Generation of novel developmental and adult zebrafish models of amyotrophic lateral sclerosis

By

Alison Hogan

MACQUARIE
University
SYDNEY·AUSTRALIA

This thesis is submitted to Macquarie University in fulfilment of the requirement for the Degree of Doctor of Philosophy.

Except where acknowledged in the customary manner, the material presented in this thesis is, to the best of my knowledge, original and has not been submitted in whole or part for a degree in any university.

Alison Hogan

Acknowledgements

"A Ph.D is an exhausting, emotional struggle. You are forced to confront all of your fears, insecurities and doubts you have about yourself and somehow overcome them. It's terrifying." (PhD humour and Facts Facebook page).

Im not sure how humorous this quote is, but it is accurate. Completing this PhD would not have been possible without a huge amount of support from a large group of people, both at Macquarie and at home.

Firstly, a huge thank you to my supervisor Ian. Thank you for giving me the opportunity to do this PhD in your lab - you have a fantastic group who do amazing work and I feel very fortunate to be a part of it. I would also like to thank you for your guidance and for somehow always making me feel like things were under control even when nothing was going according to plan.

Kelly, thank you for getting me organised right from the start of this project and thank you for sorting out my latex issues - I may have thrown it all in with 2 weeks to go without your help! Jenn, you have been an amazing support throughout, but particularly with the writing up. Thank you for you input and your encouragement, it has helped me enormously. To the rest of the genetics group Emily, Shu, Katherine, Ingrid, Sarah, Elisa, Sarah and Jasmin - thank you for the support, the help in the lab and the morning teas, you really is a great group of wonderful people.

To my other group at Macquarie - the zebrafish group. Nick, thank you for being my secondary supervisor, your ideas and input into my project has been invaluable and your enthusiasm inspiring. Emily, thank you for teaching me all the zebrafish skills and thank you for the constant support, positivity and guidance throughout this PhD (and the Masters). Angela and your team, you have been great addition to the lab, you maintain the highest of standards and it has been great working with and learning from you. Isabel, I learnt a huge amount during our daily car trips, thank you for being so generous with your knowledge and friendship. Thank you to Dasha, Rola, Tugsuu, and Jason for their care of the fish in our facility and also taking the time to teach me zebrafish husbandry and best practice. To the rest of the zebrafish group Sharron, Marco, Adam, Maxinne, Kristy, Serene, Jack and Yagiz I have learnt from each and every one of you. Thank you.

Away from the lab, I would like to thank my family for their support – for not calling me crazy for walking away from my vet career to do a PhD and for your belief that I would succeed. The biggest thank you to goes to Gordon, who supported me and tolerated my obsession with this project without complaint. I could not have achieved this without you.

This thesis is dedicated to Charlie.

List of Publications

Publications and manuscripts contained within this thesis

Paper 1: Galper J*, Rayner S*, **Hogan A***, Fifita J, Lee A, Chung R, Blair I and Yang S. (2017). *Cyclin F: a component of a E3 ubiquitin ligase complex with roles in neurodegeneration and cancer.* Int. J. Biochem. Cell Biol. 89: 216-220.
(* denotes equal first authorship).

Paper 2: **Hogan AL**, Don EK, Rayner SL, Lee A, Laird AS, Watchon M, Winnick C, Tarr I, Morsch M, Fifita JA, Gwee S, Formella I, Hortle E, Yuan K, Molloy MP, Williams KL, Nicholson GA, Chung RS, Blair IP, Cole NJ (2017). *Expression of ALS/FTD-linked mutant CCNF in zebrafish leads to increased cell death in the spinal cord and an aberrant motor phenotype.* Hum, Mol. Gen. 26(14) 26162626.

Manuscript 1: **Hogan AL**, Don EK, Fifita JA, Williams KL, Laird AS, Chung RS, Blair IP, Cole NJ (2018) *Apparent toxicity of constitutive overexpression of the ALS-linked gene CCNF precludes generation of transgenic zebrafish models* Under review, Science Matters.

Manuscript 2: **Hogan AL**, Don EK, Laird AS, Chow S, Gwee S, Fifita JA, Williams KL, Hall T, Cole NJ Blair IP (2018) *A mutant CCNF, doxycycline-inducible, adult zebrafish model of ALS* Prepared for submission to Dis. Mod. Mech.

Additional publications during this candidature

- Williams KL, Topp S, Yang S, Smith B, Fifita JA, Warraich ST, Zhang KY, Farrawell N,Vance C, Hu X, Chesi A, Leblond CS, Lee A, Rayner SL, Sundaramoorthy V, Dobson- Stone C, Molloy MP, van Blitterswijk M, Dickson DW, Petersen RC, Graff-Radford NR, Boeve BF, Murray ME, Pottier C, Don E, Winnick C, McCann EP, **Hogan A**, Daoud H, Levert A, Dion PA, Mitsui J, Ishiura H, Takahashi Y, Goto J, Kost J, Gellera C, Gkazi AS, Miller J, Stockton J, Brooks WS, Boundy K, Polak M, Muoz-Blanco JL, Esteban-Prez J, Rbano A, Hardiman O, Morrison KE, Ticozzi N, Silani V, de Belleroche J, Glass JD, Kwok JB, Guillemin GJ, Chung RS, Tsuji S, Brown RH Jr, Garca-Redondo A, Rademakers R, Landers JE, Gitler AD, Rouleau GA, Cole NJ, Yerbury JJ, Atkin JD, Shaw CE, Nicholson GA, Blair IP (2016). *CCNF mutations in amyotrophic lateral sclerosis and frontotemporal dementia.* Nat Commun. 15(7):11253.

- Don EK, Formella I, Badrock A, Hall TE, Morsch M, Hortle E, **Hogan AL**, Chow S, Gwee SL,Stoddart JJ, Nicholson GA, Chung R, Cole NJ (2016) *A Tol2 Gateway-Compatible Toolbox for the Study of the Nervous System and Neurodegenerative Disease.* Zebrafish, 14, 69-72.

- Fifita JA1, Zhang KY, Galper J, Williams KL, McCann EP, **Hogan AL**, Saunders N, Bauer D, Tarr IS, Pamphlett R, Nicholson GA, Rowe D, Yang S, Blair IP. *Genetic and Pathological Assessment of hnRNPA1, hnRNPA2/B1, and hnRNPA3 in Familial and Sporadic Amyotrophic Lateral Sclerosis.* Neurodegener Dis. 2017;17(6):304-312.

Amyotrophic lateral sclerosis (ALS) is a fatal neurodegenerative disease characterised by the death of upper and lower motor neurons. Approximately 10% of ALS patients have a known family history of the disease and genetic analysis of ALS-affected families has identified causal mutations in multiple genes. The identification of these mutations has provided the opportunity to develop models of ALS, essential tools for studies investigating the biology of the disease and for preclinical testing of potential

therapeutics. While many of the mechanisms underlying ALS have been elucidated, these mechanisms remain poorly understood. Further studies using both established and novel models of ALS are required to enhance the current understanding of these mechanisms. A greater understanding of disease biology will lead to the identification of potential therapeutic targets.

Mutations in *CCNF* linked to both familial and sporadic ALS were recently reported. Patients who carry these *CCNF* mutations develop TDP-43 positive protein aggregates within the their motor neurons – pathology considered to be the hallmark of the disease in over 95% of cases. Therefore, the identification of ALS-linked mutations in *CCNF* provides an opportunity to develop novel models that reflect the most common pathology seen in ALS patients. This project aimed to develop these novel models in the zebrafish.

Zebrafish have emerged as useful tools to identify and investigate mechanisms of human disease. As vertebrates, they share significant genetic, anatomical and physiological similarities with humans, while their speed of development, their high fertility and the relative ease of manipulating their genome contribute to efficient development of disease models. This project investigated the suitability of zebrafish to model ALS-linked mutations in *CCNF* by characterising the zebrafish *ccnf* homologue and its encoded protein, cyclin F. Comparison of zebrafish and human cyclin F identified significant structural similarities between the proteins, suggesting that they perform similar functions in the two species. Further, cyclin F was found to be persistently expressed in the zebrafish central nervous system throughout development. This suggests that models in which cyclin F is artificially expressed in the central nervous system will have physiological relevance. These findings supported the hypothesis that zebrafish are a suitable species in which to model cellular changes associated with ALS-linked mutant *CCNF*.

Based on these findings, generation of the *CCNF*-based zebrafish commenced. A variety of model paradigms were explored to identify strategies that produced models suitable for investigative studies. Several strategies failed to generate viable models, including persistent embryonic overexpression of *CCNF* and selective expression of *CCNF* within the motor neurons. Two strategies emerged that did produce suitable models with which to study ALS - transient overexpression of ALS-linked mutant *CCNF* and inducible overexpression of ALS-linked mutant *CCNF* in adult zebrafish. Evidence presented in this thesis indicates that the transient model will prove useful for efficient analysis of the cellular changes associated with mutant *CCNF* and will be suitable for use in preclinical trials of potential therapeutics, while the inducible transgenic model will prove useful for longitudinal studies aimed at investigating disease biology in an adult animal. Such studies will contribute to a greater understanding of the mechanisms involved in disease onset and progression. The presence of TDP-43 pathology in patients who carry a *CCNF* mutation suggests that findings from these models will be applicable to wider ALS. A greater understanding of the biology of ALS will lead to the identification of potential therapeutic targets, an essential step in the development of desperately needed effective therapies.

Abbreviations

ALS	amyotrophic lateral sclerosis
ALS TDI	ALS Therapy Development Institute
AO	acridine orange
bp	base pair
actb2	beta actin 2 promoter (ubiquitous)
CCNF	human *CCNF* gene
ccnf	zebrafish *ccnf* homologue
cDNA	complementary DNA
CMV	cytomegalovirus promoter (ubiquitous)
CNS	central nervous system
CRISPR	clustered regularly interspaced short palindromic repeats
CRND	cycle-related neuronal death
CSF	cerebrospinal fluid
CRT	uninjected control group
DAVID	database for annotation, visualization and integrated discovery

DMSO   dimethyl sulfoxide

DNA   deoxyribonucleic acid

dpf   days post fertilisation

DPRs   dipeptide repeat proteins

ECL   chemilluminescent western blotting

EGFP   enhanced green fluorescent protein

ER   endoplasmic reticulum

ERT   modified human oestrogen receptor

F1   1st generation

F2   2nd generation

FALS   familial ALS

FBS   fetal bovine serum

FTD   frontotemporal dementia

GO   gene ontology

H_2O_2 hydrogen peroxide

hpf   hours post fertilisation

IPA   ingenuity pathway snalysis

iPSC   induced pluripotent stem cell

ISH   *in situ* hybridisation

kb   kilobase pairs

LB   Luria-Bertani broth

LMN	lower motor neuron
MND	motor neuron disease
mRNA	messenger ribonucleic acid
mpf	months post fertilisation
NCBI	National Centre for Biotechnology Information
NEB	New England Biolabs
NLS	nuclear localisation signal
NMJ	neuromuscular junction
NSC-34	mouse motor neuron-like hybrid cell line
Neuro-2a	mouse neuroblastoma cell line
PBS	phosphate buffered saline
PBS-T	phosphate buffered saline with 0.1% Tween 20
PCR	polymerase chain reaction
PFA	paraformaldehyde
PMR	photomotor response
QFWB	quantifiable fluorescence based western blot
qPCR	quantitative polymerase chain reaction
r	Spearmans correlation coefficient
RAN	repeat-associated non-ATG
RT-PCR	reverse transcription polymerase chain reaction
RNA	ribonucleic acid

SALS   sporadic ALS

SB   sleeping beauty transposase

SCF   Skp1-Cul1-F-box

SEM   standard error of the mean

SH-SY5Y   human cell line established from metastatic neuroblastoma cells from bone marrow

TAB   AB/Túbingen wild type zebrafish line

TEER   touch evoked escape response

TUB   Túbingen wild type zebrafish line

UMN   upper motor neuron

UPS   ubiquitin proteasomal system

Contents

List of Figures

List of Tables

1

Introduction

1.1   General introduction to this thesis

Amyotrophic lateral sclerosis (ALS) is a fatal neurodegenerative disease that is characterised by the progressive death of upper and lower motor neurons. The disease generally progresses rapidly and the majority of ALS patients die from respiratory complications within 3-5 years (Rowland and Shneider, 2001). Currently available treatments extend the life of patients by just a few months. This scarcity of effective treatments reflects our need for a greater understanding of the biology of ALS, and the need for valid models for therapeutic discovery and preclinical studies. The ongoing identification of ALS-linked gene mutations has provided valuable insight into the biological pathways disrupted in ALS, but much remains to be understood.

ALS gene discovery has also facilitated the development of models that reflect aspects of patient pathology. ALS pathology can only be examined in humans at post mortem, at which point disease processes are well advanced. To gain insight into pre-clinical pathological changes and consequently, potential therapeutic targets suitable for early intervention, animal models are essential. Such models are also required to test the safety and efficacy of potential therapeutics. However, no current model adequately represents all aspects of ALS pathology. Consequently, no model can accurately reflect disruption in the multiple biological pathways that have been implicated in disease pathogenesis. Therefore, multiple models, based on different ALS-linked genes that function in different pathways are required. Our laboratory recently identified novel mutations in *CCNF* that are linked to the most common form of the disease - ALS with TDP-43 pathology. This discovery presents an opportunity to develop novel models to examine the biology of ALS from a fresh perspective.

The protein degradation pathways are strongly implicated in the pathogenesis of ALS (Webster et al., 2017). Cyclin F, encoded by *CCNF*, plays a role in protein degradation through the ubiquitin proteasome system (UPS) (Galper et al., 2017). This suggests that models based on ALS-linked mutations in *CCNF* will provide tools with which to investigate dysfunction in this key pathway. The aim of this project was to develop such models in the zebrafish.

This thesis begins with an overview of the current state of ALS research, including the ALS-linked genes identified to date and the biological pathways that have been implicated in the pathogenesis of the disease. This is followed by a review of the *in vivo* models that have been established based on ALS-linked gene mutations and the key insights that these models have provided into disease biology. The thesis then details the characterisation of zebrafish *ccnf*, which established the suitability of the species to model ALS-linked mutations in the gene, followed by a description of the transgenic strategies that were assessed in this project and the two viable models that these strategies generated. The thesis concludes with a discussion of potential studies

for this these two viable models may be suited.

1.2 Introduction to ALS

1.2.1 Motor neuron disease, amyotrophic lateral sclerosis and frontotemporal dementia

The motor neuron diseases (MNDs) are a group of disorders that are characterised by progressive degeneration of motor neurons. The motor neurons are classified as upper motor neurons (UMNs), which originate in the cerebral cortex and brainstem, and lower motor neurons (LMNs), which transmit nerve impulses to the muscles. The LMNs may innervate either the limbs (spinal LMNs) or the muscles of the face and tongue (cranial nerve LMNs). Degeneration of the UMNs leads to muscle spasticity, while degeneration of the spinal LMNs leads to muscle weakness and atrophy. Degeneration of the cranial nerve LMNs leads to bulbar motor neuron signs, which include difficulty speaking and swallowing. Clinical presentation varies between MND patients, however the disease is invariably progressive and ultimately fatal.

Amyotrophic lateral sclerosis (ALS) is the most common and most rapidly progressive form of MND. ALS is a heterogeneous disease that demonstrates significant variability with respect to dominant clinical features (upper or lower motor neuron), age of onset and speed of progression. This variability is observed even amongst patients who carry the same ALS-linked gene mutation (Xi et al., 2014). Survival time of patients is highly variable, however in most cases, death typically occurs within 3-5 years of symptom onset (Rowland and Shneider, 2001).

ALS is linked clinically, pathologically and genetically to a form of presenile dementia - frontotemporal dementia (FTD) (Figure 1.1). Frontotemporal dementia is characterised by degeneration of the frontotemporal lobes, which clinically leads to progressive behavioural changes and language deficits (Warren et al., 2013). Up to 50% of

ALS patients develop some degree of frontotemporal dysfunction and this dysfunction is severe enough in approximately 15% of patients to meet the criteria for diagnosis of co-morbid ALS-FTD (Giordana et al., 2011). Conversely, approximately 15% of primary FTD patients meet the criteria for diagnosis of ALS (Ringholz et al., 2005). In addition to this clinical overlap, the two conditions share a key pathological feature - the cytoplasmic aggregation of ubiquitinated misfolded proteins within neurons (Ling et al., 2013). Furthermore, the two conditions are linked by several gene mutations which are found in both ALS and FTD patients. As a result of these common features, ALS and FTD are regarded as two ends of a spectrum of neurodegenerative disease (Couratier et al., 2017).

1.2.2 Epidemiology of ALS

ALS has an estimated worldwide incidence of 1.5-1.85 people per 100 000 population (Marin et al., 2017). The incidence of the disease is approximately 1.3 times higher in men than women, however this ratio varies with both age and ethnicity (McCombe and Henderson, 2010). Geographically, the incidence of ALS is similar across Europe, North America and New Zealand (approximately 1.89 per 100 000) (Marin et al., 2017). This is significantly higher than the reported incidence of ALS in Asia (approximately 0.88 per 100 000) (Marin et al., 2017). The age of onset of ALS is variable. The average age of onset is reported to be 64.3 years of age (Paulukonis et al., 2015), however, rare juvenile (under 25 years of age) and young onset (under 45 years of age) forms of the disease have reported (Turner et al., 2012).

FIGURE 1.1: Clinical, pathological and genetic overlap between ALS and FTD.
A. Clinically, a high incidence of cognitive dysfunction is evident in ALS patients and conversely, a high degree of motor impairment is seen in FTD patients. **B.** The key pathological feature of both ALS and FTD is the formation of ubiquitinated protein aggregates within surviving neurons. Graphs indicate key proteins that have been identified within these aggregates. **C.** Genes in which ALS and FTD-linked mutations have been identified. Figure adapted from Ling et al. (2013). FTD-linked mutations reviewed in Turner et al. (2017).
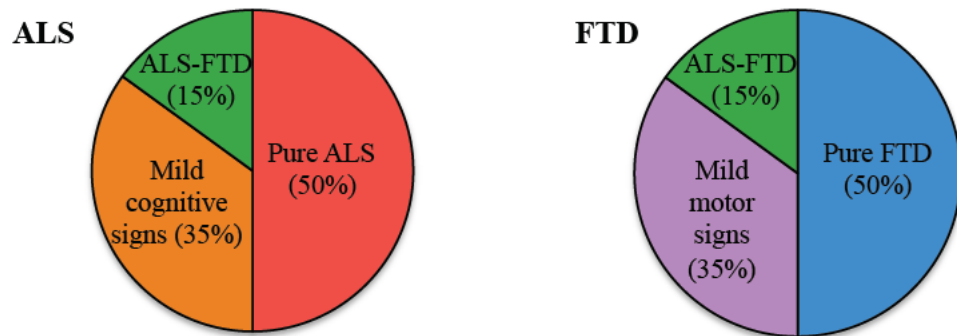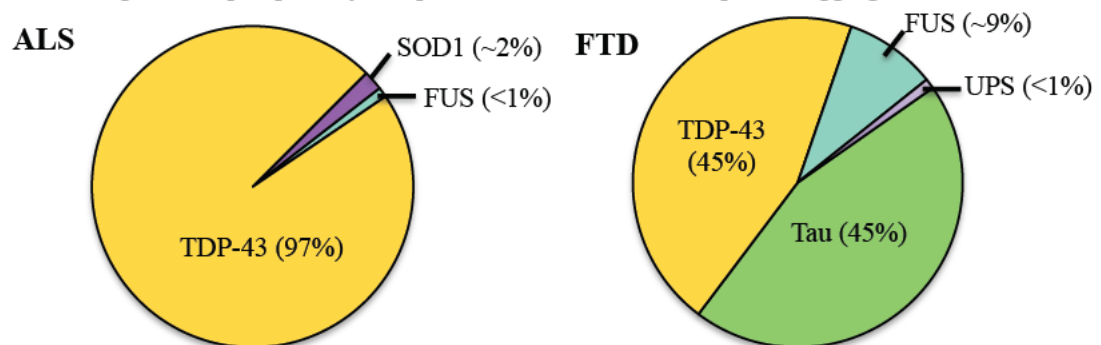
1.2.3   Familial ALS

Approximately 10% of ALS cases demonstrate familial inheritance of the disease (familial ALS, FALS) (Iguchi et al., 2013) and currently, gene mutations are the only known cause of ALS. To date, mutations in over 25 genes have been confidently linked to ALS (ALS-linked genes), accounting for approximately 60% of familial cases (McCann et al., 2017). Gene mutations have also been identified which appear to be act as disease risk factors or disease modifiers (ALS-associated genes) (Table 1.1). ALS-linked mutations often display classic Mendelian inheritance patterns, however significant variability is seen with respect to disease penetrance and clinical presentation (Al-Chalabi and Lewis, 2011).

Over 50% of familial ALS cases are attributable to mutations in just four genes - *SOD1*, *TARDBP*, *FUS* and *C9orf72* (McCann et al., 2017). These genes are briefly discussed in this section, followed by a more comprehensive review of the gene at the centre of this project - *CCNF*.

SOD1

The identification of ALS-linked mutations in *SOD1* was the first genetic breakthrough in ALS research (Rosen, 1993). The *SOD1* protein, superoxide dismutase, is a metalloenzyme, required to convert superoxide free radicals to less reactive oxygen species. To date, over 160 mutations distributed throughout this gene have been reported, accounting for 12-23% of ALS patients worldwide (Andersen, 2006) and approximately 13.7 % of Australian FALS cases (McCann et al., 2017).

TARDBP

Over 95% of ALS patients and approximately 45% of FTD patients develop neuronal protein aggregates that are positive for the protein encoded by *TARDBP* - TDP-43

Table 1.1: ALS-linked and ALS-associated genes identified to date.

ALS-linked Gene	Incidence	Primary functional pathway
SOD1 (Rosen, 1993)	~20%	Antioxidant
TARDBP (Sreedharan et al., 2008)	~4%	RNA processing
FUS (Vance et al., 2009; Kwiatkowski et al., 2009)	3-5%	RNA processing
ALS2 (Hadano et al., 2001)	<1%	Activation of GTPases, neurite outgrowth
SETX (Chen et al., 2004)	<1%	DNA repair, RNA synthesis
VAPB (Nishimura et al., 2004)	<1%	ER membrane protein
ANG (Greenway et al., 2006)	<1%	Angiogenesis, RNA processing
FIG4 (Chow et al., 2009)	<1%	Vesicle trafficking (?)
OPTN (Maruyama et al., 2010)	<1%	Golgi protein, protein homeostasis
VCP (Johnson et al., 2010)	<1%	Protein homeostasis
UBQLN2 (Deng et al., 2011)	<1%	Protein homeostasis
SIGMAR1 (Luty et al., 2010)	<1%	ER transport
PFN1 (Wu et al., 2012a)	<1%	Actin dynamics
C9ORF72 (DeJesus-Hernandez et al., 2011; Renton et al., 2011)	~40%	Protein homeostasis, transcription
SPG11 (Orlacchio et al., 2010)	<1%	Neuronal skeleton, axonal transport, synaptic vesicles
CHMP2B (Parkinson et al., 2006)	<1%	Endocytosis, protein trafficking,
hnRNPA1 (Kim et al., 2013)	<1%	RNA processing
MATR3 (Johnson et al., 2014)	<1%	RNA processing
CCNF (Williams et al., 2016)	0.6-3.3%	Protein homeostasis
DCTN1 (Munch et al., 2004)	<1%	ER-golgi transport
SQSTM1 (Fecto et al., 2011)	<1%	Protein homeostasis
NEFH (Figlewicz et al., 1994)	<1%	Axoskeleton protein
PRPH (Gros-Louis et al., 2004)	<1%	Cytoskeletal protein
TUBA4A (Smith et al., 2014)	<1%	Neuronal skeleton
hnRNPA2B1 (Kim et al., 2013)	<1%	RNA processing
EWSR1 (Couthouis et al., 2012)	<1%	Transcription suppression
CHCHD10 (Bannwarth et al., 2014; Chaussenot et al., 2014)	<1%	Mitochondrial protein
ALS-associated genes	**Incidence**	**Primary functional pathway**
TBK1 (Freischmidt et al., 2015; Chase, 2015)	Unknown	Innate immunity, autophagy
ATXN2 (Elden et al., 2010)	Unknown	RNA processing, endocytosis
NEK1 (Kenna et al., 2016; Brenner et al., 2016)	Unknown	DNA damage and repair
C21orf2 (van Rheenen et al., 2016)	Unknown	DNA damage and repair
TAF15 (Couthouis et al., 2011)	Unknown	Transcription initiation
SPAST (Meyer et al., 2005)	Unknown	Neurofilament, cytoskeletal, microtubule development
CREST (Chesi et al., 2013)	Unknown	Transcription initiation
ELP3 (Simpson et al., 2009)	Unknown	Unknown
DAO (Mitchell et al., 2010)	Unknown	Unknown
UNC13A (van Es et al., 2009)	Unknown	Neurite outgrowth, synaptic transmission
ERBB4 (Takahashi et al., 2013)	Unknown	Protein kinase
NTE (Rainier et al., 2008)	Unknown	ER protein
PON1-3 (Cronin et al., 2007)	Unknown	Antioxidant
C19orf12 (Kim et al., 2016)	Unknown	Mitochondrial protein
EPHA4 (Van Hoecke et al., 2012)	Unknown	Tyrosine kinase receptor activity
CHGB (Gros-Louis et al., 2009)	Unknown	ER-golgi transport
SMN (Orrell et al., 1997)	Unknown	snRNP synthesis

(Neumann et al., 2007). This suggests that TDP-43 dysfunction is a key feature of both diseases, a hypothesis that was confirmed by the identification of ALS and FTD-linked mutations within *TARDBP* (Sreedharan et al., 2008; Van Deerlin et al., 2008; Kabashi et al., 2008; Yokoseki et al., 2008). TDP-43 is an RNA binding protein which has a role in regulation of transcription, RNA transport and translation, mRNA splicing and DNA repair (Sephton et al., 2012). Over 50 ALS-linked mutations within this gene have now been reported, accounting for up to 4% of familial cases worldwide (Sreedharan et al., 2008) and approximately 1.9% of Australian FALS cases (McCann et al., 2017).

FUS

TDP-43 shares significant structural and functional similarities with another RNA binding protein, fused in sarcoma (FUS). Due to these similarities, Vance et al. (2009) identified the FUS-encoding gene (*FUS*) as a prime candidate for ALS mutation screening in patient cohorts. This screening identified three mutations within the gene that segregated with disease (Vance et al., 2009). To date, 49 ALS-linked mutations in *FUS* have been reported, accounting for 3-5% of ALS cases worldwide (reviewed in Shang and Huang (2016)) and approximately 2.4% of Australian FALS patients (McCann et al., 2017).

C9orf72

The most common genetic cause of ALS is a hexanucleotide repeat (GGGGCC) expansion in a non-coding region of the *C9orf72* gene. Unaffected individuals typically carry up to 23 copies of the hexanucleotide repeat sequence, whereas ALS and FTD patients with the *C9orf72* mutation carry hundreds to thousands of repeats. The *C9orf72* mutation accounts for approximately 40.6% of Australian FALS patients (McCann et al., 2017) and is also the most common genetic cause of FTD, accounting for 25.9% of FTD patients (van Blitterswijk et al., 2012). The cellular functions of *C9orf72* are only now being elucidated. So far, the protein has been shown to be involved in the maintenance of multiple homeostatic pathways, including protein homeostasis through autophagy (more specifically, microautophagy)(Nassif et al., 2017), nuclear transport (Freibaum et al., 2015; Zhang et al., 2016) and actin dynamics (Sivadasan et al., 2016).

CCNF

Introduction to *CCNF*

Cyclin F, encoded by *CCNF*, is an E3 ubiquitin ligase, a substrate recognition component of the UPS. Known substrates of cyclin F include cell cycle proteins and proteins

that function in DNA repair and replication. By regulating the expression levels of these substrates, cyclin F has a role in regulating both cell cycle progression and the maintenance of genome stability (Galper et al., 2017). The function of cyclin F within the UPS and its downstream biological effects are detailed in a review article (Paper 1) published in the *International Journal of Biochemical Cell Biology.*

Paper 1

Declaration of Contributions

The three co-first authors (JG, SR and AH) all contributed equally to the writing and editing of this paper. All other authors provided intellectual input and contributed to the editing process.
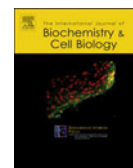
Molecules in focus

Cyclin F: A component of an E3 ubiquitin ligase complex with roles in neurodegeneration and cancer

Jasmin Galper[1], Stephanie L. Rayner[1], Alison L. Hogan[1], Jennifer A. Fifita, Albert Lee, Roger S. Chung, Ian P. Blair, Shu Yang[*]

Centre for MND Research, Faculty of Medicine and Health Sciences, Macquarie University, Sydney, NSW, Australia

ARTICLE INFO

ABSTRACT

Cyclin F, encoded by *CCNF*, is the substrate recognition component of the Skp1-Cul1-F-box E3 ubiquitin ligase complex, SCF^cyclin F. E3 ubiquitin ligases play a key role in ubiquitin-proteasome mediated protein degradation, an essential component of protein homeostatic mechanisms within the cell. By recognising and regulating the availability of several protein substrates, SCF^cyclin F plays a role in regulating various cellular processes including replication and repair of DNA and cell cycle checkpoint control. Cyclin F dysfunction has been implicated in various forms of cancer and *CCNF* mutations were recently linked to familial and sporadic amyotrophic lateral sclerosis and frontotemporal dementia, offering a new lead to understanding the pathogenic mechanisms underlying neurodegeneration. In this review, we evaluate the current literature on the function of cyclin F with an emphasis on its roles in cancer and neurodegeneration.

1. Introduction

First reported in 1994, cyclin F (encoded by *CCNF*, alias *FBXO1*) is the founding member of the F-box family of proteins, which are characterised by the presence of an F-box motif (Bai et al., 1994). F-box proteins act as the substrate recognition subunits of Skp1–Cul1–F-box (SCF) E3 ubiquitin ligase complexes, which recognise and mediate the ubiquitination of target proteins via an enzyme cascade. First, E1 ubiquitin-activating enzymes transfer activated ubiquitin to an E2 ubiquitin-conjugating enzyme. E3 ubiquitin ligase complexes then mediate the transfer of activated ubiquitin from the E2 ubiquitin-conjugating enzyme to specific substrates (Fig. 1A) (Tanaka and Matsuda, 2014). Ubiquitinated proteins are then directed to the proteasome for proteolysis. This system is collectively known as the ubiquitin-proteasome system (UPS). Cyclin F also belongs to the cyclin family and is involved in regulating various cell cycle processes, including centrosome duplication (D'Angiolella et al., 2010), genome stability maintenance (Walter et al., 2016) and DNA replication and repair (D'Angiolella et al., 2012). In contrast to other cyclins, which utilise cyclin-dependent kinases (cdk) to phosphorylate protein substrates and promote cell cycle events, cyclin F regulates the cell cycle independent of cdk activity. Alternatively, it ubiquitinates or directly interacts with substrates (D'Angiolella et al., 2012; D'Angiolella et al., 2010; Klein et al., 2015).

In line with its role in regulating the cell cycle, *CCNF* dysfunction has been linked to various forms of cancer and cyclin F expression levels have been proposed as a biomarker of hepatocellular carcinoma (Fu et al., 2013). Recently, *CCNF* mutations were linked to amyotrophic lateral sclerosis (ALS) and frontotemporal dementia (FTD) (Williams et al., 2016), highlighting a pathogenic role of cyclin F in neurodegenerative diseases.

2. Structure

Cyclin F is a 786-amino acid protein that is encoded by the 17 exon *CCNF* gene (Bai et al., 1994). Cyclin F contains two nuclear localisation signals (NLS), an F-box domain, two functional D-box motifs, a cyclin box and a PEST sequence rich in Pro (P), Glu (E), Ser (S) and Thr (T) residues (Fig. 2). The two NLS ensure cyclin F remains predominantly nuclear (Kong et al., 2000). The F-box domain binds S-phase kinase-associated protein 1 (Skp1) within the SCF complex (Schulman et al., 2000), whilst the D-boxes, composed of an RxxL sequence, are required for anaphase promoting complex/cyclosome (APC/C)-mediated degradation of cyclin F (Choudhury et al., 2016). The cyclin box domain shares structural similarities with other cyclins, and is responsible for binding substrates through hydrophobic residues (D'Angiolella et al., 2012; D'Angiolella et al., 2010; Walter et al., 2016). The PEST sequence
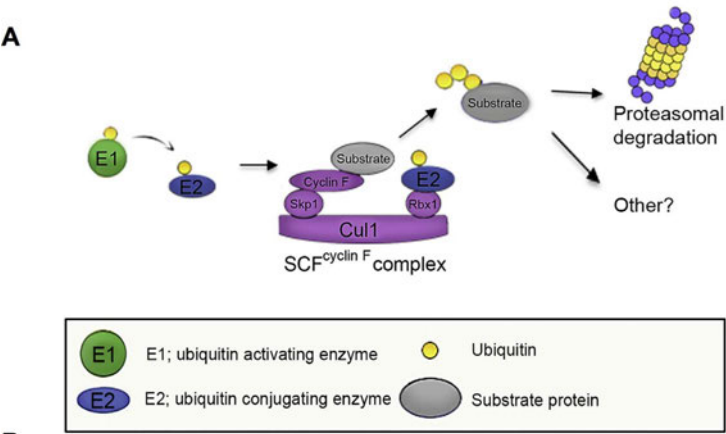
Fig. 1. (A) The SCF^cyclin F complex in the ubiquitin proteasome system pathway. Cyclin F, Skp1, Cul1 and RING box protein 1 (Rbx1) form a Skp1-Cul1-F-box (SCF) E3 ubiquitin ligase complex. E1 ubiquitin-activating enzymes transfer ubiquitin to E2 ubiquitin-conjugating enzymes, which then interact with the SCF^cyclin F complex to transfer ubiquitin to a target substrate. This directs the substrate to the proteasome for degradation. The question mark denotes that outcomes besides proteasomal degradation of ubiquitinated substrates are possible, although this has not been specifically explored for cyclin F. **(B)** Substrates targeted by SCF^cyclin F for protein degradation and cyclin F binding partners, with functional outcomes.

SCF^cyclin F Substrate	Function	Reference
NuSAP	Mitotic spindle formation	(Emanuele et al., 2011)
CDC6	Correct DNA replication	(Walter et al., 2016)
SLBP	Histone expression	(Dankert et al., 2016)
RRM2	dNTP balance, DNA repair and synthesis	(D'Angiolella et al., 2012)
CP110	Centrosome duplication	(D'Angiolella et al., 2010)
EXO1	DNA excision and repair	(Elia et al., 2015)
Cyclin F Binding Partner		
cyclin B/cdc2 / Cyclin F	Onset of mitosis	(Kong et al., 2000)
fzr1 / Cyclin F	S-phase entry	(Choudhury et al., 2016)
b-myb / Cyclin F	DNA damage-induced checkpoint control	(Klein et al., 2015)

Fig. 2. Structure of the *CCNF* gene (transcript ID ENST00000397066.8) and cyclin F protein (protein ID ENSP00000380256). *CCNF* has 17 exons that cover a 29.46 kb region on chromosome 16. Cyclin F is a 786-amino acid protein that contains two nuclear localisation signals (NLS), an F-box, a cyclin box and a PEST (Pro (P), Glu (E), Ser (S) and Thr (T)) region. Black numbers on the *CCNF* gene schematic denote exon number and black numbers on the protein schematic denote amino acid position. Grey dotted lines show which exon(s) encode each protein domain. UTR   untranslated region. Red arrows and text indicate the location of each of the ALS/FTD-linked mutations within *CCNF* identified to date. Gene structure adapted from Ensembl (Yates et al., 2015). (For interpretation of the references to colour in this figure legend, the reader is referred to the web version of this article.)

is located at cyclin F's C-terminal. PEST regions are typically present in proteins that are rapidly degraded and in agreement with this, expression of cyclin F lacking the PEST region leads to an accumulation of cyclin F in cells (Fung et al., 2002).

3. Expression, activation and turnover

In humans, cyclin F mRNA is ubiquitously expressed (Bai et al., 1994), however mRNA expression levels differ between tissues (Uhlen et al., 2015, http://www.proteinatlas.org/) and this difference may be attributed to the proportion of cycling cells within a specific tissue (Bai et al., 1994). High mRNA expression occurs in skeletal muscle and brain whilst low expression occurs in the heart and pancreas (Bai et al., 1994). In humans, cyclin F protein is most abundant in the lung, skin, bone marrow and immune system (Uhlen et al., 2015, http://www.proteinatlas.org/). Cyclin F mRNA and protein abundances oscillate throughout the cell cycle (Bai et al., 1994). Cyclin F mRNA accumulates in S phase, peaks at G_2 phase and decreases at M phase (Bai et al., 1994). Within the cell, cyclin F is predominately nuclear, however it has also been noted in perinuclear regions in dividing cells (Bai et al., 1994).

The E3 ubiquitin ligase activity of SCF$^{cyclin F}$ is modified by the neural precursor cell expressed developmentally downregulated protein 8 (NEDD8). NEDD8 post translationally modifies SCF$^{cyclin F}$ by forming a covalent attachment to the C-terminal of the SCF$^{cyclin F}$ subunit Cul1. This neddylation induces 'open' and 'closed' conformational rearrangements, resulting in SCF$^{cyclin F}$ activation or inactivation respectively (Duda et al., 2008). SCF activation by NEDD8 likely enables E2-ligase recruitment whilst preventing the binding of an SCF inhibitor, cullin-associated NEDD8-dissociated protein 1 (CAND1), resulting in ubiquitin ligase activity (Choudhury et al., 2016; Duda et al., 2008).

Cyclin F is known to be phosphorylated, although the functional consequences of this phosphorylation are unclear (Bai et al., 1994). Typically, PEST regions of proteins are heavily phosphorylated, impacting processes such as protein interactions and ligase activity (Garcia-Alai et al., 2006).

Two potential mechanisms of cyclin F degradation have been proposed. The PEST region of cyclin F confers instability to the protein and this has been proposed to promote degradation through the action of metalloproteases (Fung et al., 2002). In another study, cyclin F was identified as a direct substrate of the APC/C^{fzr} (fizzy-related protein homolog) ubiquitin ligase, leading to its ubiquitination and subsequent proteasome-mediated degradation (Choudhury et al., 2016). These studies presented different cyclin F degradation mechanisms, however, each study utilized differing cell cycle stages, so it is possible that the degradation mechanism of cyclin F is cell cycle stage dependent, although this needs further investigation.

4. Biological functions

Cell cycle activity is tightly regulated through the production and degradation of cell cycle-associated proteins (Choudhury et al., 2016; D'Angiolella et al., 2012; D'Angiolella et al., 2010; Murray et al., 1989). By binding and/or ubiquitinating several cell cycle-associated protein substrates, SCF$^{cyclin F}$ plays a role in regulating various cell cycle-associated functions, including maintenance of genome stability and cell cycle transitions (Fig. 1B).

4.1. DNA synthesis and repair/genome stability

SCF$^{cyclin F}$ limits the availability of ribonucleotide reductase (RNR) during the G_2 phase of the cell cycle by promoting the ubiquitination and subsequent degradation of an RNR subunit – RRM2 (D'Angiolella et al., 2012). RNR catalyses the conversion of ribonucleotides to deoxyribonucleotides (dNTPs), required for both replicative and reparative DNA synthesis. Misregulation of dNTP homeostasis leads to

genome instability and a hypermutator phenotype. Experimental downregulation of cyclin F expression has been shown to lead to an increase of RRM2 and consequently an abnormal increase in dNTP levels. In response to DNA damage from genotoxic stimuli, cyclin F degradation lead to the accumulation of RRM2 and an increased production of dNTPs to facilitate DNA repair (D'Angiolella et al., 2012).

SCF$^{cyclin F}$ also targets cell division cycle 6 (CDC6), a protein that is involved in DNA replication. Critically, CDC6 degradation by SCF$^{cyclin F}$ prevents DNA from re-replication or over-replication, which is highly disruptive to DNA integrity and promotes genome instability. This can activate ataxia telangiectasia mutated protein dependant responses, including the arrest of the cell cycle, DNA repair or apoptosis (Walter et al., 2016).

Recently, it was found that cyclin F responded to DNA damage by maintaining G_2 phase arrest, which enables the induction of DNA repair mechanisms that precede mitosis. This is achieved by cyclin F-mediated suppression of Myb-related protein B (B-Myb), an oncoprotein that drives a transcriptional program to promote accumulation of crucial mitosis-promoting proteins (Klein et al., 2015). Also in response to DNA damage, cyclin F ubiquitinates exonuclease 1 (Exo1). The purpose of cyclin F-mediated degradation of Exo1 is unclear, although it is speculated to prevent unnecessary DNA resection under stress (Elia et al., 2015). Cyclin F may additionally respond to DNA damage by regulating phosphorylated H2A.X histone protein pro-apoptotic signalling. By targeting stem-loop binding protein (SLBP), a factor necessary for expression of H2A.X, SCF$^{cyclin F}$ indirectly limited H2A.X synthesis, thereby reducing phosphorylated H2A.X-mediated pro-apoptotic signalling under genotoxic stress (Dankert et al., 2016). In summary, cyclin F regulates the availability of RNR, CDC6, B-Myb, Exo1 and SLBP to help maintain the integrity of the genome during DNA repair and synthesis.

4.2. The cell cycle

SCF$^{cyclin F}$ controls several mechanisms that maintain both the normal progression and checkpoint control of the cell cycle. Through ubiquitin-mediated proteolysis, SCF$^{cyclin F}$ decreases levels of centrosomal protein of 110 kDa (CP110). CP110 promotes centrosome duplication, a process that must occur only once per cell cycle. The timely degradation of CP110 by SCF$^{cyclin F}$ is critical to prevent centrosome duplications from re-occurring (D'Angiolella et al., 2010).

At the end of G_2 phase, SCF$^{cyclin F}$ inactivates APC/C^{fzr} to allow entry into S-phase, by targeting the fzr subunit of APC/C^{fzr} for proteolytic degradation (Choudhury et al., 2016). SCF$^{cyclin F}$ also controls the assembly of the mitotic spindle by decreasing nucleolar and spindle associated protein (NuSAP1), a protein involved in the organisation of microtubules (Emanuele et al., 2011). Independently of the SCF$^{cyclin F}$ complex, cyclin F also forms a complex with cyclin B and cdc2 (together known as M-phase promoting factor), which acts to promote the onset of mitosis (Kong et al., 2000).

In vivo mouse studies by Tetzlaff and colleagues have demonstrated important roles for cyclin F in development and cell cycle regulation (Tetzlaff et al., 2004). Cyclin F $^{/+}$ mice examined up to 24 months of age exhibited no detectable phenotype. In contrast, cyclin F $^{/}$ mice were embryonically lethal at midgestation and exhibited gross defects, including failure to initiate chorio-allantoic fusion during development. Interestingly, tissue-specific knockout of cyclin F$^{flox/}$ mice in the eye, bone, gut and bladder revealed no specific sensitivity to cyclin F function during embryogenesis or adulthood in rodents (Tetzlaff et al., 2004). Mouse embryonic fibroblasts deficient for cyclin F appeared viable in culture, although they exhibited a delayed rate of both growth and cell cycle re-entry, implicating cyclin F in cell cycle entry and progression (Tetzlaff et al., 2004). These mouse studies suggest that cyclin F is indispensable for the completion of embryogenesis, but not essential for the development or physiology in the tissues examined. It should be noted that the differences between *in vivo* and *in vitro* models

used cannot be ruled out as a source of the phenotype disparities observed between tissue-specific knockout and embryonic fibroblasts. The possibility remains that cyclin F knockout in untested tissues, such as nervous tissue, could generate a phenotype and therefore an investigation into this is warranted.

5. Cyclin F in cancer and neurodegenerative disease

5.1. Cancer

The cBioPortal for Cancer Genomics lists 74 studies covering numerous cancers in which *CCNF* alterations (mutation, amplification or deletion) have been identified (Cerami et al., 2012). However, the contribution of these genomic alterations to tumorigenesis is yet to be established. Causal somatic mutations in *CCNF* have been identified in breast cancer (Stephens et al., 2009) and in Endemic Burkitt Lymphoma (Abate et al., 2015).

Evidence suggests that cyclin F has a tumour suppressor role (Wang et al., 2014). Overexpression of cyclin F in U-2OS cells (D'Angiolella et al., 2010) and C33A cells (Bai et al., 1994) has been shown to induce G$_2$ phase arrest, impeding the initiation of mitosis. It has also been shown to reduce centrosome duplications, the amplification of which is a hallmark of cancer. Consistent with this tumour suppressive role, cyclin F expression is significantly downregulated in hepatocellular carcinoma (HCC) tumour tissue. Indeed, the magnitude of its downregulation correlates with a range of HCC prognostic markers and thus cyclin F expression levels have been proposed as a prognostic indicator in the disease (Fu et al., 2013).

Experimental downregulation of cyclin F has been shown to increase RRM2 expression, effectively disrupting the balance of dNTPs, leading to an increased frequency of genomic mutations (D'Angiolella et al., 2012). Consequently, increased RRM2 expression is a common feature of numerous cancers, including pancreatic, breast, lung, ovarian, bladder and gastric cancer, HCC and osteosarcoma (Huret et al., 2013). RRM2 expression is not solely regulated by cyclin F, and additional modifiers, most notably the oncogenic KRAS gene, have been shown to upregulate its expression (Yoshida et al., 2011). Further investigation into the contributory roles of upstream modifiers of RRM2, including cyclin F, is required to enhance our understanding of the pathways involved, and to identify potential therapeutic targets.

5.2. Neurodegenerative disease

Cyclin F has recently been linked to a spectrum of neurodegenerative diseases – ALS, FTD and co-morbid ALS-FTD (Williams et al., 2016). To date, ten missense mutations in *CCNF* have been identified which segregate with disease in both familial and sporadic ALS and FTD patients (Fig. 2). These mutations are scattered throughout the gene domains but their functional consequences are yet to be determined. Experimentally, overexpression of mutant, but not wildtype, cyclin F in NSC-34 cells leads to UPS dysfunction upstream of the proteasome and an accumulation of ubiquitinated proteins, including TAR DNA-binding protein 43 (TDP-43), a hallmark pathology of ALS/FTD (Williams et al., 2016). This study suggests that *CCNF* mutations could contribute to the overall protein homeostasis disruption in ALS/FTD. Currently, the relationship between cyclin F and TDP-43 remains unclear, and it will be interesting to investigate whether TDP-43 is a substrate of cyclin F. In addition, overexpression of cyclin F^{S621G} in zebrafish resulted in an aberrant motor neuron phenotype (Hogan et al., 2017). Taken together with the mouse study conducted by Tetzlaff et al. (2004) where tissue-specific knockout of cyclin F did not exhibit an effect, *CCNF* mutations are likely to be due to a toxic gain-of-function.

It should be noted that although commonly used to model motor neurons in ALS, NSC-34 cells are dividing and would therefore not recapitulate all features of post-mitotic neurons. In addition, the nature of the polyubiquitin chains associated with mutant compared to wildtype

cyclin F is unknown and warrants further investigation.

The role of cyclin F in neurons has not been well studied. Cell cycle proteins are differentially expressed in post-mortem tissue from patients with a range of neurodegenerative diseases, including ALS (Yang and Herrup, 2007). Some of these cell cycle proteins, such as cyclin B, are known interactors of cyclin F (Busser et al., 1998), suggesting that inappropriate activation of cell cycle proteins may play a role in neurodegeneration. There is evidence to suggest that post-mitotic neurons are able to re-enter the cell cycle (Yang and Herrup, 2007), however this re-entry appears to initiate neuronal apoptosis, a process known as cycle-related neuronal death. Cycle-related neuronal death has been reported in models of Parkinson's disease (Hoglinger et al., 2007) and Alzheimer's disease (Yang and Herrup, 2007), and it would be of interest to establish whether a similar mechanism occurs in *CCNF*-associated ALS/FTD.

6. Concluding remarks

In conclusion, cyclin F is a unique multifunctional protein that carries features of both cyclin and F-box proteins. Further characterisation of cyclin F, including the identification of additional substrates and its interaction with TDP-43, will provide further insights into neurodegenerative disease mechanisms. F-box proteins, including cyclin F, provide potential targets for cancer treatment, for example, altered expression of the F-box protein SKP2 has demonstrated significant promise in *in vitro* and *in vivo* cancer models (Chan et al., 2013). Further work to elucidate the expression pattern of cyclin F and its other primary substrates in various forms of cancer may provide additional biomarkers and valuable insight into new therapeutics.

References

Abate, F., Ambrosio, M.R., Mundo, L., Laginestra, M.A., Fuligni, F., Rossi, M., Zairis, S., Gazaneo, S., De Falco, G., Lazzi, S., Bellan, C., Rocca, B.J., Amato, T., Marasco, E., Etebari, M., Ogwang, M., Calbi, V., Ndede, I., Patel, K., Chumba, D., Piccaluga, P.P., Pileri, S., Leoncini, L., Rabadan, R., 2015. Distinct viral and mutational spectrum of endemic burkitt lymphoma. PLoS Pathog. 11 (10), e1005158.
Bai, C., Richman, R., Elledge, S.J., 1994. Human cyclin F. EMBO J. 13 (24), 6087 6098.
Busser, J., Geldmacher, D.S., Herrup, K., 1998. Ectopic cell cycle proteins predict the sites of neuronal cell death in Alzheimer's disease brain. J. Neurosci. 18 (8), 2801 2807.
Cerami, E., Gao, J., Dogrusoz, U., Gross, B.E., Sumer, S.O., Aksoy, B.A., Jacobsen, A., Byrne, C.J., Heuer, M.L., Larsson, E., Antipin, Y., Reva, B., Goldberg, A.P., Sander, C., Schultz, N., 2012. The cBio cancer genomics portal: an open platform for exploring multidimensional cancer genomics data. Cancer discovery 2 (5), 401 404.
Chan, C.H., Morrow, J.K., Li, C.F., Gao, Y., Jin, G., Moten, A., Stagg, L.J., Ladbury, J.E., Cai, Z., Xu, D., Logothetis, C.J., Hung, M.C., Zhang, S., Lin, H.K., 2013. Pharmacological inactivation of Skp2 SCF ubiquitin ligase restricts cancer stem cell traits and cancer progression. Cell 154 (3), 556 568.
Choudhury, R., Bonacci, T., Arceci, A., Lahiri, D., Mills Christine, A., Kernan Jennifer, L., Branigan Timothy, B., DeCaprio James, A., Burke Daniel, J., Emanuele Michael, J., 2016. APC/C and SCFcyclin F constitute a reciprocal feedback circuit controlling S-phase entry. Cell Rep. 16 (12), 3359 3372.
D'Angiolella, V., Donato, V., Vijayakumar, S., Saraf, A., Florens, L., Washburn, M.P., Dynlacht, B., Pagano, M., 2010. SCF(Cyclin F) controls centrosome homeostasis and mitotic fidelity through CP110 degradation. Nature 466 (7302), 138 142.
D'Angiolella, V., Donato, V., Forrester, F.M., Jeong, Y.T., Pellacani, C., Kudo, Y., Saraf, A., Florens, L., Washburn, M.P., Pagano, M., 2012. Cyclin F-mediated degradation of ribonucleotide reductase M2 controls genome integrity and DNA repair. Cell 149 (5), 1023 1034.
Dankert, J.F., Rona, G., Clijsters, L., Geter, P., Skaar, J.R., Bermudez-Hernandez, K., Sassani, E., Fenyo, D., Ueberheide, B., Schneider, R., Pagano, M., 2016. Cyclin F-mediated degradation of SLBP limits H2A.X accumulation and apoptosis upon genotoxic stress in G2. Mol. Cell 64 (3), 507 519.
Duda, D.M., Borg, L.A., Scott, D.C., Hunt, H.W., Hammel, M., Schulman, B.A., 2008. Structural insights into NEDD8 activation of cullin-RING ligases: conformational control of conjugation. Cell 134 (6), 995 1006.
Elia, A.E.H., Boardman, A.P., Wang, D.C., Huttlin, E.L., Everley, R.A., Dephoure, N., Zhou, C., Koren, I., Gygi, S.P., Elledge, S.J., 2015. Quantitative proteomic atlas of

ubiquitination and acetylation in the DNA damage response. Mol. Cell 59 (5), 867 881.

Emanuele, Michael J., Elia, Andrew E.H., Xu, Q., Thoma, Claudio R., Izhar, L., Leng, Y., Guo, A., Chen, Y.-N., Rush, J., Hsu Paul, W.-C., Yen, H.-Chi S., Elledge, Stephen J., 2011. Global identification of modular cullin-RING ligase substrates. Cell 147 (2), 459 474.

Fu, J., Qiu, H., Cai, M., Pan, Y., Cao, Y., Liu, L., Yun, J., Zhang, C.Z., 2013. Low cyclin F expression in hepatocellular carcinoma associates with poor differentiation and unfavorable prognosis. Cancer Sci. 104 (4), 508 515.

Fung, T.K., Siu, W.Y., Yam, C.H., Lau, A., Poon, R.Y., 2002. Cyclin F is degraded during G2-M by mechanisms fundamentally different from other cyclins. J. Biol. Chem. 277 (38), 35140 35149.

Garcia-Alai, M.M., Gallo, M., Salame, M., Wetzler, D.E., McBride, A.A., Paci, M., Cicero, D.O., de Prat-Gay, G., 2006. Molecular basis for phosphorylation-dependent: PEST-mediated protein turnover. Structure (London, England: 1993) 14 (2), 309 319.

Hogan, A.L., Don, E.K., Rayner, S.L., Lee, A., Laird, A.S., Watchon, M., Winnick, C., Tarr, I.S., Morsch, M., Fifita, J.A., Gwee, S., Formella, I., Hortle, E., Yuan, K., Molloy, M.P., Williams, K.L., Nicholson, G.A., Chung, R.S., Blair, I.P., Cole, N.J., 2017. Expression of ALS/FTD-linked mutant CCNF in zebrafish leads to increased cell death in the spinal cord and an aberrant motor phenotype. Hum. Mol. Genet.. http://dx.doi.org/10.1093/hmg/ddx136. ddx136.

Hoglinger, G.U., Breunig, J.J., Depboylu, C., Rouaux, C., Michel, P.P., Alvarez-Fischer, D., Boutillier, A.L., Degregori, J., Oertel, W.H., Rakic, P., Hirsch, E.C., Hunot, S., 2007. The pRb/E2F cell-cycle pathway mediates cell death in Parkinson's disease. Proc. Natl. Acad. Sci. U. S. A. 104 (9), 3585 3590.

Huret, J.-L., Ahmad, M., Arsaban, M., Bernheim, A., Cigna, J., Desangles, F., Guignard, J.-C., Jacquemot-Perbal, M.-C., Labarussias, M., Leberre, V., Malo, A., Morel-Pair, C., Mossafa, H., Potier, J.-C., Texier, G., Viguié, F., Chun, Yau, Wan-Senon, S., Zasadzinski, A., Dessen, P., 2013. Atlas of genetics and cytogenetics in oncology and haematology in 2013. Nucleic Acids Res. 41 (Database issue), D920 D924.

Klein, D.K., Hoffmann, S., Ahlskog, J.K., O'Hanlon, K., Quaas, M., Larsen, B.D., Rolland, B., Rösner, H.I., Walter, D., Kousholt, A.N., Menzel, T., Lees, M., Johansen, J.V., Rappsilber, J., Engeland, K., Sørensen, C.S., 2015. Cyclin F suppresses B-Myb activity to promote cell cycle checkpoint control. Nat. Commun. 6.

Kong, M., Barnes, E.A., Ollendorff, V., Donoghue, D.J., 2000. Cyclin F regulates the nuclear localization of cyclin B1 through a cyclin cyclin interaction. EMBO J. 19 (6), 1378 1388.

Murray, A.W., Solomon, M.J., Kirschner, M.W., 1989. The role of cyclin synthesis and degradation in the control of maturation promoting factor activity. Nature 339 (6222), 280 286.

Schulman, B.A., Carrano, A.C., Jeffrey, P.D., Bowen, Z., Kinnucan, E.R., Finnin, M.S., Elledge, S.J., Harper, J.W., Pagano, M., Pavletich, N.P., 2000. Insights into SCF ubiquitin ligases from the structure of the Skp1-Skp2 complex. Nature 408 (6810), 381 386.

Stephens, P.J., McBride, D.J., Lin, M.-L., Varela, I., Pleasance, E.D., Simpson, J.T., Stebbings, L.A., Leroy, C., Edkins, S., Mudie, L.J., Greenman, C.D., Jia, M., Latimer, C., Teague, J.W., Lau, K.W., Burton, J., Quail, M.A., Swerdlow, H., Churcher, C., Natrajan, R., Sieuwerts, A.M., Martens, J.W.M., Silver, D.P., Langerod, A., Russnes, H.E.G., Foekens, J.A., Reis-Filho, J.S., van/'t Veer, L., Richardson, A.L., Borresen-Dale, A.-L., Campbell, P.J., Futreal, P.A., Stratton, M.R., 2009. Complex landscapes of somatic rearrangement in human breast cancer genomes. Nature 462 (7276), 1005 1010.

Tanaka, K., Matsuda, N., 2014. Proteostasis and neurodegeneration: the roles of proteasomal degradation and autophagy. Biochim. Biophys. Acta 1843 (1), 197 204.

Tetzlaff, M.T., Bai, C., Finegold, M., Wilson, J., Harper, J.W., Mahon, K.A., Elledge, S.J., 2004. Cyclin F disruption compromises placental development and affects normal cell cycle execution. Mol. Cell. Biol. 24 (6), 2487 2498.

Uhlen, M., Fagerberg, L., Hallstrom, B.M., Lindskog, C., Oksvold, P., Mardinoglu, A., Sivertsson, A., Kampf, C., Sjostedt, E., Asplund, A., Olsson, I., Edlund, K., Lundberg, E., Navani, S., Szigyarto, C.A., Odeberg, J., Djureinovic, D., Takanen, J.O., Hober, S., Alm, T., Edqvist, P.H., Berling, H., Tegel, H., Mulder, J., Rockberg, J., Nilsson, P., Schwenk, J.M., Hamsten, M., von Feilitzen, K., Forsberg, M., Persson, L., Johansson, F., Zwahlen, M., von Heijne, G., Nielsen, J., Ponten, F., 2015. Proteomics: tissue-based map of the human proteome. Science 347 (6220), 1260419.

Walter, D., Hoffmann, S., Komseli, E.-S., Rappsilber, J., Gorgoulis, V., Sørensen, C.S., 2016. SCF(Cyclin F)-dependent degradation of CDC6 suppresses DNA re-replication. Nat. Commun. 7, 10530.

Wang, Z., Liu, P., Inuzuka, H., Wei, W., 2014. Roles of F-box proteins in cancer. Nat. Rev. Cancer 14 (4), 233 247.

Williams, K.L., Topp, S., Yang, S., Smith, B., Fifita, J.A., Warraich, S.T., Zhang, K.Y., Farrawell, N., Vance, C., Hu, X., Chesi, A., Leblond, C.S., Lee, A., Rayner, S.L., Sundaramoorthy, V., Dobson-Stone, C., Molloy, M.P., van Blitterswijk, M., Dickson, D.W., Petersen, R.C., Graff-Radford, N.R., Boeve, B.F., Murray, M.E., Pottier, C., Don, E., Winnick, C., McCann, E.P., Hogan, A., Daoud, H., Levert, A., Dion, P.A., Mitsui, J., Ishiura, H., Takahashi, Y., Goto, J., Kost, J., Gellera, C., Gkazi, A.S., Miller, J., Stockton, J., Brooks, W.S., Boundy, K., Polak, M., Munoz-Blanco, J.L., Esteban-Perez, J., Rabano, A., Hardiman, O., Morrison, K.E., Ticozzi, N., Silani, V., de Belleroche, J., Glass, J.D., Kwok, J.B.J., Guillemin, G.J., Chung, R.S., Tsuji, S., Brown Jr, R.H., Garcia-Redondo, A., Rademakers, R., Landers, J.E., Gitler, A.D., Rouleau, G.A., Cole, N.J., Yerbury, J.J., Atkin, J.D., Shaw, C.E., Nicholson, G.A., Blair, I.P., 2016. CCNF mutations in amyotrophic lateral sclerosis and frontotemporal dementia. Nat. Commun. 7.

Yang, Y., Herrup, K., 2007. Cell division in the CNS: protective response or lethal event in post-mitotic neurons? Biochim. Biophys. Acta (BBA) Mol. Basis Dis. 1772 (4), 457 466.

Yates, A., Akanni, W., Amode, M.R., Barrell, D., Billis, K., Carvalho-Silva, D., Cummins, C., Clapham, P., Fitzgerald, S., Gil, L., Girón, C.G., Gordon, L., Hourlier, T., Hunt, S.E., Janacek, S.H., Johnson, N., Juettemann, T., Keenan, S., Lavidas, I., Martin, F.J., Maurel, T., McLaren, W., Murphy, D.N., Nag, R., Nuhn, M., Parker, A., Patricio, M., Pignatelli, M., Rahtz, M., Riat, H.S., Sheppard, D., Taylor, K., Thormann, A., Vullo, A., Wilder, S.P., Zadissa, A., Birney, E., Harrow, J., Muffato, M., Perry, E., Ruffier, M., Spudich, G., Trevanion, S.J., Cunningham, F., Aken, B.L., Zerbino, D.R., Flicek, P., 2015. Ensembl 2016. Nucleic Acids Res. 44 (D1), D710 D716.

Yoshida, Y., Tsunoda, T., Doi, K., Tanaka, Y., Fujimoto, T., Machida, T., Ota, T., Koyanagi, M., Takashima, Y., Sasazuki, T., Kuroki, M., Iwasaki, A., Shirasawa, S., 2011. KRAS-mediated up-regulation of RRM2 expression is essential for the proliferation of colorectal cancer cell lines. Anticancer Res. 31 (7), 2535 2539.

<u>*CCNF* in ALS</u>

Our laboratory recently identified ALS and FTD-linked mutations in *CCNF* through a combination of genetic linkage analysis and next-generation sequencing (Williams et al., 2016). To date, 10 missense mutations in this gene have been reported in ALS cohorts, with a worldwide frequency that ranges from 0.6 to 3.3% (Williams et al., 2016). Significantly, patients who carry an ALS-linked mutation in *CCNF* have been shown to develop TDP-43 pathology (Williams et al., 2016).

ALS-linked mutations in *CCNF* have been shown to induce UPS dysfunction *in vitro*. Analysis of Neuro-2A cells transfected with mutant *CCNF* (*CCNF*^{S621G}) demonstrated an accumulation of ubiquitinated proteins, including TDP-43, and a reduction in UPS activity (Williams et al., 2016). Overexpression of *CCNF*^{S621G} in both Neuro-2A and SH-SY5Y cells has been shown to alter UPS-mediated protein ubiquitination and induce disruption of the second major proteolytic pathway - autophagy (Lee et al., 2017b). The zebrafish models presented in this thesis are the first *in vivo* models based on ALS-linked mutations in *CCNF*.

1.2.4 Sporadic ALS

Approximately 90% of ALS cases have no known family history of the disease and are classified as sporadic (SALS). Approximately 10% of these apparently sporadic cases carry a mutation in a known ALS gene, which may be a reflection of misclassification due to incomplete family history or reduced penetrance of a mutation (Iguchi et al., 2013). For the 90% of SALS cases that do not carry a known ALS-linked mutation, the cause of their disease remains unclear. It is hypothesised that a combination of genetic and environmental risk factors, rather than a single causative factor are involved in the development of disease in these patients (Simpson and Al-Chalabi, 2006). Gene variants that appear to increase susceptibility to ALS have been reported (Table 1.1) and multiple environmental factors have been proposed as risk factors for the disease. These environmental factors include smoking (Armon, 2009), exposure to heavy metals

and pesticides (reviewed in Bozzoni et al. (2016)) and exposure to a cyanotoxin, N-methylamino-L-alanine (BMAA) found in cycad seeds and cyanobacteria (blue green algae) (Bozzoni et al., 2016; Caller et al., 2012). However, no study has yet conclusively demonstrated a link between any of these environmental factors and ALS and the underling cause of the majority of SALS cases remains unclear.

1.2.5 Pathology of ALS

Despite the distinction between familial and sporadic ALS, the two forms of the disease are pathologically and clinically indistinguishable. The dominant pathological features of both FALS and SALS are the progressive loss of motor neurons in the motor cortex, corticospinal tracts, brainstem and spinal cord, and the presence of ubiquitin positive protein aggregates within the neuronal cytoplasm (Neumann et al., 2007). In over 95% of patients, these protein aggregates are immunopositive for the TDP-43 protein (Scotter et al., 2015). Patients who carry a mutation in the *SOD1* gene are an exception. These patients develop neuronal aggregates that are ubiquitin and SOD1 positive but TDP-43 negative, suggesting that different mechanisms are at play in this subset of patients (Mackenzie et al., 2007). Additional pathology that has been identified in ALS patient tissue includes eosinophilic intraneuronal inclusions (Bunina bodies) (Okamoto et al., 2008), gliosis and microglial activation (Kawamata et al., 1992; McCombe and Henderson, 2011)).

1.2.6 Pathological mechanisms of ALS

Converging pathological mechanisms

A combination of gene discovery, post mortem tissue analysis and analysis of disease models has identified multiple mechanisms that are involved in the pathogenesis of ALS. These mechanisms include aberrant protein homeostasis due to dysfunction in both the UPS and the autophagic pathways (reviewed in Webster et al. (2017)), altered RNA processing and transport (reviewed in Ling et al. (2013)), ER-golgi dysfunction (reviewed in Soo et al. (2015a)), oxidative stress (reviewed in Barber and Shaw (2010)),

disruption to nuclear-cytoplasmic transport (reviewed in Boeynaems et al. (2016), mitochondrial damage (reviewed in Bozzo et al. (2017)), excitotoxicity associated with over stimulation of glutamate receptors (reviewed in Van Den Bosch et al. (2006)), dysfunction in the DNA damage and repair mechanisms (reviewed in Coppede (2011)), defective axonal transport (reviewed in De Vos and Hafezparast (2017)) and neuroinflammation (reviewed in Hooten et al. (2015)). The key evidence implicating these mechanisms in the biology of ALS are shown in Table 1.2. Due to the role of *CCNF* in the UPS, this pathway and the evidence linking it ALS are discussed in detail in Section 1.2.6.

TABLE 1.2: Mechanisms implicated in ALS

Mechanism	Genetic evidence	Key neuropathological evidence implicating pathway in ALS
RNA processing	*TARDBP, FUS,*	Neuronal aggregates containing RNA binding proteins TDP-43 and FUS (Keller et al., 2012)
	C90rf72, ANG,	MicroRNA dysregulation in patient spinal cord (Campos-Melo et al., 2013)
	TAF1, HnRNAP2B1,	Aberrant RNA splicing in ALS patient tissue (Lin et al., 1998)
	ATNX2, MATR3	Altered RNA splicing in a *TARDBP* mouse model (Arnold et al., 2013)
	SETX,HnRNPA1	
Protein homeostasis	*CCNF, VCP*	The presence of ubiquitinated aggregates in patient neurons (Lowe, 1994)
	UBQLN2, SOD1,	Protein aggregate formation in multiple animal models of ALS (reviewed in Picher-Martel et al. (2016))
	C9orf72, ALS2,	UPS inhibition induces neurodegeneration and TDP-43 pathology *in vitro* (van Eersel et al., 2011)
	OPTN, SQSTM1	UPS inhibition induces neurodegeneration and TDP-43 pathology *in vivo* (Kabashi et al., 2012)
		Reduced expression of the 20S proteasomal subunit in post mortem spinal cord (Kabashi et al., 2012)
		Marked activation of autophagy in post mortem spinal cord (Hetz et al., 2009)
		Proteasomal inhibition induces MN degeneration, motor defects and aggregation (Kabashi et al., 2012)
		Accumulation of autophagosomes in patient spinal cord (Sasaki, 2011)
ER dysfunction	*VAPB, SIGMA1,*	Marked activation of the UPR in post mortem spinal cord (Hetz et al., 2009; Sasaki, 2010a)
	SOD1, VCP,	Upregulation of UPR chaperones in the CSF and MNs of patients (Atkin et al., 2008)
	DCTN	Elevated UPR stress sensors in *SOD1* mouse models (Atkin et al., 2006, 2008)
		ER stress, activation of the UPR stress response in *in vitro* models (Atkin et al., 2008; Saxena et al., 2009)
Endosomal trafficking	*C9orf72, ALS2,*	Loss of TDP-43 function inhibits endosomal trafficking in primary neurons (Schwenk et al., 2016)
	VAPB, OPTN	Reduced transferrin levels in serum and CSF of ALS patients (Brettschneider et al., 2008),
	CHMP	
Mitochondrial dysfunction	*SIGMA1*	Aberrant mitochondrial morphology in patient tissue (Atsumi, 1981; Sasaki, 2010b)
	CHCHD10	Aberrant mitochondrial morphology in *SOD1* mice (Wong et al., 1995; Higgins et al., 2003; Vinsant et al., 2013)
		Aberrant mitochondrial morphology in multiple animal models of ALS (reviewed in Smith et al. (2017))
		Reduced mitochondrial enzyme activity in spinal cord of *SOD1* mouse models (Jung et al., 2002)
		Reduced cellular respiration and ATP production in ALS patients and models (reviewed in Smith et al. (2017))
DNA damage and repair	*NEK1, C9orf72*	Up-regulation of markers of the DNA damage response in *C9orf72* patient neurons (Farg et al., 2017)

Continued on next page

Table 1.2 – continued from previous page

Mechanism	Genetic evidence	Key neuropathological evidence implicating pathway in ALS
Axonal transport	*DCTN1, SPG11*	Defective axonal transport in *SOD1* patient neurons (De Vos et al., 2007)
		Defective axonal transport in *SOD1* mouse models (Williamson and Cleveland, 1999; Bilsland et al., 2010)
Oxidative stress	*SOD1*	Elevated markers of oxidative damage in post mortem tissue (reviewed in Barber and Shaw (2010))
		Increased oxidative damage in *SOD1* mouse models (Andrus et al., 1998; Liu et al., 1998; Ferrante et al., 1997)
Excitotoxicity	*DAO*	Loss of the astrocytic glutamate transporter protein EAAT2 in patient tissue (Rothstein et al., 1995)
		Elevated levels of glutamate in CSF of some ALS patients (Spreux-Varoquaux et al., 2002)
		Cortical hyperexcitability precedes lower motor neuron dysfunction in ALS patients (Menon et al., 2015)
		Hyperexcitability demonstrated in *SOD1* mouse models (Thielsen et al., 2013)
Neuroinflammation		Activated microglia and infiltrating lymphocytes in patient NS (Henkel et al., 2004)
		Pro-inflammatory mediators in the CSF of patients (Kuhle et al., 2009)
		Biochemical indicators of immune response activation in bloods samples (Mantovani et al., 2009)

MN = motor neuron   UPS = ubiquitin proteasomal system   NS = nervous system   UPR = unfolded protein response

CSF = cerebral spinal fluid   ROS = reactive oxygen species

The UPS in ALS

Overview of the UPS

The UPS is responsible for the degradation of many short lived and misfolded proteins. It is a selective, energy dependent system in which specific proteins are tagged for proteasomal degradation by the addition of polyubiquitin chains. The system is comprised of three families of enzymes - E1 enzymes, of which there are two known members, E2 enzymes, of which approximately 40 members have been identified (Stewart et al., 2016) and E3 enzymes, of which there are over 600 (Iconomou and Saunders, 2016). The E1 enzymes activate ubiquitin molecules. Once activated, the ubiquitin molecules bind to the E2 ubiquitin-conjugating enzymes. E3 ubiquitin ligase complexes mediate the transfer of ubiquitin from the E2 enzyme to a target substrate. A schematic representation of the UPS and the role of cyclin F within this system is shown in Paper 1.

In some cases, the UPS attaches a single ubiquitin molecule to a substrate, but in the majority of cases, polyubiquitin chains are formed, the configuration of which determines the fate of the protein (Lecker et al., 2006). Ubiquitin carries seven lysine residue sites and the configuration of the polyubiquitin chains is determined by the site at which binding occurs (Lys6, Lys11, Lys27, Lys29, Lys33, Lys48, Lys63) (Li and Ye, 2008). Different chain configurations direct the substrate to different pathways. For example, Lys48 and Lys11 chains direct their proteins to the proteasome for degradation (Newton et al., 2008; Wickliffe et al., 2011), while Lys63 chains direct their proteins to the autophagic pathway (Ravid and Hochstrasser, 2008). Further regulation of protein fate is provided by de-ubiquitinases (DUBs) which disassemble polyubiquitin chains and remove ubiquitin from substrates (Heideker and Wertz, 2015).

An additional component of the UPS are the chaperone proteins. These proteins are responsible for identifying misfolded proteins, facilitating their recognition by the UPS and transferring Lys48 and Lys11-tagged proteins to the proteasome for degradation (Dantuma and Bott, 2014; Shiber and Ravid, 2014). Dysfunction at any point in this

highly regulated UPS system has the potential to disrupt protein homeostasis and induce pathological change.

Evidence implicating UPS dysfunction in ALS

There is strong genetic, pathological and molecular evidence implicating UPS dysfunction in the biology of ALS as summarised in Table 1.2. Genetically, ALS-linked mutations have been identified in multiple genes that have a role in this pathway, including *CCNF* and the chaperone proteins *UBQLN2* (Deng et al., 2011) and *VCP* (Johnson et al., 2010). Evidence indicates that mutations in other ALS-linked genes, including *SOD1* and *C9orf72* also induce UPS dysfunction (discussed in Section 1.3.3).

Pathologically, the presence of ubiquitinated protein aggregates within ALS patient neurons suggests UPS dysfunction is a feature of ALS (Neumann et al., 2007). Indeed, reduced proteasomal activity has been reported in post mortem spinal cord tissue of ALS patients (Kabashi et al., 2012) and experimental inhibition of the proteasome has been shown to induce ALS-like pathology both *in vitro* and *in vivo*. For example, proteasomal inhibition in primary neurons was shown to induce the formation of TDP-43 positive protein aggregates reminiscent of those found in ALS patient neurons (van Eersel et al., 2011), and inhibition of a proteasome subunit (Rp3) within mouse motor neurons was shown to induce the formation of cytoplasmic protein aggregates, motor neuron death and associated motor deficits (Tashiro et al., 2012). Unravelling UPS dysfunction in ALS has significant potential to identify possible therapeutic targets, the modification of which may restore UPS function and consequently alter disease progression.

1.2.7   Current treatments for ALS

Riluzole, a benzothiazole derivative, is currently the only drug approved to treat ALS in Australia. The mechanisms of action of riluzole remain incompletely characterised, however its effects are known to include inhibition of glutamate release, stabilisation

of inactivated sodium channels and inhibition of the effects of transmitter binding at excitatory amino acid receptors (https://pubchem.ncbi.nlm.nih.gov/). In the first human clinical trials, the drug was shown to have significant benefits with respect to both disease progression and survival (Bensimon et al., 1994). However, queries over the design, duration and statistical analysis of the clinical trial were raised following publication of the results (Rowland, 1994) and since its approval, riluzole has demonstrated limited clinical benefit, extending the lifespan of patients by an average of 2 months (Miller et al., 2002).

Edaravone was recently approved as an ALS treatment in America, however its clinical efficacy remains unclear. Edaravone is a free radical scavenger and therefore is proposed to reduce the oxidative stress that is a feature of ALS (Watanabe et al., 2004). The drug demonstrated beneficial effects in a $SOD1^{G93A}$ mouse model of ALS, significantly slowing the decline of motor function (Ito et al., 2008). However, these results failed to translate to the majority of ALS patients in a phase 2 clinical trial (Abe et al., 2014). A small subset of patients within that trial did show some benefit from edaravone treatment and consequently, a phase 3 trial was performed in which stringent selection criteria was used to select for patients within that subset (Abe et al., 2017). Edaravone was shown to have significant clinical benefit in this second trial, leading to FDA approval of the drug as a treatment for ALS. However, based on the selection criteria, less than 7% of ALS patients would have been considered eligible for the phase 3 trial, raising the question as to the value of the drug as a treatment for the majority of ALS patients. Additionally, the trial period was shorter than European Medical Agency standards and the clinical relevance of the monitoring criteria used (ALSFRS-R) has not been established (Hardiman and van den Berg, 2017).

The current therapeutic approach that has the greatest benefit to patients is supportive therapy. Respiratory and nutritional support have both been shown to improve quality of life and survival of patients (Traynor et al., 2003), while symptomatic treatment, such as physical therapy to minimise cramps and muscle spasticity aim to improve

patient comfort (reviewed in Majmudar et al. (2014)).

1.3   *In vivo* models of ALS

1.3.1   Overview

Disease gene discovery in ALS research has allowed the development of *in vivo* models
that reflect some aspects of disease pathology. These models are invaluable tools for
the mechanistic investigation of ALS-linked mutations, providing insight into disease
pathobiology. Numerous strategies have been used to develop these models, including
strategies that overexpress an ALS-linked mutant gene, silence a gene of interest or
introduce a point mutation into a gene of interest. The primary strategies used to
generate animal models and their advantages and limitations are shown in Table 1.3.
The strategies used in this project include transient overexpression through mRNA
injection (Chapter 3), constitutive overexpression of a transgene (Chapter 4) and in-
ducible overexpression of a transgene (Chapter 5). These strategies are discussed in
greater detail within each chapter.

TABLE 1.3: Common strategies used to generate animal models.

Techniques	Key advantages	Key limitations
Transient overexpression (mRNA injection)	Rapid model development	Brief expression may limit phenotype development
		Embryonic model of adult onset disease
		Ubiquitous expression only
Transient silencing (Antisense morpholinos, shRNAs)	Rapid model development	High potential for off target effects
		Embryonic model of adult onset disease
Random mutagenesis (ethyl-nitroso-urea)	Mutant gene expressed at physiologically relevant levels	Highly inefficient
Constitutive transgenic overexpression	Efficient, well established	Overexpression not physiologically accurate
	Accelerated disease course	Positional effects due to random integration
	Spatial control over gene expression	
Inducible transgenic overexpression	Spatial and temporal control of transgene expression	Overexpression not physiologically accurate
		Positional effects due to random integration
		Potential leakage of transgene expression
Genome edited gene silencing (CRISPR, TALEN, ZFN)	Permanent gene knockdown	Potential off target effects
Genome edited point mutation (CRISPR, TALEN, ZFN)	Mutant gene expressed at physiologically relevant levels	Low efficiency, off target effects, mosaicism (all improving)

1.3.2   Species used to model ALS

A range of animal species have been used to model ALS, from invertebrate models such as *Caenorhabditis elegans* (nematode worm), to non-human primates. Each species has their particular advantages and limitations, as discussed in this section and outlined in Table 1.4.

TABLE 1.4: Key species used to model human disease.

	C.elegans	*Drosophila*	Zebrafish	Rodents
% of genes with human homologues	∼38% (Shaye and Greenwald, 2011)	∼60% (Reiter and Bier, 2002)	>70% (Howe et al., 2013)	∼99% (Guenet, 2005)
Protein conservation	∼35% (Van Damme et al., 2017)	∼40% (Van Damme et al., 2017)	∼75% (Van Damme et al., 2017)	∼85% (Van Damme et al., 2017)
Age of maturity	3 days	7 days	3 months	8 weeks
Average lifespan	Short	Short	Long	Long
Efficiency of model development	High	Intermediate	Intermediate	Low
Suitability for compound screening	Yes	Yes	Yes	No
Costs	Low	Low	Intermediate	High
ALS related publications	77(Van Damme et al., 2017)	184 (Van Damme et al., 2017)	62 (Van Damme et al., 2017)	>4500 (Van Damme et al., 2017)

Caenorhabditis elegans

As models of neurological disease, *C.elegans* have the advantage of a very simple nervous system that is readily visualised *in vivo* due to their optical transparency. *C.elegans* reach maturity within 3 days, which together with low costs of housing, breeding and maintenance, allows highly efficient and cost effective generation of disease models (Markaki and Tavernarakis, 2010). However, as invertebrates, there is a large evolutionary distance between *C.elegans* and humans. Consequently, the two species share approximately 38% genetic sequence homology (Shaye and Greenwald, 2011) and some mammalian systems are not conserved, such as an active immune system (Teschendorf and Link, 2009). Nevertheless, *C.elegans* models have provided important insights into ALS biology (reviewed in Therrien and Parker (2014)) and been used extensively as a tool for preliminary testing of potential therapeutic agents (reviewed in Chen et al. (2015b)).

Drosophila melanogaster

Drosophila melanogaster provides an intermediate model between the invertebrate *C.elegans* and vertebrate species, sharing many of the advantages of both. *Drosophila* have been used in medical research for over 100 years and consequently, an extensive set of resources have been developed to genetically manipulate and study these insects. Compared to *C.elegans*, *Drosophila* have a relatively complex nervous system that has similar organisation to the mammalian brain, including the presence of a blood brain barrier (McGurk et al., 2015). Genetically, approximately 60% of human disease genes have homologs in *Drosophila* (Lloyd and Taylor, 2010) and physiologically, there is good conservation of basic signalling pathways and cellular processes between *Drosophila* and humans (Prussing et al., 2013). With regards to cost and efficiency of model development, *Drosophila* provides similar advantages to the *C.elegans* model, with their small size, high fecundity and rapid development, requiring just 10 days to

reach maturity. Due to these advantages, *Drosophila* models have been used extensively in ALS research and provided valuable insights into disease biology (reviewed in Casci and Pandey (2015)).

Zebrafish (*Danio rerio*)

Zebrafish (*Danio rerio*) provide a disease model with many of the advantages of invertebrate species with the greater complexity that has evolved in vertebrates. The complexity of the zebrafish nervous system lies between the invertebrate models and mammals, so is more comprehensible than the human system, but retains similar cell types and structure (reviewed in Babin et al. (2014); Panula et al. (2010)). In addition, zebrafish and humans share similar brain neurochemistry, including similar neurotransmitter expression, binding and signalling properties (Panula et al., 2010).

Like *C.elegans*, zebrafish embryos have the advantage of optical transparency, allowing *in vivo* live imaging, a significant advantage for studies investigating the progression of disease pathology (Lieschke and Currie, 2007). Zebrafish are closer in evolutionary distance to humans than *C.elegans* and *Drosophila* and consequently, approximately 75% of zebrafish genes have a human orthologue (Howe et al., 2013). Additional advantages of zebrafish as models of human disease include their high fertility and fecundity and their external fertilisation, which translates to an ease of genetic manipulations. These characteristics permit relatively efficient and cost effective development of disease models (Dooley and Zon, 2000; Kabashi et al., 2011b).

Mammalian species

While non-mammalian species have a significant role to play in ALS research, mammals share genetic and physiological similarities that are not reflected in non-mammalian species. For this reason, rats and mice remain the most commonly used animals in medical research (Van Damme et al., 2017). However, their greater size, lower fecundity and slower maturation rates equate to significantly higher costs of breeding and

maintenance, while their internal fertilisation complicates embryonic genetic manipulations. The high rate of inbreeding in laboratory colonies is an additional caveat of rodent models. Rodent models of ALS based on the same genetic mutation, generated in the same manner, have been shown to display significantly different phenotypes as a consequence of their different genetic backgrounds (Pfohl et al., 2015). This raises the question of how accurately rodent colonies reflect the genetics of ALS patients, despite the high homology between the human and rodent genomes (Van Damme et al., 2017).

Mammals other than rats and mice have been used to model ALS, including pigs (Yang et al., 2014) and non-human primates (Uchida et al., 2012). Models of ALS in both of these species have been shown to better replicate key pathological features of the disease, however, the significant costs and ethical concerns of using such species have limited their use as models of human disease.

1.3.3   *In vivo* models based on ALS-linked gene mutations

Key animal models and their contribution to current understanding of the biology of ALS are discussed below and summarised in Tables 1.5, 1.6, 1.7 and 1.8.

Models based on ALS-linked mutations in *SOD1*

As discussed in Section 1.2.3, the SOD1 protein is involved in the conversion of superoxide free radicals to less reactive oxygen species such as hydrogen peroxide (H_2O_2). Evidence indicates that ALS-linked mutations do not impair the ability of SOD1 to metabolise free radicals, rather these mutations appear to induce a toxic-gain of protein function. Evidence supporting this conclusion includes a study which demonstrated reduced levels of superoxide free radicals and increased levels of the products of superoxide metabolism in $SOD1^{\text{G93A}}$ transgenic mice compared to $SOD1^{\text{WT}}$ transgenic mice (Liu et al., 1999). Further supporting a toxic gain of function mechanism is the ALS-relevant phenotype that has been demonstrated in multiple mouse models that overexpress ALS-linked mutant *SOD1* (Gurney et al., 1994; Bruijn et al., 1998; Ripps

et al., 1995; Tu et al., 1996; Wang et al., 2003; Wong et al., 1995; Jonsson et al., 2006a; Zang and Cheema, 2002). While there is some variability with respect to age of onset and speed of progression, these models all reflect some of the key pathology seen in ALS patients, including motor neuron degeneration, cytoplasmic aggregation of ubiquitinated proteins, locomotor deficits progressing to paralysis and premature death. Similar phenotypes have also been demonstrated in rat (Aoki et al., 2005; Howland et al., 2002; Nagai et al., 2001), zebrafish (Lemmens et al., 2007; Ramesh et al., 2010), *Drosophila* (Watson et al., 2008) and *C.elegans* (Wang et al., 2009a; Gidalevitz et al., 2009) *SOD1* overexpression models.

As previously discussed (Section 1.2.5), the characteristic pathology seen in motor neurons of patients who carry a *SOD1* mutation differs from the pathology seen in the majority of ALS patients. *SOD1* patients develop ubiquitin positive protein aggregates that are not immunoreactive for the TDP-43 protein (Mackenzie et al., 2007). Instead, these aggregates predominately consist of misfolded SOD1, which appears to escape degradation by the UPS. Evidence from multiple *SOD1* mouse models indicates that this misfolded SOD1 not only escapes degradation by the UPS, but also inhibits the activity of the proteasome (Cheroni et al., 2009; Kabashi et al., 2004; Urushitani et al., 2002; Marino et al., 2015).

Misfolded SOD1 aggregates appear to have multiple deleterious effects in addition to inhibition of proteasomal activity. One of these effects is induction of the ER stress response, which has been demonstrated in multiple $SOD1^{G93R}$ mouse models (Saxena et al., 2009; Chen et al., 2015a; Atkin et al., 2006, 2008). Saturation of the ER stress response and its subsequent failure to clear aggregated proteins has been shown to induce cellular apoptosis (Nakagawa et al., 2000) and it is hypothesised that this process is a key mechanism of *SOD1*-linked ALS (reviewed in Jaronen et al. (2014)). Additional effects of the SOD1 aggregates include mitochondrial dysfunction, as indicated by the deposition of SOD1 aggregates on the outer mitochondrial membrane of $SOD1^{G93R}$

mice (Liu et al., 2004), and sequestration of wildtype proteins, which has been demonstrated in multiple *SOD1 in vitro* models (Okado-Matsumoto and Fridovich, 2002; Rakhit et al., 2002; Yu et al., 2014) as well as in spinal cord extracts from a $SOD1^{\text{G93A}}$ mouse model (Lu et al., 2009). Interestingly, analysis of the $SOD1^{\text{G93A}}$ mouse spinal cord demonstrated sequestration of key regulatory RNA-binding proteins within the SOD1 aggregates, suggesting dysregulation of transcription as a further mechanism of ALS-linked mutant *SOD1*.

$SOD1^{\text{G93A}}$ mouse models have been used extensively to investigate the role of non-cell autonomous mechanisms in ALS onset and progression. Ubiquitous overexpression of $SOD1^{\text{G93A}}$ has been shown to induce pathology reminiscent of that seen in ALS patients (Gurney et al., 1994). However, motor neuron specific expression of $SOD1^{\text{G93A}}$ fails to produce similar pathological changes (Pramatarova et al., 2001; Lino et al., 2002), suggesting that non-cell autonomous mechanisms play a significant role. This is supported by a study in which $SOD1^{\text{G93A}}$ was expressed in all cells except the motor neurons. This mouse model displayed delayed disease onset compared to ubiquitously expressing $SOD1^{\text{G93A}}$ mice, but a normal rate of progression following onset. Interestingly, $SOD1^{\text{G93A}}$ mice in which the mutant transgene was expressed in all cells except the microglia or the astrocytes developed disease symptoms at the same time as ubiquitously expressing $SOD1^{\text{G93A}}$ mice, but showed a significantly slower disease progression (Boillee et al., 2006; Yamanaka et al., 2008; Wang et al., 2009a). Collectively, these studies suggest that non-neuronal cells significantly influence the onset and progression of motor neuron degeneration in ALS.

TABLE 1.5: Animal models based on ALS-linked

mutations in *SOD1*

Animal	Model	Mutation	Phenotype	Reference
C.elegans	Neuronal overexpression	WT	Reduced motor function	Ogawa et al. (2015)
	Neuronal overexpression	G85R	Reduced motor function, SOD1 inclusions	Ogawa et al. (2015)
	Neuronal overexpression	C6S, C57S, C111S, C146S	No abnormalities detected	Ogawa et al. (2015)
	MN overexpression	G93A	SOD1 inclusions, defective axonal outgrowth	Li et al. (2013a)
	MN overexpression	G93A	SOD1 inclusions, defective axonal outgrowth	Wang et al. (2009a)
	Ubiquitous silencing	n/a	Increased superoxide free radicals, compensation by *sod5*	Yanase et al. (2009)
Drosophila	MN overexpression	A4V, G85R	SOD1 aggregates, progressive climbing deficits	Watson et al. (2008)
	Ubiquitous overexpression	D83S	Reduced activity, mitochondrial pathology	Bahadorani et al. (2013)
Zebrafish	Transient overexpression	A4V, G93R, G93A	MN axonopathy	Lemmens et al. (2007)
	Ubiquitous overexpression	G93A	NMJ defects, MN loss (50%)	Sakowski et al. (2012)
	Ubiquitous overexpression	G93R	NMJ defects, MN loss, motor deficits, mitochondrial pathology	Ramesh et al. (2010)
Mice	Ubiquitous overexpression	WT	Mitochondrial pathology, MN loss (20-30%)	Jaarsma et al. (2000)
	Ubiquitous overexpression	WT	SOD1 inclusions, MN loss, glial cell aggregates	Graffmo et al. (2013)
	Ubiquitous overexpression	A4V	SOD1 inclusions, MN loss	Deng et al. (2006)
	Ubiquitous overexpression	G93R	Progressive loss of motor function, MN loss	Wong et al. (1995)
	Ubiquitous overexpression	G93R	Loss of motor function, MN loss, mitochondrial degeneration	Filali et al. (2011)
	Ubiquitous overexpression	H46R	SOD1, ubiquitin inclusions, Lewy body-like inclusions	Chang-Hong et al. (2005)
	Ubiquitous overexpression	H46R, H48Q	Ubiquitin, hyaline inclusions	Wang et al. (2002)
	Ubiquitous overexpression	H46R, H48Q, H63, H120G	SOD1, ubiquitin inclusions	Wang et al. (2003)
	Point mutation	D83G	MN loss (20%)	Joyce et al. (2015)
	Ubiquitous overexpression	G85R	SOD1, ubiquitin inclusions	Bruijn et al. (1997)
	Ubiquitous overexpression	G85R	Disease course accelerated by WT overexpression	Wang et al. (2009b)
	Ubiquitous overexpression	G86R	Rapidly progressive disease course	Ripps et al. (1995)
	Ubiquitous overexpression	D90A	SOD1 inclusions, MN loss	Jonsson et al. (2006b)
	Ubiquitous overexpression	G93A	SOD1 inclusions, MN loss, early NMJ loss	Gurney et al. (1994)

Table 1.5 – continued from previous page

Animal	Model	Mutation	Phenotype	Reference
	Ubiquitous overexpression	G93A	SOD1 inclusions, MN loss, early NMJ loss	Quarta et al. (2015)
	Ubiquitous overexpression	G93A	Disease course accelerated by WT overexpression	Jaarsma et al. (2000)
	Overexpression in MNs	G93A	SOD1 aggregates	Jaarsma et al. (2008)
	Ubiquitous overexpression	L126Z	MN loss, ubiquitin inclusions	Wang et al. (2005)
	Ubiquitous overexpression	L126Z	MN loss, ubiquitin inclusions	Deng et al. (2006)
	Ubiquitous overexpression	G127X	SOD1, ubiquitin inclusions, rapid disease course	Jonsson et al. (2004)
	Ubiquitous overexpression	G93A	ER stress, motor dysfunction	Tobisawa et al. (2003)
	Ubiquitous silencing	n/a	Reduced motor performance, no MN loss	Flood et al. (1999)
	Ubiquitous silencing	n/a	Oxidative stress, muscular atrophy	Muller et al. (2006)
	Ubiquitous silencing	n/a	Oxidative stress, axonal degeneration	Fischer and Glass (2010)
Rats	Ubiquitous overexpression	H46R	SOD1, ubiquitin inclusions, MN loss, Lewy body-like inclusions	Nagai et al. (2001)
	Ubiquitous overexpression	G93A	SOD1, ubiquitin inclusions, MN loss	Nagai et al. (2001)
	Ubiquitous overexpression	G93A	SOD1, ubiquitin inclusions, MN loss	Howland et al. (2002)
Dogs	Naturally occurring mutation	T18S	SOD1 aggregates, impaired motor function, no neuronal loss	Wininger et al. (2011)
	Naturally occurring mutation	E40K	SOD1 aggregates, impaired motor function	Awano et al. (2009)
Pigs	Ubiquitous overexpression	G93A	SOD1, ubiquitin inclusions, MN loss, motor deficits	Yang et al. (2014)

MN = motor neurons   NMJ = neuromuscular junction   ER = endoplasmic reticulum

Models based on ALS-linked mutations in *TARDBP*

TDP-43 is an RNA binding protein that is ubiquitously expressed and primarily localised to the nucleus (Sephton et al., 2012). In over 95% of ALS patients, TDP-43 mislocalises from the nucleus to the cytoplasm of affected neurons, where it aggregates to form a component of the ubiquitinated inclusions characteristic of ALS pathology (Neumann et al., 2007). This pathology suggests that cytoplasmic mislocalisation of TDP-43 plays a pathogenic role in the majority of ALS cases. Indeed, experimental manipulation to induce mislocalisation of wildtype TDP-43 has been shown to be sufficient to produce an ALS-like phenotype in animal models. Two transgenic mouse models that overexpressed a *TARDBP* transgene that carried a disrupted nuclear localisation sequence (ΔNLS) have been reported. The first of these studies expressed *TARDBP*$^{\Delta\text{NLS}}$ selectively in the forebrain, which was found to induce neuronal loss, corticospinal tract degeneration and muscular spasticity (Igaz et al., 2011). The second model conditionally expressed *TARDBP*$^{\Delta\text{NLS}}$ in the brain and spinal cord of the mouse (Walker et al., 2015). This model demonstrated a progressive disease course, characterised by defects at the neuromuscular junction followed by motor neuron loss, muscle atrophy and impaired motor function (Walker et al., 2015).

Two mechanisms potentially underlie this apparent toxicity of TDP-43 mislocalisation. Firstly, the loss of nuclear TDP-43 may lead to a loss of its nuclear functions (RNA metabolism), secondly, the accumulation of TDP-43 in the cytoplasm may lead to a toxic gain of function. Animal models support the notion that ALS-linked mutations in *TARDBP* have both a loss and a gain of function effect. For example, loss of function through the selective silencing of *TARDBP* in the spinal cord of mice (Wu et al., 2012b; Iguchi et al., 2013) and ubiquitous silencing of *TARDBP* in the zebrafish (Schmid et al., 2013) has been shown to induce progressive motor dysfunction in both species. Conversely, overexpression of mutant *TARDBP* in numerous animal models has been shown to induce expression-dependant neurodegeneration (Table 1.6).

TABLE 1.6: Animal models based on ALS-linked mutations

in *TARDBP*

Animal	Model	Mutation	Phenotype	Reference
C.elegans	Pan neuronal overexpression	WT	Impaired movement	Ash et al. (2010)
	Pan neuronal overexpression	G290A, A315T, M337V	Reduced motor function (WT < Mutants)	Liachko et al. (2010)
	Neuronal overexpression	A315T	TDP-43 mislocalisation, MN loss, paralysis (WT< Mutant)	Vaccaro et al. (2012)
Drosophila	MN overexpression	WT	TDP-43 inclusions, MN loss, motor deficits	Li et al. (2010)
	MN overexpression	WT	Motor deficits, defects at NMJ, cytoplasmic inclusions	Lin et al. (2011)
	MN overexpression	F147L, G287S, A315T, G348C, A382T, ΔNLS	Progressive motor deficits, MN loss (WT< Mutant)	Voigt et al. (2010)
	MN overexpression	WT	Motor deficits, MN loss	Cheng et al. (2015)
	MN overexpression	WT	motor dysfunction and reduced life span	Hanson et al. (2010)
Zebrafish	Transient overexpression	A315T, G348C,A382T	Motor deficits, decreased axonal length (WT< Mutant)	Kabashi et al. (2010)
	Transient overexpression	A315T	Decreased axonal length	Laird et al. (2010)
	Transient silencing	n/a	Axonopathy and muscle degeneration	Schmid et al. (2013)
	Transient silencing	n/a	Axonopathy and motor dysfunction	Kabashi et al. (2010)
Mice	Neuronal overexpression	WT	Cytosolic ubiquitin accumulation, axonal degeneration	Xu et al. (2010)
	Neuronal overexpression	WT	MN loss, rapid disease progression	Wils et al. (2010)
	Neuronal overexpression	WT	Mitochondrial aggregation	Shan et al. (2010)
	Neuronal overexpression	WT	MN loss, brain atrophy	Igaz et al. (2011)
	Ubiquitous overexpression	WT	Motor deficits, no paralysis	Swarup et al. (2011)
	Neuronal overexpression	WT	TDP-43, ubiquitin inclusions, motor deficits	Tsai et al. (2010)
	Panneuronal overexpression	A315T	Muscle atrophy, paralysis	Stallings et al. (2010)
	Panneuronal overexpression	A315T	Ubiquitin inclusions, MN loss	Wegorzewska et al. (2009)
	Ubiquitous overexpression	A315T	TDP-43, ubiquitin inclusions, motor deficits	Swarup et al. (2011)
	Ubiquitous overexpression	A315T	mitochondrial dysfunction, TDP-43 inclusions, MN loss	Stribl et al. (2014)
	Neuronal overexpression	Q331K	Reduced motor function	Arnold et al. (2013)
	Neuronal overexpression	Q331K	TDP-43, ubiquitin inclusions, MN loss	Mitchell et al. (2015)

Table 1.6 – continued from previous page

Animal	Model	Mutation	Phenotype	Reference
	Neuronal overexpression	M337V	TDP-43 inclusions	Xu et al. (2011)
	Neuronal overexpression	M337V	Motor deficits	Arnold et al. (2013)
	Neuronal overexpression	M337V	TDP-43, ubiquitin inclusions, motor deficits	Janssens et al. (2013)
	Ubiquitous overexpression	G348C	TDP-43, ubiquitin inclusions, motor deficits	Swarup et al. (2011)
	Ubiquitous overexpression	M337V	M337V induced early death, WT moderate neuronal death	Tian et al. (2011)
	Neuronal overexpression	ΔNLS	motor neuron loss, progressive motor dysfunction	Walker et al. (2015)
	Neuronal overexpression	ΔNLS	neuronal loss, corticospinal tract degeneration	Igaz et al. (2011)
	Silencing in the spinal cord	n/a	Progressive motor dysfunction	Wu et al. (2012b)
	Silencing in the spinal cord	n/a	Progressive motor dysfunction	Iguchi et al. (2013)
Rats	Ubiquitous overexpression	M337 inducible (day 4)	MN loss, TDP-43 staining	Zhou et al. (2010)
	MN, neuronal, muscle overexpression	M337 inducible	Paralysis, MN loss	Huang et al. (2012)
	Astrocytic overexpression	M337 inducible (day 40)	MN loss, muscle atrophy	Tong et al. (2013)

MN = motor neurons   NMJ = neuromuscular junction

In addition to indicating a concomitant loss and gain of function mechanism of *TARDBP* mutations, animal models have provided insight into the pathways disrupted by these mutations. For example, ER stress has been shown to be a feature of the *TARDBP*^A315T transgenic mouse (Walker and Atkin, 2011), and mitochondrial dysfunction has been demonstrated in mouse models that overexpress wildtype *TARDBP* (Shan et al., 2010; Xu et al., 2010).

The role of the TDP-43 positive aggregates in disease progression remains elusive. Like the SOD1 aggregates, sequestration of wildtype proteins within the TDP-43 positive aggregates is hypothesised to play a role in the pathology of ALS-linked mutant *TARDBP* (reviewed in Wegorzewska and Baloh (2011)). However, established *TARDBP* rodent models rarely develop aggregates that are immunopositive for TDP-43 (Wils et al., 2010; Stallings et al., 2010; Xu et al., 2010; Wegorzewska and Baloh, 2011; Shan et al., 2010), potentially suggesting that TDP-43 aggregates are not required for TDP-43-associated neurodegeneration.

Interestingly, two separate rodent studies have suggested that the symptoms associated with expression of mutant *TARDBP* are to some extent reversible. The first of these studies was a *TARDBP*^M337V inducible rat model. Overexpression of *TARDBP*^M337V led to motor neuron loss and impaired motor function. However, significant functional recovery was observed following silencing of transgenic expression (Huang et al., 2012). The second study utilised an inducible *TARDBP*^ΔNLS mouse model, characterised by pronounced motor neuron loss and progressive motor dysfunction (Walker et al., 2015). This model also demonstrated significant functional recovery upon silencing of the mutant transgene (Walker et al., 2015).

Models based on ALS-linked mutations in *FUS*

FUS shares many similarities with TDP-43. It is a predominately nuclear, ubiquitously expressed RNA binding protein (Zinszner et al., 1997). Given these similarities, ALS-linked mutations in *TARDBP* and *FUS* are hypothesised to share similar mechanisms of action. This hypothesis is supported by complementary studies in zebrafish (Kabashi et al., 2011a) and *Drosophila* (Wang et al., 2011), which indicated that TDP-43 and FUS act in the same functional pathway, with FUS acting downstream of TDP-43. Both studies used models that suppressed FUS or TDP-43 expression. Reduced expression of either FUS or TDP-43 in zebrafish induced an axonopathy and motor dysfunction, while similar suppression in *Drosophila* resulted in impaired locomotion and reduced lifespan. In both studies, overexpression of FUS was shown to rescue the phenotype of the TDP-43 knockdown model. However, TDP-43 was unable to rescue the phenotype associated with suppression of FUS expression (Kabashi et al., 2011a; Wang et al., 2011). Interestingly, the zebrafish study also demonstrated that pathology induced by silencing SOD1 expression was unable to be rescued by either FUS or TDP-43, and that SOD1 was unable to rescue the pathology induced by silencing either of the RNA binding proteins. These findings suggest that *SOD1* mutations function via a separate pathological pathway to the *TARDBP* and *FUS* mutations (Kabashi et al., 2011a).

Like TDP-43, cytoplasmic mislocalisation and aggregate formation is a feature of the pathology of ALS-linked mutant FUS. FUS mislocalisation has been shown to have toxic effects in *Drosophila* (Lanson et al., 2011) and mouse models (Shelkovnikova et al., 2013). Lanson et al. (2011) demonstrated that overexpression of FUS^{R518K} in the motor neurons of *Drosophila* induced cytosolic accumulation of the FUS protein, progressive motor neuron loss and impaired motor function (Lanson et al., 2011). Reduction of the cytosolic expression of FUS^{R518K} in this model, through silencing of the nuclear export signal of the transgene, significantly reduced the observed toxic effects (Lanson et al., 2011). Shelkovnikova et al. (2013) developed a mouse model that expressed a FUS transgene in which the NLS and RNA binding motifs were disrupted

(FUS$^{\Delta\text{NLS}}$). This model demonstrated cytoplasmic accumulation and aggregation of the protein, neuroinflammation and neuronal death. Additional FUS-based models in *C.elegans* (Murakami et al., 2012) and the mouse (Sharma et al., 2016) support this apparent toxicity of FUS mislocalisation. Both studies demonstrated that overexpression of ALS-linked mutations in this gene (*FUS*$^{\text{R522G}}$ and *FUS*$^{\text{P525L}}$) induced cytoplasmic mislocalisation, which was associated with progressive motor dysfunction.

As with TDP-43, the cytoplasmic mislocalisation of FUS suggests both a loss and a gain of function mechanism of ALS-linked mutations in *FUS*. Evidence supporting a toxic gain of function includes the multiple animal models that develop an ALS-relevant phenotype associated with overexpression of the mutant protein (Table 1.7). Loss of expression models have proven more difficult to establish due to embryonic lethality that results from silencing *FUS* expression (Hicks et al., 2000) and those that have been reported provide conflicting results. Inducible silencing of *FUS* in the post-natal mouse failed to induce detectable motor neuron degeneration or changes at the neuro-muscular junction (Kino et al., 2015; Sharma et al., 2016). In contrast, zebrafish and *Drosophila FUS* knockdown models did demonstrate impaired motor activity (Armstrong and Drapeau, 2013; Wang et al., 2011) and reduced survival (Wang et al., 2011). Each of these studies used a different technique to suppress *FUS* expression, which may explain the disparity between the models. It is also feasible that extension of the mice studies beyond one year of age may have identified a late onset ALS-relevant phenotype.

TABLE 1.7: Animal models based on ALS-linked mutations in *FUS*.

Animal	Model	Mutation	Phenotype	Reference
C.elegans	Panneuronal overexpression	Multiple	Neuronal cytosolic inclusions	Murakami et al. (2012)
	Overexpression in GABAergic neurons	S57Δ	progressive paralysis, MN degeneration	Vaccaro et al. (2012)
Drosophila	Overexpression in GABAergic neurons	R524S, P525L	Reduced motor function, NMJ defects	Chen et al. (2011)
	Overexpression in GABAergic neurons	R518K, R521C, R521H	Impaired motor function, FUS mislocalisation	Lanson et al. (2011)
	Transient suppression	n/a	Reduced survival	Wang et al. (2011)
Zebrafish	Transient overexpression	R521C, R521H, S57Δ	Impaired motor function, NMJ defects	Kabashi et al. (2011a)
	Transient overexpression	R521C	Impaired motor function, NMJ defects	Armstrong and Drapeau (2013)
	Transient suppression	n/a	Impaired motor function, NMJ defects	Armstrong and Drapeau (2013)
Mice	Overexpression under prion promoter	WT	FUS mislocalisation, NMJ defects, MN loss	Mitchell et al. (2013)
	Ubiquitous overexpression	R521G	Impaired motor function, NMJ defects	Sephton et al. (2014)
	Overexpression	R521C, P525L	NMJ defects, progressive MN loss	Sharma et al. (2016)
	Neuronal overexpression	ΔNLS	FUS aggregate formation, MN death	Shelkovnikova et al. (2013)
	Inducible knockout	n/s	Postnatal induction has no effect on MNs	Sharma et al. (2016)
	Knockdown	n/a	No ALS relevant phenotype	Kino et al. (2015)
Rats	Inducible overexpression	R521C	MN loss, NMJ defects, aggregates	Huang et al. (2011)

MN = motor neurons   NMJ = neuromuscular junction

Models based on the *C9orf72* repeat expansion

Patients who carry a *C9orf72* repeat expansion mutation develop TDP-43 pathology in affected neurons. They also develop two additional pathological characteristics – nuclear RNA foci (Mendez and Sattler, 2015) and aggregates that consist of dipeptide repeat proteins (DPRs) (Mori et al., 2013). Transcription from the expanded repeat sequence occurs in the absence of an ATG start codon, a process known as repeat associated non-ATG (RAN) translation. RNA foci form from the extended RNA sequences transcribed from the *C9orf72* expansion and evidence from animal models indicates that these foci have multiple deleterious effects. For example, a zebrafish model that expressed 72 copies of the repeat sequence demonstrated that the RNA foci sequestered wildtype proteins in a similar manner to SOD1 and TDP-43 aggregates. Multiple RNA binding proteins were shown to be sequestered within the foci in the model, suggesting dysregulation of transcription as a mechanism of *C9orf72*-associated ALS (Lee et al., 2013). A *Drosophila* model indicated that the RNA foci also affect nuclear-cytosolic transport (Zhang et al., 2015a). This model, which carried 58 copies of the repeat sequence, demonstrated that the RNA foci bind to the nuclear pore proteins, thereby impeding transport (Zhang et al., 2015a). *In vitro* models have provided further insight into the deleterious effects of the RNA foci. Impaired mitochondrial function, induction of oxidative stress and DNA damage have been demonstrated in induced pluripotent stem cell-derived motor neurons (Lopez-Gonzalez et al., 2016), and binding of the RNA foci to the proteasome and subsequent inhibition of its activity has been demonstrated in primary rat spinal cord neurons (Gupta et al., 2017).

The second unique pathological feature of *C9orf72* patients are the DPR aggregates. RAN translation occurs in all three reading frames in both the sense and antisense direction, generating six dipeptide repeat proteins, all of which are highly aggregation-prone (Mori et al., 2013). Evidence from animal models indicates that the formation of DPR aggregates alone is sufficient to induce toxicity. This evidence includes a mouse model in which one of the DPRs - Poly-Gly-Ala (PolyGA), was overexpressed. This

overexpression lead to aggregate formation, neurodegeneration and behavioural abnormalities (Zhang et al., 2016). This study further demonstrated that the PolyGA aggregates formed in the model sequestered wildtype proteins involved in the UPS, thereby inhibiting UPS mediated protein degradation (Zhang et al., 2016). Further evidence supporting a toxicity of the DRPs has been provided by *Drosophila* (Mizielinska et al., 2014; Wen et al., 2014) and zebrafish models (Ohki et al., 2017). Model in both species also demonstrated neuronal toxicity associated with expression of a DPR (polyGA or polyPA).

In addition to the toxicity of RNA foci and DRPs, a loss of *C9orf72* function has been associated with the repeat expansion. Reduced expression of *C9orf72* has been shown in *C9orf72* patient tissue (DeJesus-Hernandez et al., 2011; Ciura et al., 2013; Waite et al., 2014). Additionally, zebrafish (Ciura et al., 2013) and *C.elegans* (Therrien et al., 2013) loss of expression models have both been shown to develop neurodegenerative changes. However, these findings failed to be replicated in a second zebrafish model (Schmid, Hruscha, Haass, unpublished) or in multiple mouse models (Lagier-Tourenne et al., 2013; Koppers et al., 2015; Atanasio et al., 2016; Burberry et al., 2016; Ji et al., 2017). One mouse study did demonstrate a reduced lifespan of both homozygote and heterozygote *C9orf72* knockout mice, however no motor phenotype or other ALS-relevant pathology was identified in the models (Ugolino et al., 2016). The models did however demonstrate an upregulation of autophagy, which lead the authors to propose a functional role of *C9orf72* in this pathway and consequently, a potential mechanism of autophagic dysfunction in the pathogenesis of the *C9orf72* mutation.

Multiple animal models have been developed that overexpress the *C9orf72* repeat expansion mutation with the aim of investigating a potential gain of function mechanism of the mutation. These models and the phenotype that they display are shown in Table 1.8.

TABLE 1.8: Animal models based on ALS-linked mutations in *C9orf72*.

Animal	Model	Phenotype	Reference
C.elegans	Transient knockdown	MN loss and paralysis	Therrien et al. (2013)
Drosophila	Expression of <103 repeats in the CNS	RNA foci and DPR	Mizielinska et al. (2014)
	Expression of 160 repeats	RNA foci and DPR	Tran et al. (2015)
	Expression of 30 repeats in glutamatergic neurons	Reduced motor function	Xu et al. (2013)
	Expression of 500 repeats in glutamatergic neurons	Reduced motor function, DPR	Freibaum et al. (2015)
Zebrafish	Transient knockdown	Aberrant MNs, reduced motor function	Ciura et al. (2013)
	Overexpression of a dipeptide repeat	Generalised toxicity	Ohki et al. (2017)
	Mosaic expression of 38 and 72 repeats	RNA foci, neurotoxicity, protein sequestration	Lee et al. (2013)
Mice	Expression of 66 repeats in the CNS	RNA foci, DPR, TDP-43 +ve aggregates, reduced motor function	Chew et al. (2015)
	Expression of 450 repeats	RNA foci, DPR	Jiang et al. (2016)
	Knockout	No ALS-relevant phenotype	Jiang et al. (2016)
	Expression of 500 repeats	RNA foci, DPR	Peters et al. (2015)
	Expression of 500 repeats	RNA foci, DPR, motor neuron loss	Liu et al. (2016)
	Expression of 100-100 repeats	RNA foci, DPR	O'Rourke et al. (2015)

MN = motor neurons   DPR = dipeptide repeat proteins   CNS = central nervous system

1.3.4   Limitations of disease models

No animal model adequately mimics all of the pathological aspects of ALS. For example, a commonly used mouse model of ALS, based on the $TARDBP^{\text{A315T}}$ mutation, develops motor deficits but fails to develop TDP-43 pathology and dies from gastrointestinal dysfunction rather than complications arising from motor neuron degeneration (Hatzipetros et al., 2014). This inability of animal models to reflect all aspects of ALS pathology is likely to be a consequence of multiple factors, key amongst them being species differences and limitations of the strategies currently available to generate the models.

The significance of species differences is illustrated by a comparison of ALS models based on $SOD1$ mutations. The $SOD1^{\text{G93A}}$ pig model has been shown to demonstrate ALS-relevant pathological changes, such as the formation of nuclear inclusions, and SOD1 protein interactions that are not replicated in models in other species (Yang et al., 2014). This suggests that species-specific targets may be significant to the development of some ALS-associated pathological changes (Yang et al., 2014).

The advantages and limitations of the strategies available to generate animal models are shown in Table 1.3. A limitation that is common to all current animal models, regardless of the strategy used to generate them, is that they aim to reflect a complex, multi-factorial disease by expressing or silencing a single ALS-linked gene mutation in an animal that is housed under standard laboratory conditions. In addition to the known ALS-linked genes (Table 1.1), disease-modifying gene variants (reviewed in Lamar and McNally (2014)), epigenetic factors (reviewed in Belzil et al. (2016)) and environmental factors (reviewed in Cannon and Greenamyre (2011)) are believed to have a significant impact on the development and progression of ALS. Indeed, these disease modifiers are hypothesised to account for the substantial phenotypic variability and irregular disease penetrance observed among carriers of the same ALS-linked gene mutation (Xi et al., 2014). Inbred models that are based on a single gene mutation and maintained under stringent environmental conditions cannot recapitulate the genetic,

epigenetic and environmental interactions involved in ALS.

The $SOD1^{\text{G93A}}$ mouse is the model that has been most widely used in preclinical therapeutic testing for ALS (Philips and Rothstein, 2015). The limitations of this model are made evident by the failure, thus far, of candidate therapeutics that show promise in preclinical trials to translate to patient trials. To date there have been over 50 publications describing therapeutic agents that extend the lifespan of the $SOD1^{\text{G93A}}$ mouse, however none of these drugs have shown significant benefits in human patients (Zwiegers and Shaw, 2015). This failure of translation appears to be due to a combination of factors, key amongst them being the use of the $SOD1^{\text{G93A}}$ mouse in isolation. As discussed previously, no model, the $SOD1^{\text{G93A}}$ mouse included, is capable of accurately reflecting all aspects of ALS. Therefore, studies need to utilise multiple models to identify pathologic features and therapeutic responses that are consistent both across species and across models based on different ALS-linked genes. An additional caveat that is specific to *SOD1*-based models, is that neither *SOD1* patients, nor *SOD1* models demonstrate the TDP-43 pathology seen in over 95% of ALS patients (discussed in Section 1.3.3). In addition, most ALS patients do not develop SOD1 pathology. Therefore, *SOD1*-based models may not accurately represent wider ALS.

In addition to the use of multiple models in therapeutic trials, an adherence to stringent guidelines for preclinical testing is critical. In 2008, the ALS Therapy Development Institute (ALS-TDI) retested over 70 compounds reported to have beneficial effects in the $SOD1^{\text{G93A}}$ mouse. The ALS TDI was unable to replicate any of the positive data. Flawed study design and biological noise were identified as the primary reasons for the original, positive findings (Scott et al., 2008). This study highlights the need for stringent guidelines of animal studies to avoid the time and monetary costs associated with taking poor drug candidates to clinical trial.

The limitations of animal models must be recognised. However, by using multiple models that reflect different aspects of the disease, and using these models to answer

specific questions, animal models can, and do, provide valuable insights into the biological mechanisms involved in disease and provide essential tools for preclinical testing to examine the safety and efficacy of potential therapeutics.

1.4   Aims and significance of this project

ALS is an adult onset disease. However, ALS-linked mutations, such as those in *CCNF* are expressed throughout life. This project therefore aimed to develop multiple *CCNF*-based models, to allow investigative studies into both developmental and adult onset aspects of ALS. The advantages of the zebrafish as outlined in Section 1.3.2, permits time and cost effective testing of multiple transgenic strategies to identify those that develop viable disease models. This project utilised those advantages to investigate multiple strategies to establish *CCNF*-based zebrafish models suitable for investigative studies and for use in preclinical trials. The role of cyclin F in regulating protein degradation through the UPS and findings from *in vitro CCNF* studies suggests that these *CCNF* zebrafish will provide a useful tool with which to investigate the mechanisms of disrupted protein degradation in ALS, a pathway that is strongly implicated in the pathogenesis of the disease. A significant advantage of *CCNF*-based models is that patients who carry a *CCNF* mutation develop the TDP-43 pathology seen in the majority of ALS patients (Williams et al., 2016). Therefore, unravelling the mechanisms of ALS-linked mutant *CCNF* has great potential to further our understanding of the biology of wider ALS. A greater understanding of disease biology will lead to the identification of potential therapeutic drug targets and disease biomarkers.

Specifically, the aims of the project were:

1. To characterise zebrafish *ccnf* to determine the suitability of the species to model ALS-linked mutations in the gene.

2. To develop and characterise an embryonic zebrafish model of ALS that transiently expresses mutant *CCNF*, as a tool for rapid discovery, analysis and preliminary testing of potential therapeutics.

3. To identify a strategy that allowed the development of suitable *CCNF* transgenic zebrafish for longitudinal studies of ALS biology in an adult animal.

1.5 Structure of this thesis

Aims one and two are addressed in Chapter 3 of this thesis. The characterisation of the zebrafish *ccnf* orthologue and the development of the transient *CCNF* zebrafish models are detailed in a paper published in *Human Molecular Genetics* (Paper 2). Aim three is addressed in Chapters 4 and 5. Chapter 4 details the efforts to establish transgenic zebrafish lines that constitutively overexpress *CCNF*. The key findings from this study are described in a paper which has been accepted for publication in *Science Matters* (Paper 3). Chapter 5 details the development and characterisation of transgenic lines that inducibly overexpress *CCNF*. The key findings from his study are described in a manuscript which has been prepared for submission to *Disease Models and Mechanisms* (Manuscript 1).

2

Methods

2.1 Introduction to this chapter

This chapter details the general methods used throughout this project. The Tol2 Multisite Gateway cloning system Kwan et al. (2007) was used to generate the *CCNF* expression constructs. The principles of this system and the molecular methods used to generate the constructs are described in Section 2.2.1, followed by the zebrafish husbandry protocols used in the laboratory and the general methods used to study the zebrafish. Methods used for different stages of the project are described in Chapter Specific Methods, Sections 3.2, 4.2 and 5.2. Recipes for buffers and solutions are shown in Appendix A.2.

2.2   Molecular Methods

2.2.1   Cloning - the Tol2 Gateway system

The Tol2 Multisite Gateway Three-Fragment Vector Construction kit (Life Technologies) was used to develop the expression constructs required for the generation of the *CCNF* transgenic zebrafish (Chapter 4 and Chapter 5). This system uses two recombination reactions to generate the expression constructs. The first, termed the BP reaction, inserts the cDNA of interest (promoter, fluorophore or gene) into an entry clone. The second, the LR reaction, combines three entry clones (5', middle and 3' entry clones) into a single expression plasmid. Both reactions take advantage of specific recombination sites, denoted *att* sites, to mediate the order and orientation of the recombination reactions. The principles of these reactions are detailed in this section.

BP reactions

BP reactions generate 5' entry clones, middle entry clones and 3' entry clones. Each carry specific *att* sites. The principles of the BP reactions are shown in Figure 2.1. The majority of entry clones used in this project had previously been generated (Table 2.1). However, BP reactions were required to generate 3' entry clones that carried *CCNF*. Four *CCNF* entry clones were generated:

1. Human wildtype *CCNF* - $CCNF^{\mathrm{WT}}$

2. Human *CCNF* that carried an ALS-linked mutation - $CCNF^{\mathrm{S621G}}$

3. Zebrafish wildtype *ccnf* - $ccnf^{\mathrm{WT}}$

4. Zebrafish *ccnf* that carried the equivalent ALS-linked mutation - $ccnf^{\mathrm{S623G}}$.

The 3' entry vector into which the *CCNF* sequences were inserted by the
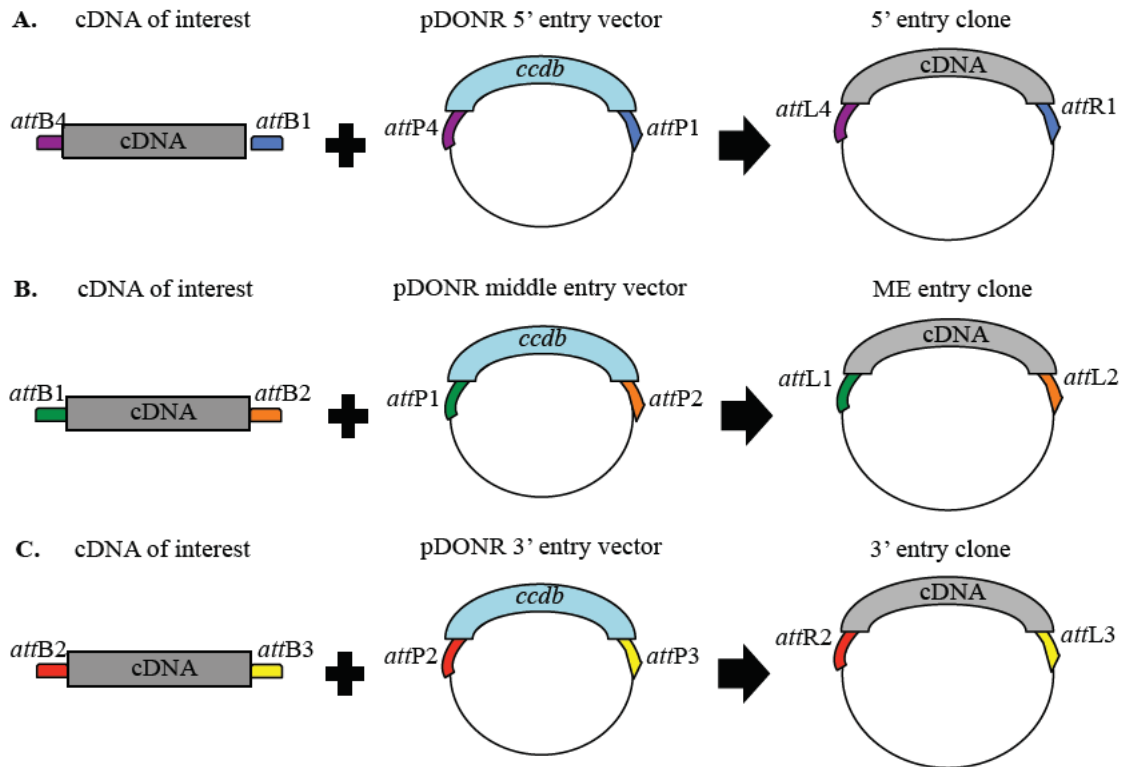
FIGURE 2.1: **BP recombination reactions used to generate Tol2 entry clones. A.** BP reaction used to generate 5' entry vectors using complementary *att*B4-P4 and *att*B1-P1 sites. **B.** BP reactions used to generate middle entry (ME) vectors using complementary *att*B1-P1 and *att*B2-P2 sites. **C.** BP reactions used to generate 3' entry vectors using complementary *att*B2-P2 and *att*B3-P3 sites. Figure adapted from (Kwan et al., 2007).

BP reaction was provided in the Tol2 kit (Life Technologies) and the *att*-flanked *CCNF* sequences were synthesised by GeneArt (ThermoFisher Scientific). Due to the relatively high cytosine (C) and guanine (G) content of *CCNF* (57.3%), codon optimisation was required to allow synthesis of the gene. Codon optimisation was performed using the GeneArt GeneOptimizer software (https://www.thermofisher.com/au/en/home/life-science/cloning/gene-synthesis/geneart-gene-synthesis/geneoptimizer.html). This software substituted a C/G nucleotide with an adenine (A) or a thymine (T) where doing so did not alter the amino acid sequence of the protein. The optimised *CCNF* sequence shared 81% nucleotide identity to *CCNF*, but 100% amino acid identity. The optimised *ccnf* sequence shared 78% nucleotide identity with the zebrafish orthologue, but 100%

TABLE 2.1: Entry clones used in this project

Vector type	Vector	Reference/ Source
5' vectors	p5E:*actb2*	(Higashijima et al., 1997)
	p5E:-*3mnx1*	(Morsch et al., 2015)
	p5E:TRE	(Campbell et al., 2012)
Middle Entry Vectors	pME:mCherry	Chien laboratory
	pME:EGFP	(Campbell et al., 2012)
	pME:rtTA	(Campbell et al., 2012)
3' vectors	P3E:*CCNF*^{WT}	BP reactions (GeneArt)
	P3E:*CCNF*^{S621G}	BP reactions (GeneArt)
	P3E:*ccnf*^{WT}	BP reactions (GeneArt)
	P3E:*ccnf*^{S623G}	BP reactions (GeneArt)
	p3E:pA	Chien laboratory
Destination vectors	Tol2:PA2	Chien laboratory
	Tol2:CG2	Chien laboratory
	Tol2:FusionRed	GeneArt

amino acid identity.

The BP reactions used to generate the *CCNF* 3' entry clones consisted of 50 fmoles of the *CCNF* cDNA, 150 ng of the 3' entry vector (Life Technologies), 2 µl of BP clonase enzyme mix (Life Technologies) and 1 X TE buffer (pH 8, Thermofisher Scientific) to a final volume of 10 µl. Reactions were assembled at room temperature and incubated at 25 °C for two hours. Constructs generated from this reaction were transformed, purified and validated as detailed in Sections 2.2.2 and 2.2.3. Validated constructs were used in the subsequent LR reactions.

LR reactions

The LR reactions recombined 5', middle entry and 3' entry clones into a destination vector. The destination vector carried a Tol2 transposable element, used to increase the efficiency of transgenic insertion into the genome (discussed in Chapter 4, Section 4.1.3). The principles of this reaction are shown in Figure 2.2 Kwan et al. (2007). Specific LR reactions used for each component of the project are shown in chapter specific methods.
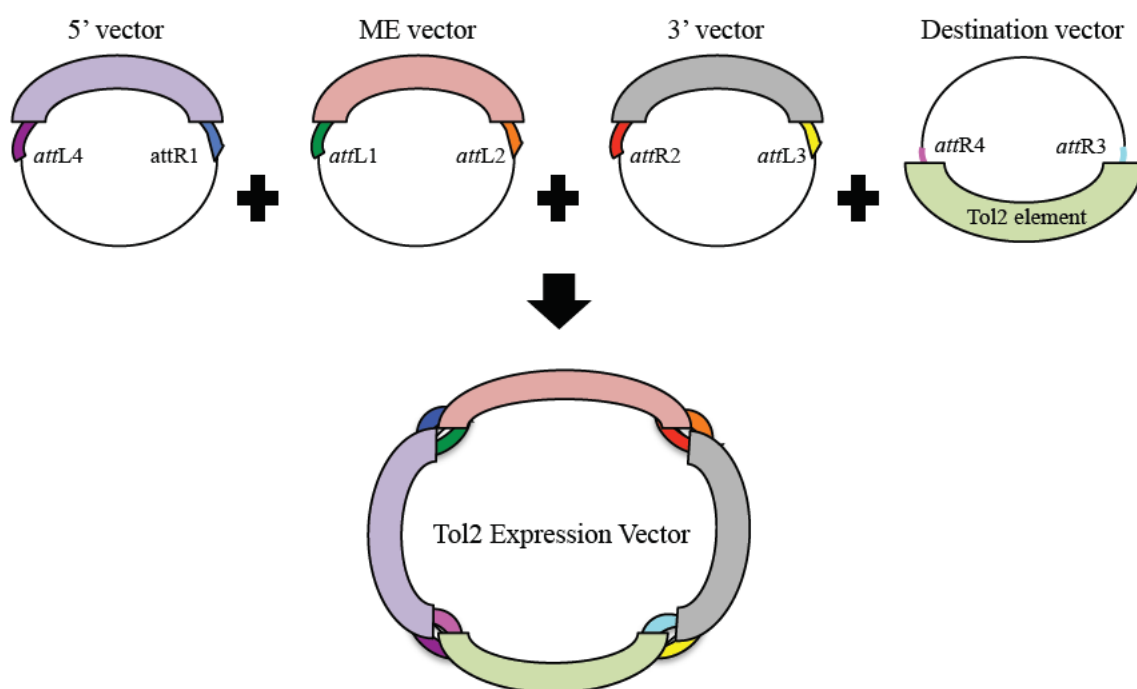
FIGURE 2.2: **LR recombination reactions used to generate Tol2 expression vectors.** LR reactions recombine three entry vectors with a Tol2 backbone vector using complementary *att* sites. Figure adapted from (Kwan et al., 2007).

LR reactions were assembled on ice and consisted of 10 fmoles of the 5' entry clone, 10 fmoles of the middle entry clone, 10 fmoles of the 3' entry clone, 20 fmoles of the destination vector, 2 µl LR clonase enzyme mix (Life Technologies) and 1 X TE buffer (pH 8, Thermofisher Scientific) to a final volume of 10 µl. The reaction was incubated at 25 °C for 24 hours, following which, 1 µl Proteinase K (20mg/ml, Life Technologies) was added to the reaction, and incubated for 10 minutes at 37 °C.

2.2.2 Transformations

Constructs generated through Tol2 cloning were transformed into Alpha-Select Gold
efficiency competent cells (Bioline) according to manufacturer instructions. Briefly, 2
µl of the BP or LR recombination reaction was gently mixed with 50 µl of competent
cells and cooled on ice for 30 minutes. Cells were heat shocked at 42 °C for 30 seconds,
then immediately returned to ice for 10 minutes. Two-hundred and fifty microliters
of S.O.C. medium (Life technologies) was added to the heat-shocked cells, and the
mixture incubated at 37 °C with shaking at 200 rpm. For transformations using the
BP reaction product, this incubation was performed for 1 hour, for transformations
using the LR reaction incubation time was extended to 1.5 hours.

Cells were then plated onto Luria-Bertani (LB) agar plates containing either 50
µg/ml kanamycin (Sigma-Aldrich) for BP recombination reactions or 100 µg/ml
ampicillin (Sigma-Aldrich) for LR recombination reactions. Plates were inverted and
incubated at 37 °C overnight.

2.2.3 Miniprep

Individual bacterial colonies were added to 5 ml LB medium containing either 50
µg/ml kanamycin (Sigma-Aldrich) for products of BP recombination reactions, or
100 µg/ml ampicillin (Sigma-Aldrich) for products of LR recombination reactions.
Mixtures were incubated overnight at 37 °C with shaking at 200 rpm. Glycerol
stocks of each bacterial culture were prepared by adding 250 µl of 100% glycerol
(Sigma-Aldrich) to 750 µl of culture and mixing. Glycerol stocks were stored at 80 °C.

Plasmids were purified from the bacteria using either the ISOLATE II Plasmid
MiniKit (Bioline) or the Spin Miniprep Kit (Qiagen) as per manufacturer's instruc-
tions. Purified plasmid was eluted into 30 µl of RNAse-free water and the final

concentration and purity of the constructs determined using a QIAxpert spectropho-
tometer (Qiagen).

2.2.4   Construct validation

Constructs were validated through a combination of restriction digests and Sanger
sequencing (Macrogen). To perform the restriction digests, one restriction site within
the Tol2 backbone and one restriction site within the middle entry or 3' entry clone
were selected within each construct. Restriction enzymes used are specified in Chapter
Specific methods, Chapter 4, Section 4.2 and Chapter 5, Section 5.2. Digest reactions
consisted of 500 ng of purified construct, 0.5 µl of the restriction enzymes and 1 µl 10
X CutSmart buffer (NEB) made up to 10 µl with RNAse free water. Reactions were
incubated at 37 °C for a minimum of 20 minutes. The products of digestion were gel
electrophoresed (1% agrose gel 100V, 60 minutes) and imaged on Gel Doc EZ System
(BioRad).

Constructs that produced products of digestion of the expected size were sent
to Macrogen (Korea) for Sanger sequencing using an ABI3730XL sequencer and
BigDye terminator sequencing (Life Technologies). Sequencing primers were designed
using Primer3 online software (http://bioinfo.ut.ee/primer3-0.4.0/). Sequenc-
ing results were analysed using Sequencher v4.8 software (GeneCodes Corporation,
USA).

2.3   Zebrafish Husbandry

The housing, breeding and experimental protocols used in this project were approved
by the Animal Ethics Committee, Macquarie University (ARA 2012-050 and ARA
2015-34, Appendix A.1) and the Internal Biosafety Committee (NLRD 5201401007)
and follow guidelines detailed in The Zebrafish Book (Westerfield, 2000).

The zebrafish strains used for this study were AB/ Túbingen (TAB) wildtype, Túbingen (TUB) wildtype and the Casper (*nacre-roy*) unpigmented line. The lines used for each component of the study are specified within each chapter.

2.3.1 Aquarium conditions

The aquarium was maintained at a constant temperature of 28 °C with a neutral pH (7.1 – 7.4), a stable conductivity (600-800 µS/m) and a day/night cycle of 11 hours light and 13 hours dark.

2.3.2 Breeding

The zebrafish used in this study were obtained from natural spawning. The afternoon prior to planned injections, male and female fish were placed in a false-bottomed pair-mating tank, separated by a divider. At the onset of light the following morning, the divider was removed. Eggs produced from the resulting mating passed through the false bottom of the tank and were collected using a plastic tea strainer. Eggs were rinsed with system water and transferred to a Petri dish containing E3 embryo medium with 0.5% methylene blue (Sigma-Aldrich).

2.3.3 Raising of embryos

Embryos were raised in E3 medium in an incubator set at 28 °C until 5 days post fertilisation (dpf). At 5 dpf, hatched larvae were transferred to juvenile tanks containing E3 medium to a depth of approximately two centimeters. A consistent temperature was maintained in the larval tanks by water bath set at 28 °C. Larvae were fed live paramecium cultures daily. At 10 dpf, live artemia was added to the diet. At approximately three weeks post fertilisation (wpf), the larvae were moved to

the main system and fed a combination of live artemia and juvenile pellets. At two months post fertilisation (mpf), the juvenile pellets were replaced with adult pellets.

2.4 Zebrafish manipulations

2.4.1 Dechorination

Depending on end use, embryos were dechorinated manually or enzymatically. Manual dechorination was performed under a Nikon SMZ745 stereo microscope using Dumont #5 watchmaker forceps (Sigma-Aldrich). Enzymatic digestion was performed with 2 mg/ml Pronase (Sigma-Aldrich), which was added to the E3 medium and incubated at 28 °C for 10 minutes.

2.4.2 Analysis of swimming behaviour at 6 dpf

Embryos to be used for behavioural analysis were raised in equal numbers (n=30 per petri dish) in the standard light/dark cycle. At 6 dpf, embryos were placed into a 24-well plate and given an hour to recover. Behavioural analysis was performed using the Zebrabox with the Zebralab software (View-point). A 14 minute protocol was used, consisting of 6 minutes of light (first two minutes not recorded), four minutes of dark, followed by an additional four minutes of light. The distance swum by each fish under light and dark conditions was recorded.

2.4.3 Anaesthetic and Euthanasia

For anaesthesia, fish were immersed in tricaine methanesulfonate solution (Sigma Aldrich) diluted to approximately 0.2 mg/ml until adequately sedated or anaesthetised. For euthanasia, fish were immersed in 4 g/l tricaine methanesulfonate solution.

2.4.4   Fixation

Following euthanasia, zebrafish were washed 2 X with E3 media, then fixed in 4%
paraformaldehyde in phosphate buffered saline (PBS) either overnight at 4 °C or at
room temperature for 2 hours on a gentle rocker. Zebrafish were then rinsed in PBS
and stored at 4 °C.

3

Transient *CCNF* overexpression

3.1 Introduction

3.1.1 Introduction to the Chapter

This chapter addresses aims 1 and 2 of the project:

- Aim 1: Characterisation of endogenous zebrafish *ccnf*.
- Aim 2: Development of transient zebrafish models that overexpress human *CCNF*.

The chapter begins with a discussion of whole genome duplication - its role in evolution and its potential effects on zebrafish models of human disease. The chapter

then reviews the transient zebrafish models of ALS that have been reported to date. Data from the current study is presented in a paper published in *Human Molecular Genetics* (Paper 2). This paper details the characterisation of zebrafish *ccnf*, which indicated the suitability of the species to model ALS-linked mutations in the gene, and it presents an analysis of transient zebrafish models that overexpress either wildtype CCNF ($CCNF^{WT}$) or ALS-linked mutant *CCNF* ($CCNF^{S621G}$). Also detailed in Paper 2 are findings from proteomic profiling analysis of *CCNF* transfected Neuro-2a cells (led by Ms Stephanie Raynor and Dr Albert Lee, Centre for MND Research, Macquarie University). Paper 2 is followed by unpublished data, which indicates the suitability of the transient models for use in drug screens. The chapter concludes with a discussion of the advantages and limitations of this current study and the potential utility of the transient models in future investigative studies and preclinical trials.

3.1.2 Zebrafish models in ALS research

Duplication of the zebrafish genome

Gene duplication greatly increases genetic complexity and diversity and is therefore considered to be a key driver of evolution (Magadum et al., 2013). Errors during cell division may result in duplication of an individual gene or, if homologous chromosomes fail to separate during mitosis, duplication of the whole genome. While some duplicated genes (paralogues) retain similar functions, most undergo either a shift in function, sub-functionalisation or a loss of function (Levasseur and Pontarotti, 2011). It is hypothesised that the considerable alterations in gene function that have resulted from whole genome duplication are largely responsible for vertebrate evolution (Pennisi, 2001; Ohta, 2003; Fortna et al., 2004; Kellis et al., 2004; Hurles, 2004).

Evidence suggests that the teleost class of fish (including zebrafish) underwent a whole genome duplication that did not occur in other vertebrates, termed the

teleost-specific genome duplication (Meyer and Schartl, 1999; Postlethwait et al., 1998; Gates et al., 1999). Since this duplication event, over 100 million years ago, evolutionary loss of function has eliminated the majority of paralogues from the zebrafish genome. However, it is estimated that approximately 20% of zebrafish genes still retain a functional paralogue (Postlethwait et al., 2000). The potential presence of a functional paralogue must be considered in the design and interpretation of zebrafish models that express a human mutation. Zebrafish models based on the ALS-linked gene *TARDBP* are a key example. *TARDBP* has two functional paralogues in the zebrafish - *tardbp* and *tardbpl.* Inhibition of one paralogue is compensated for by upregulation of the other (Schmid et al., 2013). This is highly significant as evidence suggests that ALS-linked mutations in *TARDBP* have concurrent loss and gain of function effects (reviewed in Chapter 1, Section 1.6). The compensatory ability of the *tardbp* and *tardbpl* paralogues has significant potential to mediate the loss of function effects of an ALS-linked mutation, thereby impacting the ability of the model to accurately reflect the cellular changes associated with the mutation. In this study, examination of the zebrafish genome identified a single *ccnf* orthologue (Paper 2), which greatly simplified the design and interpretation of the models.

Transient zebrafish models of ALS

Transient zebrafish overexpression models are generated by injecting mRNA of a gene of interest, often fused to a fluorescent reporter, into zebrafish embryos at the single cell stage of development (Yuan and Sun, 2009). The advantage of this strategy is the speed and relative ease of model development. With an experienced operator, hundreds of eggs can be injected with high accuracy within an hour (Rosen et al., 2009). Translation from the mRNA occurs rapidly, resulting in high levels of protein expression during early embryonic development (Yuan and Sun, 2009). Consequently, these models typically develop an early phenotype, allowing investigative studies to be performed with great efficiency. However, care is required to ensure the injection technique does not affect model phenotype. Injection volume must be

precisely measured to ensure equal expression levels between control and treatment groups. Additionally, timing of the injections must be uniform across experimental groups. Injection at timepoints beyond the single cell stage of development has increased potential to produce mosaic, rather than ubiquitous expression of the protein.

Multiple transient models of ALS have been developed in zebrafish and these models have provided valuable insight into the biological mechanisms of disease (summarised in Table 3.1). Transient zebrafish models have also been used in preclinical studies to investigate the potential efficacy of drug candidates. For example, transient *TARDBP*^{A315T} and *SOD1*^{A4V} zebrafish models have been used to examine the neuroprotective effects of progranulin overexpression (Laird et al., 2010). Mutations in the progranulin encoding gene, *GRN*, have been linked to FTD (Cruts et al., 2006; Gass et al., 2006; Baker et al., 2006). These mutations appear to induce a loss of progranulin function (Van Damme et al., 2008) and consequently, overexpression of the protein has been proposed as a therapeutic approach for FTD. Indeed, two clinical trials of drugs aimed at elevating progranulin levels in FTD patients who carry a *GRN* mutation have been performed (https://www.clinicaltrials.gov/, reference NCT02149160 and NCT01835665. Results not reported). Given the close association of ALS and FTD (reviewed in Chapter 1, Section 1.2.1) the rescue effect of progranulin overexpression was examined in the zebrafish models of ALS. Both *TARDBP*^{A315T} and *SOD1*^{A4V} transient zebrafish models develop an axonopathy characterised by shortened primary motor axons and an increased incidence of aberrant axonal branching (Lemmens et al., 2007; Laird et al., 2010). Interestingly, progranulin was shown to rescue this phenotype in the *TARDBP*^{A315T} model, but not in the *SOD1*^{A4V} model (Laird et al., 2010). These results appear to support the hypothesis, discussed in Chapter 1, Section 1.3.3, that ALS-linked mutations in these two genes function through different pathways. The study therefore, not only demonstrated the suitability of transient zebrafish models for preclinical trials, but also provided some insight into disease biology.

precisely measured to ensure equal expression levels between control and treatment groups. Additionally, timing of the injections must be uniform across experimental groups. Injection at timepoints beyond the single cell stage of development has increased potential to produce mosaic, rather than ubiquitous expression of the protein.

Multiple transient models of ALS have been developed in zebrafish and these models have provided valuable insight into the biological mechanisms of disease (summarised in Table 3.1). Transient zebrafish models have also been used in preclinical studies to investigate the potential efficacy of drug candidates. For example, transient *TARDBP*$^{\text{A315T}}$ and *SOD1*$^{\text{A4V}}$ zebrafish models have been used to examine the neuroprotective effects of progranulin overexpression (Laird et al., 2010). Mutations in the progranulin encoding gene, *GRN*, have been linked to FTD (Cruts et al., 2006; Gass et al., 2006; Baker et al., 2006). These mutations appear to induce a loss of progranulin function (Van Damme et al., 2008) and consequently, overexpression of the protein has been proposed as a therapeutic approach for FTD. Indeed, two clinical trials of drugs aimed at elevating progranulin levels in FTD patients who carry a *GRN* mutation have been performed (https://www.clinicaltrials.gov/, reference NCT02149160 and NCT01835665. Results not reported). Given the close association of ALS and FTD (reviewed in Chapter 1, Section 1.2.1) the rescue effect of progranulin overexpression was examined in the zebrafish models of ALS. Both *TARDBP*$^{\text{A315T}}$ and *SOD1*$^{\text{A4V}}$ transient zebrafish models develop an axonopathy characterised by shortened primary motor axons and an increased incidence of aberrant axonal branching (Lemmens et al., 2007; Laird et al., 2010). Interestingly, progranulin was shown to rescue this phenotype in the *TARDBP*$^{\text{A315T}}$ model, but not in the *SOD1*$^{\text{A4V}}$ model (Laird et al., 2010). These results appear to support the hypothesis, discussed in Chapter 1, Section 1.3.3, that ALS-linked mutations in these two genes function through different pathways. The study therefore, not only demonstrated the suitability of transient zebrafish models for preclinical trials, but also provided some insight into disease biology.

TABLE 3.1: Transient overexpression zebrafish models of ALS.

Gene	Conclusions drawn from study	Reference
SOD1	Gain of function mechanism rescued by upregulation of IGF-I	Sakowski et al. (2012)
	Gain of function mechanism rescued by upregulation growth factor VEGF	Lemmens et al. (2007)
TARDBP	Gain of function mechanism	Kabashi et al. (2010)
	Gain of function mechanism rescued by upregulation of Progranulin	Laird et al. (2010)
FUS	Suggests roles for cytoplasmic mislocalisation of FUS and stress granule formation	Bosco et al. (2010)
	Suggests a role of the stress responses in disease biology	Armstrong and Drapeau (2013)
	Loss of function due to rescue effect of WT, but not mutant FUS,	Kabashi et al. (2011a)
VAPB	Loss of function mechanism	Kabashi et al. (2013)
UBQLN2	Gain of function mechanism rescued by inhibition of beta-catenin	Edens et al. (2017)

3.2 Chapter-Specific Methods

The methods detailed in Paper 2 are shown in Table 3.2. Additional methods used in this study are detailed in this section.

TABLE 3.2: Summary of methods detailed in Paper 2.

Section	Technique
Characterisation of zebrafish *ccnf*	Sequence analysis of the zebrafish genome
	Alignment of human and zebrafish *CCNF*
Molecular methods	Site directed mutagenesis
	Sub-cloning of mCherry_*CCNF* into PCS2+ vector
	Generation of *CCNF* mRNA
Proteomic analysis	Transfection of Neuro-2A cells
	Trypsin digest
	Mass spectrometry analysis
	Western blotting
Zebrafish assays	RT-PCR of zebrafish cDNA
	In situ hybridisation
	Collection of protein lysates from whole embryos
	Microinjection of mRNA
	Birefringence analysis
	Acridine orange staining
	Whole mount immunostaining with Caspase-3 antibody
	Analysis of motor axon morphology
	Analysis of the photomotor response
	Correlation analysis between motor function and axonal morphology
Statistical analysis	One-way ANOVA
	Correlation analysis

3.2.1 Microplate reader analysis of acridine orange staining

At 24 hpf, zebrafish embryos were stained with acridine orange (AO) as described in Paper 2. Following staining, embryos were placed into an individual well of a 96-well plate and the intensity of the AO fluorescence measured using a PHERAstar FS microplate reader (BMG labtech) (n=60 embryos per group).

3.3 Results

3.3.1 Paper 2

Declaration of contributions

The candidate (AH) performed sequence analysis of zebrafish *ccnf* and cyclin F, the *in situ* hybridisation (ISH) and the RT-PCR analysis. Cell transfections and proteomic profiling was performed by SR and AL. JF assisted with site-directed mutagenesis and subcloning. The candidate generated the *CCNF* mRNA, performed all microinjections and screening, the birefringence analysis, immunohistochemistry staining, analysis of motor neuron morphology and behavioural analysis. MW, KY, and EH assisted the candidate with western blot analysis. The candidate and ED performed the acridine orange staining and analysis. AL and ED assisted the candidate with imaging for the correlation analysis. The images were analysed by the candidate and IT provided intellectual input into the statistical analysis. The candidate wrote the manuscript. All authors provided intellectual input and contributed to editing of the manuscript. The overall contribution of the candidate is estimated to be ∼85%.

3.3.2 Duration of cyclin F expression in transient zebrafish models

mCherry fused *CCNF* expression was shown to persist for less that 24 hours in the transient *CCNF* zebrafish model. Expression was examined by both fluorescent microscopy and western blotting (Figure A.1)
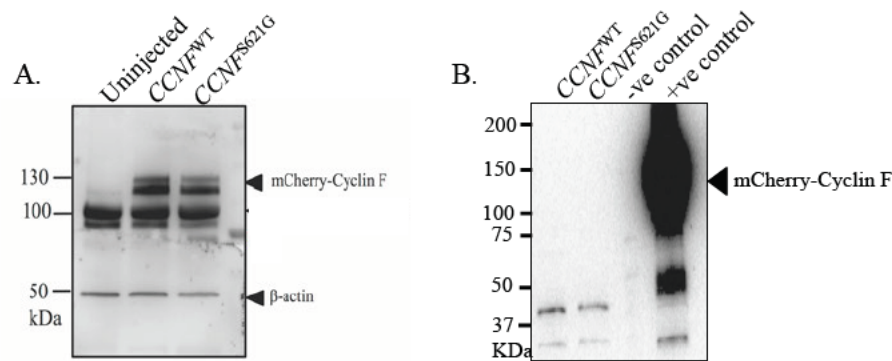

FIGURE 3.1: **CCNF mRNA is expressed for less than 24 hours in zebrafish embryos A.** Cyclin F antibody staining of a western blot performed on zebrafish lysates collected at 8 hpf following microinjection of mCherry-fused *CCNF*. Staining indicates equal expression of cyclinF^{WT} and cyclin F^{S621G}. **B.** Cyclin F antibody staining of a western blot performed on zebrafish lysates collected at 24 hpf following microinjection of mCherry-fused *CCNF*. No cyclin F expression is detectable in either of the injected groups. Previously validated Neuro-2a cells transfected with *CCNF*^{WT} was used as a positive control (Williams et al., 2016) and RIPA buffer containing no protein sample used as a negative control

.

3.3.3 Microplate reader analysis of acridine orange staining

Cell death was assessed in Paper 2 by manually counting the number of cells that stained positive for AO or caspase-3 antibody within a specific region of the spinal cord (method previously described Armstrong and Drapeau (2013)). Significantly higher levels of cell death were observed in the *CCNF*^{S621G} group compared to controls. To investigate whether analysis of cell death could be performed in a more efficient manner for use in preclinical therapeutic trials, AO staining was repeated in 24 hpf embryos and overall fluorescence determined using a 96-well microplate reader. This analysis detected significantly higher overall fluorescence in the *CCNF*^{S621G} group

compared to both $CCNF^{\text{WT}}$ and uninjected groups (p<0.0001). Fluorescence in the $CCNF^{\text{WT}}$ group was also found to be significantly increased when compared to the uninjected controls (p<0.0001) (Figure 3.2). This data suggests that the AO assay performed in Paper 2 could be adapted to more efficiently analyse the ability of potential therapeutics to mediate the toxic effects of ALS-linked mutant *CCNF*.

FIGURE 3.2: **Analysis of AO stained embryos using a microplate reader to assess total fluorescence.** Significantly higher fluorescence was detected in 24 hpf zebrafish injected with $CCNF^{\text{S621G}}$ compared to $CCNF^{\text{WT}}$ (P<0.0001) and uninjected groups (P<0.0001). Significantly higher fluorescence was also detected in the $CCNF^{\text{WT}}$ group compared to uninjected controls (P<0.0001). n=60 per group.

3.4 Discussion

This chapter describes the development and characterisation of the first reported animal model based upon an ALS-linked mutation in *CCNF*. The phenotypic features of the model included increased levels of cell death, a significant axonopathy and impaired motor function. These features suggest that the transient *CCNF* model will be useful in studies aimed at investigating the biological basis of *CCNF*-linked ALS and has potential for use in preclinical therapeutic trials. The advantages and limitations of the techniques and strategies used in this study and potential projects

for which the models may prove suitable are discussed in this section.

3.4.1   Characterisation of zebrafish *ccnf*

Summary

Examination of the zebrafish genome identified a single *ccnf* orthologue.   This facilitated the development of the *CCNF*-based models, as potential complications associated with compensatory mechanisms of a functional paralogue did not need to be considered. The significant sequence and structural similarities demonstrated between zebrafish and human cyclin F suggests that the protein is likely to play a similar functional role in both species. This supports the hypothesis that zebrafish are a suitable species in which to investigate mechanisms associated with ALS-linked mutant *CCNF*.

This study used a combination of whole mount ISH and RT-PCR to investigate the expression of zebrafish *ccnf*. Whole mount ISH is limited by the difficulty of permeablising post-embryonic larvae (post 6 dpf) sufficiently to allow RNA probes to penetrate the tissue. This difficulty necessitated the use of RT-PCR to examine mRNA expression beyond this timepoint. Due to the predominantly CNS expression of cyclin F indicated by the ISH, and the central role of the CNS in ALS, the RT-PCR was performed selectively on brain lysates. This study, for the first time, demonstrated that *ccnf* mRNA transcripts are consistently expressed in the CNS throughout development. This finding suggests that models in which *CCNF* expression is artificially driven within the CNS will have physiological relevance.

Further Studies

Both the RT-PCR and the ISH assays could be extended in further studies. The RT-PCR assay could be performed at timepoints at which the fish is considered

to be middle aged (3-15 mpf) and aged (>15 mpf) (Gilbert et al., 2014), to assess potential age-associated changes in *ccnf* mRNA expression. To further characterise *ccnf* expression, the ISH assay could be performed on either sections of the whole fish, or on brain sections taken at various stages of development. Additional studies of interest would include immunohistochemistry to confirm that cyclin F expression reflects the observed *ccnf* mRNA expression and quantitative RT-PCR (qRT-PCR) analysis to quantify expression levels at different stages of development. This level of characterisation were beyond the scope of this study.

The in situ expression of ccnf in older larva/adult could have been done on sectioned material. It looks like ccnf is expressed in the CNS in old larva but that probe penetration and staining is poor in the whole-mounts.

3.4.2   Transient zebrafish models

Limitations of transient models

Transient zebrafish models of ALS have significant advantages as discussed in Section 3.1.2. However, their limitations must also be recognised. The brief duration of overexpression of the protein of interest may preclude development of slow or late onset disease relevant pathology. Detectable expression of human cyclin F in the zebrafish models was limited to less than 24 hours (Appendix A.3). While this brief period of expression was sufficient for the development of a motor neuron axonopathy, impaired embryonic motor function and increased levels of cell death, it is possible that the brief duration of expression precluded the development of additional pathological changes. For example, expression of $CCNF^{S621G}$ in Neuro-2a and SH-SY5Y cells has been shown to induce an accumulation of ubiquitinated proteins, suggesting that dysfunction in the protein degradation pathways is a feature of *CCNF* associated ALS (Williams et al., 2016; Lee et al., 2017b). An accumulation of ubiquitinated proteins was not detected by western blotting performed on lysates collected at 8 hpf from the zebrafish mRNA models (Paper 2, Supplementary Figure 12). This failure

to replicate the *in vitro* results may have been a consequence of the brief period of *CCNF* expression at 8 hpf . Alternatively, different levels of overexpression in the transfected cells compared to the transient zebrafish models may have been the reason for the disparate results. Repeat western blotting on zebrafish lysates collected at a later timepoint may clarify this.

Transient models have two additional caveats. One, they are overexpression models that do not express a mutant gene at physiologically accurate levels and two, they are an embryonic model of an adult onset disease. The expression of a protein at greater than physiological levels can have toxic effects unrelated to expression of a disease-causative mutation. To account for this, studies using overexpression models must have controls in which the wildtype protein is expressed at the same level as the mutant protein. Additionally, assays to identify non-specific toxic effects of protein overexpression must be performed. The measures taken in this study to identify overexpression effects included embryonic staging, measurement of body length at various timepoints and birefringence analysis of skeletal muscle morphology. Despite these measures, additional models are required to validate the findings from the transient *CCNF* models. For example, a model in which the $CCNF^{S621G}$ mutation is integrated into the endogenous gene and expressed at endogenous levels would address the question of whether exogenous protein overexpression induces non-specific toxic changes. Genome editing-based methods offer an opportunity to develop such models. Additionally, an adult onset model in which expression of $CCNF^{S621G}$ is delayed until the fish matures, through the use of an inducible promoter, would address the question of the relevance of the developmental changes identified in the transient model to an adult onset disease.

Limitations of Western Blot analysis

As reported in Paper 2, chemiluminescent (ECL) western blot analysis was used in this study to validate some of the key proteomic findings, to confirm equal expression levels of cyclin F^{WT} and cyclin F^{S621G}, and to examine ubiquitination levels between the two models. Western blotting is a highly useful tool, particularly when used in combination with other methods such as mass spectroscopy. However, ECL analysis has only limited capacity for quantitative analysis and significant variability can arise from multiple sources (reviewed in Taylor and Posch (2014)). One potential source of variability comes from the loading control used to normalise expression levels of the protein of interest. The loading control used in this study, GAPDH, is one of the most frequently used controls. However, differential expression of GAPDH has been demonstrated under various physiological and pathological conditions (Greer et al., 2010; Ferguson et al., 2005). Therefore, expression levels may vary between samples. Furthermore, image saturation is a common concern with the protein, indeed with all loading controls, due to the typically high concentration of these proteins. The linear range of GAPDH imaging extends up to 5 µg of protein, beyond which increased protein concentration is not reflected by an detectable increase in band density (Welinder and Ekblad, 2011).

While the loading control can introduce variability into western blot analysis, the primary source of variability arises from image analysis. Three key factors affect image analysis - the algorithm used to remove background from the image, the area of the membrane selected for analysis and the variable used for analysis (Gassmann et al., 2009). The algorithm used to remove background varies between different software and can significantly affect the intensity of the bands to be analysed (Gassmann et al., 2009). The size of the area to be analysed is to some extent determined by the software used. Image J for example, requires the selected area to be taller than it is wide. This necessitates the inclusion of a large area of the membrane above and below the band of interest, an area that may have variable background or non-specific, irregular staining. Finally, different software uses different variables to measure the intensity of

a band of interest, including analysis of peak height (i.e. greatest intensity), average band intensity or total band volume. Different variables can provide a different result (Gassmann et al., 2009). Gassmann et al. (2009) clearly demonstrated the variability inherent in measurement of protein expression levels by western blotting by utilising a range of commonly used analysis protocols on a single image of a western blot. Image J (NIH), QuantityOne basic 4.6.3 (Bio-Rad Laboratories) and MCID Analysis 7.0 (Imaging Research Inc.) were each used with a variety of settings to quantify the relative expression of erythropoietin between different species. Highly variable results were obtained from this analysis, ranging from highly significant differences between species (p=0.000013) to no significant difference between species (p=0.76).

A more recently developed method that minimises these sources of variability is Quantifiable Fluorescence based Western Blot (QFWB). The use of fluorescent reporters in QFWB provides higher sensitivity, a wider range of linear detection and automatic elimination of background (Eaton et al., 2014). This technology is soon to be implemented in our laboratory and will be used in future studies. Of particular interest in these future studies will be the relative ubiquitination levels in lysates collected from the $CCNF^{\text{WT}}$ and $CCNF^{\text{S621G}}$ injected zebrafish. As discussed in Section 3.4.2, the previously reported increase in ubiquitination associated with $CCNF^{\text{S621G}}$ expression in Neuro-2a and SH-SY5Y cells (Williams et al., 2016; Lee et al., 2017b) was not reflected in the transient zebrafish models. It is possible this was due to the brief mRNA expression. Alternatively, the failure to replicate the results may be due to differences in the analysis, a consequence of the two studies being performed and analysed by different researchers. The use of alternative methods such as QFWB will help clarify this question.

Caspase-3 and AO staining

The proteomic profiling data shown in Paper 2 indicated that the cell death pathways were significantly upregulated in Neuro-2a cells transfected with $CCNF^{\text{S621G}}$. Consequently, the level of cell death was assessed in the transient zebrafish models. Two indicators of cell death were used for this analysis, AO staining and caspase-3 staining. AO is a live stain with advantages and limitations. Live staining avoids the need for fixation, which contributes to the high efficiency of the rapid AO staining protocol. However, because cell death is a dynamic process, imaging must be performed rapidly and in small experimental groups to accurately compare the level of cell death at the same timepoint (Sorrells et al., 2013). In contrast, caspase-3 antibody staining requires both fixation and a significantly longer protocol. However, the use of fixation allows imaging to be performed on larger groups without time constraints (Sorrells et al., 2013).

The AO and caspase-3 assays can reflect different cell death pathways. As discussed in Paper 2, multiple forms of cell death have been described, including apoptosis (a caspase-mediated form of programmed cell death) (Walsh, 2014), necroptosis (Re et al., 2014), paraptosis (Sperandio et al., 2004) and ferroptosis (Dixon et al., 2012). The predominant pathway involved in ALS-associated motor neuron death is yet to be clarified (Sathasivam and Shaw, 2005). Due to the different properties of the AO and caspase-3 assays, a combination of the two, performed in the same embryo at the same timepoint, could be used to investigate the relative roles of caspase mediated and caspase independent cell death associated with $CCNF^{\text{S621G}}$. Such a study is feasible as the caspase-3 antibody is unlikely to identify cells dying via the caspase independent pathways (necroptosis, paraptosis or ferroptosis). In contrast, AO will stain cells dying via both caspase-mediated and caspase-independent pathways. This is because AO staining relies on a loss of chromatin integrity associated with cell death, which allows the stain to intercalate with double stranded DNA, causing the cells to fluoresce (Weber and Koster, 2013).

Alternatively, to avoid the time constrains associated with the AO live staining, caspase-3 immunostaining could be used in combination with terminal deoxynucleotide transferase (TdT) dUTP nick-end labelling (TUNEL). TUNEL staining utilises TdT, an enzyme that binds to fragmented DNA in fixed embryos. Therefore, like AO staining, TUNEL staining would provide an indication of cell death regardless of pathway (Kyrylkova et al., 2012), however unlike AO staining, it could be performed on fixed embryos. This approach would ensure the same timepoint was analysed in each embryo, which would allow a direct comparison of the levels of caspase mediated and caspase independent cell death in the transient *CCNF* models.

Microplate reader analysis of AO staining

The AO analysis presented in Paper 2 demonstrated increased levels of cell death in the spinal cord of embryos expressing $CCNF^{S621G}$ compared to controls. Cell death in the spinal cord was initially assessed in this study due to the particular focus on the effect of $CCNF^{S621G}$ expression on the motor neurons and to reflect findings from an established transient *FUS* model of ALS (Armstrong and Drapeau, 2013). However, the key advantages of zebrafish as disease models are their rapidity of model development and their high fertility and fecundity. To take full advantage of these features in the efficient testing of multiple therapeutics, analysis of cell death in a more efficient manner is essential. The utility of microplate reader analysis of acridine orange stained zebrafish embryos to assess drug efficacy has previously been demonstrated. Parng et al. (2002) tested the effect of 18 different chemicals on a range of variables in zebrafish embryo and concluded that microplate reader analysis of AO staining intensity provided a suitable screening system for drugs which aimed to modulate apoptosis (Parng et al., 2002). The data presented in this study (Section 3.3.3), suggests that the transient *CCNF* zebrafish models may prove suitable for similar drug trials. The results presented in Section 3.3.3 do suggest that two clusters are present within the $CCNF^{S621G}$ group - one half which demonstrated similar levels of apoptosis to the $CCNF^{WT}$ group, and one half which demonstrated elevated levels of apoptosis. While analysis was performed in

triplicate, repeated analysis is required to investigate whether this pattern is repeatable.

Primary motor axon morphology

Analysis of the length and incidence of aberrant branching in primary motor axons as performed in Paper 2 is a well-established means of assessing pathogenicity of ALS-linked mutations in zebrafish. Aberrant morphology of the primary motor axons has been described in zebrafish models of ALS based on mutations in *SOD1* (Lemmens et al., 2007; Ramesh et al., 2010), *TARDBP* (Kabashi et al., 2010; Laird et al., 2010), *FUS* (Kabashi et al., 2011a), *C9orf72* (Ciura et al., 2013), *ALS2* (Gros-Louis et al., 2008) and *VAPB* (Kabashi et al., 2013). While a similar axonopathy was shown to develop in all of these models and impaired motor function has been demonstrated in some, a direct relationship between axonal development and motor function has not previously been demonstrated. The correlation analysis performed in this study provided the first evidence for a direct relationship between aberrant axonal outgrowth and motor impairment, a finding that validates the functional relevance of the axonopathy observed in the established zebrafish models.

Assessment of motor function

The photomotor response (PMR) is a non-visual reflex in which a motor response is activated by stimulation of photoreceptors in the hindbrain of the zebrafish (Kokel et al., 2013). The PMR is present between 30 and 42 hpf (Kokel and Peterson, 2011) and consequently, was highly suited to the early analysis of motor function required for the transient *CCNF* model. An alternative measure of motor function commonly used at a similar stage of development is the touch evoked escape response (TEER). The PMR was selected for this study in preference to the TEER for the following reasons. First, the PMR relies only on motor function and hindbrain photoreceptors, whereas the TEER relies on motor function, mechanosensory neurons, the ascending sensory tract and the hindbrain (Umeda et al., 2016). Second, the PMR has the advantage over the TEER with respect to its uniformity of stimulus. The zebrabox used to

assess the PMR delivers the same stimuli to all embryos, whereas the TEER relies on manual application of a stimulus, which has inherent variability with respect to its intensity, timing and location (Smith et al., 2013). Finally, the PMR is well suited to high throughout analysis as it can be performed in 96-well plates. The robust and highly repeatable results from the PMR assay performed in this study, suggest that this measure of motor function may be of value in future preclinical therapeutic trials.

Of interest would be a study in which assessment of motor function was extended throughout the development of the fish into adulthood. The assessment of motor function in adult fish is described in Manuscript 1 (Chapter 5, Section 5.4. This analysis could be performed monthly on the transient models to assess the impact of a developmental defect in axonal morphology on swimming behaviour in mature and aged fish. Such a study was beyond the time frame of this project, but would have the potential provide some insight into the role of developmental defects in the onset of ALS.

3.4.3 Future directions

Investigation of disease mechanisms

The transient *CCNF* zebrafish models presented in this study have the potential to be used in *in vivo* studies that aim to understand the pathogenic mechanisms of the $CCNF^{S621G}$ mutation. To maximise the advantages of the zebrafish as disease models, many of these investigative studies will be performed using a combination of models - both transient embryonic *CCNF* models, which will allow rapid analysis, and adult models in which *CCNF* is persistently expressed, which will facilitate longitudinal studies. The use of these complementary models in potential future studies are discussed in detail in Chapter 6, Section 6.4.

One study for which the transient *CCNF* zebrafish appear well suited is proteomic profiling analysis. Such a study could provide *in vivo* validation of the findings from the *in vitro* analysis performed in Paper 2. As discussed in Chapter 1, Section 1.2, non-cell autonomous mechanisms are strongly implicated in the biology of ALS. One limitation of *in vitro* assays is that the cells are maintained in isolation and therefore, cannot reflect non-cell autonomous mechanisms. Lysates collected from the transient *CCNF* zebrafish provide an opportunity to repeat the proteomic profiling analysis in a model which reflects both cell autonomous and non-cell autonomous mechanisms. Dysregulated proteins and pathways that are common to both the *in vitro* and *in vivo* models would be of significant interest in further studies.

Also of interest would be targeted analysis of the expression levels of UPS-associated proteins in both the *in vitro* and *in vivo* models (ubiquitinomic analysis). Ubiquitinated proteins could be isolated through immunoprecipitation and profiling of this subset of proteins would provide more detailed insight into the effect of $CCNF^{S621G}$ on UPS function. One key advantage of the transient *CCNF* zebrafish for the proposed proteomic studies is the rapid expression of cyclin F following mRNA injections. Expression of the protein is evident from approximately 4 hpf. This would allow highly efficient analysis and would also allow lysates to be collected at the same timepoints used for the *in vitro* study presented in Paper 2 (8 hpf and 24 hpf).

Testing of candidate therapeutics

Evidence presented in this chapter suggests that the transient *CCNF* models will prove suitable for preliminary testing of potential therapeutics. The early onset phenotype displayed by the $CCNF^{S621G}$ model will allow highly efficient analysis in the early embryonic stage. This analysis may include quantification of cell death (AO staining) and motor function (the PMR), both of which can be performed in 96-well plates. The use of 96-well plates will maximise the efficiency of the screening process and minimise the amount of drug required, saving both time and money, thereby

allowing multiple compounds to be tested at multiple concentrations. More detailed analysis, such as morphological assessment of the primary motor axons, could be performed to further assess the effect of the most promising drugs.

Excitingly, the transient *CCNF* zebrafish model developed here has already been used in a preclinical study that supports its suitability to investigate potential therapeutic approaches. This study, lead by Dr Audrey Ragagin and A/Prof Julie Atkin (Centre for MND Research, Macquarie University), investigated the neuroprotective effects of the ER-golgi transport protein, Rab1, in the models. Dysfunction in the Rab1-dependant ER-golgi protein transport system has been implicated in ALS (reviewed in Soo et al. (2015a)) and overexpression of Rab1 has been shown to have a rescue effect in Neuro-2a cells transfected with ALS-linked mutant *FUS* (FUS^{P525L} and FUS^{R522G}) (Soo et al., 2015b). To investigate the rescue effect of *RAB1* on *CCNF*-associated ALS, *RAB1* and *CCNF* mRNA were co-injected into zebrafish embryos as described in Paper 2. The resulting overexpression of RAB1 was shown to rescue both the axonopathy and the impaired motor dysfunction (PMR) displayed in the transient $CCNF^{\text{S621G}}$ model. The effect of *RAB1* overexpression on cell death was not assessed (unpublished).

Data from the proteomic profiling, western blot analysis of the *in vitro* model and analysis of the zebrafish model suggests that a therapeutic trial of apoptosis inhibitors, more specifically, caspase-3 inhibitors may be worthwhile. As discussed in Paper 2, upregulation of caspase-3 has been implicated in multiple neurodegenerative diseases, including ALS (reviewed in Khan et al. (2015)) and inhibition of caspase-3 has been recognised as a potential therapeutic approach (Khan et al., 2015). However, therapeutic trials of caspase-3 inhibitors are yet to be reported in animal models of ALS. The therapeutic effect of pan-caspase inhibition with N-benzyloxycarbonyl-Val-Ala-Asp fluoromethyl-ketone (Z-VAD-fmk) has been examined in the $SOD1^{\text{G93A}}$ mouse model of ALS (Li et al., 2000). This study demonstrated that administration of Z-VAD-fmk into the cerebral ventricle of pre-symptomatic mice resulted in a delayed

disease onset and an extended lifespan (Li et al., 2000). This finding suggests that caspase inhibition is a potentially viable approach in the treatment of ALS. While adverse effects were not reported with non-specific caspase inhibition, a more targeted approach, such as specific caspase-3 inhibition, may prove to be both more efficacious and less prone to adverse effects. The transient *CCNF* zebrafish provide a tool with which to investigate this question.

3.5   Concluding Remarks

This chapter details the development of the first animal model based on an ALS-linked mutation in *CCNF*. The characterisation of zebrafish *ccnf* performed in this study supports the suitability of this species to model ALS-linked *CCNF* mutations and the ALS-relevant phenotype identified in the model suggests that they will be suitable for future studies to investigate the pathological mechanisms of ALS. Additionally, viable assays of the identified phenotypes offer potential for the future assessment of candidate therapeutics. However, as with all models, zebrafish that transiently overexpress *CCNF*^S621G have limitations as disease models. Consequently, additional *CCNF* based zebrafish models are required to complement future studies. The development of one such model, in which *CCNF*^S621G is overexpressed in adult zebrafish, is detailed in Chapters 4 and 5.

4

Constitutive overexpression of *CCNF*

4.1 Introduction

4.1.1 Introduction to the chapter

The goal of the study detailed in this chapter was to establish transgenic zebrafish in which *CCNF* was constitutively overexpressed throughout the lifetime of the fish. The chapter begins with a review of the techniques available for the development of constitutive overexpression zebrafish models, with a focus on the Tol2 transposase system used in this study. Data from the study is presented in two sections:

- Efforts to establish a ubiquitously overexpressing *CCNF* model are detailed in a paper that has been accepted to *Science Matters* (Paper 3).

- Efforts to establish a model in which the *CCNF* transgene was expressed selectively in the motor neurons are detailed in Section 4.4.

The data presented in this chapter suggests that overexpression of *CCNF* throughout the early stages of embryonic development is toxic in the zebrafish and this toxicity precludes the development of zebrafish models that constitutively overexpress *CCNF*. Accordingly, the chapter concludes with a discussion of potential future studies to investigate this apparent toxicity, followed by a discussion of the alternative transgenic strategies available to establish *CCNF* transgenic zebrafish models.

4.1.2 Zebrafish constitutive overexpression models

Constitutive overexpression models are developed through the injection of a transgene (cDNA) into the zebrafish embryo at the single cell stage of development. The majority of the injected transgenic DNA is degraded, but some is integrated into the genome through DNA repair mechanisms (Stuart et al., 1988). This integration occurs randomly, and commonly at multiple genomic locations (Wilson et al., 1990). When integration occurs within germline cells, the transgene is transmitted to the next generation, producing stable transgenic lines that overexpress the transgene throughout the lifetime of the fish (Lieschke and Currie, 2007).

The first reported transgenic zebrafish was generated through the microinjection of linearised cDNA (Stuart et al., 1988). While successful, this approach had low efficiency, with germline transmission rates of approximately 5% (Stuart et al., 1988). Multiple strategies have since been developed that utilise various vectors to improve the efficiency of genomic integration. Higher efficiency induces earlier integration, reducing mosaicism and increasing germline transmission rates. The use of vectors to facilitate transgenic integration has the additional benefit of reducing concatemer formation (Lin et al., 1994; Thermes et al., 2002; Kawakami et al., 2000). Concatemers

are formed by the integration of multiple copies of a transgene into a single genomic location. While the presence of concatemers does results in high expression levels of a transgene,they do frequently result in variable expression (Stuart et al., 1990), silencing of the transgene (Stuart et al., 1988).

The key vectors used in zebrafish to maximise the efficiency of transgene integration are shown in Table 4.1. The use of a transposase vector, as used in this project, is discussed in detail in Section 4.1.3.

TABLE 4.1: Common strategies used to generate transgenic zebrafish

Strategy	Efficiency	Advantages	Limitations	Reference
Injection of linearised DNA	5%	Simplicity, low cost	High mosaicism, concatemer formation	Stuart et al. (1988)
Use of viral vectors	70-100%	Highly efficient, Reduced concatemers	Laborious, strict safety measures, low cargo size (<2kb)	Lin et al. (1994)
Use of meganucleases	< 45%	Ease of construction, Reduced concatemers	Lower efficiency than retroviruses	Thermes et al. (2002)
Use of transposons	≤ 50%	Ease of construction, Reduced concatemers	Lower efficiency than retroviruses	Kawakami et al. (2000)

4.1.3 Transposon-mediated transgenesis

Principles of transposon-mediated transgenesis

Transposon-mediated transgenesis takes advantage of naturally occurring transposons – segments of DNA that move from one genomic location to another due to endogenous transposase enzymes (McClintock, 1950). A large number of transposons are found in all plant and animal species (Kazazian, 2004) and some have been co-opted to improve efficiency of transgenic insertion for the development of animal models. To utilise this system, transposase mRNA is co-injected with constructs that carry a transgene flanked by transposase restriction sites (*att* sites) (Ivics et al., 2009). This system has been shown to produce highly efficient germline integration with low concatemer formation (Kwan et al., 2007).

Two naturally occurring transposons have been identified in zebrafish, Sleeping

Beauty (SB) (Ivics et al., 1997) and Tol2 (Kawakami et al., 2000), both of which have been utilised to develop transgenic lines in zebrafish. In comparison to the SB system, the Tol2 system has a higher efficiency of transgene integration (up to 50% Balciunas et al. (2006)), is capable of integrating larger fragments of DNA (up to 160 kb), and is less vulnerable to overexpression inhibition (Balciunas et al., 2006). The Tol2 system has therefore become the predominant transposase tool in zebrafish research (Sugano and Neuhauss, 2013). The development of the Tol2-kit (Kwan et al., 2007) greatly enhanced the efficiency of the system, providing a catalogue of interchangeable vectors that can be readily recombined to develop Tol2 expression constructs. The principles of the Tol2-kit are detailed in Chapter 2, Section 2.2.1.

Tol2-mediated transgenic zebrafish

Tol2-mediated transgenesis is a well-established strategy in the zebrafish. The system has successfully been used to establish a transgenic zebrafish model that ubiquitously overexpressed $SOD1^{\text{G93A}}$ under a *cytomegalovirus (CMV)* promoter (Sakowski et al., 2012). Sakowski et al. (2012) generated six independent $SOD1^{\text{G93A}}$ transgenic lines using the Tol2 system, all of which developed defects at the neuromuscular junction, death of motor neurons and motor dysfunction. However, the study was limited by the lack of a $SOD1^{\text{WT}}$ control - the phenotype of the $SOD1^{\text{G93A}}$ transgenic lines was compared to non-transgenic wildtype siblings.

In addition to the Sakowski et al. (2012) $SOD1^{\text{G93A}}$ model, the Tol2 transposase system has been utilised to establish numerous transgenic reporter lines in zebrafish. These include motor neuron reporter lines (*-3mnx1* promoter) (Arkhipova et al., 2012), microglial reporter lines (*mpeg* promoter) (Ellett et al., 2011), astrocytic reporter lines (*gfap* promoter) (Bernardos and Raymond, 2006), Annexin A5 reporter lines (*annexin* A5 promoter) (van Ham et al., 2010) and an ER stress reporter line (*ef1* promoter) (Li et al., 2015a). Due to the established efficacy of the Tol2 system as evidenced by these models, and the availability of the Tol2-kit Kwan et al. (2007),

this system was selected to generate the *CCNF* transgenic zebrafish models in this project.

4.1.4 Tol2 model Design

Promoters

Cyclin F is a ubiquitously expressed protein, therefore a ubiquitous promoter was selected to drive expression of the *CCNF* transgene. The Tol2 kit Kwan et al. (2007) provides two ubiquitous promoters; human *CMV* and zebrafish *beta actin 2* (*actb2*, formerly *β-actin*). The *CMV* promoter has been shown to undergo rapid methylation in zebrafish, which results in a loss of transgene expression across generations (Collas, 1998). In contrast, no methylation issues have been reported with the *actb2* promoter, which has been shown to drive strong, ubiquitous expression from the embryonic stage throughout the lifetime of the fish (Yoshinari et al., 2012). For this reason, the *actb2* promoter was selected for use in this project. Due to the specific interest in the effect of mutant *CCNF* on motor neurons, a second set of constructs was generated in which *CCNF* expression was driven by the zebrafish motor neuron promoter, *-3mnx1* (previously homeobox gene 9, *hb9*).

Fluorophores

Fluorescent reporters fused to a protein of interest are currently the gold standard strategy to examine protein expression and localisation in zebrafish. Fluorescent reporters also allow efficient selection of zebrafish embryos that have successfully integrated a transgene into the genome. The Tol2 kit system contains mCherry and EGFP fluorophores, both of which are reported to have excellent photostability and brightness with low toxicity (Day and Davidson, 2009). Both fluorophores were used for this study.

CCNF

The majority of zebrafish models of ALS constitutively overexpress a human ALS-linked gene. This includes zebrafish models based on *TARDBP* (Kabashi et al., 2010, 2011a), *SOD1* (Sakowski et al., 2012), *FUS* (Kabashi et al., 2011a) and *VAPB* (Kabashi et al., 2013). One zebrafish model has been established that overexpressed the zebrafish orthologue of an ALS-linked gene – a *sod1*$^{\text{G93R}}$ model (Ramesh et al., 2010). Ramesh et al. (2010) hypothesised that the different body temperatures of humans and fish may affect protein physiology and therefore, expression of the zebrafish gene was preferable to expression of the human orthologue in disease models. No study has yet described a direct comparison between models that express a human gene and models that express the zebrafish orthologue, therefore the preferable model design is yet to be established. To investigate this, the study detailed in this chapter aimed to develop two sets of models – one that overexpressed human *CCNF* and a second that overexpressed the zebrafish orthologue (*ccnf*).

The unanticipated findings from this study were that constitutive overexpression of both *CCNF* and *ccnf* appeared to be equally toxic in zebrafish embryos, and this toxicity precluded the development of either *CCNF* or *ccnf* transgenic lines. The findings from this study are outlined in Paper 3 and Section 5.8.

4.2   Chapter specific methods

The methods detailed in Paper 3, are shown in Table 4.2. The constructs generated for this study and the restriction digests used to select constructs for validation by Sanger sequencing are detailed in this section.

4.2.1   Generation of constructs

The LR recombination reactions used to generate the Tol2 constructs for this project are shown in Table 4.3. These reactions were performed as described in Chapter

Table 4.2: Methods described in Paper 3.

Section	Technique
Molecular methods	Tol2 recombination reactions
	Generation of transposase mRNA
Zebrafish assays	Microinjeciton of Tol2 constructs
	Live imaging (light microscopy)
	Founder screening
	Acridine orange staining

2, Section 2.2.1. The expression constructs generated by these reactions are shown schematically in Figure 4.1.

Table 4.3: LR reactions performed to generate the Tol2 expression constructs

5' vector	Middle Entry Vector	3' vector	Destination vector
p5E:*actb2*	pME:mCherry	P3E:$CCNF^{\mathrm{WT}}$	Tol2:PA2
p5E:*actb2*	pME:mCherry	P3E:$CCNF^{\mathrm{S621G}}$	Tol2:PA2
p5E:*actb2*	pME:mCherry	P3E:$ccnf^{\mathrm{WT}}$	Tol2:PA2
p5E:*actb2*	pME:mCherry	P3E:$ccnf^{\mathrm{S623G}}$	Tol2:PA2
p5E:*actb2*	pME:mCherry	p3E:pA	Tol2:PA2
p5E:*actb2*	pME:EGFP	P3E:$CCNF^{\mathrm{WT}}$	Tol2:PA2
p5E:*actb2*	pME:EGFP	P3E:$ccnf^{\mathrm{WT}}$	Tol2:PA2
p5E:*-3mnx1*	pME:mCherry	P3E:$CCNF^{\mathrm{WT}}$	Tol2:PA2
p5E:*-3mnx1*	pME:mCherry	P3E:$CCNF^{\mathrm{S621G}}$	Tol2:PA2
p5E:*-3mnx1*	pME:mCherry	P3E:$ccnf^{\mathrm{WT}}$	Tol2:PA2
p5E:*-3mnx1*	pME:mCherry	P3E:$ccnf^{\mathrm{S623G}}$	Tol2:PA2
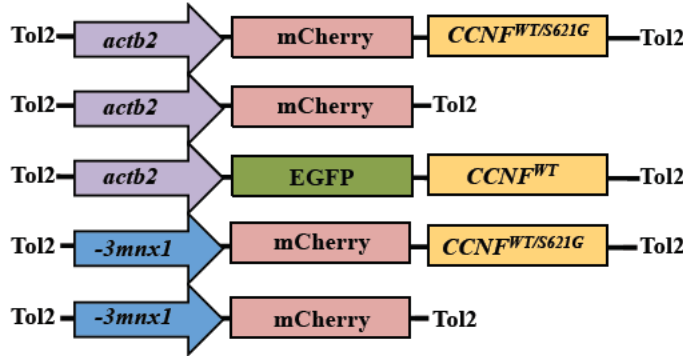
*CCNF refers to both the human and zebrafish *CCNFf* orthologues

FIGURE 4.1: **Constitutive overexpression constructs generated with the Tol2 Gateway cloning system (Life Technologies).** Constructs were designed to induce either ubiquitous (*actb2* promoter) or motor neuronal (*-3mnx1* promoter) expression of a transgene. Transgenes consisted of either a fluorophore alone or a fluorophore tagged *CCNF*. Constructs for expression of both the human *CCNF* and zebrafish *ccnf* homologues (wildtype and mutant) were generated.

4.2.2   Restriction site digests

Constructs were selected for Sanger sequencing based on observed restriction fragments following restriction enzyme digests. Digests were performed as described in Chapter 2, Section 2.2.4 using restriction enzymes shown in Table 4.4.

TABLE 4.4: Restriction digests used to select Tol2 constructs for sequencing.

Construct	Restriction enzymes	Size of product of digestion
actb2:mCherry	NdeI and NotI (NEB)	6.6 kb and 3.8 kb
actb2:mCherry_*CCNF*	BamHI and NdeI (NEB)	7.1 kb and 5.5 kb
actb2:EGFP_*CCNF*	BamHI and NdeI (NEB)	7.1 kb and 5.5 kb
-3mnx1:mCherry	Not1	linearised
-3mnx1:mCherry_*CCNF*	BamHI and NotI	6.9 kb and 3.3 kb

4.3 Results: Ubiquitous overexpression of *CCNF*

4.3.1 Paper 3

Declaration of contributions All experiments presented in this paper were performed by AH. All authors contributed intellectual input and were involved in editing of the manuscript.

Constitutive overexpression of the ALS-linked gene *CCNF* fusions results in cytotoxicity to preclude generation of transgenic zebrafish models

Alison L Hogan, Emily K Don, Jennifer A Fifita, Kelly L Williams, Roger S Chung, Angela S Laird, Ian P Blair, Nicholas J Cole

Biomedical Sciences, Macquarie University

Abstract

The E3 ubiquitin ligase protein, cyclin F (encoded by *CCNF*) has a role in substrate recognition for protein degradation within the ubiquitin proteasomal system. Mutations in this gene have recently been linked to the neurodegenerative diseases amyotrophic lateral sclerosis and frontotemporal dementia. To investigate the role of *CCNF* dysfunction in neurodegenerative disease, we aimed to develop novel transgenic zebrafish models that constitutively overexpress *CCNF* fusion proteins. After several attempts at establishing these transgenic lines, with side-by-side successful controls, it became apparent that generation of constitutively overexpressing *CCNF* fusion transgenic lines was not feasible. This failure appears to be a result of toxicity associated with persistent overexpression of *CCNF* fusion proteins in the developing embryo that precludes germ-line transmission of the transgene. The observations from our study indicate that an additional screening stage of zebrafish embryos, and/or the use of a temporal inducible system/mechanism is warranted in studies that aim to develop transgenic models expressing potentially toxic proteins, to circumvent the issues produced by expression during early developmental stages.

Introduction

Cyclin F is a key component of the ubiquitin proteasomal system (UPS), involved in mediating the transfer of ubiquitin molecules to specific substrates, thereby tagging them for degradation by the proteasome. By regulating the degradation and consequently the expression levels of specific substrates through the UPS, cyclin F governs DNA repair and replication and controls cell cycle progression [1]. Dysfunction of cyclin F and a subsequent dysregulation of these pathways have been linked to various forms of cancer [2] [3] [4]. Additionally, mutations in *CCNF* have recently been reported in two clinically, pathologically and genetically linked neurodegenerative diseases- amyotrophic lateral sclerosis (ALS) and frontotemporal dementia (FTD) [5]. To date, only one *in vivo* model has been established as a tool to investigate *CCNF* dysfunction- a zebrafish model that transiently overexpressed an ALS-FTD mutation in *CCNF* (*CCNF*S621G) [6]. This model demonstrated neurological defects associated with expression of *CCNF*S621G, including a motor axonopathy and impaired motor function. To supplement the existing transient models, this study aimed to use the Tol2 transposase system [7] to develop zebrafish models that constitutively expressed fluorescently labelled human *CCNF* under a quasi-ubiquitous (actb2) promoter.

Objective

To develop novel transgenic zebrafish models that constitutively overexpress CCNF-fluorophore fusion for use in studies investigating disease-associated dysfunction of this gene.
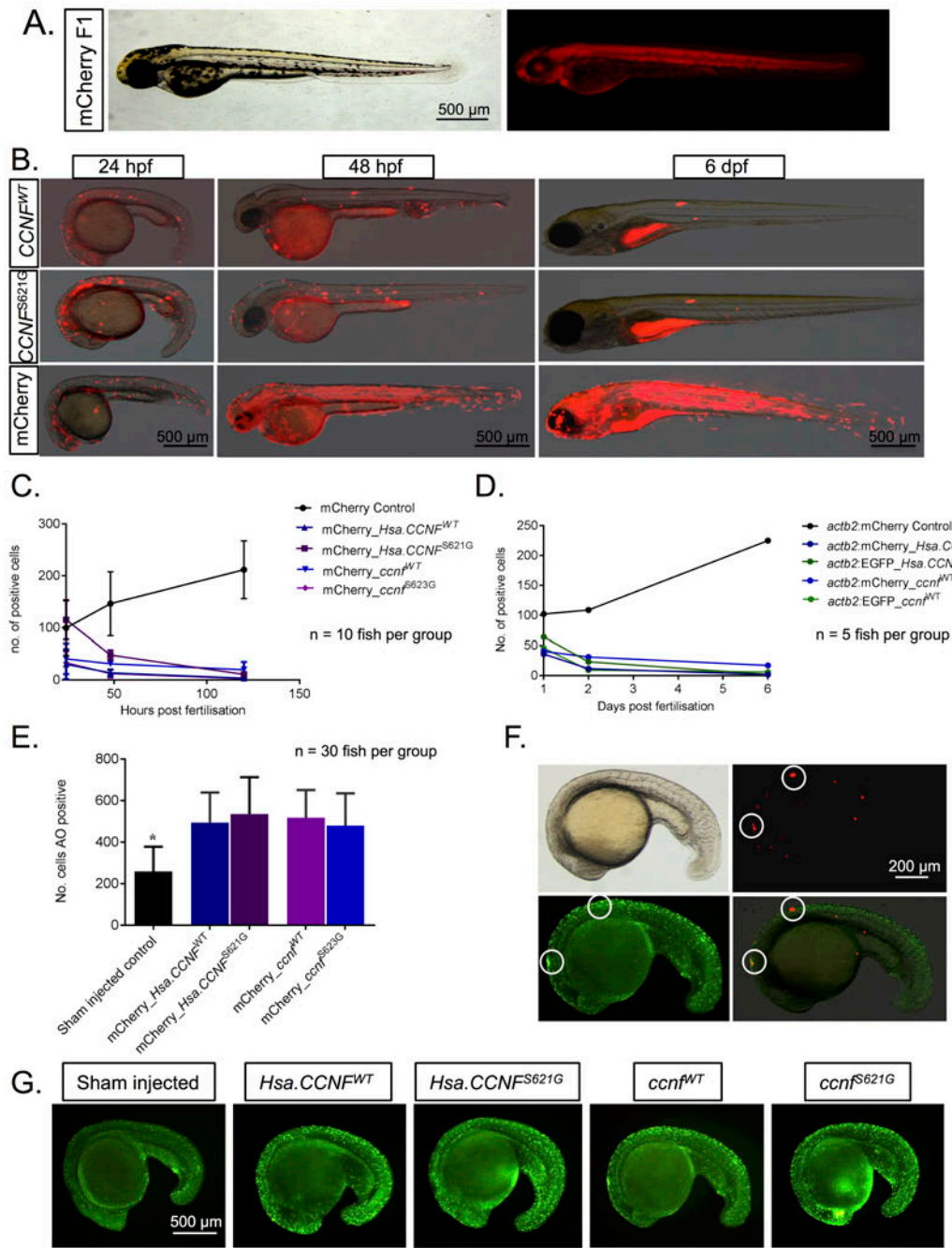
Figure Legend

Figure 1. Progressive loss of transgenic *CCNF* expression in zebrafish embryos through early development.

(A) F1 offspring from a *actb2*:mCherry founder demonstrating successful development of the transgenic line.

(B) Representative images of a single fish from different injection groups imaged at 1, 2 and 6 dpf demonstrating a loss of expression in both *CCNF*-expressing groups and an

increase in expression in the mCherry-expressing control.

(C) Quantification of the average number of mCherry positive cells per injection group over the first 5 days of development (n=10 per group).

(D) Quantification of the average number of mCherry/GFP positive cells per injection group over the first 5 days of development (n=5 per group). No difference was seen between embryos injected with GFP constructs or mCherry constructs.

(E) Quantification of the number of acridine orange-positive cells demonstrated significantly higher levels of cell death in embryos expressing *CCNF* compared to controls (n=30 per group).

(F) Example of co-expression of mCherry- tagged *CCNF* and an area of strong AO staining.

(G) Representative images of acridine orange-stained fish from each of the 5 experimental groups indicating higher levels of cell death in fish expressing *CCNF* compared to sham injected controls.

Results & Discussion

No founders were identified in the *CCNF* injected groups

Offspring from 102 fish injected with a *CCNF* construct (32 *Hsa.CCNF*WT, 28 *Hsa.CCNF*S621G, 18 *ccnf* WT and 24 *ccnf* S6213G) were screened and no founders were identified. Offspring from 8 fish injected with the mCherry control construct were screened and 4 founders were identified (Fig. 1A). The efficiency of transgenic integration in the mCherry control line, (reported at 30–50% for Tol2 system [8]) validated the injection and screening methods and suggested a gene-specific issue caused the failure to identify *CCNF* founders.

CCNF expression is lost over the first 6 days of development

To investigate this failure, the embryonic injections were repeated, and the screening protocol was altered. Instead of the standard screening at 2–3 days post fertilisation (dpf), screening was performed at 24 h post fertilisation (hpf) followed by subsequent analysis every 24 h up to 6 dpf. A dramatic loss of mCherry expression was observed in all *CCNF*-injected fish over this time period. In comparison, an increase in the number of mCherry positive cells was evident in the mCherry control fish (Fig. 1B). To quantify this, the number of mCherry positive cells in 10 fish from each injection group was estimated. This demonstrated no significant difference in the number of mCherry expressing cells between any of the injection groups at 24 hpf (p=0.08). However, significantly more mCherry positive cells were detectable in the control fish than any of the *CCNF* groups by 2 dpf (p<0.0001) and this difference increased over the next 5 days (Fig. 1C).

Similar loss of expression was seen between mCherry and EGFP fused *CCNF*

To eliminate an unexpected toxicity associated with mCherry fusion to *CCNF*, mCherry was substituted with the EGFP fluorophore in the Hsa. *CCNF*WT and *ccnf* WT constructs. Quantification of the number of fluorophore positive cells in 5 fish in each injection group demonstrated a similar loss of expression between the mCherry and the EGFP groups over the first 6 days of development (Fig. 1D).

Higher levels of cell death were evident in *CCNF* injected groups compared to mCherry controls

To investigate the mechanism responsible for the loss of cells expressing the transgene, cell death was assessed at the time of peak mCherry-*CCNF* expression (24 hpf) using acridine orange (AO). This analysis demonstrated significantly higher levels of cell death in all of the *CCNF* groups compared to sham injected controls (p<0.05). No significant difference was seen between any of the *CCNF* groups (n=30 per group) (Fig. 1E). Cells that both expressed mCherry fused *CCNF* and stained positive with AO were observed (Fig. 1F).

This AO staining assay suggests that toxicity associated with overexpression of *CCNF* is an impediment to establishing transgenic lines based on this gene. It is possible that all, or the majority, of cells in which the *CCNF* transgene is integrated into the genome, including germline cells, undergoes apoptosis, precluding germline transmission. Given the high level of programmed cell death that occurs during early development [9] and

the regenerative capacity of the zebrafish, this *CCNF*-associated cell death could occur without causing detectable morphological abnormalities.

Conclusions

This study demonstrates that the development of zebrafish transgenic lines that constitutively overexpress CCNF-fluorophore fusions using the described methods is not a feasible option, despite the clearly possible expression of the full-length ORF of the transgenic construct as apparent by fluorescence signal. The authors, therefore, suggest that levels of transgene expression to be re-assessed at 6–7 dpf to detect potential toxic overexpression effects at this early stage. In addition, models with temporal control of transgene expression to bypass overexpression during this period of development and cell death may be warranted.

Limitations

One limitation of this study is that fluorophore fusion proteins were used instead of the native CCNF ORF. For a possible follow-up, a native CCNF ORF could be tested with a transgenesis reporter in cis (i.e. myl7:EGFP or alpha-crystallin:Venus) to uncouple transgene detection from CCNF. In addition, studies to further investigate the failure to establish *CCNF* transgenic lines could be performed. For example, DNA could be extracted from embryos at 24 hpf to confirm transgenic integration, then repeated at later timepoints to establish whether cells that successfully integrate *CCNF* survive and to confirm if the loss of expressed CCNF is at a protein or DNA level. The presence of integrated *CCNF* DNA may assist in the elucidation of any gene silencing effects in the model.

The role of CCNF in regulating the cell cycle provides a possible explanation for the apparent toxicity of CCNF overexpression in the embryonic zebrafish. The cell cycle is highly regulated and the coordination of transcription, cell proliferation, migration, differentiation and apoptosis is essential for embryonic development [9] [12]. It is feasible that disruption to this highly regulated system associated with overexpression of CCNF in an organism undergoing rapid cell replication would have toxic effects.

It is likely that the toxicity reported here extends beyond CCNF. There is the potential for toxicity to arise when overexpression is introduced into a system and this is of importance during early development when vital systems such as the nervous system are being established. In particular, the generation of models of ALS (and likely most neurodegenerative diseases) may be fraught with difficulties as many of these genes are ubiquitously expressed during development before becoming restricted to the central nervous system [6] [13]. This suggests that the toxicity detailed here is not specific to CCNF expression during developmental stages and may be a factor in the establishment of other models.

To overcome this problem, we hypothesise that inducible transgenic lines, that allow for precise temporal control of gene expression will be necessary for the generation of novel models of ALS. The adoption of inducible transgenic lines such as the heat shock-inducible Cre line [14] [15] and Tet-on transgenic lines for doxycycline-inducible gene expression [16] will be crucial in establishing zebrafish models of ALS. Use of such lines will allow for temporal control of *CCNF* (or other ALS-linked genes) expression to be delayed until the fish matures beyond the developmental stage. We believe that this delay in expression will avoid the issues of early cell toxicity and allow for stable integration of the transgene in the germline, which in turn will facilitate transmission of transgene to the next generation. This would ultimately permit the development of transgenic overexpression CCNF-based zebrafish models of ALS. These inducible models are currently being generated and it is hoped that these models will yield insights into the biological mechanisms causing ALS as well as providing a platform for testing future therapeutics.

Additional Information

Methods and Supplementary Material

Please see https://sciencematters.io/articles/201802000012.

Ethics Statement

All husbandry and experimental procedures were performed in compliance with the Animal Ethics and Internal Biosafety Committees, Macquarie University (ARAs 2012/050 and 2015/034; NLRD 5201401007) (NSW, Australia).

Citations

[1] D'Angiolella Vincenzo et al. "Cyclin F-Mediated Degradation of Ribonucleotide Reductase M2 Controls Genome Integr ty and DNA Repair". In: *Cell* 149.5 (2012), pp. 1023–1034. DOI: 10.1016/j.cell.2012.03.043. URL: https://doi.org/10.1016/j.cell.2012.03.043.

[2] D'Angiolella Vincenzo et al. "SCFCyclin F controls centrosome homeostasis and mitotic fidelity through CP110 degradation". In: *Nature* 466.7302 (2010), pp. 138–142. DOI: 10.1038/nature09140. URL: https://doi.org/10.1038/nature09140.

[3] Emanuele Michael J. et al. "Global Identification of Modular Cullin-RING Ligase Substrates". In: *Cell* 147.2 (2011), pp. 459–474. DOI: 10.1016/j.cell.2011.09.019. URL: https://doi.org/10.1016/j.cell.2011.09.019.

[4] Monica Kong et al. "Cyclin F regulates the nuclear localization of cyclin B1 through a cyclin-cyclin interaction". In: *The EMBO Journal* 19.6 (2000), pp. 1378–1388. DOI: 10.1093/emboj/19.6.1378. URL: https://doi.org/10.1093/emboj/19.6.1378.

[5] Kelly L. Williams et al. "CCNF mutations in amyotrophic lateral sclerosis and frontotemporal dementia". In: *Nature Communications* 7 (2016), p. 11253. DOI: 10.1038/ncomms11253. URL: https://doi.org/10.1038/ncomms11253.

[6] Alison L. Hogan et al. "Expression of ALS/FTD-linked mutant CCNF in zebrafish leads to increased cell death in the spinal cord and an aberrant motor phenotype". In: *Human Molecular Genetics* 26.14 (2017), pp. 2616–2626. DOI: 10.1093/hmg/ddx136. URL: https://doi.org/10.1093/hmg/ddx136.

[7] Kawakami Koichi et al. "A Transposon-Mediated Gene Trap Approach Identifies Developmentally Regulated Genes in Zebrafish". In: *Developmental Cell* 7.1 (2004), pp. 133–144. DOI: 10.1016/j.devcel.2004.06.005. URL: https://doi.org/10.1016/j.devcel.2004.06.005.

[8] Koichi Kawakami, Akihiro Shima, and Noriko Kawakami. "Identification of a functional transposase of the Tol2 element, an Ac-like element from the Japanese medaka fish, and its transposition in the zebrafish germ lineage". In: *Proceedings of the National Academy of Sciences* 97.21 (2000), pp. 11403–11408. DOI: 10.1073/pnas.97.21.11403. URL: https://doi.org/10.1073/pnas.97.21.11403.

[9] L.K. Cole and L.S. Ross. "Apoptosis in the Developing Zebrafish Embryo". In: *Developmental Biology* 240.1 (2001), pp. 123–142. DOI: 10.1006/dbio.2001.0432. URL: https://doi.org/10.1006/dbio.2001.0432.

[10] Karl J. Clark et al. "Chapter 8 - Transgenic Zebrafish Using Transposable Elements". In: *Methods in Cell Biology- The Zebrafish: Genetics and Genomics and Informatics* 104 (2011), pp. 137–149. DOI: 10.1016/b978-0-12-374814-0.00008-2. URL: https://doi.org/10.1016/b978-0-12-374814-0.00008-2.

[11] Courtney M. Akitake et al. "Transgenerational analysis of transcriptional silencing in zebrafish". In: *Developmental Biology* 352.2 (2011), pp. 191–201. DOI: 10.1016/j.ydbio.2011.01.002. URL: https://doi.org/10.1016/j.ydbio.2011.01.002.

[12] Joseph C. Siefert, Emily A. Clowdus, and Christopher L. Sansam. "Cell cycle control in the early embryonic development of aquatic animal species". In: *Comparative Biochemistry and Physiology Part C: Toxicology and Pharmacology* 178 (2015), pp. 8–15. DOI: 10.1016/j.cbpc.2015.10.003. URL: https://doi.org/10.1016/j.cbpc.2015.10.003.

[13] Bettina Schmid et al. "Loss of ALS-associated TDP-43 in zebrafish causes muscle degeneration, vascular dysfunction, and reduced motor neuron axon outgrowth". In: *Proceedings of the National Academy of Sciences* 110.13 (2013), pp. 4986–4991. DOI: 10.1073/pnas.1218311110. URL: https://doi.org/10.1073/pnas.1218311110.

[14] Hans Stefan et al. "Generation of a non-leaky heat shock-inducible Cre line for cond tional Cre/lox strategies in zebrafish". In: *Developmental Dynamics* 240.1 (2010), pp. 108–115. DOI: 10.1002/dvdy.22497. URL: https://doi.org/10.1002/dvdy.22497.

[15] Christian Mosimann et al. "Ubiquitous transgene expression and Cre-based recombination driven by the ubiquitin promoter in zebrafish". In: *Development* 138.1 (2011), pp. 169–177. DOI: 10.1242/dev.059345. URL: https://doi.org/10.1242/dev.059345.

[16] Leah J. Campbell, John J. Willoughby, and Abbie M. Jensen. "Two Types of Tet-On Transgenic Lines for Doxycycline-Induc ble Gene Expression in Zebrafish Rod Photoreceptors and a Gateway-Based Tet-On Toolkit". In: *PLOS ONE* 7.12 (2012), e51270. DOI: 10.1371/journal.pone.0051270. URL:

https:
//doi.org/10.1371/journal.pone.0051270.

[17] Kwan Kristen M. et al. "The Tol2kit: A multisite gateway-based construction kit for Tol2 transposon transgenesis constructs". In: *Developmental Dynamics* 236.11 (2007), pp. 3088–3099. DOI: 10.1002/dvdy.21343. URL: https://doi.org/10.1002/dvdy.21343.

[18] Richard Mark White et al. "Transparent Adult Zebrafish as a Tool for In Vivo Transplantation Analysis". In: *Cell Stem Cell* 2.2 (2008), pp. 183–189. DOI: 10.1016/j.stem.2007.11.002. URL: https://doi.org/10.1016/j.stem.2007.11.002.

[19] Westerfield M. "The Zebrafish Book: A Guide for the Laboratory Use of Zebrafish Danio". In: *Eugene: Univ. of Oregon Press* (2000).

4.4   Results: Motor neuron expression of *CCNF*

4.4.1   Introduction

Generation and injection of the *actb2* and the *-3mnx1* driven constructs was per-formed concurrently. Attempts to establish the models that constitutively overex-pressed *CCNF* selectively in the motor neurons are detailed in this section.

4.4.2   No founders were identified in *-3mnx1_CCNF* injected zebrafish

Embryos injected with the *-3mnx1* constructs were screened for mCherry expression at 3 dpf. mCherry positive embryos were raised to maturity and their offspring screened as detailed in Paper 3. No founders were identified from six *-3mnx1*:mCherry_*CCNF* injected fish that survived to maturity. In comparison, three *-3mnx1*:mCherry injected fish were identified as founders from the eight raised to maturity (37.5% efficiency, Figure 4.2).

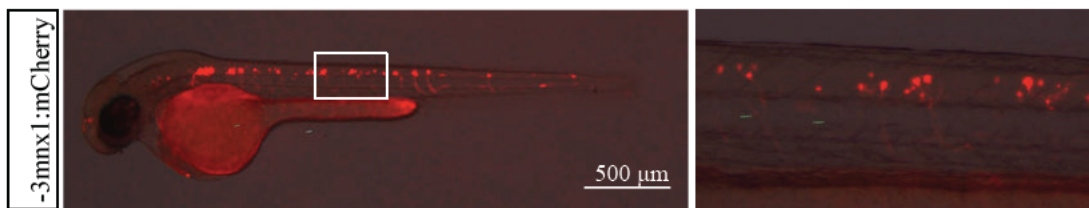FIGURE 4.2: **Representative image of *-3mnx1*:mCherry F1 embryo** demonstrating motor neuron expression of the fluorophore with no apparent off target effects.

4.4.3   Expression of *-3mnx1_CCNF* was lost over the first three days of development

Examination of *-3mnx1* driven mCherry expression at 24 hpf, 48 hpf and 72 hpf demon-strated that both the number of positive embryos and the number of positive cells

within each embryo increased over the first three days of development in the control group. In contrast, the number of mCherry positive embryos and the number of positive cells within each embryo declined in all *CCNF* expressing groups (Figure 4.3). These results reflected the findings from the *actb2*:mCherry_*CCNF* injected embryos presented in Paper 3.
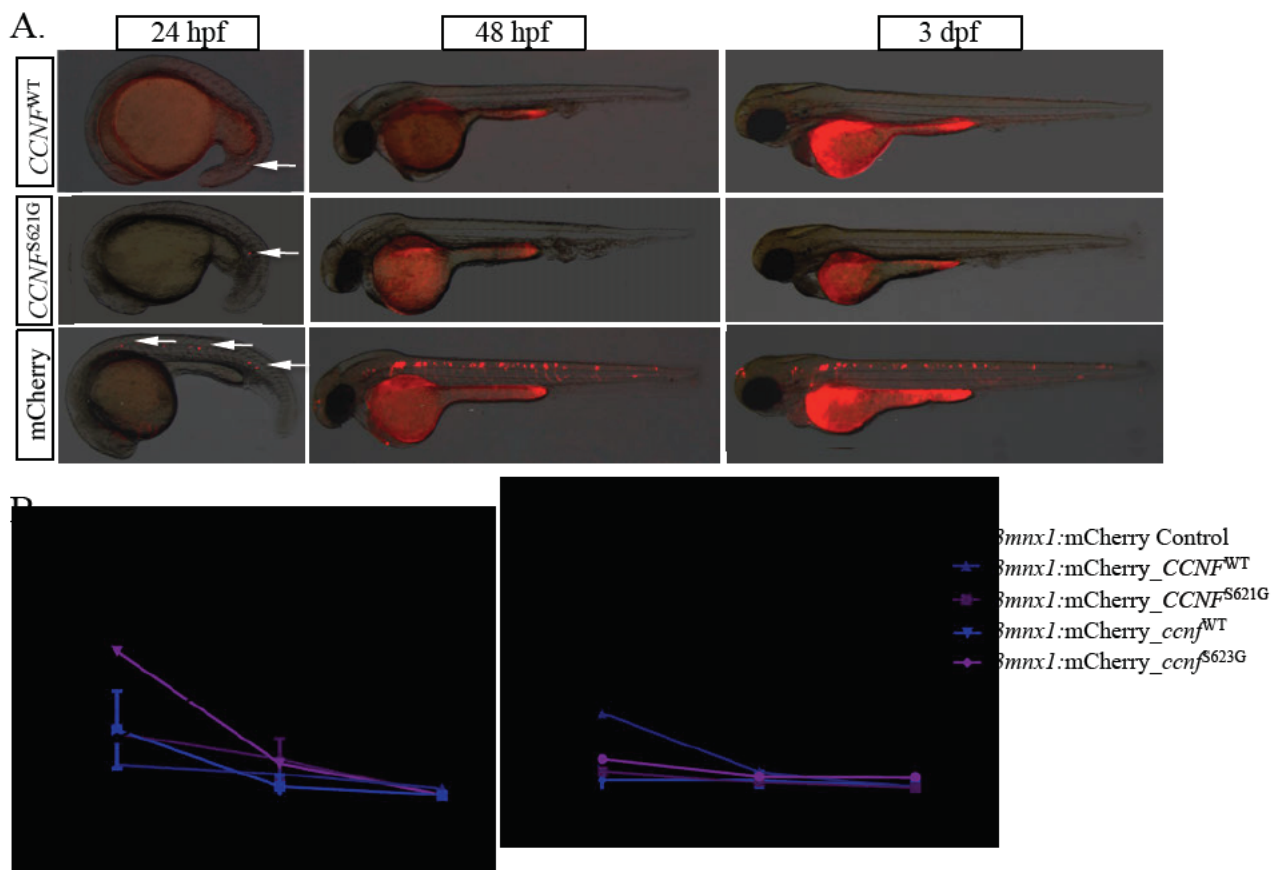
FIGURE 4.3: **Loss of mCherry expression in zebrafish injected with -*3mnx1* driven *CCNF*. A.** Representative images of a single fish from each injection group imaged at 1,2 and 3 dpf, demonstrating similar expression levels of mCherry in all three experimental groups at 24 hpf, followed by a progressive loss of expression in both the *CCNF* groups and an increase in expression in the control group. **B.** Quantification of the percentage of embryos per clutch demonstrating mCherry expression over the first 3 days of development (n=60 per group). **C.** Quantification of the average number of cells expressing mCherry per group over the first 3 days of development (n=5 per group).

4.5 Discussion

4.5.1 Summary

The results presented in this chapter indicate that constitutive overexpression of *CCNF* is not a feasible strategy for the development of transgenic zebrafish. The data suggests that overexpression of *CCNF* is toxic, leading to death of cells that successfully integrate either *CCNF* or *ccnf* into their genome. However, explanations other than toxicity are possible and further studies to investigate these are discussed in this section, as are alternative approaches that may circumvent the apparent toxicity demonstrated in this study.

4.5.2 Constitutive overexpression is not a feasible approach to develop *CCNF* transgenic zebrafish

Generation of the control *actb2* and *-3mnx1* mCherry transgenic lines occurred at expected rates of efficiency (50% and 37.5% respectively). In contrast, no *CCNF* transgenic lines were generated from 108 fish that were injected with a *CCNF* construct and raised to maturity. It is possible that continued screening of additional fish may have identified a founder. However, the random nature of transgene integration with the Tol2 system can lead to significant positional effects that have the potential to affect model phenotype (Wilson et al., 1990). In order to account for this, multiple wildtype and mutant transgenic lines are required to confirm an observed phenotype is consistently observed. Therefore, the failure to identify any *CCNF* transgenic founders from over 100 screened fish was a strong indication that establishing the multiple transgenic lines required for this study was not feasible using this strategy.

The successful establishment of mCherry control lines validated the experimental steps, including the injection technique, the Tol2 control construct design and cloning, the transposase mRNA activity and the screening process. The only variable

between the mCherry and *CCNF* groups was the size of the transgene that was integrated into the genome. The mCherry transgene was approximately 0.7 kb in size, while the *CCNF* transgene was approximately 3 kb. The Tol2 transposase system has been shown to carry transgenes up to 10 kb without any loss of efficiency (Clark et al., 2011). Therefore, this difference in size was unlikely to be a contributory factor in the failure to establish the *CCNF* transgenic lines.

The evidence presented in this chapter suggests that toxicity arising from constitutive overexpression of *CCNF* in the developing embryo was a more likely reason for the failure to establish these *CCNF* transgenic lines. While not previously reported in zebrafish, similar toxicity issues have been found to impede development of constitutive overexpression models of ALS in other species, including a *TARDBP* rat model (Zhou et al., 2010) and a *TARDBP*^M337V mouse model (Tian et al., 2011). This apparent toxicity is perhaps unsurprising given the roles that both *CCNF* and *TARDBP* play in essential cellular processes. It seems feasible that similar issues may arise in future studies that aim to establish *CCNF* transgenic lines in other species, and potentially in studies that aim to establish transgenic lines based on other ALS-linked genes. This suggests that a direct progression to inducible transgenic systems, or alternate transgenic strategies may be warranted in the development of future models of ALS.

4.5.3 Further Investigations

Correlation of *CCNF* expression and cell death

Data from the AO staining assay performed in this study suggests a relationship between *CCNF* overexpression and cell death in zebrafish embryos (Paper 3). This provides a basis for the hypothesis that toxicity associated with *CCNF* overexpression precluded development of these transgenic lines. While some correlation between AO staining and mCherry_*CCNF* expression was observed, the relationship between *CCNF*

and cell death could be further investigated to strengthen this hypothesis. One such study could take advantage of the live staining nature of AO, which allows repeated analysis of the same fish. By examining both mCherry expression (detectable from approximately 18 hpf) and AO staining at set intervals, the fate of cells expressing mCherry_*CCNF* could be to followed over the first few days of development. The feasibility of this approach has previously been demonstrated in a zebrafish model that overexpressed tau, a protein linked to both Alzheimers Disease and FTD (Paquet et al., 2009). These authors demonstrated a direct relationship between tau expression and cell death by repeatedly imaging AO stained embryos over a period of 12 hours. This analysis revealed that tau positive, AO negative cells undergo morphological changes characteristic of apoptosis. The cells were then shown to stain positive for AO before eventually becoming both tau and AO negative (Paquet et al., 2009).

Alternative causes for the failure to establish *CCNF* transgenic lines

While evidence presented in this study suggests that toxicity associated with *CCNF* overexpression in the developing embryo was the reason for the failure to establish transgenic lines, alternative explanations are feasible. A failure of transgene integration, death of *CCNF* positive offspring before screening or epigenetic silencing of the transgene could all explain the observations in this study. PCR amplification of mCherry from DNA extracted at 24 hpf and a second, later timepoint (such as 2 weeks) could be used to investigate these possibilities. Successful amplification of mCherry at 24 hpf would confirm integration of the transgene. Amplification of mCherry at 24 hpf, but not 2 wpf would support the hypothesis that cell death follows transgene integration. Amplification of mCherry at both 24 hpf and 2 wpf would suggest that either death of *CCNF* positive offspring prior to screening or silencing of transgene expression lead to the failure to identify founders in this study. Rapid epigenetic silencing of a stably integrated transgene has been reported in transgenic zebrafish (Goll et al., 2009; Akitake et al., 2011). However, silencing of expression at the rate required to explain the results presented in this study has not previously been

reported. Therefore, the more likely explanation in this case would be pre-screening death of *CCNF* expressing embryos. Such an occurrence would be difficult to detect due to the large size of zebrafish clutches (average 200 embryos Westerfield (2000)) and the typically small percentage of transgene positive offspring (average of 10-15%, Clark et al. (2011)).

4.5.4 Concluding remarks

The results presented in this chapter suggest that constitutive overexpression of *CCNF* was not a feasible strategy for the development of transgenic zebrafish. Due to time constraints, further investigation of the potential reasons underlying the failure of this approach were not performed. The aim of the project was to identify a strategy that lead to the development of viable transgenic *CCNF* models. Consequently, the project moved on to investigate an alternative strategy to establish these models. The strategy selected was make use of an inducible overexpression system. The rationale behind the selection of this approach and successful development of the *CCNF* inducible zebrafish models of ALS is detailed in Chapter 5.

5

Inducible overexpression of *CCNF*

5.1 Introduction

5.1.1 Introduction to the chapter

Two potential strategies to circumvent the apparent toxicity of *CCNF* overexpression in the developing embryo were considered for this project - one, the use of an inducible system to allow overexpression of *CCNF* to be delayed until the fish matured beyond the embryonic stage, and two, the use of genome editing tools to introduce the S621G mutation into the endogenous *ccnf* gene, thus avoiding potential toxicity associated with overexpression of the gene. The suitability of overexpression strategies to generate models that develop an ALS-relevant phenotype is well established (Chapter 1, Section 1.3.3). Specifically, the suitability of a mutant *CCNF* overexpression

model to reflect an ALS-relevant phenotype was established by the transient *CCNF* models presented in Chapter 3. Additionally, the ability of the inducible transgenic strategy to overcome toxicity associated with embryonic overexpression of a transgene (*TARDBP*) has been established (Zhou et al., 2010). For these reasons, and to best complement the already established transient model, the decision was made to proceed with an inducible transgenic strategy for development of the adult *CCNF* zebrafish models.

This chapter details the development and characterisation of zebrafish models that carry a doxycycline-inducible *CCNF* transgene. The use of the doxycycline-inducible system overcame the apparent toxicity associated with constitutive overexpression of *CCNF* detailed in Chapter 4, thereby enabling the development of *CCNF* transgenic lines. This chapter begins with an overview of the inducible systems available for use in zebrafish, with a focus on the doxycycline-inducible system. This is followed by an explanation of the rationale behind the design of the doxycycline-inducible *CCNF* models. Data from this study is presented in four sections:

- Section 5.3 describes characteristics of the doxycycline-inducible system that were observed in this study.
- Section 5.4 details the development and characterisation of models in which ubiquitous expression of *CCNF* was induced in adult zebrafish. The results from this study are presented in a manuscript that has been prepared for submission to *Disease Models and Mechanisms* (Manuscript 1).
- Section 5.5 details the characterisation of zebrafish in which ubiquitous expression of *CCNF* was induced in the embryonic stage.
- Section 5.6 describes efforts to establish zebrafish models in which *CCNF* was selectively expressed in the motor neurons.

The chapter concludes with a discussion of the success and limitations of the inducible

CCNF models, further work required to complete characterisation of the models and potential studies for which the models may prove suitable.

5.1.2   Inducible transgenic systems

Like constitutive overexpression models, these inducible systems express a randomly integrated transgene at greater than physiological levels under the control of an exogenous promoter (Elder et al., 2010). For this reason, appropriate transgenic wildtype counterparts are required to ensure that an observed phenotype is a consequence of the presence of a disease-linked mutation rather than an overexpression effect. Additionally, due to positional effects associated with the random integration of a transgene, multiple lines are required to ensure consistency of an observed phenotype.

Despite these limitations, overexpression models do have significant advantages over genome edited models in which expression of a mutation remains at physiological levels. Firstly, overexpression of a mutant transgene is more likely to induce a disease-relevant phenotype in a short-lived species, such as zebrafish (Dawson et al., 2010). Secondly, this overexpression often produces models that display an accelerated disease course, allowing the study of adult onset disease in young animals (Dawson et al., 2010). This is particularly advantageous in diseases such as ALS, where the average age on onset is 50-60 years (McCombe and Henderson, 2010). Finally, inducible overexpression strategies permit the use of exogenous promoters, which permit spatial control over gene expression. This facilitates study of the effects of a disease-linked mutation in specific cells types, avoids toxicity in vulnerable cell-types that are not relevant to disease, and provides the potential to unravel cell autonomous and non-cell autonomous mechanisms involved in disease.

Multiple inducible transgenic systems are available for use in zebrafish. These systems utilise either DNA recombination or transcriptional transactivation to induce transgene expression. Both approaches have advantages and limitations. The

advantage of transcriptional transactivation systems is that the induction of transgene expression is reversible (Lewandoski, 2001). The key limitation of these systems is that they are binary - they require two transgenes to be inserted into the genome, one of which carries the gene of interest and a second that encodes a transcriptional activator protein (Lewandoski, 2001). This binary nature compounds positional effects associated with the random integration of the transgenes into the genome (discussed in Chapter 4, Section 4.5.2). Consequently, highly variable expression levels of the protein of interest are often observed across different inducible lines (Lewandoski, 2001). This necessitates the development of multiple lines and determination of the expression levels in each to identify wildtype and mutant lines with similar expression levels.

The principles of the most commonly used inducible transgenic systems in zebrafish are detailed in this section. These systems include a DNA recombination system, the Cre-Lox system, (Jaisser, 2000) and two transcriptional transactivation systems, the modified Gal4-UAS system (Ornitz et al., 1991) and the tetracycline-regulated system (Gossen and Bujard, 1992).

The Cre-Lox system

The Cre-Lox system utilises Cre, an enzyme that catalyses the recombination of specific DNA sequences called LoxP sites (Metzger and Feil, 1999). A DNA segment that lies between two LoxP sites is termed floxed DNA. Floxed DNA is excised upon Cre-mediated recombination (Jaisser, 2000). To develop inducible zebrafish, transgenes are generated that carry floxed DNA, for example a fluorophore that carries a STOP codon. This floxed DNA is inserted upstream of a gene of interest. The floxed DNA inhibits expression of the gene of interest until its excision through the activation of Cre.

Temporal control of gene expression with the Cre-Lox system is enabled through the use of a heat shock promoter (*hsp70l*, Hans et al. (2009)), a modified oestrogen-binding

domain of the human oestrogen receptor (ERT, Feil et al. (1996)), or a combination of both (Hans et al., 2011). A key limitation of Cre-lox systems that utilise heat shock and/or oestrogen inhibition to induce expression of a transgene is that both induction methods have potential pleiotropic effects. Heat shock has been shown to induce cell stress and alter neutrophil activity (Lam et al., 2013) as well as disturb somite formation in the zebrafish embryo, leading to defective axonal outgrowth, a significant limitation for models of ALS (Roy et al., 1999). Exposure to tamoxifen has been also been shown to have (mild) effects on development in zebrafish by altering the expression of multiple endocrine-related proteins (Xia et al., 2016).

Modified Gal4-UAS system

The Gal4-UAS system utilises the transcriptional activator protein, Gal4 which binds to a specific DNA sequence, termed an upstream activator sequence (UAS). One transgene in this binary system carries a tissue specific promoter that drives expression of Gal4, which is typically fused to a portion of the herpes simplex virus protein, VP16 (Sadowski et al., 1988). The second transgene carries the UAS upstream of the gene of interest. Tissue specific binding of Gal4 to UAS activates transcription of the gene of interest (Ornitz et al., 1991). Multiple methods have been developed to provide temporal control of Gal4 expression, including the use of the ERT promoter (Akerberg et al., 2014) and the use of a temperature-sensitive Gal4 repressor protein (GAL80ts) (Fujimoto et al., 2011).

While the Gal4-UAS system is well established in zebrafish (reviewed in Asakawa and Kawakami (2008)), it does have significant disadvantages. In addition to the binary nature of the system and the potential pleiotropic effects of heat shock and hormone induction, the Gal4-UAS system has a high propensity for transgene silencing across generations (Asakawa and Kawakami, 2008; Halpern et al., 2008). Indeed, the loss of transgene expression from one generation to the next is so pronounced with the

Gal4-UAS system, that Gal4-UAS zebrafish models have been proposed as a useful tool to study the basis of transcriptional gene silencing (Goll et al., 2009; Akitake et al., 2011).

Tetracycline-regulated system

The first tetracycline-regulated system was developed in 1992 and was based on two key components – a trans-activator protein (tTA) and a tetracycline response element (TRE) (Gossen and Bujard, 1992). The tTA is a fusion protein consisting of a modified tetracycline resistance gene found in *E coli* and a transcriptional activating domain of the herpes simplex virus. The TRE consists of a series of repeated tetracycline operator (TetO) sequences (TCCCTATCAGTGATAGAGAA) located upstream of a minimal promoter derived from the human *CMV* promoter. Under normal conditions, tTA binds to the TetO sequences and this binding initiates transcription from the minimal promoter. Binding of tetracycline, or derivatives such as doxycycline, to tTA induces a conformational change in the protein that inhibits its binding to the TetO sequence, thereby inhibiting transcription. (Gossen and Bujard, 1992). This original system is termed the Tet-Off system, the principles of which are shown in Figure 5.1.

For greater flexibility, a converse system the Tet-On system was developed in 1995. Gossen et al. (1995) developed this system by randomly mutating the tTA protein and selecting for a mutant version that functions in a reverse fashion, termed reverse trans-activator protein (rtTA). The conformational change induced by tetracycline, or one of its derivatives, to rtTA enables the binding of the protein to the TetO sequence, thus activating transcription. The principles of this Tet-on system are shown in Figure 5.1).
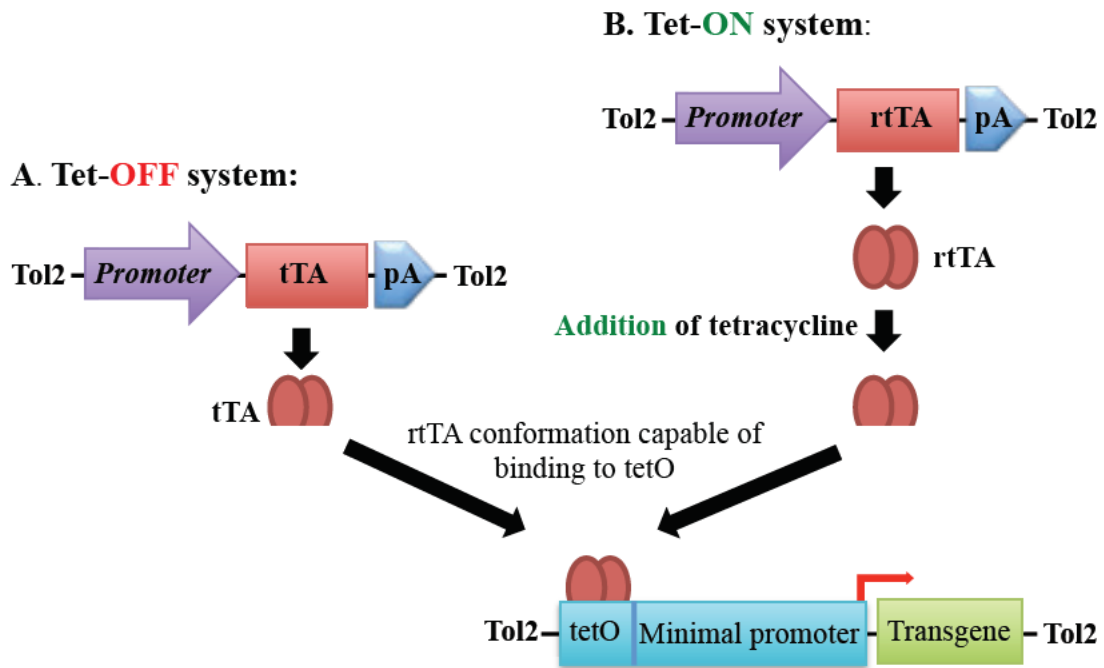
FIGURE 5.1: **Principles of the tetracycline-regulated systems.** Expression of the tTA protein (Tet-off system) or the rtTA protein (Tet-on system) is tissue specific. **A.** In the absence of doxycycline, tTA binds to the tetO sequence in the responder transgene, activating the minimal promoter and driving expression of the transgene. **B.** The addition of doxycycline alters the structure of rtTA , allowing it to bind to the tetO sequence, thus activating the minimal promoter.

Various modifications to the original tTa, rtTA and TRE elements detailed by Gossen and Bujard (1992) and Gossen et al. (1995) have provided increased stability, reduced background activity, increased sensitivity to tetracycline and reduced leakage of the system (Urlinger et al., 2000; Baron et al., 1997; Agha-Mohammadi et al., 2004; Loew et al., 2010). This optimisation has lead to the use of tetracycline-regulated systems for the development of multiple animal models of ALS. Significantly, for this study, the Tet-off system has been used to circumvent toxicity associated with constitutive overexpression of the ALS-linked $TARDBP^{M337V}$ transgene in the rat (Zhou et al., 2010). Additional tetracycline-regulated models of ALS in the rat include a ubiquitously expressing FUS^{R521C} model (Huang et al., 2011) and a model in which $TARDBP^{M337V}$ was selectively expressed in the motor neurons (Huang et al., 2012).

Two tetracycline-regulated mouse models of ALS have also been established, both of which express *TARDBP* with a silenced nuclear localisation sequence (*TARDBP*$^{\Delta \text{NLS}}$) (Walker et al., 2015; Igaz et al., 2011).

To date, no doxycycline inducible models of ALS, or other neurodegenerative diseases have been reported in zebrafish. However, multiple studies have demonstrated the utility of the system in this species. The first of these studies was Huang et al. (2005) who used the system to produce a model with inducible expression of GFP in the myocardium. Subsequent zebrafish studies have demonstrated successful transgene induction in a variety of tissues (Knopf et al., 2010; Campbell et al., 2012; West et al., 2014; Wehner et al., 2015; Li et al., 2013b). Key amongst these studies was Campbell et al. (2012), who developed zebrafish models in which expression of a fluorescent reporter in the photoreceptors was regulated by doxycycline. To develop these models, the authors compiled a "Tet-On toolkit" consisting of a range of Tol2-compatible entry vectors for use in the generation of doxycycline-inducible zebrafish models. The development of this toolkit greatly enhanced the flexibility and efficiency of generation of subsequent models.

5.1.3   Design of the inducible *CCNF* zebrafish models

The tetracycline-regulated system was selected for this study due the ease of construct generation with the Tet-on toolkit (Campbell et al., 2012), the reversibility of the system and the ease of induction with tetracyclines. Additionally, unlike the Gal4-UAS system, loss of transgene expression across generations has not previously been reported with the tetracycline-regulated system. Within the tetracycline-regulated system, the Tet-on system was selected for this study and the tetracycline derivative doxycycline was used to induce expression of *CCNF*. The rationale behind these selections is discussed in this section.

Tetracyclines

Tetracyclines are broad-spectrum antibiotics that bind to the 30S ribosomal subunit of bacteria, thereby inhibiting protein synthesis. A range of tetracycline derivatives have shown efficacy in the tetracycline-regulated system. However, doxycycline is the most commonly used tetracycline in animal models due to its low cost, its high affinity for both tTA and rtTA proteins (Krueger et al., 2004) and its low toxicity (Agwuh and MacGowan, 2006). Additionally, doxycycline has been shown to have good tissue distribution, which importantly for this study, includes penetration through the blood brain barrier (Domercq and Matute, 2004). For these reasons, doxycycline was selected for use in this study.

The stability of doxycycline in water under different environmental conditions has been investigated in multiple studies. Honnorat-Benabbou et al. (2001) demonstrated that doxycycline remained stable in tap water at 37 °C for one week and Redelsperger et al. (2016) demonstrated that doxycycline remained stable in reverse osmosis purified water (RO water) at 23 °C for one week. While mild variations in temperature did not appear to affect the stability of doxycycline, the pH of the water did, with higher acidity found to extend its duration of activity (Redelsperger et al., 2016). Tetracyclines absorb ultraviolet light and are therefore considered to be photosensitive (Zakeri and Wright, 2008). However, the stability of doxycycline has been shown to be unaffected by exposure to light (Redelsperger et al., 2016). As a result of these studies, the doxycycline used in this study was replenished weekly and the pH of all tanks was monitored daily. As a precaution, the doxycycline treated water was also protected from direct exposure to light.

Tet-on system

The aim of this study was to use an inducible system to allow expression of the *CCNF* transgene to be delayed until the fish matured beyond the embryonic stage.

This aim could have been achieved using either the Tet-on system or the Tet-off system. Use of the Tet-off system would have required embryos to be exposed to doxycycline from fertilisation to prevent embryonic expression of the *CCNF* transgene. Evidence indicates that embryonic exposure to doxycycline can induce dose-dependant developmental delays in zebrafish, including delayed hatching, reduced body length, increased yolk sac area and impaired inflation of the swim bladder (Zhang et al., 2015b). Elevated levels of oxidative stress and cell death have also been associated with embryonic exposure to doxycycline at concentrations as low as 10 µg/l (Zhang et al., 2015b). To avoid these potential side effects, the Tet-on system was selected for this study.

Construct design

Two driver lines were developed for the Tet-on models in this study - one in which rtTA was expressed ubiquitously (*actb2* promoter) and one in which expression was restricted to the motor neurons (*-3mnx1* promoter). The rationale for the use of these promoters was discussed in Chapter 4, Section 4.1.4. Responder lines were designed to express human *CCNF* (wildtype or S621G mutant) with a N-terminal EGFP fluorophore. The EGFP fluorophore was selected in preference to mCherry due to a reported propensity for the mCherry protein to aggregate (Snaith et al., 2010). Human *CCNF* was selected in preference to the zebrafish *ccnf* orthologue to reflect the transient overexpression models previously established (Chapter 3).

To allow selection of embryos that successfully integrated a transgene into their genome, the driver and responder line constructs were designed to carry a cardiac reporter (*myl7* promoter) that was expressed independently of doxycycline induction. One vector was available in the Tol2kit Kwan et al. (2007) that carried a *myl7*:EGFP reporter. This vector was used in the driver line constructs. A second, novel vector with a *myl7*:FusionRed cardiac reporter was developed in this study for use in the responder line constructs. Design of this novel vector is details in Manuscript 1.

The zebrafish models generated from these constructs are the first reported *in vivo* models that stably express an ALS-linked mutation in *CCNF*. These models are also the first inducible zebrafish models of ALS. The data presented in Manuscript 1 suggests that induction of ubiquitously expressed $CCNF^{\text{S621G}}$ in adult zebrafish produces models that will prove useful in further studies investigating the biology of ALS.

5.2 Chapter-Specific Methods

The methods detailed in Manuscript 1 are shown in Table 5.1. Additional methods used in this study are detailed in this section.

TABLE 5.1: Methods described in Manuscript 1.

Section	Technique
Molecular methods	Generation of driver and responder line constructs
	Generation of transposase mRNA
Zebrafish assays	Microinjection of Tol2 cosntructs
	Generation of double transgenic lines
	Induction of gene expression
	Assessment of motor functon (adult swimmig behaviour)
	Tissue fixation
	Cryosectioning of frozen zebrafish sections
	Cresyl Violet staining for motor neuron counts
	Western blotting

5.2.1 Cloning

Generation of constructs

The Tol2 system was used to generate the doxycycline-inducible models (Chapter 2, Section 4.3). Three experimental groups were established for this study - one that expressed a fluorophore (EGFP) to control for the effect of the florescent reporter on model phenotype, one that expressed EGFP-tagged $CCNF^{\text{WT}}$ to control for the effect

of overexpression of *CCNF* and one that expressed $CCNF^{\text{S621G}}$. The recombination reactions used in the study are shown in table 5.2, using the methods described in in Chapter 2, Section 2.2.1.

TABLE 5.2: LR reactions performed to generate the doxycycline-inducible expression constructs

5' vector	Middle Entry Vector	3' vector	Destination vector
p5E:*actb2*	pME:rtTA	p3E:pA	Tol2:*myl7*:CG2
p5E:*3mnx1*	pME:rtTA	p3E:pA	Tol2:*myl7*:CG2
p5E:TRE	pME:EGFPns	P3E:$CCNF^{\text{WT}}$	Tol2:*myl7*:FusionRed
p5E:TRE	pME:EGFPns	P3E:$CCNF^{\text{S621G}}$	Tol2:*myl7*:FusionRed
p5E:TRE	pME:EGFPns	polyA	Tol2:*myl7*:FusionRed

Restriction site digests

Constructs were selected for Sanger sequencing based on restriction enzyme digests. Digests were performed as described in Chapter 2, Section 2.2.4 using restriction enzymes shown in Table 5.3.

TABLE 5.3: Restriction digests performed to select constructs for sequence validation.

Construct	Restriction enzyme	Product size
actb2:rtTA	BamH1 and Not1	7kb and 3 kb
-3mnx1:rtTA	BamH1 and Not1	7kb and 1 kb
TRE:EGFP_*CCNF*	Xho1	5.8 kb and 3.6 kb
TRE:EGFP	BamH1 and Xhol1	6.7kb, 350bp and 106 bp

5.2.2   Generation of inducible models

Establishing double transgenic lines

Instability of transgene inheritance has been reported in doxycycline-inducible zebrafish that carry both the driver and responder transgene (Personal communication from the Jensen Laboratory, developers of the Tet-on toolkit). To avoid issues associated with unpredictable inheritance, separate driver and responder lines were established to the second (F2) generation as detailed in Manuscript 1. A minimum of three transgenic lines were established for each driver and responder group. The

F2 generations of the driver and responder lines were then crossed, and their offspring (F3) used for analysis. Only morphologically normal embryos which demonstrated similar expression levels, as assessed by fluorescent microscopy, were selected.

Induction of transgene expression

Doxycycline (Sigma Aldrich) was diluted to a working concentration of 20 µg/ml as detailed in Manuscript 1. For embryonic induction, 20 µg/ml doxycycline was added to petri dishes which were incubated at 28 °C. For adult induction, fish were taken off the main system and placed in individual 3.5 litre tanks. Direct exposure to light was prevented with foil covering of tank lids. A 10% water change was performed twice weekly and fresh doxycycline added weekly. Water parameters, including pH and conductivity were checked daily.

5.2.3 Zebrafish assays

Examination of cardiac oedema following embryonic induction

Severe cardiac oedema was observed in embryos following induction of transgene expression at fertilisation. To investigate whether cardiac oedema would develop following later induction of transgene expression, $CCNF^{\text{WT}}$ and $CCNF^{\text{S621G}}$ clutches (3 clutches per group) were pooled, then separated into four groups. The four groups were induced at 24 hourly intervals, with the first group induced at fertilisation. Five days after the addition of doxycycline, embryos were screened to establish whether they were single or double transgenic, then classified as positive (detectable cardiac oedema at 5 X magnification) or negative (no detectable cardiac oedema at 5 X magnification).

Immunohistochemistry analysis of adult zebrafish sections

Frozen sections of adult zebrafish prepared as described in Manuscript 1 were thawed at room temperature and washed 3 X 5 minutes PBST. Sections were blocked in

10% bovine serum albumin (BSA) for 1 hour at room temperature, and incubated in primary antibody in 10% BSA overnight at 4 °C. Primary antibodies used were rabbit TDP-43 C-terminus 1:500 (Cosmo Bio) and rabbit Ubiquitin 1:500 (Cell Signalling Technology). Following incubation, sections were washed in PBST, then incubated in alexafleur 594 donkey anti rabbit secondary antibody 1:300 (Invitrogen) for 1 hour at room temperature in the dark. Sections were mounted with Vectrashield fluorescence mounting medium with DAPI.

5.3   Results: Characterisation of the doxycycline-inducible system in zebrafish

5.3.1   Introduction

The doxycycline-inducible system has not yet been widely used in zebrafish, therefore the characteristics of the system in this species are not well established. Two key issues have been identified in inducible systems that have been more commonly used in zebrafish - leakage of transgene expression (predominantly seen with the Cre-Lox system) and transgenerational loss of transgene expression (commonly seen with the Gal4-UAS system). This study aimed to investigate whether these issues were evident in the *CCNF* doxycycline-inducible zebrafish to provide an indication of the relative advantages and limitations of the system in this species.

5.3.2   Transgene expression without induction

The doxycycline-inducible system is reported to demonstrate lower incidence of transgene expression without induction than other commonly used transgenic systems (Knopf et al., 2010). To assess the accuracy of these reports, the incidence of ubiquitous expression of EGFP in embryos not exposed to doxycycline was quantified. 0.7% of EGFP embryos (1 of 138), 1.1% of $CCNF^{\text{WT}}$ embryos (1 of 88) and 1.7% of

$CCNF^{S621G}$ embryos (1 of 120) demonstrated detectable expression of the transgene
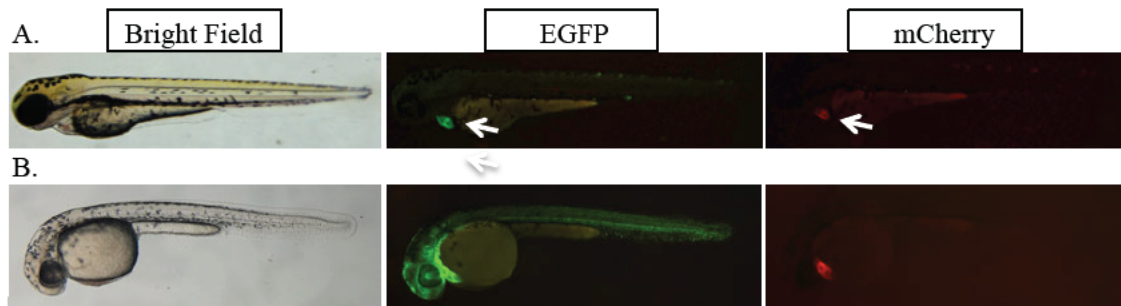without exposure to doxycycline (Figure 5.2).

FIGURE 5.2: **Leakage of transgene expression in doxycycline-inducible zebrafish.**
A. Zebrafish embryo not exposed to doxycycline. Both driver (green cardiac reporter) and
responder (red cardiac reporter) transgenes were present within the embryo, however no ubiq-
uitous expression of EGFP was evident. **B.** A small percentage of embryos did demonstrated
some ubiquitous expression of the EGFP fluorophore without exposure to doxycycline .

5.3.3 Duration of transgene expression following doxycycline exposure

Expression of a transgene (EGFP or EGFP fused *CCNF* was evident in all double
transgenic embryos 24 hours after the addition of doxycycline. To determine how
long expression of the transgene persisted without continued exposure to doxycycline,
embryos that carried the EGFP transgene were removed from the doxycycline treated
water and imaged at 24 hourly intervals. Consistent exposure and gain settings were
used for each image, which demonstrated persistent expression of the EGFP transgene
at 8 days post doxycycline removal. Beyond this timepoint, expression progressively
declined (Figure 5.3.

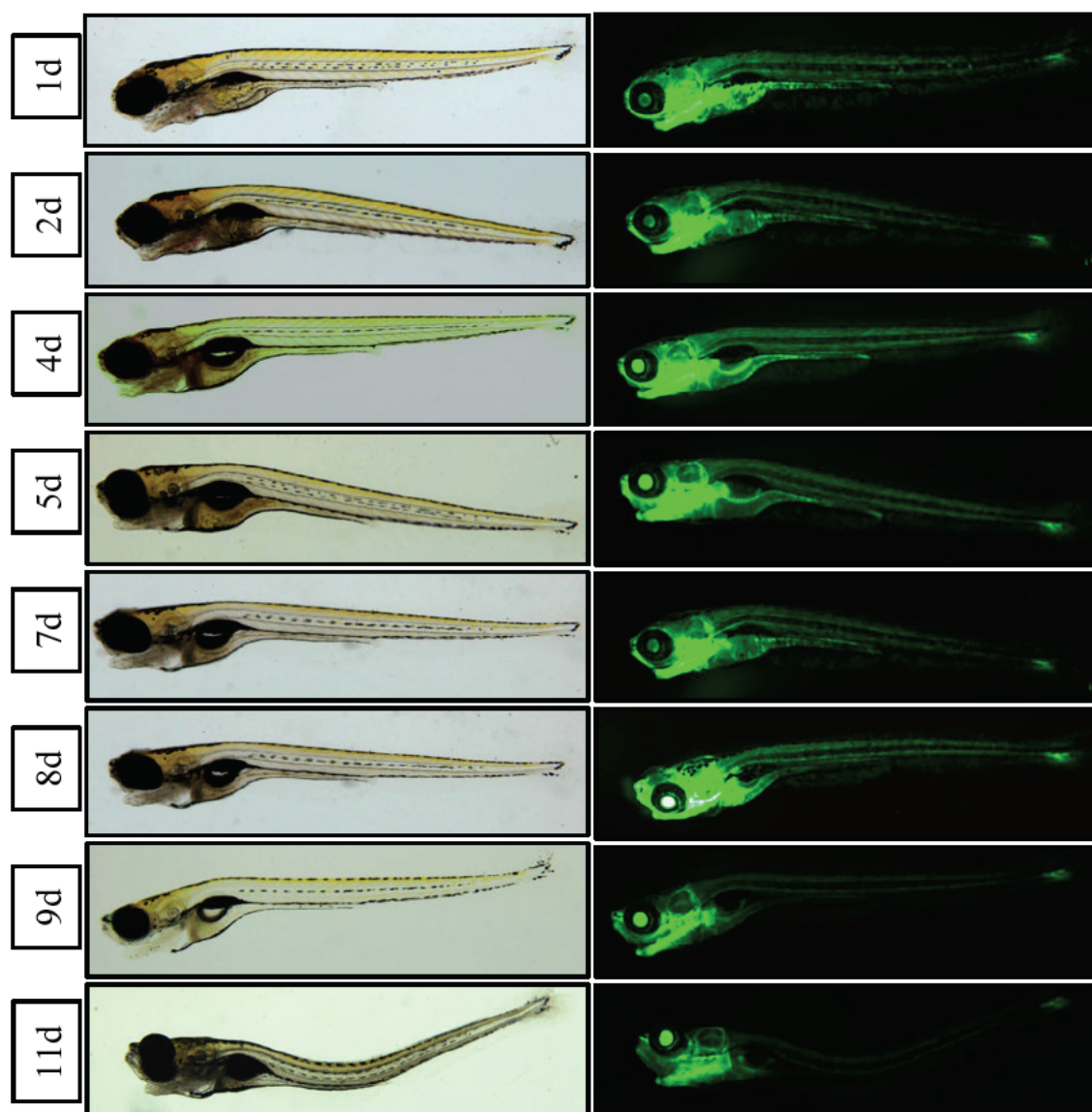FIGURE 5.3: **Duration of expression of the EGFP transgene following withdrawal of doxycycline.** Expression of EGFP was evident after 24 hours of doxycycline exposure. This expression was found to persist in the absence of doxycycline for eight days, beyond which, expression progressively declined. All images taken of the same fish, with a consistent exposure time of 640 and a gain setting of 1.

5.4 Results: Induction of ubiquitous *CCNF* expression in adult zebrafish

5.4.1 Introduction

The primary goal of this study was to establish models in which *CCNF* was persistently expressed in adult zebrafish, to provide tools to complement the transient models presented in Chapter 3. To achieve this aim, zebrafish that carried both the driver and responder transgenes were raised to maturity (3 mpf) before induction of *CCNF* expression. The data from this study is presented as a Manuscript which has been prepared for submission to *Disease Models and Mechanisms*.

5.4.2 Manuscript 1

Declaration of contributions All experiments presented in this manuscript were performed by AH. SG assisted with microinjection of the expression constructs into zebrafish embryos. All authors contributed intellectual input and provided input to the editing of the manuscript.

A doxycycline-inducible adult zebrafish model of ALS

Alison L. Hogan*[1], Emily K. Don[1], Angela Laird[1], Sharron Chow[1], Serene Gwee[1], Jennifer A. Fifita[1], Tom Hall[2], Nicholas J. Cole[1], Ian P. Blair[1]

[1]Centre for MND Research, Department of Biomedical Sciences, Faculty of Medicine & Health Sciences, Macquarie University, North Ryde, NSW, 2109, Australia.

[2] Institute for Molecular Bioscience, University of Queensland, Brisbane, QLD, 4072, Australia

Summary statement

This study presents a transgenic zebrafish model that inducibly expresses an ALS-linked mutation in *CCNF*. This model provides a novel tool with which to investigate the biology of *CCNF* mutations.

Abstract

Amyotrophic lateral sclerosis (ALS) is an adult onset neurodegenerative disease characterised by rapidly progressive death of motor neurons. The disease is invariably fatal, typically resulting in patient death within three to five years of symptom onset. The only established causes of ALS are gene mutations. Novel ALS-linked mutations were recently reported in *CCNF*. Cyclin F, encoded by *CCNF,* is an E3 ubiquitin ligase protein, involved in regulating protein degradation through the ubiquitin proteasome system. Evidence suggests that disruption to protein homeostasis is a key feature of ALS biology and ALS-linked mutations in *CCNF* provide an opportunity to develop novel disease models to study dysfunction in this pathway. This study presents a transgenic animal model of ALS-linked mutant *CCNF*. The model was developed in the zebrafish using the doxycycline inducible system, allowing both temporal and spatial control of *CCNF* expression. Ubiquitous expression of mutant *CCNF* in adult zebrafish led to a progressive loss of motor function and a significant reduction in motor neuron number within the spinal cord. These findings suggest that the doxycycline inducible zebrafish models will be useful tools for investigating the mechanisms of ALS-linked mutant *CCNF* in an adult model.

Introduction

Amyotrophic lateral sclerosis (ALS) is characterised by the rapidly progressive death of motor neurons. This neuronal death leads to spasticity and wasting of the skeletal muscles which affects movement, speech, swallowing and breathing. Current treatments for ALS have limited clinical benefit and patients typically die as a result of respiratory complications within 2-5 years of

symptom onset (Rowland, L. P. & Shneider 2001). ALS is linked clinically, pathologically and genetically to a form of presenile dementia - frontotemporal dementia (FTD) (Ling et al. 2013). Clinically, there is significant overlap between the two conditions, with up to 50% of ALS patients found to develop some degree of cognitive impairment (Ringholz et al. 2005). Pathologically, the two conditions are linked by their hallmark pathology - the formation of ubiquitin positive protein aggregates in the cytoplasm of affected neurons (Ling et al. 2013). Furthermore, over 95% of ALS patients and 50% of FTD patients, these aggregates contain a common protein – TDP-43 (Neumann et al. 2006). Genetically, approximately 10% of ALS cases (Kirby et al. 2016) and 20-40% of FTD cases (Rohlfing & Tu 2017) present familial inheritance of the disease, and mutations common to both diseases have been identified in multiple genes (Guerreiro et al. 2015). Mutations in *CCNF* were recently linked to both diseases, accounting for 0.6 to 3.3% of ALS/FTD cases (Williams et al. 2016). Cyclin F, encoded by *CCNF* is a E3 ubiquitin ligase, a substrate recognition component of the ubiquitin proteasome system (UPS) and consequently, a regulator of protein degradation (reviewed in Galper et al. 2017).

Multiple converging mechanisms have been proposed to contribute to the onset and progression of ALS/FTD, key amongst them being disruption to the tightly regulated protein homeostatic pathways (Ling et al. 2013). The role of cyclin F in the UPS suggests that altered protein degradation may be a mechanism of ALS/FTD-linked mutations in *CCNF*. Indeed, ALS/FTD-linked mutant *CCNF (CCNF^{S621G})* has been shown to induce dysfunction in this pathway *in vitro*. Analysis of Neuro-2a and SH-SY5Y cells transfected with *CCNF^{S621G}* demonstrated altered ubiquitination of cyclin F substrates and an overall accumulation of ubiquitinated proteins (Lee et al. 2017). This study also demonstrated that expression of *CCNF^{S621G}* was associated with disruption to another protein degradation pathway, autophagy (Lee et al. 2017). These findings strongly implicate aberrant protein degradation in the biology of mutant *CCNF*.

To date, a single animal model has been reported with which to investigate *CCNF*-associated dysfunction *in vivo* - a transient zebrafish model that overexpressed human mutant *CCNF (CCNF^{S621G})* (Hogan et al. 2017). These zebrafish developed an ALS-relevant phenotype that included a motor neuron axonopathy and impaired motor function, indicating the potential suitability of overexpression zebrafish models to study ALS-linked mutations in *CCNF*. Transient models have significant value in investigative studies and the preliminary testing of potential therapeutics. However, transgenic models provide highly useful complementary tools to allow longitudinal studies that examine the cellular and molecular changes that occur as the disease

progresses. Additionally, transgenic models provide the opportunity to model adult onset diseases such as ALS and FTD in an adult model.

This study presents one such model in the zebrafish. The suitability of zebrafish to model human neurodegenerative diseases is well established (Santoriello et al. 2012) . Further, significant similarities have been demonstrated between human cyclin F and the zebrafish homologue (Hogan et al. 2017), which suggests similar functions of the protein in the two species and consequently, the suitability of zebrafish to model disease-linked mutations in *CCNF*. As disease models, zebrafish have the advantage over mammalian species with respect to the speed and ease of model generation and the costs associated development and maintenance. The *CCNF*-based zebrafish model was developed using the doxycycline inducible system (Campbell et al. 2012), which provides both temporal and spatial control over expression of the *CCNF* transgene. This system allowed expression of *CCNF* to be delayed until the zebrafish reached maturity, thus circumventing potential problems associated with overexpression of a disease-linked gene in the embryonic stage of development.

Zebrafish in which expression of ALS/FTD-linked mutant *CCNF (CCNF^{S621G})* was induced at maturity (three months post fertilisation, mpf) demonstrated progressively impaired motor function and a reduced number of motor neurons in their spinal cords. These findings suggest that the inducible *CCNF* zebrafish will be suitable tools with which to investigate the mechanisms of mutant *CCNF*.

Results

Doxycycline induction of EGFP-tagged *CCNF* in adult zebrafish

The constructs used to generate the inducible *CCNF* zebrafish are shown in (**Fig. 1A**). The driver line construct carried a ubiquitous promoter (*actb2)* and a transcriptional activator protein (rtTA). The responder lines carried a tetracycline response element (TRE) upstream of either EGFP or EGFP-tagged *CCNF* (WT or S621G). Once established to the F2 generation, the driver and responder transgenic lines were crossed and double transgenic embryos selected for analysis. This generated three experimental groups – EGFP, *CCNF*^{WT}, and *CCNF*^{S621G}. Addition of doxycycline to the water of adult zebrafish induced ubiquitous expression of the EGFP, *CCNF*^{WT} and *CCNF*^{S621G} transgenes within 24 hours. Level of transgene expression was comparale between the *CCNF*^{WT} and *CCNF*^{S621G} experimental groups (**Fig. 1B**). Importantly for this study, transgenic expression was confirmed in both adult fish (**Fig. 1C**) and in the central nervous system (**Fig. 1D).** Following withdrawal of the doxycycline, transgene expression was found to persist for a minimum of a week.
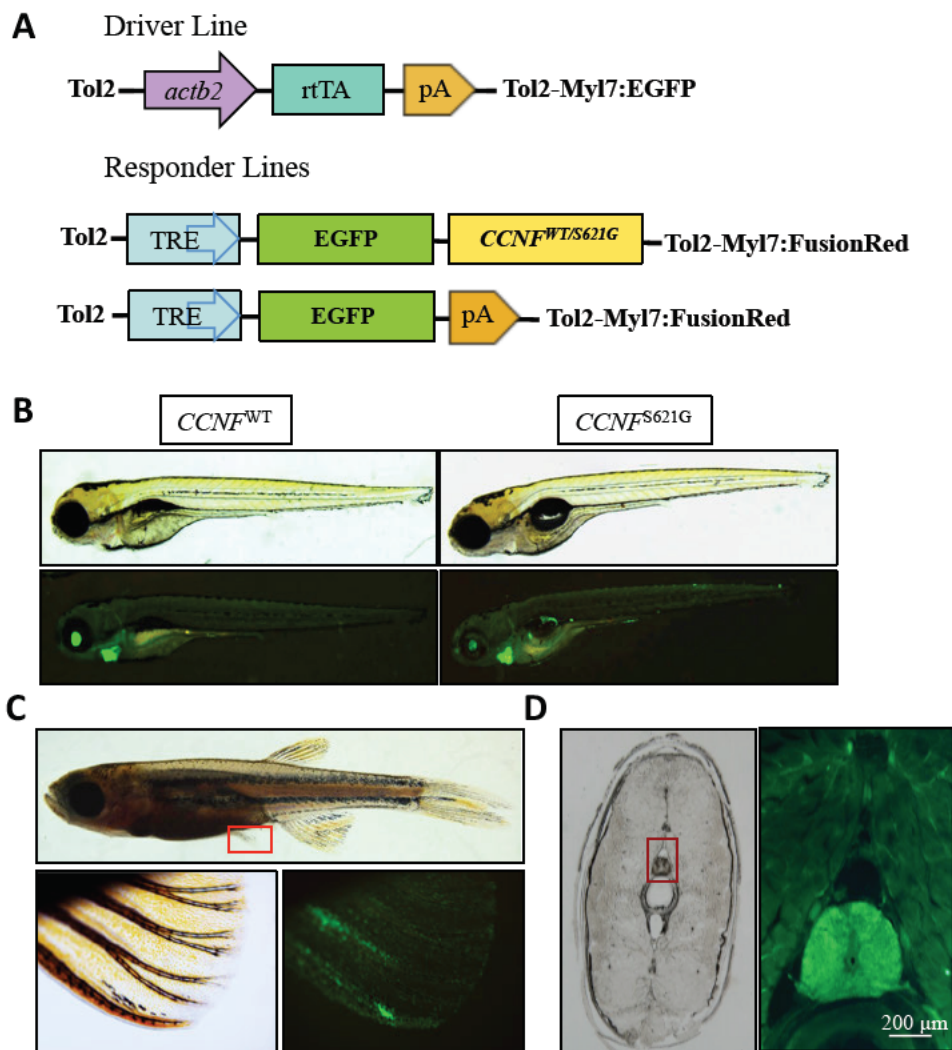
Fig. 1.

Development of Doxycycline inducible zebrafish. A. Schematic of the constructs used to generate the driver and responder transgenic lines required for model development. In the presence of doxycycline, the rtTA protein binds to the doxycycline response element (TRE), which activates a minimal promoter present within the TRE, driving expression of the EGFP-*CCNF* or EGFP transgene. **B.** Expression of GFP-fused *CCNF* following addition of doxycycline at 3 days post fertilisation, demonstrating equal levels of expression in the fish expressing $CCNF^{WT}$ and $CCNF^{S621G}$. C. Confirmation of induction of transgene expression in adult zebrafish (pectoral fin). **D.** Cross section of an induced adult fish demonstrating expression of the *CCNF* transgene within the spinal cord (SC).

Induction of $CCNF^{S621G}$ expression in adult zebrafish induces a progressive loss of motor function

The motor function of zebrafish from each experimental group was assessed weekly following induction of transgene expression at 3 mpf. The Zebrabox analysis system (Viewpoint) was used to measure the distance swum by each fish in three minutes under dark conditions. No significant

difference was observed between the three experimental groups for the first four weeks following induction (n=12). Some variability was observed in the following weeks, however, from twelve weeks post induction, to the endpoint of the study, a significant reduction in the distance swum by the $CCNF^{S621G}$ group compared to both control groups was consistently observed (P<0.05) (**Fig. 2**).
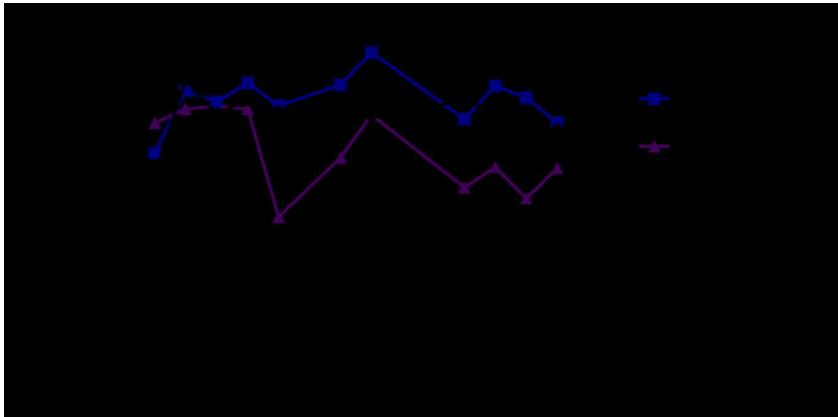

Fig. 2

Expression of $CCNF^{S621G}$ is associated with impaired motor function. Weekly analysis of motor function was performed on zebrafish in which transgene expression was induced at 3 months post fertilisation. Initially, no difference was observed in the average distance swum by fish in each of the three treatment groups. However, from 12 weeks post induction, the zebrafish expressing EGFP-tagged $CCNF^{S621G}$ consistently swam shorter distances that either of the control groups (EGFP-tagged $CCNF^{WT}$ and EGFP controls) p<0.05, n=12 per group at the beginning of the analysis, n=7 at week 16.

Overexpression of $CCNF^{S621G}$ is associated with reduced motor neuron counts in the spinal cord

Zebrafish were euthanised at 15 weeks post induction to allow examination of the spinal motor neurons. Motor neuron counts were performed by a blinded observer on Nissel stained cross sections of the spinal cord as previously described (Ramesh et al. 2010). Zebrafish that expressed $CCNF^{S621G}$ were found to have significantly fewer mature motor neurons in the spinal cord in comparison to $CCNF^{WT}$ (P< 0.001) and EGFP (P<0.0001) expressing fish (n=4 fish, 30-35 sections per fish) (**Fig. 3**).
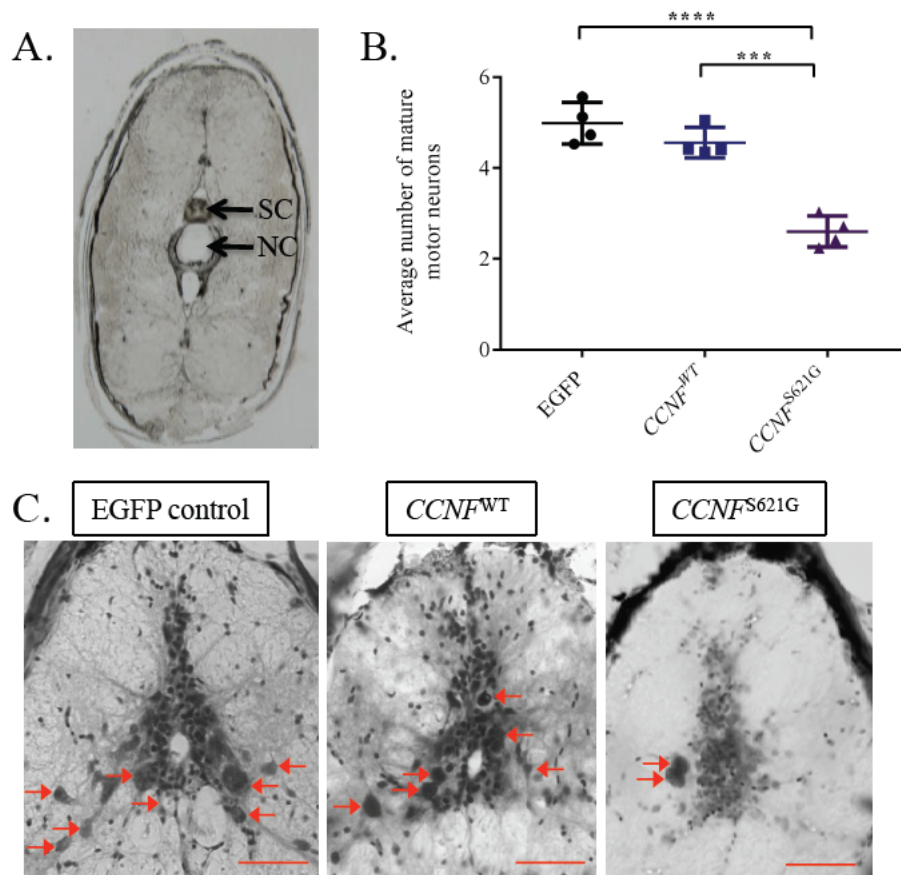
Fig. 3

Reduced number of mature motor neurons in zebrafish expressing
CCNF[S621G]. Nissel stained motor neurons in spinal cord sections of adult
zebrafish following 15 weeks of transgenic expression. **A.** Cross section of adult
zebrafish indicating the location of the spinal cord (SC) and the notocord (NC).
B. Quantification of the average number of mature motor neurons within the
spinal cord demonstrated significantly reduced motor neurons in the *CCNF*[S621G]
expressing fish compared to the *CCNF*[WT] and GFP controls (n=4 fish per group,
average taken over 30-35 30 μm thick sections per fish). **C.** Representative
images from each group. Arrows indicate motor neurons. Scale bars = 50 μm.

Discussion

This study presents the first transgenic models based on an ALS\FTD-linked mutation in *CCNF*.
The models were developed using the doxycycline inducible system, which allowed expression of
mutant *CCNF* to be delayed until the fish reached maturity, thus generating an adult-onset model of
an adult onset disease. The use of the doxycycline system also circumvented an apparent toxicity
associated with persistent overexpression of *CCNF* in the developing zebrafish embryo, which had
previously been found to preclude development of constitutive overexpression lines (unpublished).

Following prolonged expression of $CCNF^{S621G}$, adult zebrafish were found to swim significantly shorter distances than zebrafish expressing $CCNF^{WT}$ or EGFP, a finding that has previously been correlated with increased fatigue and reduced motor function (Sakowski et al. 2012). Importantly, this result was not a single observation – although minor variability was observed, the reduced swimming ability of the $CCNF^{S621G}$ zebrafish was persistent from 12 weeks post induction. This behavioural phenotype in combination with the significantly reduced number of motor neurons in the $CCNF^{S621G}$ models suggests that the ALS-linked mutation has neurotoxic effects in the zebrafish, reflecting the key pathology seen in ALS patients. This evidence indicates that the $CCNF$ zebrafish may prove suitable for studies aimed at unravelling the mechanisms of $CCNF$-linked ALS.

Zebrafish models that transiently overexpress $CCNF$ have previously been reported (Hogan et al. 2017). These developmental models demonstrated a motor neuron axonopathy, which importantly was shown to correlate with impaired motor function (Hogan et al. 2017). Addition of doxycycline to the water of the inducible zebrafish models at fertilisation (resulting in transgene expression by 24 hours post fertilisation) did not give rise to detectable abnormalities in the motor neuron axons at the same timepoint analysed in the transient models (**Supplementary Fig. 1**). A similar disparity between transient mRNA models and transgenic lines has previously been reported in $SOD1$ models of ALS (Ramesh et al. 2010). In both cases, this disparity is likely to be a consequence of lower, and perhaps more physiologically relevant, expression levels of the mutant gene in the transgenic models and a function of the rapidity of protein expression following injection of mRNA compared to cDNA. These findings suggest that the transient and inducible $CCNF$ zebrafish models will provide complementary tools for use in future studies.

No single disease model is ideal for all mechanistic and preclinical studies, thus the need for multiple models. For example, the inducible models presented in this study are less suited to high-throughput testing of potential therapeutics due to potential interactions between doxycycline and drugs undergoing testing and the slow onset of their motor phenotype. However, the transient zebrafish models, with their small size and rapidly developing phenotype appear to be well suited for such studies (Hogan et al. 2017). Conversely, the inducible $CCNF$ models presented in this study are better suited to longitudinal studies investigating the progressive effects of $CCNF^{S621G}$ expression. Analysis of the cellular and molecular changes that occur early in disease and the progression of these changes has great potential to provide significant insight into the basic biology of ALS and identify targets that may be suitable for therapeutic modification early in disease.

Of particular interest will be studies that examine the effect of $CCNF^{S621G}$ on the protein degradation pathways. *In vitro* studies have demonstrated that expression of *CCNF^{S621G}* is associated with an accumulation of ubiquitinated proteins (Williams et al. 2016) and impaired autophagy (Lee et al. 2017). These findings suggest that *CCNF* overexpression models, such as the model presented in this study, will be suitable for use in studies aimed at investigating disruption to this key ALS-linked pathway. Also of interest will be studies investigating the effect of the $CCNF^{S621G}$ mutation on the substrates of the cyclin F protein. To date, six substrates of cyclin F have been identified. These substrates have roles in two key pathways - regulation of the cell cycle (CP110, NuSAP) and DNA replication and repair (RRM2, CDC6, EXO1). Cyclin F mediates the ubiquitination of these substrates, thereby regulating their expression (Galper et al. 2017). Altered expression of these proteins may have as yet unidentified roles in the biology of *CCNF*-linked ALS.

The behavioural phenotype and reduced motor neuron number demonstrated in the inducible *CCNF^{S621G}* transgenic zebrafish models support their suitability to model ALS. The models may also prove suitable for studies investigating the biology of the closely related disease, FTD. The *CCNF^{S621G}* mutation has been shown to segregate with disease in a subset of FTD patients (Williams et al. 2016) and evidence suggests that aberrant proteostasis is also a key pathogenic mechanism in FTD (Ling et al. 2013). Zebrafish are well established as useful models of dementia and have become increasingly utilised in Alzheimer's Disease research (reviewed in (Newman et al. 2014, Caramillo & Echevarria 2017). Mutant *CCNF* models may provide insight into the mechanisms of FTD in addition to their primary role as models of ALS.

The models presented in the study are the first reported doxycycline inducible zebrafish models of ALS. The models provide proof of principle that the doxycycline inducible system is suitable for the development of neurodegenerative disease models in the zebrafish and that adult onset expression of a disease-linked mutation can induce a disease-relevant phenotype in this species. The models are also the first reported transgenic models of ALS-linked mutant *CCNF*. The ALS-relevant phenotype that developed as a consequence of $CCNF^{S621G}$ overexpression appears to suggest a toxic gain-of-function mechanism, a finding supported by the previously established transient $CCNF^{S621G}$ zebrafish model (Hogan et al. 2017) and *in vitro* models (Williams et al. 2016, Lee et al. 2017). However, models aimed at examining a potential loss-of-function mechanism of mutant *CCNF* are yet to be reported.

The evidence presented by this study supports the suitability of the inducible *CCNF*-based zebrafish models to reflect adult-onset motor dysfunction in human patients and indicates that the adult

CCNF transgenic zebrafish will provide a useful tool for future studies investigating the biology of ALS-linked mutant *CCNF* and the role of aberrant proteostasis in the disease.

Materials and Methods

Generation of constructs

The driver and responder constructs used in this study were generated using the Tol2 Multisite Gateway kit (Life Technologies) and the Tet-on toolkit (Campbell et al. 2012). The driver lines ubiquitously expressing reverse doxycycline-controlled transactivator (rtTa) protein were generated by recombining a *actb2* 5' entry vector (Life Technologies), rtTA middle entry vector (Campbell et al. 2012) and a 3' polyA vector (Life Technologies) into a Tol2 backbone vector carrying a GFP cardiac reporter (*myl7* promoter) in a single LR reaction as per manufactures instructions (Life Technologies).

To generate the responder lines, human *CCNF* (WT and S621G) was synthesised by Genscript and cloned into a Tol2 3' entry vector. GenScript also synthesised and cloned a novel Tol2 backbone vector that carried a FusionRed cardiac reporter flanked by restriction sites (NdeI-*myl7*-AvrII-FusionRed-BglII). These constructs were recombined with the doxycycline response element (TRE) 5' entry vector (Campbell et al. 2012), and the EGFP middle entry vector (Life Technologies) in a LR reaction as per manufactures instructions (Life Technologies).

All constructs were validated through Sanger sequencing (Macrogen).

Generation of Tol2 transposase mRNA

Transposase mRNA was transcribed from a NotI-linearised pCS_zT2TP vector using the Sp6 mMESSAGE mMachine Kit (Ambion). The resulting mRNA was lithium purified as per manufacturers instructions (Ambion), resuspended in RNAse-free water and stored in aliquots at -80 °C until use.

Zebrafish husbandry

Zebrafish used in this study were Tübingen wild type (TUB). Fish were bred and maintained under established conditions (Westerfield 2000) and all husbandry and experimental procedures were performed in compliance with the Animal Ethics and Internal Biosafety Committees, Macquarie University (ARAs 2012/050 and 2015/034; NLRD 5201401007) (NSW, Australia).

Generation of doxycycline inducible transgenic zebrafish

Separate driver and responder transgenic lines were established. 200 ng of the driver and responder constructs were co-injected with 160 ng of Tol2 transposase mRNA into wildtype eggs at the 1-2 cell stage of development. Embryos were screened for cardiac expression of GFP (driver lines) or FusionRed (responder lines) at 3 dpf and 7 dpf using a M165F stereo dissection microscope (Leica). Embryos that expressed the cardiac reporter were raised to maturity and outcrossed to wildtype fish in order to identify founders. Positive F1 offspring were raised to maturity and outcrossed to wildtype fish to establish F2 generations for both driver and responder lines. F2 driver lines were crossed to F2 responder lines to generate double transgenic offspring. Morphologically normal offspring from this generation that demonstrated similar expression levels of the transgene as assessed by fluorescent microscopy were used for all analysis in this stage of the project.

Induction of expression

Doxycycline (Sigma Aldrich) was diluted to 10 mg/ml in 100\% methanol and stored at 4°C as previously described (Campbell et al. 2012). This solution was further diluted in system water to a final concentration of 20 μg/ml. Fish were raised in equal numbers to maturity, then equal numbers of each group (n=12) were transferred to a separate system containing doxycycline at 20 μg/ml which was replenished weekly. Direct exposure to light was prevented with foil covering of tank lids.

Assessment of motor function

Fish used for this analysis were raised and housed in equal numbers. At the beginning of the behaviour trial, 12 fish were analysed per group, with equal numbers of males and females. By the end of the trial, there were 7 fish per group with equal male female ratio maintained. The swimming behaviour of these fish was assessed weekly using the ZebraTower (View-point) and Zebralab software (View-point). The home tanks of the fish were transferred to the behavior room two hours prior to testing and testing was performed at the same time each week. Following a period of acclimatisation, spontaneous swimming was tracked in individual tanks in low light conditions (3 minutes). Temperature of the behavior room was found to vary significantly from week to week (range 15.5°C – 25.5°C). Temperatures below 20°C significantly reduced overall distance swum by

all groups (P<0.0001) (**Supplementary Fig. 2**). Therefore measurements taken in these weeks were excluded from analysis. The full dataset from this analysis is presented in **Supplementary Fig. 3**.

Tissue preparation

Following euthanasia in 4 g/L tricaine methanesulfonate solution (Sigma Aldrich), adult zebrafish were sectioned into thirds. and fixed in 4\% paraformaldehyde in phosphate buffered saline (PBS) overnight at 4°C. Samples were placed in 30% sucrose in PBS overnight in preparation for cryosectioning, then placed in an embedding mould containing 100% Optimal Cutting Temperature Compound (OCT, Fisher HealthCare) and frozen at -80°C. Sections were cut at 30 μm using a Leica CM1050 cryostat and mounted on superfrost plus slides (Thermofisher).

Nissel staining of the spinal motor neurons

Sections for motor neuron counts were taken from the region of the spinal cord along the length of the dorsal fin. Spinal motor neuron counts were performed using 0.2 % Cresyl Violet (Sigma-Aldrich) and 0.003/% glacial acetic acid solution. Frozen sections were thawed at room temperature, washed in PBS (2 X 5 minutes), then incubated in the Cresyl Violet solution for 15 minutes at room temperature. Sections were rinsed in milliQ water and immersed in 70% ethanol for 15 seconds, then dehydrated in 95% ethanol (10 minutes X 2) and 100% ethanol (10 minutes X 2). Sections were cleared in 100/% Xylene (10 minutes X 2) (Sigma-Aldrich) and a coverslip attached using Permount mounting medium (Fisher Scientific). Images were acquired with a Leica DMi8 inverted microscope using Leica Application Suite X software. The number of large motor neurons in the ventral horn, averaged across 30-35 sections per fish, was counted by a blinded observer as previously described (Ramesh et al. 2010) (n=4 fish per group).

Western blot analysis

Protein concentration of lysates collected in RIPA buffer from adult zebrafish was determined using the Pierce™ BCA Protein Assay Kit. Western blotting performed as previously described (Krishnan et al. 2006). Briefly, lysates were electrophoresed into 10% SDS-PAGE gel and transferred to a nitrocellulose membrane which was blocked with 3% BSA for 1 hour at room temperature, followed by an overnight incubation in primary antibody at 4°C. Primary antibodies used were Cyclin F rabbit polyclonal 1:250 (Santa Cruz), Ubiquitin rabbit polyclonal 1:500 (Cell Signalling Technology) and GAPDH rabbit polyclonal 1:5000 (Sigma-Aldrich). Secondary antibodies used were anti-rabbit (Promega) or anti-mouse (Sigma-Aldrich), both at a dilution of 1:5000. Blots were developed with a chemiluminescent substrate (BioRad, Clarity Western ECL Substrate) and imaged with ImageQuant LAS4000 (GE Healthcare Life Sciences).

Statistical analysis

All statistical analysis was performed in biological triplicates. Statistical analysis was performed using an ordinary one-way ANOVA and the Tukey's HSD post hoc test to determine significant differences at a 95% confidence interval.

All values in the figures are shown as means ± standard error of the mean (SEM) (* $p \leq 0.05$; **$p \leq 0.01$, *** $p \leq 0.001$, ****$p \leq 0.0001$).

References

Campbell, L.J., Willoughby, J.J. & Jensen, A.M., 2012. Two types of Tet-On transgenic lines for doxycycline-inducible gene expression in zebrafish rod photoreceptors and a gateway-based tet-on toolkit. *PloS one*, 7(12), p.e51270.

Caramillo, E.M. & Echevarria, D.J., 2017. Alzheimer's disease in the zebrafish: where can we take it? *Behavioural pharmacology*, 28(2 and 3 - Special Issue), pp.179–186.

D'Angiolella, V., Esencay, M. & Pagano, M., 2013. A cyclin without cyclin-dependent kinases: cyclin F controls genome stability through ubiquitin-mediated proteolysis. *Trends in cell biology*, 23(3), pp.135–140.

Da Costa, M.M. et al., 2014. A new zebrafish model produced by TILLING of SOD1-related amyotrophic lateral sclerosis replicates key features of the disease and represents a tool for in vivo therapeutic screening. *Dis Model Mech*, 7(1), pp.73–81.

Galper, J. et al., 2017. Cyclin F: A component of an E3 ubiquitin ligase complex with roles in neurodegeneration and cancer. *The international journal of biochemistry & cell biology*, 89, pp.216–220.

Guerreiro, R., Bras, J. & Hardy, J., 2015. SnapShot: Genetics of ALS and FTD. *Cell*, 160(4), p.798.e1.

Hogan, A.L. et al., 2017. Expression of ALS/FTD-linked mutant CCNF in zebrafish leads to increased cell death in the spinal cord and an aberrant motor phenotype. *Human molecular genetics*.

Kirby, J. et al., 2016. The genetics of amyotrophic lateral sclerosis: current insights. *Degenerative Neurological and Neuromuscular Disease*, p.49.

Krishnan, J. et al., 2006. Role of heat shock response and Hsp27 in mutant SOD1-dependent cell death. *Experimental neurology*, 200(2), pp.301–310.

Lee, A. et al., 2017. Pathogenic mutation in the ALS/FTD gene, CCNF, causes elevated Lys48-linked ubiquitylation and defective autophagy. *Cellular and molecular life sciences : CMLS*.

Ling, S.-C., Polymenidou, M. & Cleveland, D.W., 2013. Converging mechanisms in ALS and FTD: disrupted RNA and protein homeostasis. *Neuron*, 79(3), pp.416–438.

McGown, A., Shaw, D.P.J. & Ramesh, T., 2016. ZNStress: a high-throughput drug screening protocol for identification of compounds modulating neuronal stress in the transgenic mutant sod1G93R zebrafish model of amyotrophic lateral sclerosis. *Molecular Neurodegeneration*, 11, p.56.

Neumann, M. et al., 2006. Ubiquitinated TDP-43 in frontotemporal lobar degeneration and amyotrophic lateral sclerosis. *Science (New York, N.Y.)*, 314(5796), pp.130–133.

Newman, M., Ebrahimie, E. & Lardelli, M., 2014. Using the zebrafish model for Alzheimer's disease research. *Frontiers in Genetics*, 5, p.189.

Ramesh, T. et al., 2010. A genetic model of amyotrophic lateral sclerosis in zebrafish displays phenotypic hallmarks of motoneuron disease. *Disease Models & Mechanisms*, 3(9-10), pp.652–662.

Ringholz, G.M. et al., 2005. Prevalence and patterns of cognitive impairment in sporadic ALS. *Neurology*, 65(4), pp.586–590.

Rohlfing, F.W. & Tu, R.K., 2017. Genetics of Frontotemporal Dementia. *American Journal of Neuroradiology*, 38(1), pp.10–11.

Rowland, L. P. & Shneider, N.A., 2001. Amyotrophic lateral sclerosis. *New England Journal of Medicine*, 344(22), pp.1688–1700.

Sakowski, S.A. et al., 2012. Neuromuscular effects of G93A-SOD1 expression in zebrafish. *Mol Neurodegener*, 7, p.44.

Santoriello, C. & Leonard, I.Z. 2012. Hooked! modeling human disease in zebrafish. *Journal of Clinical Investigation*, 122(7), pp2337-2343.

Westerfield, M., 2000. Westerfield (1993) The zebrafish book: A guide for the laboratory use of zebrafish (Brachydanio rerio). *Eugene: University of Oregon Press.*

Williams, K.L. et al., 2016. *CCNF* mutations in amyotrophic lateral sclerosis and frontotemporal dementia. *Nature communications*, 7, pp.11253-11261.

Supplementary material
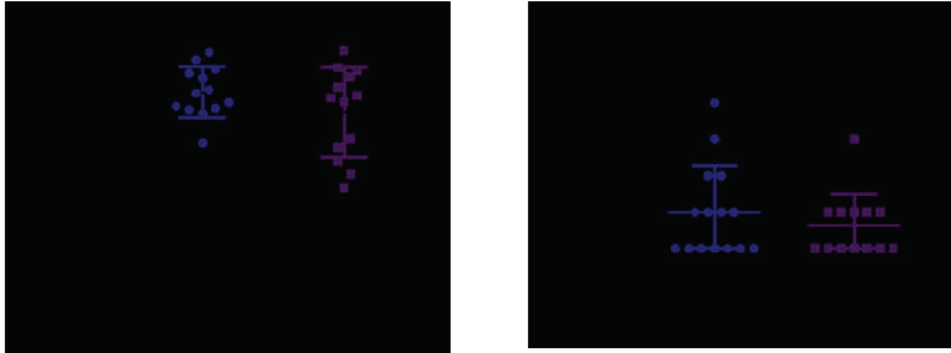
Supplementary Fig.1

Induction of *CCNF* expression at fertilisation does not induce a detectable axonopathy at 30 hpf. Analysis of primary motor axons at 2 dpf in embryos doxycycline-induced at 0 hpf demonstrated **A.** No significant difference in the length of the primary motor axons between $CCNF^{WT}$ and $CCNF^{S621G}$ expressing fish and **B.** No significant difference in branching of the primary motor axons between$CCNF^{WT}$ and $CCNF^{S621G}$ groups. (n=15). Analysis of the photomotor response of the embryos at 42 hpf demonstrated
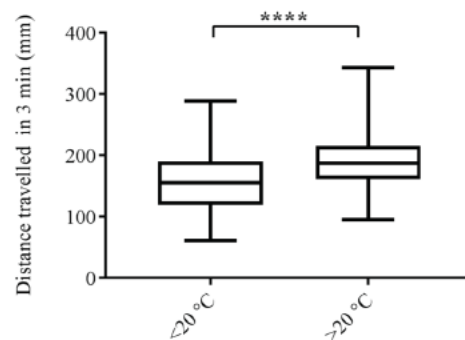
Supplementary Fig. 2

Effect of room temperature on zebrafish behavior. The temperature of the behavior room varied between weeks, over the course of the motor function assay. Room temperatures below 20 °C was found to significantly affect the swimming behavior of the all fish regardless of experimental group (p<0.0001). <20°C n= 97, >20°C n= 135. Weeks in which room temperature was below 20 °C were therefore excluded from analysis.

Supplementary Fig. 3

Complete data set of weekly swimming behavior of adult fish measured over a 3 minute period under dark conditions. Room temperature was recorded from 6 weeks post induction to investigate an observed variability in distance swum between weeks. Lower room temperature equated with a reduced distance swum across all treatment groups (weeks 6, 9 and 10). From 6 weeks post induction, at room temperatures above 20°C, reduced swimming distance was noted in the $CCNF^{S621G}$ group compared to $CCNF^{WT}$ and GFP controls (weeks 7,11,12,13,14).

5.4.3 Immunohistochemistry staining of adult zebrafish sections

Staining of spinal cord sections taken from adult zebrafish that had been induced for 16 weeks was performed as described in Section 5.2.3. Sections were examined for the presence of either ubiquitin or TDP-43 positive neuronal aggregates. No aggregate formation was detected in any of the three experimental groups.

5.5 Results: Induction of ubiquitous *CCNF* expression in zebrafish embryos

5.5.1 Introduction

This study aimed to investigate whether the utility of the ubiquitously expressing inducible zebrafish could be extended to include embryonic studies. If found suitable for embryonic studies, these models would provide an alternative to the transient mRNA models (Chapter 3), eliminating the need for repeated mRNA injections, thereby further increasing the efficiency of investigative and therapeutic studies.

To generate the models, F2 driver lines were crossed to F2 responder lines and doxycycline (20 µg/ml) was added to the water of the eggs immediately following fertilisation (0 hpf). Twenty-four hours post induction, ubiquitous expression of EGFP was evident in embryos that carried both the driver and responder transgenes (double transgenic embryos) (Figure 5.4).
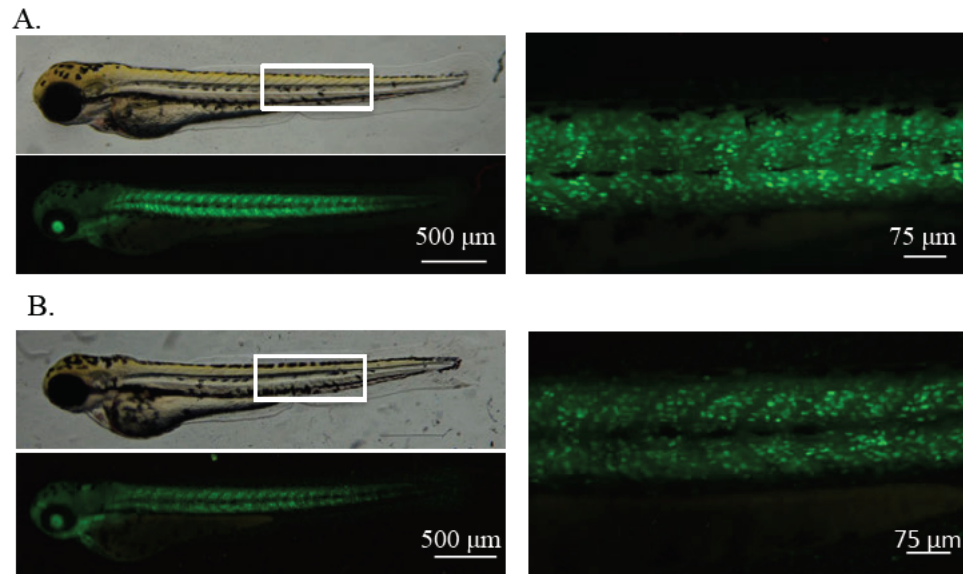
FIGURE 5.4: **Induction of *actb2*-driven *CCNF* expression in the zebrafish embryo. A.** Fish expressing *CCNF*$^{\text{WT}}$, and **B.** Fish expressing *CCNF*$^{\text{S621G}}$. In both cases, EGFP expression was evident by 24 hours post induction, and similar levels of expression were seen in the two transgenic strains.

5.5.2 High incidence of cardiac oedema following embryonic induction of transgene expression

Daily imaging of the embryos to assess the persistence of transgene expression identified a high incidence (up to 90%) of severe cardiac oedema at 6 dpf in zebrafish induced at fertilisation. It was hypothesised that this cardiac oedema may have developed as a result of embryonic exposure to doxycycline or the methanol in which it was dissolved, the expression of two cardiac reporters within double transgenic embryos, or toxicity associated with *CCNF* expression. To investigate this, the incidence of cardiac oedema was quantified in :

- single transgenic embryos exposed to doxycycline
- double transgenic embryos not exposed to doxycycline
- double transgenic embryos exposed to doxycycline

A significantly higher percentage of double transgenic embryos induced at fertilisation

were found to develop severe cardiac oedema by 6 dpf compared to double transgenic embryos that were not exposed to doxycycline (p<0.0001), suggesting that the presence of two cardiac reporters alone was not responsible for the observed phenotype. The incidence of cardiac oedema was also significantly higher in double transgenic induced embryos compared to single transgenic embryos that were exposed to doxycycline (p<0.0001), suggesting that the oedema was not a consequence of embryonic exposure to doxycycline. The incidence of cardiac oedema was found to be consistent for all three experimental groups, suggesting the oedema was not a consequence of toxicity associated with *CCNF* expression (Figure 5.5) (n= 3 clutches per group).
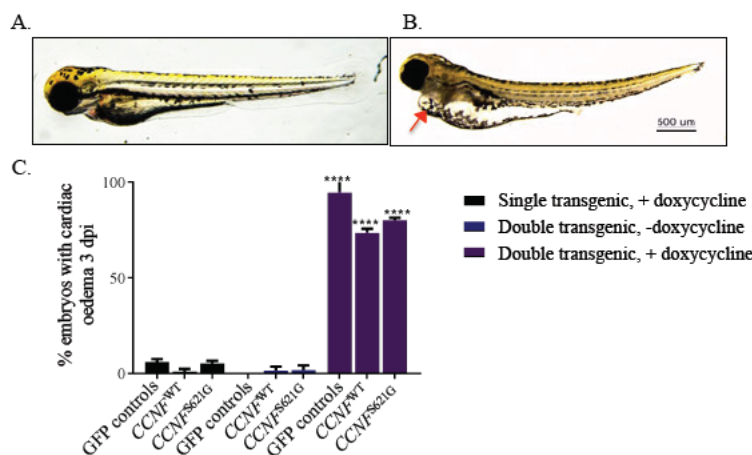

FIGURE 5.5: **Severe cardiac oedema was observed in a high percentage of zebrafish embryos induced at fertilisation. A.** Representative image of uninduced embryos at 3 dpf. **B.** Representative image of embryos in which transgene expression was induced at fertilisation, demonstrating severe cardiac oedema at 3 dpf (arrow). **C.** Percentage of embryos within each experimental group that developed cardiac oedema by 6 dpf. Significantly higher incidence of cardiac oedema was was observed in double transgenic fish from all three experimental groups that were exposed to doxycycline compared to controls (p<0.0001, n= 3 clutches per group).

The study then examined whether the cardiac toxicity associated with induction of transgene expression developed in embryos that were induced at a later timepoint. The incidence of cardiac oedema six days after the addition of doxycycline at 1 dpf, 2 dpf and 3 dpf was determined in single and double transgenic clutch mates (Method

described in Section 5.5.2). As previously observed, induction at 0 hpf gave rise to a significantly increased incidence of cardiac oedema in the double transgenic embryos (84%) compared to their single transgenic clutch mates (1.7%) ($p < 0.0005$). Similarly, the incidence of cardiac oedema was significantly higher in double transgenic embryos (78.5%) compared to single transgenic clutch mates (3%) following induction at 24 hpf ($p < 0.0005$) and 48 hpf (58.2% compared to 6%, $p < 0.005$). No significant difference in incidence of cardiac oedema six days post induction was observed between single and double transgenic embryos induced at 72 hpf ($<1\%$, $p > 0.05$) (Figure 5.6). This finding suggests that the earliest timepoint at which the *actb2*-driven models are suitable for induction of transgenic expression is 3 dpf.
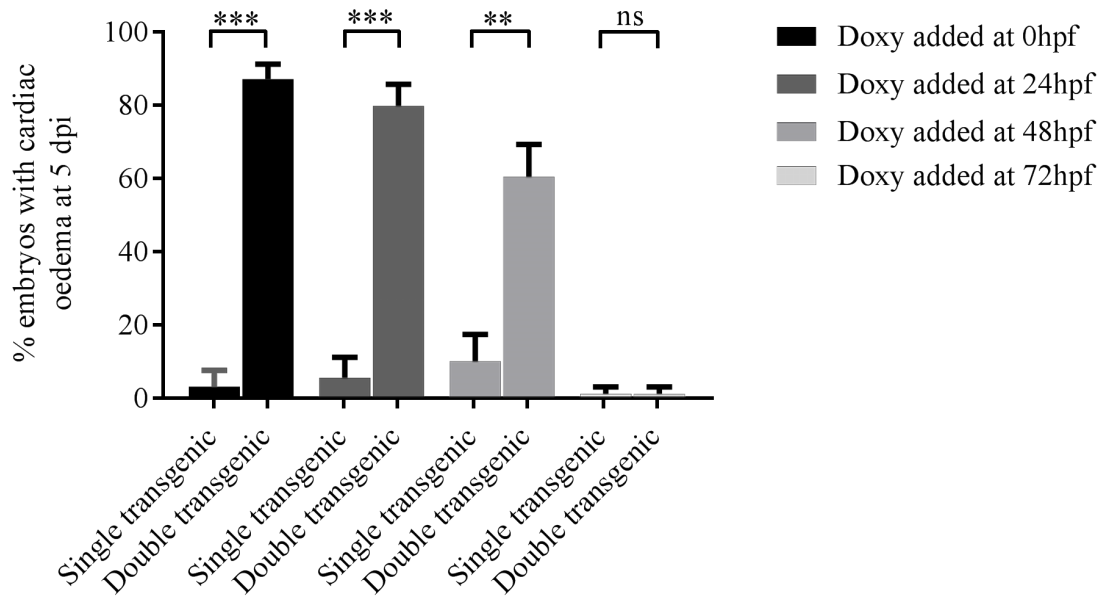
FIGURE 5.6: **Incidence of cardiac oedema in single and double transgenic embryos following induction of transgene expression.** The incidence of cardiac oedema at five days post induction (dpi) was significantly higher in double transgenic embryos compared to their single transgenic clutch mates following induction at 0 hpf ($p < 0.0005$), 24 hpf ($p < 0.0005$) and 48 hpf ($p < 0.005$). No significant difference was observed between single and double transgenic embryos following induction at 3 dpf (n=3 $CCNF^{\text{WT}}$ clutches and 3 $CCNF^{\text{S621G}}$ clutches).

5.5.3　Assessment of motor function at 6 dpf

Results from this study suggested that 3 dpf was the earliest timepoint suitable for induction of transgene expression and that expression of the transgene declined significantly beyond 7 dpf. To investigate whether this period of expression was sufficient to induce motor dysfunction in embryos that expressed $CCNF^{\text{S621G}}$, swimming behaviour was assessed at 6 dpf following induction at 3 dpf. The zebrabox (viewpoint) was used to quantify the distance swum by each embryo over a 3 minute period under light and dark conditions (Method described in Chapter 2, Section 2.4.2). No significant difference was detected between any of the the experimental groups under either light or dark conditions (Figure 5.7), (n= 15 per group).
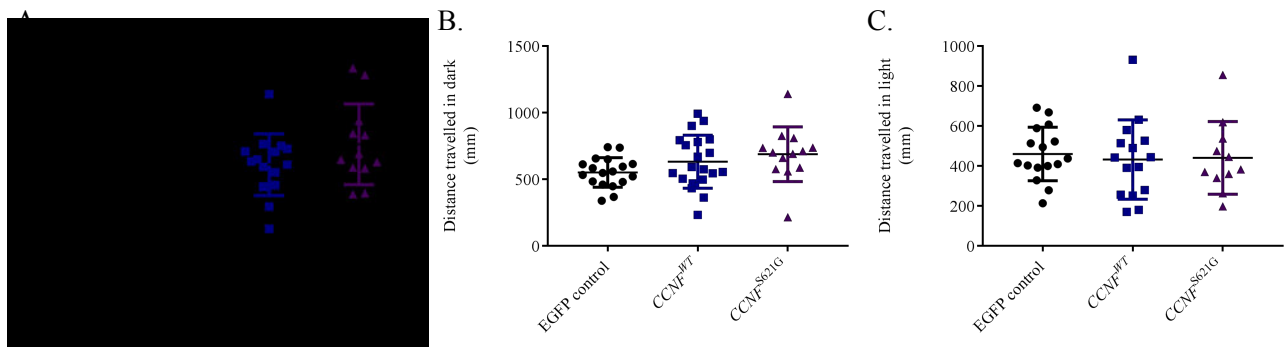
FIGURE 5.7: **Motor function at 6 dpf in zebrafish induced at 3 dpf.** The distance swum by induced embryos under both light and dark conditions was assessed at 6 dpf. No significant difference in motor function was evident between the three experimental groups in either light (**A** and **C**) or dark conditions (**B**).

Collectively, the results from this study suggest that the functionality of the *CCNF* inducible zebrafish as an embryonic model is limited.

5.6 Results: Induction of motor neuron *CCNF* expression

5.6.1 Introduction

The aim of this study was to investigate the suitability of the inducible models to investigate the cellular changes associated with motor neuron specific expression of $CCNF^{S621G}$. To confirm the functionality of this system, *-3mnx1* driver lines were crossed with each of the responder lines. Embryos from this mating were induced at 0 hpf.

5.6.2 Inducible transgene expression in motor neurons
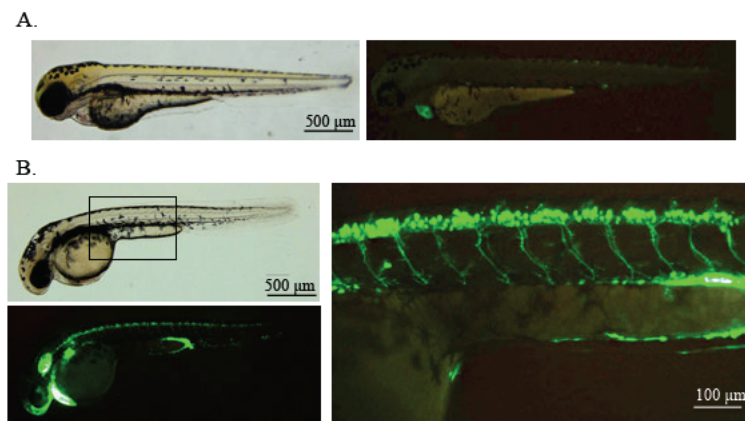
FIGURE 5.8: **Induction of *-3mnx1*-driven transgene expression** Embryos that carried the *-3mnx1* driver transgene and a responder transgene were induced at 24 hpf. **A.** No expression of the EGFP tagged *CCNF* transgene (WT or S621G) was observed. **B.** Embryos that carried the EGFP transgene demonstrated strong motor neuron expression following induction.

Twenty-four hours post induction, motor neuron expression of the EGFP transgene was evident. However, no expression of the EGFP_$CCNF^{WT}$ or EGFP_$CCNF^{S621G}$ transgenes was observed (Figure 5.8). Six *-3mnx1* driver lines were crossed with each of the seven *CCNF* responder lines (four $CCNF^{WT}$ and three $CCNF^{S621G}$). No expression of *CCNF* was evident in any of the induced embryos. Extended doxycycline exposure

(up to 5 days) and increased concentration of doxycycline (up to 40 µg/ml) failed to induce detectable expression of the *CCNF* transgene. Due to time constraints, this lack of detectable *CCNF* expression in the motor neurons was not further investigated.

5.7 Discussion

5.7.1 Summary

The use of the doxycycline-inducible system successfully permitted the development of the first transgenic animal models based on an ALS-linked mutation in *CCNF*. The adult zebrafish that ubiquitously overexpressed *CCNF*^S621G developed an ALS-relevant phenotype characterised by progressive motor impairment and a reduction in motor neuron numbers within the spinal cord. These findings suggest that the adult *CCNF* models will be suitable for use in longitudinal studies investigating the biology of ALS in adult zebrafish. Data from this study also indicates that the inducible zebrafish will have limited value as an embryonic model of ALS and preliminary data presented in this chapter suggests that the inducible models in their current form may not be suitable for investigations into motor neuron specific changes associated with ALS-linked mutant *CCNF*. Further studies to investigate the apparent failure to selectively induce *CCNF* expression in the motor neurons of these models are discussed in Section 5.7.4. The potential applications of the inducible *CCNF* zebrafish models in investigative studies are discussed in Section 5.7.5 and additional models that could be developed in future studies to complement those presented in this study are discussed in Section 5.7.5.

5.7.2 Ubiquitous expression of *CCNF* in adult zebrafish

Limitations of model design

Requirement for doxycycline

Doxycycline was added to the tank water once weekly and the treated fish were maintained on a separate system to the rest of the zebrafish colony for the duration of the drug treatment. Both of these factors added costs and labour to maintenance of the model. The prolonged expression of the transgene without continued exposure to doxycycline (Section 5.3) did permit the fish to be treated for 24 hour periods once weekly, rather than requiring continual maintenance on separate systems and the low dose of doxycycline combined with the relatively the low cost of the drug made weekly dosing feasible. However, there are caveats associated with the use of doxycycline. One key caveat is the potential for the drug to affect the physiology of the fish. Doxycycline has lower potential for pleiotropic effects than the heat shock and steroid-derivative induction methods used in alternate inducible systems (discussed in Section 5.1.2). However, the drug does have known physiological effects, the best documented being an inhibitory effect on microglial activation (Yrjanheikki et al., 1998; Tikka et al., 2001), suppression of reactive oxygen species and inhibition of apoptosis (Orsucci et al., 2009).

Microglial activity, reactive oxygen species and apoptosis are all of significance in models of ALS as all of these processes have been implicated in disease pathogenesis (Chapter 1, Section 1.2). The potential significance of these pleiotropic effects is hilighted by studies that have demonstrated neuroprotective effects of tetracycline derivatives in models of neurodegenerative diseases (reviewed in Orsucci et al. (2009)), including a model of ALS (Zhu et al., 2002). Zhu et al. (2002) demonstrated that the tetracycline derivative, minocycline, delayed the onset of motor impairment and extended the lifespan of the $SOD1^{\text{G93A}}$ mouse model (Zhu et al., 2002). However, the significance of this result is unclear as subsequent Phase1/2 (Gordon et al., 2004) and Phase 3 clinical trials (Gordon et al., 2007) actually demonstrated a mildly detrimental effect of minocycline in ALS patients (Gordon et al., 2007).

A second caveat of the requirement for doxycycline in the Tet-on models is the potential interaction of the drug with therapeutic agents in preclinical trials. Doxycycline is known to interact with multiple drugs, for example chemotherapeutic agents

(Foroodi et al., 2009) and anti-epileptic medication (Patsalos and Perucca, 2003). Therefore, doxycycline inducible models are not ideal for use in preclinical trials. The development of alternate models based on the Tet-off system would be required to circumvent this problem if the adult *CCNF* zebrafish were to be considered for such studies.

Expression of the *CCNF* fusion protein

A second limitation of the design of the models used in this study was the N-terminal EGFP tag. The fusion of a fluorescent reporter has the potential to influence the behaviour of a protein of interest (Stadler et al., 2013). Stadler et al. (2013) compared the cellular localisation of 873 proteins (not including *CCNF*) which had been tagged with either a N-terminal or C-terminal fluorophore. Approximately 26% of the proteins examined showed different localisation patterns when they carried an N-terminal tag compared to a C-terminal tag. The majority of the proteins that did demonstrate dissimilar localisation patterns were mitochondrial proteins and proteins that localise to secretory-pathway organelles (Stadler et al., 2013). This suggests that similar issues are less likely for fluorescently labelled cyclin F. However, alternate designs could be considered for future models to eliminate potential effects of the EGFP fusion. Options include the insertion of a ribosome skipping sequence (P2A sequence) between the fluorophore and *CCNF* (Daniels et al., 2014) or the use of a bi-directional tetracycline-response element (BiTRE) in the responder line constructs, in place of the TRE sequence (Campbell et al., 2012). Both strategies would lead to the translation of two separate proteins, rather than a single, fused protein (Daniels et al., 2014). Time constrains precluded the development of these additional models for this project, but would be of value for future studies.

Motor dysfunction in $CCNF^{S621G}$ models

All behavioural experiments are susceptible to variation, hence the importance of replicating results at multiple timepoints as performed in this study. There are numerous factors that can introduce variability to the swimming behaviour of adult zebrafish. These include water temperature, pH, conductivity, density of housing, time of the day, environmental distractions and sex of the fish. To minimise variability in this study, water pH and conductivity were monitored daily to ensure consistency between tanks, fish were raised and maintained in equal numbers and an equal male to female ratio was used for analysis. Behavioural testing was performed at the same time each week, in a purpose-specific room to keep environmental distractions to a minimum. While the fish room was maintained at a constant temperature, the temperature of the behaviour room could not be controlled at the time of the study. The variability in room temperature had a significant effect on the behaviour of all three experimental groups, which necessitated the exclusion of some results from analysis as detailed in Manuscript 1.

Multiple studies have demonstrated an effect of water temperature during embryonic development on the swimming behaviour of zebrafish (Ackerly and Ward, 2016; Sfakianakis et al., 2011). These studies demonstrated that fish reared in lower water temperature swim significantly shorter distances than those raised at temperatures that better reflect their native, tropical environment. The effect of water temperature on the swimming behaviour of adult zebrafish is yet to be reported. However, similar studies have been performed in other fish species, including Atlantic herring (Fuiman and Batty, 1997), salamander (Else and Bennett, 1987), salmon (Lee et al., 2003), and bass (Hasler and Tuftsa, 2009). All of these studies demonstrated a significant reduction in distances swum within a set time period at lower water temperatures. This effect was also reflected in the $CCNF$ inducible zebrafish models, which demonstrated a significant reduction (24.1%) in average distance swum by all three experimental groups at room temperatures below 20 °C (Manuscript 1, supplementary data).

Temperature control in the behaviour room will provide greater consistency for future behavioural assays (this has since been enabled in the Macquarie facility). A measure of motor function with less inherent variability would also provide greater consistency. One such measure that will be useful in future studies is the "swim test". This assay assesses motor function by measuring the ability of zebrafish to swim against a current of increasing strength (Ramesh et al., 2010).

Reduced motor neuron count in the spinal cord of the $CCNF^{\text{S621G}}$ models

Loss of motor neurons is the primary feature of ALS. The finding of reduced motor neuron numbers in the spinal cord of adult zebrafish that expressed $CCNF^{\text{S621G}}$ indicates the suitability of these zebrafish to model this key aspect of the disease. The progressive motor dysfunction demonstrated in this study suggests that the reduced number of motor neurons was due to progressive neuronal loss over the 15 weeks of $CCNF^{\text{S621G}}$ expression. However, to demonstrate progressive loss of motor neurons and to confirm a direct correlation between motor function and motor neuron numbers, this study could be expanded into a longitudinal study in which motor neuron numbers were counted at multiple timepoints, including pre-induction. Additional staining could also be performed, including staining with a choline acetyltransferase (ChAT) antibody to label mature motor neurons. Such a study could be extended to include a pan-neuronal marker to investigate whether general neuronal cell death occurs, or a cleaved caspase-3 antibody to detect apoptosis.

Immunohistochemistry analysis

Immunohistochemistry staining did not detect any ubiquitin or TDP-43 positive protein aggregates within the spinal motor neurons of adult zebrafish at 15 weeks post induction of transgene expression. It is possible that these aggregates were present but not detected due to limitations of the protocol or the antibodies tested, as no positive control was available to confirm efficacy of the assay. A lack of antibodies with proven

affinity for zebrafish proteins has long been a limitation of zebrafish studies. No current zebrafish model of ALS has been shown to develop either ubiquitin or TDP-43 positive aggregates within their motor neurons, which may be a reflection of this. Time constraints precluded extensive troubleshooting of the protocol in this project, however future studies can seek to optimise the immunohistochemical analysis in the *CCNF* zebrafish models.

An alternative approach to investigate aggregate formation would be use of the fluorescent filter trap assay, also known as the cellulose acetate filter retardation assay (Wanker et al., 1999). In this assay, lysates are passed though a membrane which traps large aggregates, the composition of which can be investigated by antibody probing. Like immunohistochemistry analysis, this assay does rely on antibody detection of zebrafish proteins which may limit its efficacy. However, the protocol for antibody staining of membranes is significantly less prone to variability than immunostaining of frozen sections. Additionally trapped proteins are highly concentrated on the membrane, which maximises the likelihood of their detection, even with antibodies with low affinity for the protein. The utility of this approach has been successfully demonstrated in multiple zebrafish models, including a model of Huntingtons Disease (Schiffer et al., 2007) and a tauopathy model based on a FTD-linked mutation (van Bebber et al., 2010).

5.7.3 Embryonic induction of ubiquitious *CCNF* expression

Cardiac oedema following embryonic induction

Severe cardiac oedema developed in a high percentage of double transgenic embryos in which ubiquitous expression of a transgene was induced in the first three days of development (Section 5.5.2). This cardiac oedema was not a consequence of toxicity associated with *CCNF* expression, as embryos that expressed EGFP developed cardiac oedema at similar frequencies. The cardiac oedema also appeared to be unrelated to

exposure to doxycycline, or the methanol in which it was dissolved, as single transgenic embryos exposed to doxycycline did not demonstrate increased frequency of cardiac oedema. Only embryos that expressed both cardiac reporters (EGFP and FusionRed) and *actb2*-driven expression of the transgene demonstrated a high incidence of cardiac oedema.

The *actb2* promoter drives strong ubiquitous expression of a transgene, which includes expression in myocardial cells. It appears highly likely that the cumulative expression of the two cardiac reporters and the *actb2*-driven myocardial expression of EGFP lead to the observed effect on cardiac development. Indeed, personal communications within the Australian zebrafish community has confirmed that toxicity associated with cardiac expression of multiple fluorophores has previously been observed (personal communication, Dr Tom Hall, University of Queensland and Dr Dan Hesselson, The Garvan Institute).

Given that *actb2*-driven transgene expression was most likely the "tipping point for development of cardiac toxicity in the zebrafish embryos, the severity and incidence of the observed cardiac oedema may be reduced in subsequent generations due to transgenerational reduction in transgenic expression that occurs with Tol2 transgenesis. Following injection of a Tol2 construct, a transgene is typically transposed into the genome at between one and eight independent positions. Approximately half of these copies are lost with outcrossing each generation. This reduction in the level of overexpression may be sufficient to overcome the cardiac toxicity observed in this study, however, new driver and/or responder line constructs that carry an alternate reporter could be developed to eliminate the possibility. For example, transgenic lines that utilised a lens reporter (α-*crystallin* promoter, Kurita et al. (2003)) in place of the *myl7* cardiac reporter could be established. The development of such lines would be necessary for the doxycycline-inducible models to be used as embryonic models. However, cardiac toxicity was not apparent in embryos older than 3 dpf and no gross abnormalities in the heart were observed in the zebrafish induced as adults, even

following prolonged doxycycline expression. Therefore, the current lines appear to be suitable for use in the adult *CCNF* models and generation of the additional lines was not performed as part of this study.

Motor function at 6 dpf

The development of cardiac oedema before 3 dpf, and the loss of transgene expression from 7 dpf, limited the duration of transgene expression in the embryonic zebrafish models. To examine whether this brief period of expression would induce an ALS-relevant phenotype, the motor function of the zebrafish was examined at 6 dpf. This analysis identified no significant difference between any of the experimental groups (Section 5.5.3). It is possible that more subtle defects, such as defects in motor neuron morphology or defects at the neuromuscular junction, did develop. Assessment of motor neuron morphology was not performed in these models as the highly convoluted nature of the primary motor axons beyond 2 dpf precludes accurate quantification of either length or branching. Analysis of the neuromuscular junctions could have been performed in the models using SV2 antibody as a pre-synaptic marker and α-bungarotoxin antibody as a post-synaptic marker (Ramesh et al., 2010). However, due to the significant limitations of inducible expression of *CCNF* in the embryonic zebrafish, this analysis was not performed.

5.7.4 Transgene expression in motor neurons

The apparent failure to induce expression of *CCNF* under the *-3mnx1* promoter in this study was an interesting finding. Successful induction of EGFP expression in the motor neurons validated the *-3mnx1* driver lines and the ability of doxycycline to penetrate the blood brain barrier. Additionally, the successful induction of *CCNF* under the *actb2* promoter validated the responder lines. All possible combinations of the five established *-3mnx1* driver lines and the seven established *CCNF* responder lines were trialled. However no expression of expression of *CCNF* was observed with

the stereomicroscope used for this project. It is possible that this method of detection was not sensitive enough to detect low expression of the *CCNF* transgene, which may require detection with a higher power compound microscope. Further investigation to establish whether this was the case would be of interest. Western blot analysis of whole embryo lysates would be unlikely to detect cyclin F at low levels of expression restricted to the motor neurons. However, lysates collected from the brain and spinal cord of induced adult zebrafish may contain sufficient cyclin F for detection. Alternatively, mRNA extraction and RT-PCR amplification of either EGFP or *CCNF* could be performed to investigate whether transcription of the *CCNF* transgene was occurring.

The *actb2*-driven models are likely to better reflect the cyclin F expression pattern in humans and provide tools more suited to complement the transient mRNA models already established. Therefore, further investigation of the *-3mnx1*-driven models was not performed as part of this project.

5.7.5 Future directions

Use of the *actb2*-driven adult zebrafish models to study the mechanisms of ALS-linked mutant *CCNF*

The data presented in this study suggests that the ubiquitously expressing *CCNF* transgenic models are well suited to studies performed in the adult animal, but less suited to embryonic studies. Therefore, the inducible models and the transient models presented in Chapter 3 appear to provide complementary tools - the transient models provide a tool for rapid analysis, and the inducible models provide a tool for longitudinal analysis. Consequently, the two models will be used in combination in future studies that aim to investigate the biology of ALS. Potential studies for which a combination of the two models may prove useful are discussed in Chapter 6, Section 6.4.

Examining the dying back vs dying forward mechanisms of ALS

The ability to perform longitudinal studies in the adult onset $CCNF^{\text{S621G}}$ models presents an opportunity to investigate one of the outstanding questions in ALS research - whether the death of motor neurons occurs through a dying-forward mechanism or a dying-back mechanism (reviewed in Cappello and Francolini (2017)). The dying-forward hypothesis suggests that the primary damage in ALS occurs at the cell body, while the dying-back hypothesis suggests that an insult to the distal axon at the neuromuscular junction precedes injury to the cell body. Studies investigating this question have produced conflicting results. For example, multiple studies in $SOD1^{\text{G93A}}$ mouse models of ALS demonstrated significant defects at the neuromuscular junction prior to the onset of clinical signs, suggesting a dying-back mechanism of disease progression (Fischer et al., 2004; Clark et al., 2016). In contrast, clinical studies have demonstrated that cortical hyperexcitability precedes the development of motor impairment in ALS patients (Eisen et al., 1993; Ziemann et al., 1997; Mills and Nithi, 1997; Vucic and Kiernan, 2006; Vucic et al., 2008), suggesting a central origin of the disease. Supporting this hypothesis, motor neurons that do not have a direct connection with the cortico-motor neurons are typically spared in ALS Kiernan et al. (2011)). Furthermore, *in vitro* and *in vivo* studies have demonstrated a vulnerability of the neuronal cell body to excitotoxins that is not evident in distal axons (Blizzard et al., 2015).

Fischer et al. (2004) examined the question of a dying-back / dying-forward mechanism in a $SOD1^{\text{G93A}}$ mouse model by examining the neuromuscular junctions, motor axons and motor neuron cell bodies at various stages of disease development. This study found that significant denervation of the neuromuscular junctions was evident by 47 days of age, followed by a significant loss of motor axons from the ventral root (between 47 and 80 days) and subsequent loss of motor neuron cell bodies in the lumbar spinal cord (from 80 days), suggesting a dying-back mechanism of disease progression. A similar study could be performed in the $CCNF$ inducible zebrafish models. Such a study would be aided by the ability to generate a large number of these models at relatively low cost, thereby allowing reasonable sample sizes to be

assessed at multiple timepoints.

Development of additional inducible *CCNF* models

Non-cell autonomous mechanisms have been implicated in disease onset and progression and it is hypothesised that non-neuronal cells such as astrocytes (Philips and Robberecht, 2011) and microglia (Vargas and Johnson, 2010) may provide potential therapeutic targets it the treatment of ALS (Lee et al., 2016). To provide models with which to investigate non-cell autonomous mechanisms, potential future studies could develop alternate driver lines to allow inducible expression of *CCNF* in specific cell types. However, this approach would require the apparent failure of induction of *CCNF* expression in the *-3mnx1* models to be overcome in order to provide a complete set of models in which the effect of ALS-linked mutant *CCNF* could be examined in the key cells affected in the disease.

In addition to the development of novel driver lines, alternative responder lines could be established that substitute human *CCNF* for the zebrafish orthologue. As discussed in Chapter 4, Section 4.1.4, the differences in gene sequence, protein structure and the different physiology of humans and zebrafish suggests that phenotypic differences may develop between these models. Knowledge of the different phenotypic effects that arise from expressing a human or zebrafish orthologue would be information that could be used to inform the design of future models.

5.7.6   Concluding Remarks

The doxycycline-inducible *CCNF* zebrafish presented in this chapter provide promising tools for use in studies which aim to further understanding of the biology of ALS in an adult model. These models have the significant advantage over transient models in that they enable longitudinal studies of disease onset and progression. Longitudinal

studies are required to unravel the pathological progression of ALS and thereby identify molecular changes that occur early in disease. Molecular changes that are involved in disease onset and early disease progression will provide ideal therapeutic targets. Future studies in which the doxycycline-inducible *CCNF* zebrafish may be used to provide insight into ALS are discussed in detail in Chapter 6.

6
Discussion

6.1   Introduction to this chapter

This chapter reviews the key findings from the project, highlights their significance and discusses possible studies in which a combination of the transient and adult *CCNF* zebrafish models may be valuable. The chapter concludes with a discussion of additional models that would complement the *CCNF* zebrafish in future investigative studies.

6.2   Summary of results

This project addressed three aims - to investigate the suitability of zebrafish to model cellular changes associated with ALS-linked mutations in *CCNF*, to generate a transient zebrafish *CCNF* model for rapid analysis of these cellular changes and to generate an adult zebrafish *CCNF* model for use in longitudinal studies. The study presented in Chapter 3 (Paper 2) demonstrated significant similarities between human and zebrafish *CCNF/ccnf* and cyclin F, and also demonstrated that cyclin F is persistently expressed within the central nervous system of the zebrafish throughout development. The similarity in the structure of cyclin F in humans and zebrafish suggests that the protein performs similar functions in the two species. Therefore, functional changes associated with mutant cyclin F in zebrafish are likely to reflect functional changes that occur in ALS patients who carry a *CCNF* mutation. This supported the rationale for developing *CCNF* models in the zebrafish.

The transient *CCNF* model was shown to develop an ALS-relevant phenotype characterised by impaired motor function and a motor neuron axonopathy. Significantly, this is the first time a correlation has been reported between motor function and axonal morphology in zebrafish. This novel correlation validates the functional relevance of the aberrant axonal morphology that has been previously reported in zebrafish models of ALS (Lemmens et al., 2007; Laird et al., 2010; Kabashi et al., 2010, 2011b; Armstrong and Drapeau, 2013). In addition to motor neuron deficits, the $CCNF^{S621G}$ zebrafish displayed elevated levels of cell death, a finding supported by proteomic data generated in parallel with this project (Paper 2). The phenotype displayed by this transient *CCNF* overexpression model suggests that it will provide a useful tool in future investigative studies. Additionally, the rapid onset of the phenotype suggests that the model will prove suitable for screening candidate therapeutic drugs.

Multiple strategies were explored to establish a paradigm that lead to the development of suitable transgenic *CCNF* zebrafish. Data presented in Chapter 4 suggested that toxic effects associated with persistent overexpression of *CCNF* in the developing embryo impeded development of both the ubiquitous and motor neuron transgenic lines. While this component of the project did not achieve its primary aim, data from the study did lead to an important change in protocol within our laboratory. To aid the early detection of similar toxicity issues during the generation of future zebrafish models, repeated screening of embryos through the first week of development is now standard. This revised protocol will confirm that transgene expression persists throughout early development, which will ensure that only those fish with a reasonable prospect of transmitting the transgene to the next generation are raised to maturity. A paper outlining these outcomes has been accepted for publication in *Science Matters*, with the aim of making the revised protocol known to the wider zebrafish community (Paper 3).

The use of the doxycycline-inducible system enabled expression of *CCNF* to be delayed until the zebrafish had matured beyond the embryonic stage, and consequently overcome the toxic effects of persistent transgene expression in the embryo. As detailed in Chapter 5, this permitted the successful development of transgenic zebrafish lines in which *CCNF* could be persistently expressed. Expression of *CCNF*$^{\text{S621G}}$ in adult zebrafish was shown to induce a progressive loss of function, a finding that was consistently demonstrated over multiple weeks of testing. Importantly, the adult *CCNF*$^{\text{S621G}}$ models were also found to have significantly reduced number of motor neurons in their spinal cord, reflecting the motor neuron loss seen in ALS patients and indicating the potential of the model to reflect key features of the disease and its potential for preclinical testing of candidate therapeutics.

6.3   Significance of the project

6.3.1   The *CCNF* zebrafish provide models with which to investigate the biological pathways implicated in the pathogenesis of ALS

Multiple cellular pathways have been implicated in the onset and progression of ALS. Unravelling the respective roles of these pathways in disease is vital to the development of targeted drug therapies. The identification of motor neuron pathology in both the transient and adult *CCNF* zebrafish models suggests that these fish will prove to be useful tools with which to investigate the pathogenic mechanisms of ALS. Importantly, patients with *CCNF*-linked ALS display TDP-43 pathology (Williams et al., 2016), pathology found in over 95% of ALS patients (Neumann et al., 2007). This suggests that models based on ALS-linked mutations in *CCNF* will provide a means with which to investigate TDP-43 dysfunction in ALS.

The presence of ubiquitin positive protein aggregates within surviving neurons is a hallmark pathological feature of all familial and sporadic ALS patients, including patients who carry a *SOD1* mutation. This suggests that aberrant protein degradation is a feature of the biology of ALS regardless of the genetic, epigenetic or environmental factors that underlie disease aetiology in individual patients (Ling et al., 2013). This further suggests that modification of the protein degradation pathways may provide a therapeutic approach that would be effective for all ALS patients (Webster et al., 2017). The role of cyclin F in regulating protein degradation through the UPS and data from *in vitro CCNF* models (Williams et al., 2016; Lee et al., 2017b,a) suggests that the *CCNF* zebrafish may prove useful in studies that aim to investigate dysfunction of this central pathway.

While it is well established that aberrant protein degradation has a central role in

the biology of ALS, the interaction of the protein degradation pathways with other ALS-associated pathways require further investigation. Multiple pathways have been implicated in ALS pathogenesis (Figure 6.1). However, the interactions of these pathways in the cascade of cellular changes that are involved in disease progression remain unclear. Unravelling these interactions would differentiate cellular dysfunction that occurs early in disease from secondary pathological changes that drive progression. For example, ER stress may develop either as a consequence of protein aggregation, or it may play a key role in aggregate formation by interfering with the ability of the ER to appropriately respond to the presence of misfolded proteins. Longitudinal studies are essential to unravel the complex pathway interactions involved in ALS onset and progression and the adult *CCNF* zebrafish provide one tool with which these longitudinal studies may be performed. Cellular dysfunction that occurs early in disease are the critical targets for pharmaceutical intervention as early intervention is likely to maximise the efficacy of any therapeutic approach.

A greater understanding of the biology of ALS and identification of cellular changes that occur early in disease will not only lead to the identification of potential therapeutic targets, but also to the identification of disease biomarkers. Biomarkers are required to allow accurate and early diagnosis, monitoring of disease progression and monitoring of patient response to therapeutics in drug trials. Currently, there is a pronounced lag between symptom onset and diagnosis for ALS patients, which ranges from 10.6-17.5 months (Donaghy et al., 2008). This lag is both an emotional burden on patients and their families and results in a delay in onset of treatment. While effective therapies are yet to be identified for ALS, early intervention is likely to maximise the efficacy of any therapeutic approach.
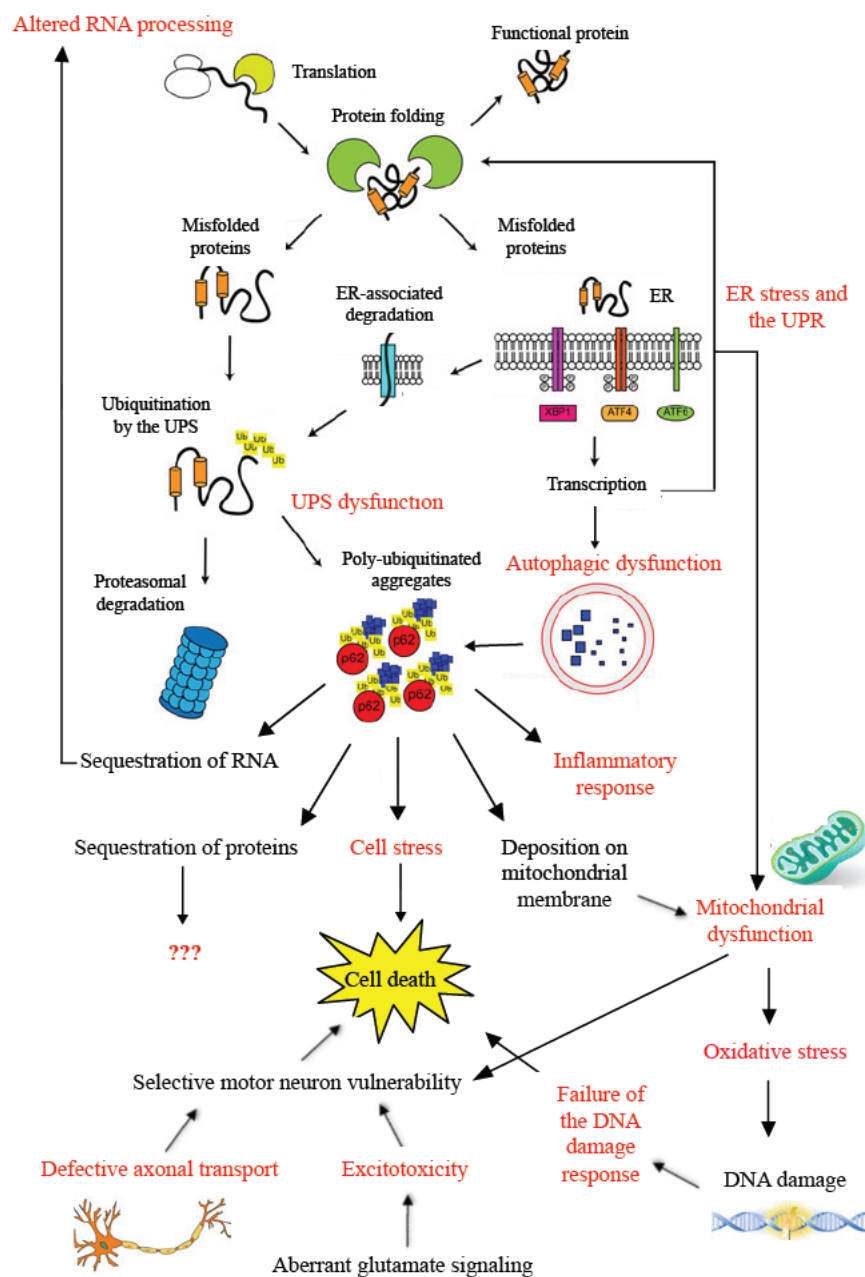
FIGURE 6.1: Interaction of pathways implicated in the pathogenesis of ALS. Multiple pathways have been implicated in the biology of ALS. Figure adapted from Webster et al. (2017)

.

6.3.2 Findings from this project may inform the design of future zebrafish models

As discussed in Chapter 1, ALS is a complex genetic disease with mutations in over 25 different genes reportedly linked to the disease. Due to both this complexity and limitations of animal models of human disease, no single model can accurately reflect all aspects of ALS biology. Consequently, validation of findings in multiple models is required and models based on different ALS-linked genes are required to allow focused analysis of dysfunction in specific pathways.

This project explored multiple strategies to establish *CCNF* transgenic zebrafish. Findings from these studies may help inform the development of future zebrafish disease models. For example, the protocol changes induced by the study which aimed to establish constitutive overexpression models (Chapter 4) are expected to increase the efficiency of development of future transgenic zebrafish models by detecting problems early in model development. As discussed in Paper 3, it is highly likely that the issues associated with establishing the *CCNF* transgenic lines are not specific to *CCNF* and may be a factor in the development of other zebrafish models. Therefore, a direct progression to an inducible strategy may be warranted for future model development. This study has established universal driver lines in our laboratory and optimised the protocols used for induction and maintenance of transgene expression, all of which should prove useful for the efficient development of future inducible zebrafish models.

6.4   Potential studies utilising the *CCNF* zebrafish to investigate the biology of ALS

6.4.1   Investigation of UPS dysfunction

Overview

There is strong genetic, pathological and molecular evidence implicating UPS dysfunction in the pathogenesis of both familial and sporadic ALS (reviewed in Chapter 1, Section 1.2.6). Unravelling UPS dysfunction in ALS has great potential to identify therapeutic targets. Indeed, the therapeutic potential of modifying the UPS to treat a range of neurodegenerative diseases is well recognised and multiple preclinical trials have supported the validity of this approach (reviewed in (Opattova et al., 2015; Webster et al., 2017)). For example, non-specific proteasome upregulation in a $SOD1^{G93A}$ mouse model of ALS was shown to reduce cytotoxicity and protein aggregate formation (Chen et al., 2012). However, non-specific up-regulation of the UPS as a therapeutic approach has significant potential for off target effects. A more targeted approach that seeks to modify specific dysfunction within the system would be less likely to induce adverse effects in patients. The identification of specific UPS dysfunction awaits a greater understanding of the role of this pathway in ALS.

In vitro studies have provided significant insight into the impact of ALS-linked mutations in *CCNF* on the UPS (Summarised in Figure 6.2). *CCNF* mutations impair overall UPS function, but not affect the activity of the proteasome, suggesting that the UPS dysfunction occurs upstream of the proteasome (Williams et al., 2016). Supporting this finding, the $CCNF^{S621G}$ mutation has been shown to alter the phosphorylation of cyclin F at the Ser621 residue, which appears to affect the E3 ligase activity of the protein, thereby disrupting the Lys48 ubiquitination of cyclin F substrates (Lee et al., 2017b,a).
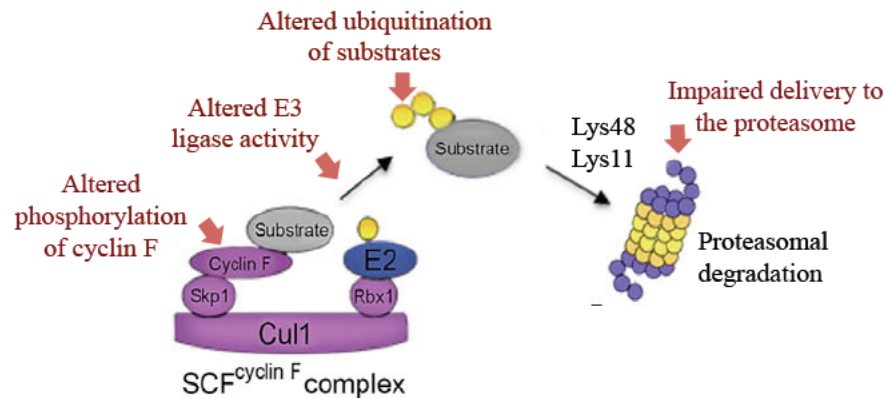
FIGURE 6.2: **Proposed mechanisms of ALS-linked mutant *CCNF* indicated by *in vitro* studies.** The phosphorylation of cyclin F at p.621 is altered by the S621G mutation, which affects the E3 ubiquitin ligase activity of the protein. This altered activity induces a change in the Lys48 ubiquitin chains formed on cyclin F substrates. Directly, or indirectly, delivery of Lys48 tagged proteins to the proteasome is reduced, leading to a reduction in ubiquitin-dependant proteasomal activity (Figure adapted from Paper 1).

In vitro models have provided important insights into the mechanisms of ALS-linked mutant *CCNF*. However, like all models, *in vitro* models have limitations, key amongst them being their inability to reflect interactions between different cell types. Given the apparent role of non-cell autonomous mechanisms in ALS (Chapter 1, Section 1.3.3), these interactions are potentially of great significance. In addition, the utility of human primary neuronal cell lines in *in vitro* studies is limited due to their terminally differentiated state and the great difficulty in accessing the cells for culturing. Consequently, most studies investigating the mechanisms of neurodegenerative disease, including those investigating $CCNF^{S621G}$, have been performed in secondary cell lines such as Neuro-2a and SH-SH5Y cells. The physiology of these secondary cell lines differs significantly from the cells from which they were derived (Gordon et al., 2013), which raises the question as to the capacity of the cell lines to reflect the physiology of ALS patients. Due to these limitations, findings from *in vitro* studies require validation in *in vivo* models.

The zebrafish *CCNF* models are currently the only *CCNF*-based *in vivo* models with which to perform this validation. While additional models will be established in other species, the *CCNF* zebrafish will continue to provide a model in which validation of *in vitro* findings can be performed in a time- and cost-effective manner. Furthermore, the *CCNF* zebrafish will continue to be a useful tool with which to study disease propagation *in vivo*, allowing sequential analysis to be formed in the same animal or animals from the same clutch at multiple timepoints, studies that are not feasible in large numbers using mammalian models. Some of the studies for which the *CCNF* zebrafish may be suited are discussed in the following sections.

Mutant cyclin F phosphorylation

The *in vitro* analysis performed by Lee et al. (2017a) demonstrated that expression of *CCNF*$^{\text{S621G}}$ induced a statistically significant reduction in the phosphorylation of the Ser621 residue of cyclin F. The phosphorylation status of E3 ubiquitin ligases is known to affect their ligase activity (Nguyen et al., 2013) and in line with this, Lee et al. (2017a) demonstrated reduced ligase activity of cyclin F$^{\text{S621G}}$ in HEK293 cells. As previously discussed, the reduced ligase activity of cyclin F$^{\text{S621G}}$ is believed to induce a dysregulation of substrate ubiquitination and a subsequent accumulation of ubiquitinated proteins. *In vivo* validation of the altered phosphorylation of cyclin F$^{\text{S621G}}$ could be readily performed in the either the transient of the adult *CCNF* zebrafish through quantifiable fluorescent western blotting (QFWB) using a phospho-specific cyclin F antibody.

The *in vitro* study of (Lee et al., 2017a) also demonstrated that casein kinase II (CK2) is responsible for the phosphorylation of cyclin F at Ser621. This finding is of potential clinical interest as modulation of CK2 has emerged as a promising therapeutic approach in the treatment of multiple cancers (reviewed in Chon et al. (2015)). Indeed, Phase I and II clinical trials are currently in progress to investigate

the clinical benefits of CK2 inhibition in the treatment of cholangiocarcinoma (ClinicalTrials.gov Identifier: NCT02128282). CK2 also been proposed as a therapeutic target for neurodegenerative disorders (Perez et al., 2011; Cozza and Pinna, 2016). However, the efficacy of this approach has not yet been reported in preclinical or clinical trials. The *CCNF* zebrafish may provide an opportunity to perform the first preclinical trials to establish whether CK2 modulators show promise in the treatment of ALS.

Ubiquitination and expression of cyclin F substrates

The impact of the $CCNF^{\text{S621G}}$ mutation on cyclin F substrates may trigger downstream mechanisms of ALS pathogenesis. The zebrafish models may prove suitable to examine this possibility *in vivo*. Analysis could include determination of the expression levels of cyclin F substrates through QFWB and examination of the ubiquitination of known cyclin F substrates though a combination of QFWB with linkage-specific antibodies (Newton et al., 2008) and deubiquitinase-based assays (Hospenthal et al., 2015). Altered expression or ubiquitination of cyclin F substrates may indicate additional pathways involved in the biology of *CCNF*-associated ALS.

As discussed in Paper 1, cyclin F substrates identified to date have key roles in the regulation of DNA replication and repair (RRM2, CDC6, EXO1) and in regulation of the cell cycle (CP110, NuSAP), both processes relevant to the development and progression of ALS. Dysregulation of DNA replication and repair mechanisms have been implicated in the pathogenesis of ALS genetically through the identification of ALS-linked mutations in *SETX* (Chen et al., 2004), *NEK1* (Kenna et al., 2016; Brenner et al., 2016) and *C21orf2* (van Rheenen et al., 2016), all of which have roles in this pathway. Experimental evidence implicating the DNA repair mechanisms in ALS includes altered expression of key regulators of DNA replication in the spinal cord of *SOD1* transgenic mice (Manabe et al., 2001; Nagano et al., 2002). The role of dysregulation of the cell cycle in ALS is less clear. Motor neurons are generally considered to

be terminally differentiated. However reactivation of the neuronal cell cycle has been reported in multiple neurodegenerative diseases, including ALS (Ranganathan et al., 2001; Ranganathan and Bowser, 2003; Nguyen et al., 2003), and it is hypothesised that this reactivation induces neuronal death, a process termed cycle-related neuronal death (CRND) (Herrup and Yang, 2007). Changes in the expression or ubiquitination of cyclin F substrates with a role in cell cycle regulation may suggest that CRND mechanisms are involved in ALS-linked mutant *CCNF*-associated neuronal death.

Ubiquitin mediated and ubiquitin independent proteasomal activity

UPS activity was shown to be significantly reduced in $CCNF^{S621G}$ transfected Neuro-2a cells (Williams et al., 2016). Further, ubiquitin independent proteasome activity was shown to be unchanged, indicating that $CCNF^{S621G}$ mediated disruption of UPS activity occurs upstream of the proteasome (Williams et al., 2016). To investigate whether these findings are reflected *in vivo*, ubiquitin-dependant proteasome activity could be investigated in the *CCNF* zebrafish models using an artificial UPS substrate (a degron) tagged with a green fluorescent protein (GFP^u). The efficiency of GFP^u degradation by the UPS can be assessed by quantification of the intensity of GFP^u expression through a combination of fluorescent microscopy, microplate reader and QFWB. The transient *CCNF* models would prove useful for this study as co-injection of GFP^u mRNA and the *CCNF* mRNA would provide a highly efficient means of assessing UPS-dependant proteasome activity. The viability of this assay has previously been demonstrated in embryonic zebrafish models of Parkinsons disease (Lichtenberg et al., 2011). The adult *CCNF* models may also prove useful for this assay. A GFP^u transgenic line that stably expressed the GFP^u protein could be generated and crossed to the *CCNF* transgenic lines. This would provide a model in which UPS function could be assessed at various timepoints following induction of $CCNF^{S621G}$ expression. This could determine whether UPS activity declines over time in these models.

UPS independent proteasome activity could be assessed in a similar manner using fluorescently labelled ornithine decarboxylase (OCD), a degron that does not require ubiquitination to be degraded by the proteasome (Melvin et al., 2013). The use of a fluorescently labelled OCD reporter has not yet been reported in zebrafish, however the feasibility of the approach to evaluate proteasome activity *in vivo* has been demonstrated in a mouse model of prostate cancer (Momose et al., 2012). As with the GFP^u assay, proteasome activity may be assessed by quantifying the expression level of the GFP-OCD reporter through a combination of fluorescent microscopy, microplate reader and QFWB. Again, the transient zebrafish model appears to be well suited to this analysis, however a longitudinal study in the adult models may also provide valuable insight.

6.4.2 Investigation of autophagy

Overview

Autophagy is a protein degradation pathway primarily responsible for the breakdown of long-lived proteins and cellular organelles, in contrast to the short-lived proteins that are the primary target of the UPS. Despite their apparently distinct targets, a compensatory relationship has been demonstrated between these two protein degradation pathways, with inhibition of the UPS shown to induce upregulation of autophagy both *in vitro* and *in vivo* (Pandey et al., 2007; Iwata et al., 2005; Rideout et al., 2004). Dysfunction in the autophagic pathway has been strongly implicated in the biology of ALS. ALS-linked mutations have been identified in multiple genes with a role in autophagy, including *SQSTM* (Fecto et al., 2011) and *OPTN* (Maruyama et al., 2010). Additionally, analysis of post-mortem tissue has demonstrated upregulation of autophagy in ALS patient spinal cord (Sasaki, 2011) and autophagic dysfunction has been demonstrated in multiple *in vitro* and *in vivo* models of ALS (reviewed in Ramesh and Pandey (2017)).

Modification of autophagy as a therapeutic approach in ALS has shown promising results. Multiple studies have demonstrated beneficial effects of Trehalose, an inducer of autophagy, in the $SOD1^{\text{G85R}}$ mouse model. These beneficial effects include delayed disease onset, reduced formation of SOD1 aggregates and extended lifespan (Li et al., 2015b; Zhang et al., 2014; Castillo et al., 2013). However, as with generalised upregulation of the UPS, generalised upregulation of autophagy has significant potential for off target effects. A greater understanding of where dysfunction occurs in this system is required to aid development of targeted therapies.

In vitro analyses of Neuro-2a and SH-SY5Y cells have demonstrated that expression of $CCNF^{\text{S621G}}$ is associated with autophagic dysfunction, specifically a failure of lysosome-autophagosome fusion (Lee et al., 2017b). The *CCNF* zebrafish models may provide a useful tool to validate this finding *in vivo*. A schematic of the autophagy system, highlighting the components of the system that may be assessed in the zebrafish models is shown in Figure 6.3.

Investigation of autophagic activity

Overall autophagy activity could be examined in lysates collected from the *CCNF* zebrafish through QFWB analysis of LC3 and p62 expression levels. To investigate the apparent inhibition of lysosome-autophagosome fusion induced by the $CCNF^{\text{S621G}}$ mutation, a combination of a GFP tagged LC3 protein (pGFP-LC3 plasmid, He et al. (2009)) and a lysosomal dye such as Lysotracker (Thermofisher) could be used. Co-localisation of these makers in the zebrafish models would provide an indication of autolysosome formation. Both the transient and the adult *CCNF* zebrafish models appear suitable for this study. To perform the assay in the transient model, the pGFP-LC3 mRNA could be co-injected with the *CCNF* mRNA. The permeability of the skin of the zebrafish during the first few days of development would allow
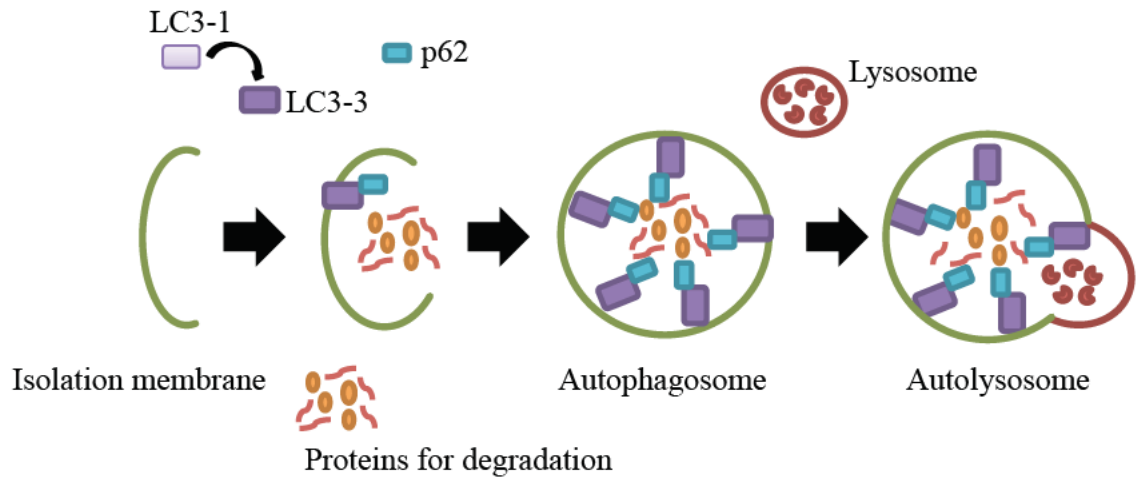
FIGURE 6.3: **Overview of autophagic protein degradation.** Ubiquitin like proteins, including LC3, bind to adapter proteins, such as p62, on the isolation membrane in the early stages of autophagosome formation. These proteins become incorporated into the autophagosome. Fusion of the autophagosome with the lysosome forms the autolysosome, within which, protein degradation, including degradation of the LC3 and p62 proteins occurs.(Adapted from Mizushima and Komatsu (2011)).

the Lysotracker dye to penetrate the embryo (He et al., 2009) and co-localisation of the markers could be assessed *in vivo* due to the optical transparency of the fish during early development. The suitability of embryoinc zebrafish for this analysis has previously been established (He et al., 2009). A similar assay could be performed in the adult zebrafish models. This would require the establishment of a pGFP-LC3 transgenic line and immunostaining of zebrafish sections with a lysosomal antibody, for example, LAMP1. While significantly more time consuming than the corresponding assay in the transient model, the use of the adult *CCNF* zebrafish would allow longitudinal analysis of autophagy.

6.4.3   Examination of the interaction between cyclin F and TDP-43

TDP-43 pathology is found in patients with ALS-linked mutations in over 25 different genes that function in a variety of cellular pathways. TDP-43 pathology is also a feature of sporadic ALS patients who carry no known disease-causative mutation. Establishing how this common pathology develops in such a wide range of ALS subtypes, is likely to provide significant insight into the shared mechanisms leading to motor neuron death in ALS.

To date, six known substrates of cyclin F have been identified - RRM2, CP110, EXO1, SLBP, CDC6 and NuSAP (reviewed in Paper 1). Despite TDP-43 not being a known cyclin F substrate, *in vitro* expression of $CCNF^{S621G}$ has been shown to increase the expression levels of ubiquitinated TDP-43 in Neuro-2a cells (Williams et al., 2016). This suggests that there is an interaction between TDP-43 and cyclin F. Supporting this hypothesis is an unpublished study, lead by Dr Albert Lee and Miss Stephanie Raynor (Centre for MND Research, Macquarie University), which used a proximity-dependant biotinylation assay, BioID, to identify proteins that interact with cyclin F *in vitro* (Roux et al., 2012). One of the proteins identified by this study was TDP-43. Interestingly, this study also showed that inhibition of the proteasome has no effect on TDP-43 expression levels, suggesting that the interaction between cyclin and TDP-43 does not induce TDP-43 degradation through the UPS. Further investigation of how dysregulation of cyclin F activity induces an accumulation of ubiquitinated TDP-43, independent of proteasome activity, is required.

The effect of $CCNF^{S621G}$ expression on TDP-43 expression levels was examined in the transient *CCNF* zebrafish through ECL western blotting. No significant difference in TDP-43 expression was detected (Chapter 3, Paper 2). However, only overall TDP-43 expression in the soluble fraction of the lysates was examined. Further analysis including quantification of ubiquitinated TDP-43 expression and

examination of the insoluble fraction was not performed due to time constraints. Further investigation using immunoprecipitation to isolate ubiquitinated proteins and/or insoluble proteins followed by QFWB analysis is therefore required to establish whether the *CCNF* zebrafish models do reflect the *in vitro* findings (Williams et al., 2016).

Also required is determination of the effect of *CCNF*[S621G] on the cellular localisation of TDP-43. Mislocalisation of TDP-43 is a pathological feature of ALS and is hypothesised to be a key factor in disease onset and progression (reviewed in Chapter 1, Section 1.6). The *CCNF* zebrafish should prove suitable for studies investigating the effect of *CCNF*[S621G] on TDP-43 localisation. For example, co-injection of mCherry-labelled *CCNF* mRNA with GFP-labelled wildtype TDP-43 mRNA would provide a rapid assessment of TDP-43 localisation in the presence of wildtype and mutant cyclin F. More in-depth analysis, not only of TDP-43 localisation, but localisation of other ALS proteins such as FUS, could be also performed using a subcellular fractionation assay of lysates collected from either the transient or adult models (de Araujo and Huber, 2007).

6.5 Further characterisation of the *CCNF* zebrafish models

Further characterisation of both the transient and adult *CCNF* zebrafish could be performed to investigate which ALS-linked pathways other than the protein degradation pathways are disrupted by the *CCNF*[S621G] mutation. This would provide a further indication of the capacity of the models to reflect the biology of ALS and their suitability to investigate interactions between dysfunctional pathways in ALS.

Investigation of ER stress in the models will be of particular interest. Overexpression of the ER-Golgi transport protein, RAB1, has been shown to mediate the toxic effects of $CCNF^{S621G}$ expression in the transient $CCNF$ zebrafish, rescuing both the axonopathy and the motor dysfunction (discussed in Chapter 3, Section 3.4.3). This rescue effect suggests that ER dysfunction is a feature of the $CCNF$ models. To investigate this, a transgenic ER stress reporter line (*ef1* promoter) (Li et al., 2015a) could be utilised. This reporter line expresses fluorescently labeled XBP1, a transcription factor that mediates the ER unfolded protein response. Under conditions of ER stress, XBP1 is upregulated and this upregulation may be quantified through fluorescent microscopy and QFWB. The use of this transgenic line would provide a rapid indication of ER stress in the transient $CCNF$ zebrafish and a longitudinal indication of ER stress levels in the adult $CCNF$ zebrafish. Use of the ER stress reporter line in combination with the GFP^u assay detailed in Section 6.4.1 may provide some insight into the linear relationship between ER stress and UPS dysfunction.

Additional reporter lines available in our laboratory may also prove useful to further characterise the $CCNF$ zebrafish. For example, a transgenic line in which fluorescently labelled Annexin A5 is expressed (van Ham et al., 2010) would be useful to investigate oxidative stress and apoptosis in the models, and a microglial reporter line (*mpeg* promoter) (Ellett et al., 2011) may be used to assess the inflammatory response. Transgenic zebrafish lines that reflect mitochondrial damage are yet to be established. However, a modified fluorescent reporter tagged to a mitochondrial-targeting sequence has been developed, which may be useful in future zebrafish studies (Hernandez et al., 2013). This reporter, termed MitoTimer, localises to the mitochondria and under normal cellular conditions, fluoresces green. Oxidation, as occurs under conditions of mitochondrial stress, shifts the emission spectrum of the fluorophore to red. The successful use of this reporter to assess mitochondrial numbers, morphology and stress has been demonstrated in *C.elegans, Drosphilia* and mice, validating the utility of the approach *in vivo* (Laker et al., 2014).

6.6 Determination of the suitability of the *CCNF* zebrafish to examine the biology of FTD

This project has focused on the suitability of the *CCNF* zebrafish models to study the biology of ALS. However, the *CCNF*[S621G] mutation, has also been linked to pure FTD and ALS-FTD (Williams et al., 2016). Zebrafish and humans share significant similarities with respect to their brain structure and brain physiology, which suggests the suitability of zebrafish to model neurological disorders (Panula et al., 2010). Structurally, the same major domains are present in zebrafish and human brains, including a diencephalon, telencephalon and cerebellum (Santana et al., 2012). At the cellular level, the same key cell types are present in both species, including motor neurons, oligodendrycytes, astrocytes and microglia (Santana et al., 2012). Zebrafish also possess the same neurotransmitters as humans, including glutamate, GABA, serotonin, histamine and acetylcholine (Kalueff et al., 2014) and have been shown to display a range of complex behaviours involving memory, learning and social interactions (Lieschke and Currie, 2007; Norton and Bally-Cuif, 2010). Consequently, zebrafish have become well recognised as a suitable species in which to model complex human brain disorders, such as dementia and have become increasingly utilised in this field of research (Kalueff et al., 2014). Indeed, the number of new studies examining cognitive dysfunction in zebrafish now exceeds the number of new studies in rodents and other species (reviewed in Meshalkina et al. (2017)).

Two zebrafish models of FTD have been established to date, both of which overexpressed FTD-linked mutant *MAPT*, which encodes the FTD-associated protein, tau. Both zebrafish models demonstrated a motor neuron axonopathy, reduced motor function as assessed by the touch-evoked escape response (TEER) and neuronal tau aggregates (Paquet et al., 2009; Lopez et al., 2017). Assessment of both models was performed in the embryonic stage and characterisation of more complex behaviours, such as learning and memory, or assessment of atrophy within the frontal region of the brain was not described. Further characterisation of zebrafish models of FTD is

required to confirm the ability of these models to reflect key aspects of the disease.

More in-depth analysis has been performed in mouse models of FTD. Multiple models have been described which display a range of FTD-associated behaviours, including a genome edited *MAPT* model which displays heightened anxiety and depressive/apathetic behaviour (Koss et al., 2016), a *C9orf72* model which displays hyperactivity and anxiety-like exploration (Chew et al., 2015) and a *MAPT* over-expression model that displays impaired nest-building behaviour, suggesting apathy or reduced attention (Warmus et al., 2014). While these models display some FTD-relevant behaviours, no established model of FTD accurately reflects the phenotype and the pathology of the disease in humans (reviewed in Ahmed et al. (2017)). Therefore, as with all complex diseases, multiple models are required to unravel the biology of the disease. The *CCNF* zebrafish may provide a novel tool suitable for use in these studies.

Further characterisation of the *CCNF* zebrafish is required to establish their suitability to investigate the biology of FTD with TDP-43 pathology. This characterisation would include an assessment of the ability of the models to reflect the key pathology seen in FTD patients - atrophy within the frontal and/or temporal cortices and the formation of neuronal TDP-43 positive aggregates (Mackenzie and Neumann, 2016). The cognitive abilities of the *CCNF* zebrafish would also be assessed. Multiple assays have been designed with which to investigate cognitive dysfunction in the zebrafish. These assess learning and memory (reviewed in Levin (2011) and the ability of the zebrafish to adapt to novel temporal, spatial, and visual cues (detailed in Yu et al. (2006)). An example of a commonly used assay in adult zebrafish is the three-chamber task, which uses a tank divided into three chambers by moveable partitions. Adult zebrafish are placed in the central chamber and trained to move into the left or right chamber in response to a visual cue. Both negative reinforcement (reduction of the size of the incorrectly selected chamber) and positive reinforcement (expanding the size of the correctly selected chamber to provide an area in which the fish can swim freely) are used to induce the correct response. Once the zebrafish has

learned to consistently select the correct chamber, an indication of learning ability
and memory, the contingencies may be changed so the opposite choice becomes the
correct one. Delayed adaptation to this alteration can be used as a further indicator
of memory (detailed in Levin (2011)).

Adult zebrafish have primarily been used for these behavioural tests as they a
have fully developed range of brain function and behaviour. However, embryonic
models have also been used in cognitive testing for rapid analysis of central nervous
system defects (Santana et al., 2012). One consideration for studies using either
embryonic or adult models is that some cognitive tests do rely on the locomotor
ability of the zebrafish. The appropriate behavioural assays therefore would have
to be selected in studies utilising the *CCNF* zebrafish. For example, assays that
assess the learning ability and memory of the fish by recording how often the
correct chamber is selected would be appropriate, whereas protocols that measure
how quickly the fish moves from one chamber to the next would not. The reduced
motor function observed in both the embryonic and adult *CCNF* models in this
study was robust, but not severe enough to interfere with the ability of the fish to
move from one area of the tank to the another. Motor function may be expected
to decline over time in the adult models, therefore the level of impairment would
require continual re-assessment to ensure the models remain suitable for cognitive
testing. For ethical reasons, a decline in motor function to the point where the ability
of the fish to move around the tank was impeded would mark the end point of the study.

6.7 Potential development of additional *CCNF* models

6.7.1 *CCNF* models in other species

The advantages of zebrafish to model human diseases are discussed in Chapter 1, Section 1.4. This study has demonstrated the suitability of the species to specifically model ALS-linked mutations in *CCNF* through characterisation of the zebrafish *ccnf* orthologue and the ALS-relevant phenotypes identified in the *CCNF* zebrafish models. However, no disease model accurately reflects all aspects of ALS or is suitable to all applications. Therefore, the development of *CCNF*-based models in additional species, both invertebrate and mammalian species, would provide valuable additional tools to future studies. The advantages of these alternate models species are also outlined in Chapter 1, Section 1.4.

6.7.2 *CCNF* knockout / knockdown models

The zebrafish models presented in this study and the *CCNF in vitro* studies published to-date (Williams et al., 2016; Lee et al., 2017b,a) suggest that the $CCNF^{S621G}$ mutation induces a toxic gain-of-function. However, additional models are required to investigate a potential concomitant loss-of-function mechanism of the mutation. To-date, a single model has been developed in which expression of *CCNF* was suppressed - a *CCNF* knockout mouse (Tetzlaff et al., 2004). Homozygous *CCNF* knockout mice displayed severe developmental abnormalities and died in early embryonic development. In contrast, no abnormalities were identified in heterozygous *CCNF* knockout mice at one year of age (Tetzlaff et al., 2004). While this suggests that a loss-of-function mechanism is not involved in the biology of ALS-linked mutant *CCNF*, this was a developmental study, aimed at establishing the role of cyclin F in early development. Consequently, the *CCNF* knockout mice were only examined for survival to maturity and their breeding ability. No behavioural testing, nor

histological examination of motor neurons or other tissues was performed. Therefore, abnormalities may be present in these mice that become evident with aging. Further characterisation of these models may provide insight into the potential role of a loss-of-function mechanism of the $CCNF^{S621G}$ mutation.

To provide additional tools to complement the overexpression models presented in this study, zebrafish models could be developed in which expression of *CCNF* was partially or completely silenced. Previous efforts to develop transient *CCNF* knockdown zebrafish models using antisense oligonucleotides (morpholinos, AMOs) were unsuccessful (Nic LeGrand, Honours Thesis, University of Sydney, 2012). Suppression of *CCNF* expression in zebrafish embryos was found to induce severe developmental defects, reflecting the findings from the *CCNF* knockout mouse study (Tetzlaff et al., 2004). The use of genome editing tools to generate heterozygous knockdown zebrafish may enable the development of models suitable for studies investigating a potential loss-of-function mechanism of ALS-linked mutant *CCNF*.

6.7.3   Genome edited $CCNF^{S621G}$ models

In addition to the development of models in which *CCNF* expression is suppressed, genome editing tools could be used to establish models in which the $CCNF^{S621G}$ mutation was introduced into the zebrafish genome. This approach would generate models in which $CCNF^{S621G}$ was expressed at physiologically relevant levels. It is hypothesised that due to this physiological expression of a mutation, genome edited models may provide a more accurate reflection of the cellular changes that occur in ALS patients than overexpression models. Multiple zebrafish models have been developed in which an ALS-linked point mutation has been introduced into the genome,including *FUS* (R521G and P525L) (Armstrong et al., 2016; Panda et al., 2013) and *TARDBP* (A382T) models (Armstrong et al., 2016). These models provide proof of principle for use of genome editing in zebrafish, no ALS-relevant phenotypes have yet been described in these models. The question therefore remains as to whether

physiological expression of an ALS-linked mutant gene is sufficient to produce a phenotype in a short-lived animal species such as the zebrafish.

The development of a $CCNF^{\text{S621G}}$ model in future studies may prove to be a valuable complementary tool to the overexpression models presented in this study. Furthermore, a comparison of the phenotype displayed by a $CCNF^{\text{S621G}}$ genome edited model and $CCNF^{\text{S621G}}$ overexpression models would provide valuable information that may inform the design of future models of ALS.

6.7.4   Induced pluripotent stem cell models

The development of induced pluripotent stem cell (iPSC)-derived models from $CCNF$ patient tissue would provide additional tools with which to study the biology of ALS-linked $CCNF$ mutations. The capacity of iPSC-derived models to reflect key aspects of ALS pathology, including the formation of TDP-43 positive neuronal aggregates has been established (Burkhardt et al., 2013). Unlike animal models, iPSC-derived cells would accurately reflect the genetic background of $CCNF$ patients, expressing not only the ALS-linked mutation within $CCNF$, but also unidentified genetic modifiers.

6.8   Final remarks

Significant progress has been made unravelling the biology of ALS over the past two decades and this progress inspires optimism for the development of effective therapeutics in the near future (Taylor et al., 2016). Gene discovery has been the driving force behind the recent advances in ALS research, providing insight into the cellular pathways that are involved in disease pathogenesis, including the protein degradation pathways, and permitting the development of disease models. While there is no ideal model of ALS that reflects all aspects of this complex disease, multiple disease models

in multiple species, based on multiple gene mutations have provided essential tools for investigative studies. The *CCNF* based zebrafish models presented in this thesis are a novel addition to this toolkit. These models display a motor neuron toxicity, reflecting the primary feature of ALS and therefore will provide an avenue through which the pathogenic mechanisms associated with ALS-linked *CCNF* mutations may be unravelled. The presence of TDP-43 pathology in *CCNF* patients suggests that findings from these studies will be applicable to wider ALS and therefore will contribute to our overall understanding of disease biology and the development of effective therapeutics for this devastating disease.

A
Appendix

A.1 Ethics approval

MACQUARIE University ANIMAL RESEARCH AUTHORITY (ARA)

AEC Reference No.: 2015/034-13   <u>**Date of Expiry:**</u> 10 December 2018

Full Approval Duration: 11 December 2015 to 10 December 2018 (36 months)
This ARA remains in force until the Date of Expiry (unless suspended, cancelled or surrendered) **and will only be renewed upon receipt of a satisfactory Progress Report before expiry (see Approval email for submission details).**

Principal Investigator:
Doctor Nicholas Cole
Faculty of Medicine and Health Sciences
Macquarie University, NSW 2109
nicholas.cole@mq.edu.au
0431 955 280

Doctor Angela Laird
Faculty of Medicine and Health Sciences
Macquarie University, NSW 2109
angela.laird@mq.edu.au
0416 808 108

Associate Investigators:
Marco Morsch	0449 126 528
Roger Chung	0402 808 958
Emily Don	0423 387 488

Others Partipating:
Alison Hogan	0401 857 972
Jennifer Fifita	0433 979 754
Yagiz Aksoy	0431 955 280
Rowan Radford	0403 605 754
Serene Gwee	0411 514 831
Sharron Chow	0413 536 028
Jack Stoddart	0402 682 745
Erin Lynch	0431 106 315
Hamideh Shahheydari	0413 243 183
Rola Bazzi	0481 148 556
Katherine Robinson	0402 734 322
Ariuntugs Ultziikhutag	0410 936 063
Maxine Watchon	0481 451 897
Kristy Yuan	0430 039 958
Emma Perri	0400 068 242
Sina Shadfar	0431 107 710
Reka Toth	0434 893 254
Luan Luu	0430 115 691

In case of emergency, please contact:
the Principal Investigator / Associate Investigator named above
or Animal Welfare Officer: 9850 7758 / 0439 497 383

The above-named are authorised by MACQUARIE UNIVERSITY ANIMAL ETHICS COMMITTEE to conduct the following research:

<u>**Title of the project:**</u> **Zebrafish models of neurodegenerative diseases**

<u>**Purpose:**</u> **5 - Research: Human or Animal Health and Welfare**

<u>**Aims:**</u> **To create fish models of neurodegenerative diseases using zebrafish**

<u>**Surgical Procedures category: 9 - Production of Genetically Modified Animals**</u>

<u>**All procedures must be performed as per the AEC-approved protocol, unless stated otherwise by the AEC and/or AWO.**</u>

Maximum numbers approved (for the Full Approval Duration):

Species	Strain	Age/Weight/Sex	Total	Supplier/Source
23 - Fish	Zebrafish (*Danio rerio*)	Larvae	30, 552	Bred In-house
23 - Fish	Zebrafish (Danio rerio)	Adult	10,000	Bred In-house
23 - Fish	Zebrafish (Danio rerio)	Adults and Larvae	90	Bred In-house
			TOTAL 40,642	

Location of research:

Location	Full street address
FMHS Laboratory	Level 1, F10A, 2 Technology Place, Macquarie University, NSW 2109

Amendments approved by the AEC since initial approval:

1. *Amendment #1* - Add Erin Lynch as Student. *(Executive Approved. Ratified by AEC 18 February 2016).*
2. *Amendment #2* - Add Dr Elinor Hortle as Associate Investigator. *(Executive Approved. Ratified by AEC 18 February 2016).*
3. *Amendment #3* - Add Dr Hamideh Shahheydari as Researcher. *(Executive Approved. Ratified by AEC 18 February 2016).*
4. *Amendment #4* - Add Rola Bazzi as Animal Technician/Research Assistant. *(Executive Approved. Ratified by AEC 17 March 2016).*
5. *Amendment #5(a)* - Amend experimental design and *Amendment #5(b)* - Amend procedure *(Approved by the AEC 14 April 2016).*
6. *Amendment #6* - Amend Zebrafish husbandry protocol to allow for the live collection of sperm and eggs for cryopreservation and IVF. *(Approved by the AEC 16 June 2016).*
7. *Amendment #7* - Add Bianca Varney as weekend fish feeder & health check *(Executive approved. Ratified by AEC 07/12/2016).*

Amendments approved by the AEC since initial approval (Cont'd)

8. *Amendment #8 - Amend experimental procedure (Executive approved. Ratified by AEC 07/12/2016).*
9. *Amendment #9 - Additional procedure (Approved by AEC 07/12/2016).*
10. *Amendment #10 - Additional 2, 800 adult zebrafish (Approved by AEC 16/03/2017).*
11. *Amendment #11 - Add Katherine Robinson as Fish Feeder (Approved by AEC 16/03/2017).*
12. *Amendment #12 - Add Ariuntugs Ulziikhutag as Fish Feeder (Approved by AEC 16/03/2017).*
13. *Amendment #13 – Add Maxine Watchon as PhD Student (Approved by AEC 16/03/2017).*
14. *Amendment #14 - Add Kristy Yuan as Research Assistant (Approved by AEC 16/03/2017).*
15. *Amendment #15 - Add Angela Laird as Chief Investigator (Approved by AEC 16/03/2017).*
16. *Amendment #16 - Additional behavioural testing to detect changes in baseline activity, cognition and memory. (Approved by AEC 16/03/2017).*
17. *Amendment #17 - Additional 90 adult zebrafish to include 30 zebrafish added as adults (three groups of n=10) and 60 zebrafish raised from embryos to adults (three groups of n=20) (Approved by AEC 16/03/2017).*
18. *Amendment #18 - Add Emma Perri as PhD student (Executive approved. Ratified by AEC 12/04/2017).*
19. *Amendment #19 - Define the role of Fish Feeder (Executive approved. Ratified by AEC 12/04/2017).*
20. *Amendment #20 – Remove Joel Berliner from protocol (Executive approved. Ratified by AEC 20 July 2017).*
21. *Amendment #21 – Remove Vinod Sundaramoorthy from protocol (Executive approved. Ratified by AEC 20 July 2017).*
22. *Amendment #22 – Remove Elinor Hortle from protocol (Executive approved. Ratified by AEC 20 July 2017).*
23. *Amendment #23 – Remove Dasha Monisha Syal from protocol (Executive approved. Ratified by AEC 20 July 2017).*
24. *Amendment #24 – Remove Isabel Formella from protocol (Executive approved. Ratified by AEC 20 July 2017).*
25. *Amendment #25 – Remove Bianca Varney from protocol (Executive approved. Ratified by AEC 20 July 2017).*
26. *Amendment #26(a) - Additional procedure involving administration of substances (Approved by AEC 20 July 2017).*
27. *Amendment #26(b) - Additional 15,552 embryo and larval zebrafish for these treatments to be tested on (Approved by AEC 20 July 2017).*
28. *Amendment #27 - Add Sina Shadfar as PhD Candidate (Executive approved. Ratified by AEC 17 August 2017).*
29. *Amendment #28 - Add Reka Petra Toth as Student (Executive approved. Ratified by AEC 17 August 2017).*
30. *Amendment #29 - Add Luan Luu as Research Fellow (Executive approved. Ratified by AEC 21 September 2017).*

Conditions of Approval:
1. *Amendments #2 & #3 - Approved subject to strict supervision until competency established.*

Being animal research carried out in accordance with the Code of Practice for a recognised research purpose and in connection with animals (other than exempt animals) that have been obtained from the holder of an animal suppliers license.

A/Prof. Nathan Hart (Chair, Animal Ethics Committee)   **Approval Date:** 16 November 2017

A.2   Recipes and buffers

E3 embryo medium (pH 7.8)

5mM NaCl

0.17mMKC l

10mM HEPES

0.33 mM MgSO4

0.33 mM $CaCl_2$

0.5% methylene blue (Sigma-Aldrich)

in situ **hybridisation buffer**

50% Deionised formamide

5 X SSC

0.1% Tween 20

1mM EDTA

0.1% CHAPS

20g/L Blocking agent (Roche)

50ug/L Yeast tRNA

100ng/L Heparin

in situ **hybridisation blocking solution**

2% FBS

2 mg/ml BSA

1 in Tris buffer (pH 7.5)

in situ **hybridisation prehybridisation Buffer (HYB-)**

50% formamide

5 x SSC

0.1

H_2O to final volume   **Luria Bertani broth (LB)**

1.0 0.5 1.0% Sodium Chloride (NaCl)

PBS(T)

0.8% NaCl

0.02% KCl

0.02 M PO_4

pH 7.3

(0.1% Tween 20)

Proteinase K solution

2 μg/μl in

10 mM Tris-HCl (pH 7.5)

20 mM $CaCl_2$

50% glycerol

RIPA buffer / Calcium free solution 10 mM Tris-Cl (pH 8.0)

1 mM EDTA

1% Triton X-100

0.1% sodium deoxycholate

0.1% SDS

140 mM NaCl

1 mM PMSF

S.O.C. medium 2% tryptone

0.5 10 mM NaCl

2.5 mM KCl

10 mM $MgCl_2$

10 mM $MgSO_4$

20 mM glucose

20xSSC stock solution

150 mM NaCl

15 mM Na3-citrate

pH to 7.0

TE buffer

10mM Tris-HCl

1mM EDTA

adjusted to a pH of 8.0

Tricaine pH 7

400 mg tricaine powder (Simga-Aldrich)

97.9 mL deionised water

2.1 mL 1M Tris

Tris buffered saline (TBS) 10 X

For 1 L:

24 g Tris base (formula weight: 121.1 g)

88 g NaCl (formula weight: 58.4 g)

Dissolve in 900 mL distilled water

pH to 7.6 with 12 N HCl

Add distilled water to a final volume of 1 L

(0.1% Tween 20)

Western Blotting Running Buffer

5 X Tris Glycine (200ml)

SDS (10ml)

H2O (800ml)

Western Blotting Transfer Buffer

5 X Tris Glycine (160mL)

methanol (200mL)

H2O (640ml)

A.3 Duration of cyclin F expression in transient zebrafish models

mCherry fused *CCNF* expression was shown to persist for less that 24 hours in the transient *CCNF* zebrafish model. Expression was examined by both fluorescent microscopy and western blotting (Figure A.1)
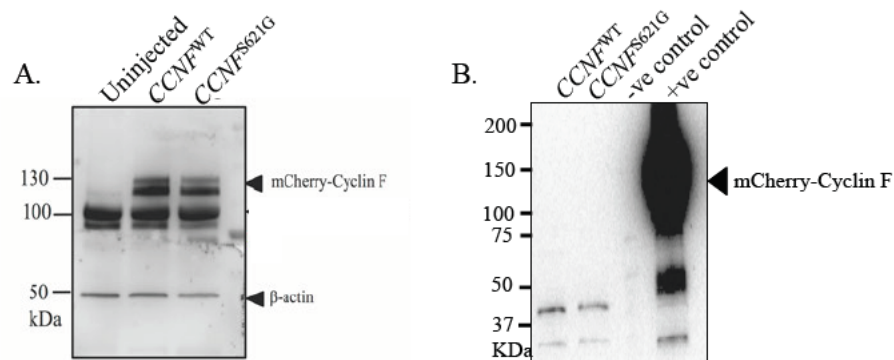

FIGURE A.1: **Duration of cyclin F expression in the transient *CCNF* zebrafish A.** Cyclin F antibody staining of a western blot performed on zebrafish lysates collected at 8 hpf following microinjection of mCherry-fused *CCNF*. Staining indicates equal expression of cyclinF$^{\text{WT}}$ and cyclin F$^{\text{S621G}}$. **B.** Cyclin F antibody staining of a western blot performed on zebrafish lysates collected at 24 hpf following microinjection of mCherry-fused *CCNF*. No cyclin F expression is detectable in either of the injected groups. Previously validated Neuro-2a cells transfected with *CCNF*$^{\text{WT}}$ was used as a positive control (Williams et al., 2016) and RIPA buffer containing no protein sample used as a negative control.

.

References

K. Abe, Y. Itoyama, G. Sobue, S. Tsuji, M. Aoki, M. Doyu, C. Hamada, K. Kondo, T. Yoneoka, M. Akimoto, and H. Yoshino. Confirmatory double-blind, parallel-group, placebo-controlled study of efficacy and safety of edaravone (MCI-186) in amyotrophic lateral sclerosis patients. *Amyotroph Lateral Scler Frontotemporal Degener*, 15(7-8):610–617, Dec 2014. 22

K. Abe, M. Aoki, S. Tsuji, Y. Itoyama, G. Sobue, M. Togo, C. Hamada, M. Tanaka, M. Akimoto, K. Nakamura, F. Takahashi, K. Kondo, H. Yoshino, K. Abe, M. Aoki, S. Tsuji, Y. Itoyama, G. Sobue, M. Togo, C. Hamada, H. Sasaki, I. Yabe, S. Doi, H. Warita, T. Imai, H. Ito, M. Fukuchi, E. Osumi, M. Wada, I. Nakano, M. Morita, K. Ogata, Y. Maruki, K. Ito, O. Kano, M. Yamazaki, Y. Takahashi, H. Ishiura, M. Ogino, R. Koike, C. Ishida, T. Uchiyama, K. Mizoguchi, T. Obi, H. Watanabe, N. Atsuta, I. Aiba, A. Taniguchi, H. Sawada, T. Hazama, H. Fujimura, H. Kusaka, T. Kunieda, H. Kikuchi, H. Matsuo, H. Ueyama, K. Uekawa, M. Tanaka, M. Akimoto, M. Ueda, A. Murakami, R. Sumii, T. Kudou, K. Nakamura, K. Morimoto, T. Yoneoka, M. Hirai, K. Sasaki, H. Terai, T. Natori, H. Matsui, K. Kotani, K. Yoshida, T. Iwasaki, F. Takahashi, K. Kondo, and H. Yoshino. Safety and efficacy of edaravone in well defined patients with amyotrophic lateral sclerosis: a randomised, double-blind, placebo-controlled trial. *Lancet Neurol*, 16(7):505–512, Jul 2017. 22

K. L. Ackerly and A. B. Ward. How temperature-induced variation in musculoskeletal

anatomy affects escape performance and survival of zebrafish (Danio rerio). *J Exp Zool A Ecol Genet Physiol*, 325(1):25–40, Jan 2016. 167

S. Agha-Mohammadi, M. O'Malley, A. Etemad, Z. Wang, X. Xiao, and M. T. Lotze. Second-generation tetracycline-regulatable promoter: repositioned tet operator elements optimize transactivator synergy while shorter minimal promoter offers tight basal leakiness. *J Gene Med*, 6(7):817–828, Jul 2004. 131

K. N. Agwuh and A. MacGowan. Pharmacokinetics and pharmacodynamics of the tetracyclines including glycylcyclines. *J. Antimicrob. Chemother.*, 58(2):256–265, Aug 2006. 133

R. M. Ahmed, M. Irish, J. van Eersel, A. Ittner, Y. D. Ke, A. Volkerling, J. van der Hoven, K. Tanaka, T. Karl, M. Kassiou, J. J. Kril, O. Piguet, J. Gotz, M. C. Kiernan, G. M. Halliday, J. R. Hodges, and L. M. Ittner. Mouse models of frontotemporal dementia: A comparison of phenotypes with clinical symptomatology. *Neurosci Biobehav Rev*, 74(Pt A):126–138, Mar 2017. 196

A. A. Akerberg, S. Stewart, and K. Stankunas. Spatial and temporal control of transgene expression in zebrafish. *PLoS ONE*, 9(3):e92217, 2014. 129

C. M. Akitake, M. Macurak, M. E. Halpern, and M. G. Goll. Transgenerational analysis of transcriptional silencing in zebrafish. *Dev. Biol.*, 352(2):191–201, Apr 2011. 122, 130

A. Al-Chalabi and C. M. Lewis. Modelling the effects of penetrance and family size on rates of sporadic and familial disease. *Hum. Hered.*, 71(4):281–288, 2011. 6

P. M. Andersen. Amyotrophic lateral sclerosis associated with mutations in the CuZn superoxide dismutase gene. *Curr Neurol Neurosci Rep*, 6(1):37–46, Jan 2006. 6

P. K. Andrus, T. J. Fleck, M. E. Gurney, and E. D. Hall. Protein oxidative damage in a transgenic mouse model of familial amyotrophic lateral sclerosis. *J. Neurochem.*, 71(5):2041–2048, Nov 1998. 19

M. Aoki, S. Kato, M. Nagai, and Y. Itoyama. Development of a rat model of amyotrophic lateral sclerosis expressing a human SOD1 transgene. *Neuropathology*, 25 (4):365–370, Dec 2005. 30

V. Arkhipova, B. Wendik, N. Devos, O. Ek, B. Peers, and D. Meyer. Characterization and regulation of the hb9/mnx1 beta-cell progenitor specific enhancer in zebrafish. *Dev. Biol.*, 365(1):290–302, May 2012. 106

C. Armon. Smoking may be considered an established risk factor for sporadic ALS. *Neurology*, 73(20):1693–1698, Nov 2009. 15

G. A. Armstrong and P. Drapeau. Loss and gain of FUS function impair neuromuscular synaptic transmission in a genetic model of ALS. *Hum. Mol. Genet.*, 22(21):4282–4292, Nov 2013. 39, 40, 63, 89, 97, 178

G. A. Armstrong, M. Liao, Z. You, A. Lissouba, B. E. Chen, and P. Drapeau. Homology Directed Knockin of Point Mutations in the Zebrafish tardbp and fus Genes in ALS Using the CRISPR/Cas9 System. *PLoS ONE*, 11(3):e0150188, 2016. 199

E. S. Arnold, S. C. Ling, S. C. Huelga, C. Lagier-Tourenne, M. Polymenidou, D. Ditsworth, H. B. Kordasiewicz, M. McAlonis-Downes, O. Platoshyn, P. A. Parone, S. Da Cruz, K. M. Clutario, D. Swing, L. Tessarollo, M. Marsala, C. E. Shaw, G. W. Yeo, and D. W. Cleveland. ALS-linked TDP-43 mutations produce aberrant RNA splicing and adult-onset motor neuron disease without aggregation or loss of nuclear TDP-43. *Proc. Natl. Acad. Sci. U.S.A.*, 110(8):E736–745, Feb 2013. 18, 35, 36

K. Asakawa and K. Kawakami. Targeted gene expression by the Gal4-UAS system in zebrafish. *Dev. Growth Differ.*, 50(6):391–399, Aug 2008. 129

P. E. Ash, Y. J. Zhang, C. M. Roberts, T. Saldi, H. Hutter, E. Buratti, L. Petrucelli, and C. D. Link. Neurotoxic effects of TDP-43 overexpression in C. elegans. *Hum. Mol. Genet.*, 19(16):3206–3218, Aug 2010. 35

A. Atanasio, V. Decman, D. White, M. Ramos, B. Ikiz, H. C. Lee, C. J. Siao, S. Brydges, E. LaRosa, Y. Bai, W. Fury, P. Burfeind, R. Zamfirova, G. Warshaw, J. Orengo,

A. Oyejide, M. Fralish, W. Auerbach, W. Poueymirou, J. Freudenberg, G. Gong, B. Zambrowicz, D. Valenzuela, G. Yancopoulos, A. Murphy, G. Thurston, and K. M. Lai. C9orf72 ablation causes immune dysregulation characterized by leukocyte expansion, autoantibody production, and glomerulonephropathy in mice. *Sci Rep*, 6: 23204, Mar 2016. 42

J. D. Atkin, M. A. Farg, B. J. Turner, D. Tomas, J. A. Lysaght, J. Nunan, A. Rembach, P. Nagley, P. M. Beart, S. S. Cheema, and M. K. Horne. Induction of the unfolded protein response in familial amyotrophic lateral sclerosis and association of protein-disulfide isomerase with superoxide dismutase 1. *J. Biol. Chem.*, 281(40):30152–30165, Oct 2006. 18, 30

J. D. Atkin, M. A. Farg, A. K. Walker, C. McLean, D. Tomas, and M. K. Horne. Endoplasmic reticulum stress and induction of the unfolded protein response in human sporadic amyotrophic lateral sclerosis. *Neurobiol. Dis.*, 30(3):400–407, Jun 2008. 18, 30

T. Atsumi. The ultrastructure of intramuscular nerves in amyotrophic lateral sclerosis. *Acta Neuropathol.*, 55(3):193–198, 1981. 18

T. Awano, G. S. Johnson, C. M. Wade, M. L. Katz, G. C. Johnson, J. F. Taylor, M. Perloski, T. Biagi, I. Baranowska, S. Long, P. A. March, N. J. Olby, G. D. Shelton, S. Khan, D. P. O'Brien, K. Lindblad-Toh, and J. R. Coates. Genome-wide association analysis reveals a SOD1 mutation in canine degenerative myelopathy that resembles amyotrophic lateral sclerosis. *Proc. Natl. Acad. Sci. U.S.A.*, 106(8): 2794–2799, Feb 2009. 33

P. J. Babin, C. Goizet, and D. Raldua. Zebrafish models of human motor neuron diseases: advantages and limitations. *Prog. Neurobiol.*, 118:36–58, Jul 2014. 28

S. Bahadorani, S. T. Mukai, J. Rabie, J. S. Beckman, J. P. Phillips, and A. J. Hilliker. Expression of zinc-deficient human superoxide dismutase in Drosophila neurons produces a locomotor defect linked to mitochondrial dysfunction. *Neurobiol. Aging*, 34 (10):2322–2330, Oct 2013. 32

M. Baker, I. R. Mackenzie, S. M. Pickering-Brown, J. Gass, R. Rademakers, C. Lindholm, J. Snowden, J. Adamson, A. D. Sadovnick, S. Rollinson, A. Cannon, E. Dwosh, D. Neary, S. Melquist, A. Richardson, D. Dickson, Z. Berger, J. Eriksen, T. Robinson, C. Zehr, C. A. Dickey, R. Crook, E. McGowan, D. Mann, B. Boeve, H. Feldman, and M. Hutton. Mutations in progranulin cause tau-negative frontotemporal dementia linked to chromosome 17. *Nature*, 442(7105):916–919, Aug 2006. 62

D. Balciunas, K. J. Wangensteen, A. Wilber, J. Bell, A. Geurts, S. Sivasubbu, X. Wang, P. B. Hackett, D. A. Largaespada, R. S. McIvor, and S. C. Ekker. Harnessing a high cargo-capacity transposon for genetic applications in vertebrates. *PLoS Genet.*, 2 (11):e169, Nov 2006. 106

S. Bannwarth, S. Ait-El-Mkadem, A. Chaussenot, E. C. Genin, S. Lacas-Gervais, K. Fragaki, L. Berg-Alonso, Y. Kageyama, V. Serre, D. G. Moore, A. Verschueren, C. Rouzier, I. Le Ber, G. Auge, C. Cochaud, F. Lespinasse, K. N'Guyen, A. de Septenville, A. Brice, P. Yu-Wai-Man, H. Sesaki, J. Pouget, and V. Paquis-Flucklinger. A mitochondrial origin for frontotemporal dementia and amyotrophic lateral sclerosis through CHCHD10 involvement. *Brain*, 137(Pt 8):2329–2345, Aug 2014. 7

S. C. Barber and P. J. Shaw. Oxidative stress in ALS: key role in motor neuron injury and therapeutic target. *Free Radic. Biol. Med.*, 48(5):629–641, Mar 2010. 16, 19

U. Baron, M. Gossen, and H. Bujard. Tetracycline-controlled transcription in eukaryotes: novel transactivators with graded transactivation potential. *Nucleic Acids Res.*, 25(14):2723–2729, Jul 1997. 131

V. V. Belzil, R. B. Katzman, and L. Petrucelli. ALS and FTD: an epigenetic perspective. *Acta Neuropathol.*, 132(4):487–502, Oct 2016. 44

G. Bensimon, L. Lacomblez, and V. Meininger. A controlled trial of riluzole in amyotrophic lateral sclerosis. ALS/Riluzole Study Group. *N. Engl. J. Med.*, 330(9): 585–591, Mar 1994. 22

R. L. Bernardos and P. A. Raymond. GFAP transgenic zebrafish. *Gene Expr. Patterns*, 6(8):1007–1013, Oct 2006. 106

L. G. Bilsland, E. Sahai, G. Kelly, M. Golding, L. Greensmith, and G. Schiavo. Deficits in axonal transport precede ALS symptoms in vivo. *Proc. Natl. Acad. Sci. U.S.A.*, 107(47):20523–20528, Nov 2010. 19

C. A. Blizzard, K. A. Southam, E. Dawkins, K. E. Lewis, A. E. King, J. A. Clark, and T. C. Dickson. Identifying the primary site of pathogenesis in amyotrophic lateral sclerosis - vulnerability of lower motor neurons to proximal excitotoxicity. *Dis Model Mech*, 8(3):215–224, Mar 2015. 173

S. Boeynaems, E. Bogaert, P. Van Damme, and L. Van Den Bosch. Inside out: the role of nucleocytoplasmic transport in ALS and FTLD. *Acta Neuropathol.*, 132(2): 159–173, Aug 2016. 17

S. Boillee, C. Vande Velde, and D. W. Cleveland. ALS: a disease of motor neurons and their nonneuronal neighbors. *Neuron*, 52(1):39–59, Oct 2006. 31

D. A. Bosco, N. Lemay, H. K. Ko, H. Zhou, C. Burke, T. J. Kwiatkowski, P. Sapp, D. McKenna-Yasek, R. H. Brown, and L. J. Hayward. Mutant FUS proteins that cause amyotrophic lateral sclerosis incorporate into stress granules. *Hum. Mol. Genet.*, 19(21):4160–4175, Nov 2010. 63

F. Bozzo, A. Mirra, and M. T. Carri. Oxidative stress and mitochondrial damage in the pathogenesis of ALS: New perspectives. *Neurosci. Lett.*, 636:3–8, Jan 2017. 17

V. Bozzoni, O. Pansarasa, L. Diamanti, G. Nosari, C. Cereda, and M. Ceroni. Amyotrophic lateral sclerosis and environmental factors. *Funct. Neurol.*, 31(1):7–19, 2016. 16

D. Brenner, K. Muller, T. Wieland, P. Weydt, S. Bohm, D. Lule, A. Hubers, C. Neuwirth, M. Weber, G. Borck, M. Wahlqvist, K. M. Danzer, A. E. Volk,

T. Meitinger, T. M. Strom, M. Otto, J. Kassubek, A. C. Ludolph, P. M. Andersen, and J. H. Weishaupt. NEK1 mutations in familial amyotrophic lateral sclerosis. *Brain*, 139(Pt 5):e28, May 2016. 7, 187

J. Brettschneider, H. Mogel, V. Lehmensiek, T. Ahlert, S. Sussmuth, A. C. Ludolph, and H. Tumani. Proteome analysis of cerebrospinal fluid in amyotrophic lateral sclerosis (ALS). *Neurochem. Res.*, 33(11):2358–2363, Nov 2008. 18

L. I. Bruijn, M. W. Becher, M. K. Lee, K. L. Anderson, N. A. Jenkins, N. G. Copeland, S. S. Sisodia, J. D. Rothstein, D. R. Borchelt, D. L. Price, and D. W. Cleveland. ALS-linked SOD1 mutant G85R mediates damage to astrocytes and promotes rapidly progressive disease with SOD1-containing inclusions. *Neuron*, 18(2):327–338, Feb 1997. 32

L. I. Bruijn, M. K. Houseweart, S. Kato, K. L. Anderson, S. D. Anderson, E. Ohama, A. G. Reaume, R. W. Scott, and D. W. Cleveland. Aggregation and motor neuron toxicity of an ALS-linked SOD1 mutant independent from wild-type SOD1. *Science*, 281(5384):1851–1854, Sep 1998. 29

A. Burberry, N. Suzuki, J. Y. Wang, R. Moccia, D. A. Mordes, M. H. Stewart, S. Suzuki-Uematsu, S. Ghosh, A. Singh, F. T. Merkle, K. Koszka, Q. Z. Li, L. Zon, D. J. Rossi, J. J. Trowbridge, L. D. Notarangelo, and K. Eggan. Loss-of-function mutations in the C9ORF72 mouse ortholog cause fatal autoimmune disease. *Sci Transl Med*, 8(347):347ra93, Jul 2016. 42

M. F. Burkhardt, F. J. Martinez, S. Wright, C. Ramos, D. Volfson, M. Mason, J. Garnes, V. Dang, J. Lievers, U. Shoukat-Mumtaz, R. Martinez, H. Gai, R. Blake, E. Vaisberg, M. Grskovic, C. Johnson, S. Irion, J. Bright, B. Cooper, L. Nguyen, I. Griswold-Prenner, and A. Javaherian. A cellular model for sporadic ALS using patient-derived induced pluripotent stem cells. *Mol. Cell. Neurosci.*, 56:355–364, Sep 2013. 200

T. A. Caller, N. C. Field, J. W. Chipman, X. Shi, B. T. Harris, and E. W. Stommel. Spatial clustering of amyotrophic lateral sclerosis and the potential role of BMAA. *Amyotroph Lateral Scler*, 13(1):25–32, Jan 2012. 16

L. J. Campbell, J. J. Willoughby, and A. M. Jensen. Two types of Tet-On transgenic lines for doxycycline-inducible gene expression in zebrafish rod photoreceptors and a gateway-based tet-on toolkit. *PLoS ONE*, 7(12):e51270, 2012. 52, 132, 166

D. Campos-Melo, C. A. Droppelmann, Z. He, K. Volkening, and M. J. Strong. Altered microRNA expression profile in Amyotrophic Lateral Sclerosis: a role in the regulation of NFL mRNA levels. *Mol Brain*, 6:26, May 2013. 18

J. R. Cannon and J. T. Greenamyre. The role of environmental exposures in neurodegeneration and neurodegenerative diseases. *Toxicol. Sci.*, 124(2):225–250, Dec 2011. 44

V. Cappello and M. Francolini. Neuromuscular Junction Dismantling in Amyotrophic Lateral Sclerosis. *Int J Mol Sci*, 18(10), Oct 2017. 173

I. Casci and U. B. Pandey. A fruitful endeavor: modeling ALS in the fruit fly. *Brain Res.*, 1607:47–74, May 2015. 28

K. Castillo, M. Nassif, V. Valenzuela, F. Rojas, S. Matus, G. Mercado, F. A. Court, B. van Zundert, and C. Hetz. Trehalose delays the progression of amyotrophic lateral sclerosis by enhancing autophagy in motoneurons. *Autophagy*, 9(9):1308–1320, Sep 2013. 190

R. Chang-Hong, M. Wada, S. Koyama, H. Kimura, S. Arawaka, T. Kawanami, K. Kurita, T. Kadoya, M. Aoki, Y. Itoyama, and T. Kato. Neuroprotective effect of oxidized galectin-1 in a transgenic mouse model of amyotrophic lateral sclerosis. *Exp. Neurol.*, 194(1):203–211, Jul 2005. 32

A. Chase. Motor neuron disease: loss-of-function mutations in TBK1 can cause familial ALS. *Nat Rev Neurol*, 11(5):246, May 2015. 7

A. Chaussenot, I. Le Ber, S. Ait-El-Mkadem, A. Camuzat, A. de Septenville, S. Bannwarth, E. C. Genin, V. Serre, G. Auge, A. Brice, J. Pouget, and V. Paquis-Flucklinger. Screening of CHCHD10 in a French cohort confirms the involvement

of this gene in frontotemporal dementia with amyotrophic lateral sclerosis patients. *Neurobiol. Aging*, 35(12):1–2884, Dec 2014. 7

D. Chen, Y. Wang, and E. R. Chin. Activation of the endoplasmic reticulum stress response in skeletal muscle of G93A*SOD1 amyotrophic lateral sclerosis mice. *Front Cell Neurosci*, 9:170, 2015a. 30

T. Chen, R. Benmohamed, J. Kim, K. Smith, D. Amante, R. I. Morimoto, D. R. Kirsch, R. J. Ferrante, and R. B. Silverman. ADME-guided design and synthesis of aryloxanyl pyrazolone derivatives to block mutant superoxide dismutase 1 (SOD1) cytotoxicity and protein aggregation: potential application for the treatment of amyotrophic lateral sclerosis. *J. Med. Chem.*, 55(1):515–527, Jan 2012. 184

X. Chen, J. W. Barclay, R. D. Burgoyne, and A. Morgan. Using C. elegans to discover therapeutic compounds for ageing-associated neurodegenerative diseases. *Chem Cent J*, 9:65, 2015b. 27

Y. Chen, M. Yang, J. Deng, X. Chen, Y. Ye, L. Zhu, J. Liu, H. Ye, Y. Shen, Y. Li, E. J. Rao, K. Fushimi, X. Zhou, E. H. Bigio, M. Mesulam, Q. Xu, and J. Y. Wu. Expression of human FUS protein in Drosophila leads to progressive neurodegeneration. *Protein Cell*, 2(6):477–486, Jun 2011. 40

Y. Z. Chen, C. L. Bennett, H. M. Huynh, I. P. Blair, I. Puls, J. Irobi, I. Dierick, A. Abel, M. L. Kennerson, B. A. Rabin, G. A. Nicholson, M. Auer-Grumbach, K. Wagner, P. De Jonghe, J. W. Griffin, K. H. Fischbeck, V. Timmerman, D. R. Cornblath, and P. F. Chance. DNA/RNA helicase gene mutations in a form of juvenile amyotrophic lateral sclerosis (ALS4). *Am. J. Hum. Genet.*, 74(6):1128–1135, Jun 2004. 7, 187

C. W. Cheng, M. J. Lin, and C. K. Shen. Rapamycin alleviates pathogenesis of a new Drosophila model of ALS-TDP. *J. Neurogenet.*, 29(2-3):59–68, 2015. 35

C. Cheroni, M. Marino, M. Tortarolo, P. Veglianese, S. De Biasi, E. Fontana, L. V. Zuccarello, C. J. Maynard, N. P. Dantuma, and C. Bendotti. Functional alterations

of the ubiquitin-proteasome system in motor neurons of a mouse model of familial amyotrophic lateral sclerosis. *Hum. Mol. Genet.*, 18(1):82–96, Jan 2009. 30

A. Chesi, B. T. Staahl, A. Jovi?i?, J. Couthouis, M. Fasolino, A. R. Raphael, T. Yamazaki, L. Elias, M. Polak, C. Kelly, K. L. Williams, J. A. Fifita, N. J. Maragakis, G. A. Nicholson, O. D. King, R. Reed, G. R. Crabtree, I. P. Blair, J. D. Glass, and A. D. Gitler. Exome sequencing to identify de novo mutations in sporadic ALS trios. *Nat. Neurosci.*, 16(7):851–855, Jul 2013. 7

J. Chew, T. F. Gendron, M. Prudencio, H. Sasaguri, Y. J. Zhang, M. Castanedes-Casey, C. W. Lee, K. Jansen-West, A. Kurti, M. E. Murray, K. F. Bieniek, P. O. Bauer, E. C. Whitelaw, L. Rousseau, J. N. Stankowski, C. Stetler, L. M. Daughrity, E. A. Perkerson, P. Desaro, A. Johnston, K. Overstreet, D. Edbauer, R. Rademakers, K. B. Boylan, D. W. Dickson, J. D. Fryer, and L. Petrucelli. Neurodegeneration. C9ORF72 repeat expansions in mice cause TDP-43 pathology, neuronal loss, and behavioral deficits. *Science*, 348(6239):1151–1154, Jun 2015. 43, 196

H. J. Chon, K. J. Bae, Y. Lee, and J. Kim. The casein kinase 2 inhibitor, CX-4945, as an anti-cancer drug in treatment of human hematological malignancies. *Front Pharmacol*, 6:70, 2015. 186

C. Y. Chow, J. E. Landers, S. K. Bergren, P. C. Sapp, A. E. Grant, J. M. Jones, L. Everett, G. M. Lenk, D. M. McKenna-Yasek, L. S. Weisman, D. Figlewicz, R. H. Brown, and M. H. Meisler. Deleterious variants of FIG4, a phosphoinositide phosphatase, in patients with ALS. *Am. J. Hum. Genet.*, 84(1):85–88, Jan 2009. 7

S. Ciura, S. Lattante, I. Le Ber, M. Latouche, H. Tostivint, A. Brice, and E. Kabashi. Loss of function of C9orf72 causes motor deficits in a zebrafish model of Amyotrophic Lateral Sclerosis. *Ann. Neurol.*, May 2013. 42, 43, 98

J. A. Clark, K. A. Southam, C. A. Blizzard, A. E. King, and T. C. Dickson. Axonal degeneration, distal collateral branching and neuromuscular junction architecture alterations occur prior to symptom onset in the SOD1(G93A) mouse model of amyotrophic lateral sclerosis. *J. Chem. Neuroanat.*, 76(Pt A):35–47, Oct 2016. 173

K. J. Clark, M. D. Urban, K. J. Skuster, and S. C. Ekker. Transgenic zebrafish using transposable elements. *Methods Cell Biol.*, 104:137–149, 2011. 121, 123

P. Collas. Modulation of plasmid DNA methylation and expression in zebrafish embryos. *Nucleic Acids Res.*, 26(19):4454–4461, Oct 1998. 107

F. Coppede. An overview of DNA repair in amyotrophic lateral sclerosis. *ScientificWorldJournal*, 11:1679–1691, 2011. 17

P. Couratier, P. Corcia, G. Lautrette, M. Nicol, and B. Marin. ALS and frontotemporal dementia belong to a common disease spectrum. *Rev. Neurol. (Paris)*, 173(5):273–279, May 2017. 4

J. Couthouis, M. P. Hart, J. Shorter, M. DeJesus-Hernandez, R. Erion, R. Oristano, A. X. Liu, D. Ramos, N. Jethava, D. Hosangadi, J. Epstein, A. Chiang, Z. Diaz, T. Nakaya, F. Ibrahim, H. J. Kim, J. A. Solski, K. L. Williams, J. Mojsilovic-Petrovic, C. Ingre, K. Boylan, N. R. Graff-Radford, D. W. Dickson, D. Clay-Falcone, L. Elman, L. McCluskey, R. Greene, R. G. Kalb, V. M. Lee, J. Q. Trojanowski, A. Ludolph, W. Robberecht, P. M. Andersen, G. A. Nicholson, I. P. Blair, O. D. King, N. M. Bonini, V. Van Deerlin, R. Rademakers, Z. Mourelatos, and A. D. Gitler. A yeast functional screen predicts new candidate ALS disease genes. *Proc. Natl. Acad. Sci. U.S.A.*, 108(52):20881–20890, Dec 2011. 7

J. Couthouis, M. P. Hart, R. Erion, O. D. King, Z. Diaz, T. Nakaya, F. Ibrahim, H. J. Kim, J. Mojsilovic-Petrovic, S. Panossian, C. E. Kim, E. C. Frackelton, J. A. Solski, K. L. Williams, D. Clay-Falcone, L. Elman, L. McCluskey, R. Greene, H. Hakonarson, R. G. Kalb, V. M. Lee, J. Q. Trojanowski, G. A. Nicholson, I. P. Blair, N. M. Bonini, V. M. Van Deerlin, Z. Mourelatos, J. Shorter, and A. D. Gitler. Evaluating the role of the FUS/TLS-related gene EWSR1 in amyotrophic lateral sclerosis. *Hum. Mol. Genet.*, 21(13):2899–2911, Jul 2012. 7

G. Cozza and L. A. Pinna. Casein kinases as potential therapeutic targets. *Expert Opin. Ther. Targets*, 20(3):319–340, 2016. 187

S. Cronin, M. J. Greenway, J. H. Prehn, and O. Hardiman. Paraoxonase promoter and intronic variants modify risk of sporadic amyotrophic lateral sclerosis. *J. Neurol. Neurosurg. Psychiatry*, 78(9):984–986, Sep 2007. 7

M. Cruts, S. Kumar-Singh, and C. Van Broeckhoven. Progranulin mutations in ubiquitin-positive frontotemporal dementia linked to chromosome 17q21. *Curr Alzheimer Res*, 3(5):485–491, Dec 2006. 62

R. W. Daniels, A. J. Rossano, G. T. Macleod, and B. Ganetzky. Expression of multiple transgenes from a single construct using viral 2A peptides in Drosophila. *PLoS ONE*, 9(6):e100637, 2014. 166

N. P. Dantuma and L. C. Bott. The ubiquitin-proteasome system in neurodegenerative diseases: precipitating factor, yet part of the solution. *Front Mol Neurosci*, 7:70, 2014. 20

T. M. Dawson, H. S. Ko, and V. L. Dawson. Genetic animal models of Parkinson's disease. *Neuron*, 66(5):646–661, Jun 2010. 127

R. N. Day and M. W. Davidson. The fluorescent protein palette: tools for cellular imaging. *Chem Soc Rev*, 38(10):2887–2921, Oct 2009. 107

M. E. de Araujo and L. A. Huber. Subcellular fractionation. *Methods Mol. Biol.*, 357: 73–85, 2007. 193

K. J. De Vos and M. Hafezparast. Neurobiology of axonal transport defects in motor neuron diseases: Opportunities for translational research? *Neurobiol. Dis.*, 105: 283–299, Sep 2017. 17

K. J. De Vos, A. L. Chapman, M. E. Tennant, C. Manser, E. L. Tudor, K. F. Lau, J. Brownlees, S. Ackerley, P. J. Shaw, D. M. McLoughlin, C. E. Shaw, P. N. Leigh, C. C. J. Miller, and A. J. Grierson. Familial amyotrophic lateral sclerosis-linked SOD1 mutants perturb fast axonal transport to reduce axonal mitochondria content. *Hum. Mol. Genet.*, 16(22):2720–2728, Nov 2007. 19

M. DeJesus-Hernandez, I. R. Mackenzie, B. F. Boeve, A. L. Boxer, M. Baker, N. J. Rutherford, A. M. Nicholson, N. A. Finch, H. Flynn, J. Adamson, N. Kouri, A. Wojtas, P. Sengdy, G. Y. Hsiung, A. Karydas, W. W. Seeley, K. A. Josephs, G. Coppola, D. H. Geschwind, Z. K. Wszolek, H. Feldman, D. S. Knopman, R. C. Petersen, B. L. Miller, D. W. Dickson, K. B. Boylan, N. R. Graff-Radford, and R. Rademakers. Expanded GGGGCC hexanucleotide repeat in noncoding region of C9ORF72 causes chromosome 9p-linked FTD and ALS. *Neuron*, 72(2):245–256, Oct 2011. 7, 42

H. X. Deng, Y. Shi, Y. Furukawa, H. Zhai, R. Fu, E. Liu, G. H. Gorrie, M. S. Khan, W. Y. Hung, E. H. Bigio, T. Lukas, M. C. Dal Canto, T. V. O'Halloran, and T. Siddique. Conversion to the amyotrophic lateral sclerosis phenotype is associated with intermolecular linked insoluble aggregates of SOD1 in mitochondria. *Proc. Natl. Acad. Sci. U.S.A.*, 103(18):7142–7147, May 2006. 32, 33

H. X. Deng, W. Chen, S. T. Hong, K. M. Boycott, G. H. Gorrie, N. Siddique, Y. Yang, F. Fecto, Y. Shi, H. Zhai, H. Jiang, M. Hirano, E. Rampersaud, G. H. Jansen, S. Donkervoort, E. H. Bigio, B. R. Brooks, K. Ajroud, R. L. Sufit, J. L. Haines, E. Mugnaini, M. A. Pericak-Vance, and T. Siddique. Mutations in UBQLN2 cause dominant X-linked juvenile and adult-onset ALS and ALS/dementia. *Nature*, 477 (7363):211–215, Aug 2011. 7, 21

S. J. Dixon, K. M. Lemberg, M. R. Lamprecht, R. Skouta, E. M. Zaitsev, C. E. Gleason, D. N. Patel, A. J. Bauer, A. M. Cantley, W. S. Yang, B. Morrison, and B. R. Stockwell. Ferroptosis: an iron-dependent form of nonapoptotic cell death. *Cell*, 149(5):1060–1072, May 2012. 96

M. Domercq and C. Matute. Neuroprotection by tetracyclines. *Trends Pharmacol. Sci.*, 25(12):609–612, Dec 2004. 133

C. Donaghy, A. Dick, O. Hardiman, and V. Patterson. Timeliness of diagnosis in motor neurone disease: a population-based study. *Ulster Med J*, 77(1):18–21, Jan 2008. 181

K. Dooley and L. I. Zon. Zebrafish: a model system for the study of human disease. *Curr. Opin. Genet. Dev.*, 10(3):252–256, Jun 2000. 28

S. L. Eaton, M. L. Hurtado, K. J. Oldknow, L. C. Graham, T. W. Marchant, T. H. Gillingwater, C. Farquharson, and T. M. Wishart. A guide to modern quantitative fluorescent western blotting with troubleshooting strategies. *J Vis Exp*, (93):e52099, Nov 2014. 95

B. M. Edens, J. Yan, N. Miller, H. X. Deng, T. Siddique, and Y. C. Ma. A novel ALS-associated variant in UBQLN4 regulates motor axon morphogenesis. *Elife*, 6, May 2017. 63

A. Eisen, B. Pant, and H. Stewart. Cortical excitability in amyotrophic lateral sclerosis: a clue to pathogenesis. *Can J Neurol Sci*, 20(1):11–16, Feb 1993. 173

A. C. Elden, H. J. Kim, M. P. Hart, A. S. Chen-Plotkin, B. S. Johnson, X. Fang, M. Armakola, F. Geser, R. Greene, M. M. Lu, A. Padmanabhan, D. Clay-Falcone, L. McCluskey, L. Elman, D. Juhr, P. J. Gruber, U. Rub, G. Auburger, J. Q. Trojanowski, V. M. Lee, V. M. Van Deerlin, N. M. Bonini, and A. D. Gitler. Ataxin-2 intermediate-length polyglutamine expansions are associated with increased risk for ALS. *Nature*, 466(7310):1069–1075, Aug 2010. 7

G. A. Elder, M. A. Gama Sosa, and R. De Gasperi. Transgenic mouse models of Alzheimer's disease. *Mt. Sinai J. Med.*, 77(1):69–81, 2010. 127

F. Ellett, L. Pase, J. W. Hayman, A. Andrianopoulos, and G. J. Lieschke. mpeg1 promoter transgenes direct macrophage-lineage expression in zebrafish. *Blood*, 117 (4):49–56, Jan 2011. 106, 194

P. L. Else and A. F. Bennett. The thermal dependence of locomotor performance and muscle contractile function in the salamander Ambystoma tigrinum nebulosum. *J. Exp. Biol.*, 128:219–233, Mar 1987. 167

M. A. Farg, A. Konopka, K. Y. Soo, D. Ito, and J. D. Atkin. The DNA damage response (DDR) is induced by the C9orf72 repeat expansion in amyotrophic lateral sclerosis. *Hum. Mol. Genet.*, 26(15):2882–2896, Aug 2017. 18

F. Fecto, J. Yan, S. P. Vemula, E. Liu, Y. Yang, W. Chen, J. G. Zheng, Y. Shi, N. Siddique, H. Arrat, S. Donkervoort, S. Ajroud-Driss, R. L. Sufit, S. L. Heller, H. X. Deng, and T. Siddique. SQSTM1 mutations in familial and sporadic amyotrophic lateral sclerosis. *Arch. Neurol.*, 68(11):1440–1446, Nov 2011. 7, 189

R. Feil, J. Brocard, B. Mascrez, M. LeMeur, D. Metzger, and P. Chambon. Ligand-activated site-specific recombination in mice. *Proc. Natl. Acad. Sci. U.S.A.*, 93(20): 10887–10890, Oct 1996. 129

R. E. Ferguson, H. P. Carroll, A. Harris, E. R. Maher, P. J. Selby, and R. E. Banks. Housekeeping proteins: a preliminary study illustrating some limitations as useful references in protein expression studies. *Proteomics*, 5(2):566–571, Feb 2005. 94

R. J. Ferrante, L. A. Shinobu, J. B. Schulz, R. T. Matthews, C. E. Thomas, N. W. Kowall, M. E. Gurney, and M. F. Beal. Increased 3-nitrotyrosine and oxidative damage in mice with a human copper/zinc superoxide dismutase mutation. *Ann. Neurol.*, 42(3):326–334, Sep 1997. 19

D. A. Figlewicz, A. Krizus, M. G. Martinoli, V. Meininger, M. Dib, G. A. Rouleau, and J. P. Julien. Variants of the heavy neurofilament subunit are associated with the development of amyotrophic lateral sclerosis. *Hum. Mol. Genet.*, 3(10):1757–1761, Oct 1994. 7

M. Filali, R. Lalonde, and S. Rivest. Sensorimotor and cognitive functions in a SOD1(G37R) transgenic mouse model of amyotrophic lateral sclerosis. *Behav. Brain Res.*, 225(1):215–221, Nov 2011. 32

L. R. Fischer and J. D. Glass. Oxidative stress induced by loss of Cu,Zn-superoxide dismutase (SOD1) or superoxide-generating herbicides causes axonal degeneration in mouse DRG cultures. *Acta Neuropathol.*, 119(2):249–259, Feb 2010. 33

L. R. Fischer, D. G. Culver, P. Tennant, A. A. Davis, M. Wang, A. Castellano-Sanchez, J. Khan, M. A. Polak, and J. D. Glass. Amyotrophic lateral sclerosis is a distal

axonopathy: evidence in mice and man. *Exp. Neurol.*, 185(2):232–240, Feb 2004. 173

D. G. Flood, A. G. Reaume, J. A. Gruner, E. K. Hoffman, J. D. Hirsch, Y. G. Lin, K. S. Dorfman, and R. W. Scott. Hindlimb motor neurons require Cu/Zn superoxide dismutase for maintenance of neuromuscular junctions. *Am. J. Pathol.*, 155(2):663–672, Aug 1999. 33

F. Foroodi, W. C. Duivenvoorden, and G. Singh. Interactions of doxycycline with chemotherapeutic agents in human breast adenocarcinoma MDA-MB-231 cells. *Anticancer Drugs*, 20(2):115–122, Feb 2009. 166

A. Fortna, Y. Kim, E. MacLaren, K. Marshall, G. Hahn, L. Meltesen, M. Brenton, R. Hink, S. Burgers, T. Hernandez-Boussard, A. Karimpour-Fard, D. Glueck, L. Mc-Gavran, R. Berry, J. Pollack, and J. M. Sikela. Lineage-specific gene duplication and loss in human and great ape evolution. *PLoS Biol.*, 2(7):E207, Jul 2004. 60

B. D. Freibaum, Y. Lu, R. Lopez-Gonzalez, N. C. Kim, S. Almeida, K. H. Lee, N. Badders, M. Valentine, B. L. Miller, P. C. Wong, L. Petrucelli, H. J. Kim, F. B. Gao, and J. P. Taylor. GGGGCC repeat expansion in C9orf72 compromises nucleocytoplasmic transport. *Nature*, 525(7567):129–133, Sep 2015. 8, 43

A. Freischmidt, T. Wieland, B. Richter, W. Ruf, V. Schaeffer, K. Muller, N. Marroquin, F. Nordin, A. Hubers, P. Weydt, S. Pinto, R. Press, S. Millecamps, N. Molko, E. Bernard, C. Desnuelle, M. H. Soriani, J. Dorst, E. Graf, U. Nordstrom, M. S. Feiler, S. Putz, T. M. Boeckers, T. Meyer, A. S. Winkler, J. Winkelman, M. de Carvalho, D. R. Thal, M. Otto, T. Brannstrom, A. E. Volk, P. Kursula, K. M. Danzer, P. Lichtner, I. Dikic, T. Meitinger, A. C. Ludolph, T. M. Strom, P. M. Andersen, and J. H. Weishaupt. Haploinsufficiency of TBK1 causes familial ALS and frontotemporal dementia. *Nat. Neurosci.*, 18(5):631–636, May 2015. 7

L. Fuiman and R. Batty. What a drag it is getting cold: partitioning the physical and physiological effects of temperature on fish swimming. *J. Exp. Biol.*, 200(Pt 12): 1745–1755, 1997. 167

E. Fujimoto, B. Gaynes, C. J. Brimley, C. B. Chien, and J. L. Bonkowsky. Gal80 intersectional regulation of cell-type specific expression in vertebrates. *Dev. Dyn.*, 240(10):2324–2334, Oct 2011. 129

J. Galper, S. L. Rayner, A. L. Hogan, J. A. Fifita, A. Lee, R. S. Chung, I. P. Blair, and S. Yang. Cyclin F: A component of an E3 ubiquitin ligase complex with roles in neurodegeneration and cancer. *Int. J. Biochem. Cell Biol.*, 89:216–220, Aug 2017. 2, 9

J. Gass, A. Cannon, I. R. Mackenzie, B. Boeve, M. Baker, J. Adamson, R. Crook, S. Melquist, K. Kuntz, R. Petersen, K. Josephs, S. M. Pickering-Brown, N. Graff-Radford, R. Uitti, D. Dickson, Z. Wszolek, J. Gonzalez, T. G. Beach, E. Bigio, N. Johnson, S. Weintraub, M. Mesulam, C. L. White, B. Woodruff, R. Caselli, G. Y. Hsiung, H. Feldman, D. Knopman, M. Hutton, and R. Rademakers. Mutations in progranulin are a major cause of ubiquitin-positive frontotemporal lobar degeneration. *Hum. Mol. Genet.*, 15(20):2988–3001, Oct 2006. 62

M. Gassmann, B. Grenacher, B. Rohde, and J. Vogel. Quantifying Western blots: pitfalls of densitometry. *Electrophoresis*, 30(11):1845–1855, Jun 2009. 94, 95

M. A. Gates, L. Kim, E. S. Egan, T. Cardozo, H. I. Sirotkin, S. T. Dougan, D. Lashkari, R. Abagyan, A. F. Schier, and W. S. Talbot. A genetic linkage map for zebrafish: comparative analysis and localization of genes and expressed sequences. *Genome Res.*, 9(4):334–347, Apr 1999. 61

T. Gidalevitz, T. Krupinski, S. Garcia, and R. I. Morimoto. Destabilizing protein polymorphisms in the genetic background direct phenotypic expression of mutant SOD1 toxicity. *PLoS Genet.*, 5(3):e1000399, Mar 2009. 30

M. J. Gilbert, T. C. Zerulla, and K. B. Tierney. Zebrafish (Danio rerio) as a model for the study of aging and exercise: physical ability and trainability decrease with age. *Exp. Gerontol.*, 50:106–113, Feb 2014. 92

M. T. Giordana, P. Ferrero, S. Grifoni, A. Pellerino, A. Naldi, and A. Montuschi. Dementia and cognitive impairment in amyotrophic lateral sclerosis: a review. *Neurol. Sci.*, 32(1):9–16, Feb 2011. 4

M. G. Goll, R. Anderson, D. Y. Stainier, A. C. Spradling, and M. E. Halpern. Transcriptional silencing and reactivation in transgenic zebrafish. *Genetics*, 182(3):747–755, Jul 2009. 122, 130

J. Gordon, S. Amini, and M. K. White. General overview of neuronal cell culture. *Methods Mol. Biol.*, 1078:1–8, 2013. 185

P. H. Gordon, D. H. Moore, D. F. Gelinas, C. Qualls, M. E. Meister, J. Werner, M. Mendoza, J. Mass, G. Kushner, and R. G. Miller. Placebo-controlled phase I/II studies of minocycline in amyotrophic lateral sclerosis. *Neurology*, 62(10):1845–1847, May 2004. 165

P. H. Gordon, D. H. Moore, R. G. Miller, J. M. Florence, J. L. Verheijde, C. Doorish, J. F. Hilton, G. M. Spitalny, R. B. MacArthur, H. Mitsumoto, H. E. Neville, K. Boylan, T. Mozaffar, J. M. Belsh, J. Ravits, R. S. Bedlack, M. C. Graves, L. F. McCluskey, R. J. Barohn, and R. Tandan. Efficacy of minocycline in patients with amyotrophic lateral sclerosis: a phase III randomised trial. *Lancet Neurol*, 6(12): 1045–1053, Dec 2007. 165

M. Gossen and H. Bujard. Tight control of gene expression in mammalian cells by tetracycline-responsive promoters. *Proc. Natl. Acad. Sci. U.S.A.*, 89(12):5547–5551, Jun 1992. 128, 130, 131

M. Gossen, S. Freundlieb, G. Bender, G. Muller, W. Hillen, and H. Bujard. Transcriptional activation by tetracyclines in mammalian cells. *Science*, 268(5218):1766–1769, Jun 1995. 130, 131

K. S. Graffmo, K. Forsberg, J. Bergh, A. Birve, P. Zetterstrom, P. M. Andersen, S. L. Marklund, and T. Brannstrom. Expression of wild-type human superoxide

dismutase-1 in mice causes amyotrophic lateral sclerosis. *Hum. Mol. Genet.*, 22(1): 51–60, Jan 2013. 32

M. J. Greenway, P. M. Andersen, C. Russ, S. Ennis, S. Cashman, C. Donaghy, V. Patterson, R. Swingler, D. Kieran, J. Prehn, K. E. Morrison, A. Green, K. R. Acharya, R. H. Brown, and O. Hardiman. ANG mutations segregate with familial and 'sporadic' amyotrophic lateral sclerosis. *Nat. Genet.*, 38(4):411–413, Apr 2006. 7

S. Greer, R. Honeywell, M. Geletu, R. Arulanandam, and L. Raptis. Housekeeping genes; expression levels may change with density of cultured cells. *J. Immunol. Methods*, 355(1-2):76–79, Apr 2010. 94

F. Gros-Louis, R. Lariviere, G. Gowing, S. Laurent, W. Camu, J. P. Bouchard, V. Meininger, G. A. Rouleau, and J. P. Julien. A frameshift deletion in peripherin gene associated with amyotrophic lateral sclerosis. *J. Biol. Chem.*, 279(44): 45951–45956, Oct 2004. 7

F. Gros-Louis, J. Kriz, E. Kabashi, J. McDearmid, S. Millecamps, M. Urushitani, L. Lin, P. Dion, Q. Zhu, P. Drapeau, J. P. Julien, and G. A. Rouleau. Als2 mRNA splicing variants detected in KO mice rescue severe motor dysfunction phenotype in Als2 knock-down zebrafish. *Hum. Mol. Genet.*, 17(17):2691–2702, Sep 2008. 98

F. Gros-Louis, P. M. Andersen, N. Dupre, M. Urushitani, P. Dion, F. Souchon, M. D'Amour, W. Camu, V. Meininger, J. P. Bouchard, G. A. Rouleau, and J. P. Julien. Chromogranin B P413L variant as risk factor and modifier of disease onset for amyotrophic lateral sclerosis. *Proc. Natl. Acad. Sci. U.S.A.*, 106(51):21777–21782, Dec 2009. 7

J. L. Guenet. The mouse genome. *Genome Res.*, 15(12):1729–1740, Dec 2005. 26

R. Gupta, M. Lan, J. Mojsilovic-Petrovic, W. H. Choi, N. Safren, S. Barmada, M. J. Lee, and R. Kalb. The Proline/Arginine Dipeptide from Hexanucleotide Repeat Expanded C9ORF72 Inhibits the Proteasome. *eNeuro*, 4(1), 2017. 41

M. E. Gurney, H. Pu, A. Y. Chiu, M. C. Dal Canto, C. Y. Polchow, D. D. Alexander, J. Caliendo, A. Hentati, Y. W. Kwon, and H. X. Deng. Motor neuron degeneration in mice that express a human Cu,Zn superoxide dismutase mutation. *Science*, 264 (5166):1772–1775, Jun 1994. 29, 31, 32

S. Hadano, C. K. Hand, H. Osuga, Y. Yanagisawa, A. Otomo, R. S. Devon, N. Miyamoto, J. Showguchi-Miyata, Y. Okada, R. Singaraja, D. A. Figlewicz, T. Kwiatkowski, B. A. Hosler, T. Sagie, J. Skaug, J. Nasir, R. H. Brown, S. W. Scherer, G. A. Rouleau, M. R. Hayden, and J. E. Ikeda. A gene encoding a putative GTPase regulator is mutated in familial amyotrophic lateral sclerosis 2. *Nat. Genet.*, 29(2):166–173, Oct 2001. 7

M. E. Halpern, J. Rhee, M. G. Goll, C. M. Akitake, M. Parsons, and S. D. Leach. Gal4/UAS transgenic tools and their application to zebrafish. *Zebrafish*, 5(2):97–110, 2008. 129

S. Hans, J. Kaslin, D. Freudenreich, and M. Brand. Temporally-controlled site-specific recombination in zebrafish. *PLoS ONE*, 4(2):e4640, 2009. 128

S. Hans, D. Freudenreich, M. Geffarth, J. Kaslin, A. Machate, and M. Brand. Generation of a non-leaky heat shock-inducible Cre line for conditional Cre/lox strategies in zebrafish. *Dev. Dyn.*, 240(1):108–115, Jan 2011. 129

K. A. Hanson, S. H. Kim, D. A. Wassarman, and R. S. Tibbetts. Ubiquilin modifies TDP-43 toxicity in a Drosophila model of amyotrophic lateral sclerosis (ALS). *J. Biol. Chem.*, 285(15):11068–11072, Apr 2010. 35

O. Hardiman and L. H. van den Berg. Edaravone: a new treatment for ALS on the horizon? *Lancet Neurol*, 16(7):490–491, Jul 2017. 22

S. C. D. H. K. C. C. S. J. P. D. P. Hasler, C. T. and B. L. Tuftsa. Effect of water temperature on laboratory swimming performance and natural activity levels of adult largemouth bass. *Canadian J.Zoology*, 87(7):589–596, April 2009. 167

T. Hatzipetros, L. P. Bogdanik, V. R. Tassinari, J. D. Kidd, A. J. Moreno, C. Davis, M. Osborne, A. Austin, F. G. Vieira, C. Lutz, and S. Perrin. C57BL/6J congenic Prp-TDP43A315T mice develop progressive neurodegeneration in the myenteric plexus of the colon without exhibiting key features of ALS. *Brain Res.*, 1584:59–72, Oct 2014. 44

C. He, C. R. Bartholomew, W. Zhou, and D. J. Klionsky. Assaying autophagic activity in transgenic GFP-Lc3 and GFP-Gabarap zebrafish embryos. *Autophagy*, 5(4):520–526, May 2009. 190, 191

J. Heideker and I. E. Wertz. DUBs, the regulation of cell identity and disease. *Biochem. J.*, 465(1):1–26, Jan 2015. 20

J. S. Henkel, J. I. Engelhardt, L. Siklos, E. P. Simpson, S. H. Kim, T. Pan, J. C. Goodman, T. Siddique, D. R. Beers, and S. H. Appel. Presence of dendritic cells, MCP-1, and activated microglia/macrophages in amyotrophic lateral sclerosis spinal cord tissue. *Ann. Neurol.*, 55(2):221–235, Feb 2004. 19

G. Hernandez, C. Thornton, A. Stotland, D. Lui, J. Sin, J. Ramil, N. Magee, A. Andres, G. Quarato, R. S. Carreira, M. R. Sayen, R. Wolkowicz, and R. A. Gottlieb. MitoTimer: a novel tool for monitoring mitochondrial turnover. *Autophagy*, 9(11): 1852–1861, Nov 2013. 194

K. Herrup and Y. Yang. Cell cycle regulation in the postmitotic neuron: oxymoron or new biology? *Nat. Rev. Neurosci.*, 8(5):368–378, May 2007. 188

C. Hetz, P. Thielen, S. Matus, M. Nassif, F. Court, R. Kiffin, G. Martinez, A. M. Cuervo, R. H. Brown, and L. H. Glimcher. XBP-1 deficiency in the nervous system protects against amyotrophic lateral sclerosis by increasing autophagy. *Genes Dev.*, 23(19):2294–2306, Oct 2009. 18

G. G. Hicks, N. Singh, A. Nashabi, S. Mai, G. Bozek, L. Klewes, D. Arapovic, E. K. White, M. J. Koury, E. M. Oltz, L. Van Kaer, and H. E. Ruley. Fus deficiency in mice results in defective B-lymphocyte development and activation, high levels of

chromosomal instability and perinatal death. *Nat. Genet.*, 24(2):175–179, Feb 2000. 39

S. Higashijima, H. Okamoto, N. Ueno, Y. Hotta, and G. Eguchi. High-frequency generation of transgenic zebrafish which reliably express GFP in whole muscles or the whole body by using promoters of zebrafish origin. *Dev. Biol.*, 192(2):289–299, Dec 1997. 52

C. M. Higgins, C. Jung, and Z. Xu. ALS-associated mutant SOD1G93A causes mitochondrial vacuolation by expansion of the intermembrane space and by involvement of SOD1 aggregation and peroxisomes. *BMC Neurosci*, 4:16, Jul 2003. 18

V. C. Honnorat-Benabbou, A. A. Lebugle, B. Sallek, and D. Duffaut-Lagarrigue. Stability study of tetracyclines with respect to their use in slow release systems. *J Mater Sci Mater Med*, 12(2):107–110, Feb 2001. 133

K. G. Hooten, D. R. Beers, W. Zhao, and S. H. Appel. Protective and Toxic Neuroinflammation in Amyotrophic Lateral Sclerosis. *Neurotherapeutics*, 12(2):364–375, Apr 2015. 17

M. K. Hospenthal, T. E. T. Mevissen, and D. Komander. Deubiquitinase-based analysis of ubiquitin chain architecture using Ubiquitin Chain Restriction (UbiCRest). *Nat Protoc*, 10(2):349–361, Feb 2015. 187

K. Howe, M. D. Clark, C. F. Torroja, J. Torrance, C. Berthelot, M. Muffato, J. E. Collins, S. Humphray, K. McLaren, L. Matthews, S. McLaren, I. Sealy, M. Caccamo, C. Churcher, C. Scott, J. C. Barrett, R. Koch, G. J. Rauch, S. White, W. Chow, B. Kilian, L. T. Quintais, J. A. Guerra-Assuncao, Y. Zhou, Y. Gu, J. Yen, J. H. Vogel, T. Eyre, S. Redmond, R. Banerjee, J. Chi, B. Fu, E. Langley, S. F. Maguire, G. K. Laird, D. Lloyd, E. Kenyon, S. Donaldson, H. Sehra, J. Almeida-King, J. Loveland, S. Trevanion, M. Jones, M. Quail, D. Willey, A. Hunt, J. Burton, S. Sims, K. McLay, B. Plumb, J. Davis, C. Clee, K. Oliver, R. Clark, C. Riddle, D. Elliot,

D. Eliott, G. Threadgold, G. Harden, D. Ware, S. Begum, B. Mortimore, B. Mortimer, G. Kerry, P. Heath, B. Phillimore, A. Tracey, N. Corby, M. Dunn, C. Johnson, J. Wood, S. Clark, S. Pelan, G. Griffiths, M. Smith, R. Glithero, P. Howden, N. Barker, C. Lloyd, C. Stevens, J. Harley, K. Holt, G. Panagiotidis, J. Lovell, H. Beasley, C. Henderson, D. Gordon, K. Auger, D. Wright, J. Collins, C. Raisen, L. Dyer, K. Leung, L. Robertson, K. Ambridge, D. Leongamornlert, S. McGuire, R. Gilderthorp, C. Griffiths, D. Manthravadi, S. Nichol, G. Barker, S. Whitehead, M. Kay, J. Brown, C. Murnane, E. Gray, M. Humphries, N. Sycamore, D. Barker, D. Saunders, J. Wallis, A. Babbage, S. Hammond, M. Mashreghi-Mohammadi, L. Barr, S. Martin, P. Wray, A. Ellington, N. Matthews, M. Ellwood, R. Woodmansey, G. Clark, J. Cooper, J. Cooper, A. Tromans, D. Grafham, C. Skuce, R. Pandian, R. Andrews, E. Harrison, A. Kimberley, J. Garnett, N. Fosker, R. Hall, P. Garner, D. Kelly, C. Bird, S. Palmer, I. Gehring, A. Berger, C. M. Dooley, Z. Ersan-Urun, C. Eser, H. Geiger, M. Geisler, L. Karotki, A. Kirn, J. Konantz, M. Konantz, M. Oberlander, S. Rudolph-Geiger, M. Teucke, C. Lanz, G. Raddatz, K. Osoegawa, B. Zhu, A. Rapp, S. Widaa, C. Langford, F. Yang, S. C. Schuster, N. P. Carter, J. Harrow, Z. Ning, J. Herrero, S. M. Searle, A. Enright, R. Geisler, R. H. Plasterk, C. Lee, M. Westerfield, P. J. de Jong, L. I. Zon, J. H. Postlethwait, C. Nusslein-Volhard, T. J. Hubbard, H. Roest Crollius, J. Rogers, and D. L. Stemple. The zebrafish reference genome sequence and its relationship to the human genome. *Nature*, 496(7446):498–503, Apr 2013. 26, 28

D. S. Howland, J. Liu, Y. She, B. Goad, N. J. Maragakis, B. Kim, J. Erickson, J. Kulik, L. DeVito, G. Psaltis, L. J. DeGennaro, D. W. Cleveland, and J. D. Rothstein. Focal loss of the glutamate transporter EAAT2 in a transgenic rat model of SOD1 mutant-mediated amyotrophic lateral sclerosis (ALS). *Proc. Natl. Acad. Sci. U.S.A.*, 99(3): 1604–1609, Feb 2002. 30, 33

C. Huang, H. Zhou, J. Tong, H. Chen, Y. J. Liu, D. Wang, X. Wei, and X. G. Xia. FUS transgenic rats develop the phenotypes of amyotrophic lateral sclerosis and frontotemporal lobar degeneration. *PLoS Genet.*, 7(3):e1002011, Mar 2011. 40, 131

C. Huang, J. Tong, F. Bi, H. Zhou, and X. G. Xia. Mutant TDP-43 in motor neurons promotes the onset and progression of ALS in rats. *J. Clin. Invest.*, 122(1):107–118, Jan 2012. 36, 37, 131

C. J. Huang, T. S. Jou, Y. L. Ho, W. H. Lee, Y. T. Jeng, F. J. Hsieh, and H. J. Tsai. Conditional expression of a myocardium-specific transgene in zebrafish transgenic lines. *Dev. Dyn.*, 233(4):1294–1303, Aug 2005. 132

M. Hurles. Gene duplication: the genomic trade in spare parts. *PLoS Biol.*, 2(7):E206, Jul 2004. 60

M. Iconomou and D. N. Saunders. Systematic approaches to identify E3 ligase substrates. *Biochem. J.*, 473(22):4083–4101, Nov 2016. 20

L. M. Igaz, L. K. Kwong, E. B. Lee, A. Chen-Plotkin, E. Swanson, T. Unger, J. Malunda, Y. Xu, M. J. Winton, J. Q. Trojanowski, and V. M. Lee. Dysregulation of the ALS-associated gene TDP-43 leads to neuronal death and degeneration in mice. *J. Clin. Invest.*, 121(2):726–738, Feb 2011. 34, 35, 36, 132

Y. Iguchi, M. Katsuno, J. Niwa, S. Takagi, S. Ishigaki, K. Ikenaka, K. Kawai, H. Watanabe, K. Yamanaka, R. Takahashi, H. Misawa, S. Sasaki, F. Tanaka, and G. Sobue. Loss of TDP-43 causes age-dependent progressive motor neuron degeneration. *Brain*, 136(Pt 5):1371–1382, May 2013. 6, 15, 34, 36

H. Ito, R. Wate, J. Zhang, S. Ohnishi, S. Kaneko, H. Ito, S. Nakano, and H. Kusaka. Treatment with edaravone, initiated at symptom onset, slows motor decline and decreases SOD1 deposition in ALS mice. *Exp. Neurol.*, 213(2):448–455, Oct 2008. 22

Z. Ivics, P. B. Hackett, R. H. Plasterk, and Z. Izsvak. Molecular reconstruction of Sleeping Beauty, a Tc1-like transposon from fish, and its transposition in human cells. *Cell*, 91(4):501–510, Nov 1997. 106

Z. Ivics, M. A. Li, L. Mates, J. D. Boeke, A. Nagy, A. Bradley, and Z. Izsvak.

Transposon-mediated genome manipulation in vertebrates. *Nat. Methods*, 6(6):415–422, Jun 2009. 105

A. Iwata, B. E. Riley, J. A. Johnston, and R. R. Kopito. HDAC6 and microtubules are required for autophagic degradation of aggregated huntingtin. *J. Biol. Chem.*, 280(48):40282–40292, Dec 2005. 189

D. Jaarsma, E. D. Haasdijk, J. A. Grashorn, R. Hawkins, W. van Duijn, H. W. Verspaget, J. London, and J. C. Holstege. Human Cu/Zn superoxide dismutase (SOD1) overexpression in mice causes mitochondrial vacuolization, axonal degeneration, and premature motoneuron death and accelerates motoneuron disease in mice expressing a familial amyotrophic lateral sclerosis mutant SOD1. *Neurobiol. Dis.*, 7 (6 Pt B):623–643, Dec 2000. 32, 33

D. Jaarsma, E. Teuling, E. D. Haasdijk, C. I. De Zeeuw, and C. C. Hoogenraad. Neuron-specific expression of mutant superoxide dismutase is sufficient to induce amyotrophic lateral sclerosis in transgenic mice. *J. Neurosci.*, 28(9):2075–2088, Feb 2008. 33

F. Jaisser. Inducible gene expression and gene modification in transgenic mice. *J. Am. Soc. Nephrol.*, 11 Suppl 16:S95–S100, Nov 2000. 128

J. Janssens, H. Wils, G. Kleinberger, G. Joris, I. Cuijt, C. Ceuterick-de Groote, C. Van Broeckhoven, and S. Kumar-Singh. Overexpression of ALS-associated p.M337V human TDP-43 in mice worsens disease features compared to wild-type human TDP-43 mice. *Mol. Neurobiol.*, 48(1):22–35, Aug 2013. 36

M. Jaronen, G. Goldsteins, and J. Koistinaho. ER stress and unfolded protein response in amyotrophic lateral sclerosis-a controversial role of protein disulphide isomerase. *Front Cell Neurosci*, 8:402, 2014. 30

Y. J. Ji, J. Ugolino, N. R. Brady, A. Hamacher-Brady, and J. Wang. Systemic deregulation of autophagy upon loss of ALS- and FTD-linked C9orf72. *Autophagy*, 13(7): 1254–1255, Jul 2017. 42

J. Jiang, Q. Zhu, T. F. Gendron, S. Saberi, M. McAlonis-Downes, A. Seelman, J. E. Stauffer, P. Jafar-Nejad, K. Drenner, D. Schulte, S. Chun, S. Sun, S. C. Ling, B. Myers, J. Engelhardt, M. Katz, M. Baughn, O. Platoshyn, M. Marsala, A. Watt, C. J. Heyser, M. C. Ard, L. De Muynck, L. M. Daughrity, D. A. Swing, L. Tessarollo, C. J. Jung, A. Delpoux, D. T. Utzschneider, S. M. Hedrick, P. J. de Jong, D. Edbauer, P. Van Damme, L. Petrucelli, C. E. Shaw, C. F. Bennett, S. Da Cruz, J. Ravits, F. Rigo, D. W. Cleveland, and C. Lagier-Tourenne. Gain of Toxicity from ALS/FTD-Linked Repeat Expansions in C9ORF72 Is Alleviated by Antisense Oligonucleotides Targeting GGGGCC-Containing RNAs. *Neuron*, 90(3):535–550, May 2016. 43

J. O. Johnson, J. Mandrioli, M. Benatar, Y. Abramzon, V. M. Van Deerlin, J. Q. Trojanowski, J. R. Gibbs, M. Brunetti, S. Gronka, J. Wuu, J. Ding, L. McCluskey, M. Martinez-Lage, D. Falcone, D. G. Hernandez, S. Arepalli, S. Chong, J. C. Schymick, J. Rothstein, F. Landi, Y. D. Wang, A. Calvo, G. Mora, M. Sabatelli, M. R. Monsurro, S. Battistini, F. Salvi, R. Spataro, P. Sola, G. Borghero, G. Galassi, S. W. Scholz, J. P. Taylor, G. Restagno, A. Chio, B. J. Traynor, F. Giannini, C. Ricci, C. Moglia, I. Ossola, A. Canosa, S. Gallo, G. Tedeschi, P. Sola, I. Bartolomei, K. Marinou, L. Papetti, A. Conte, M. Luigetti, V. La Bella, P. Paladino, C. Caponnetto, P. Volanti, M. G. Marrosu, and M. R. Murru. Exome sequencing reveals VCP mutations as a cause of familial ALS. *Neuron*, 68(5):857–864, Dec 2010. 7, 21

J. O. Johnson, E. P. Pioro, A. Boehringer, R. Chia, H. Feit, A. E. Renton, H. A. Pliner, Y. Abramzon, G. Marangi, B. J. Winborn, J. R. Gibbs, M. A. Nalls, S. Morgan, M. Shoai, J. Hardy, A. Pittman, R. W. Orrell, A. Malaspina, K. C. Sidle, P. Fratta, M. B. Harms, R. H. Baloh, A. Pestronk, C. C. Weihl, E. Rogaeva, L. Zinman, V. E. Drory, G. Borghero, G. Mora, A. Calvo, J. D. Rothstein, C. Drepper, M. Sendtner, A. B. Singleton, J. P. Taylor, M. R. Cookson, G. Restagno, M. Sabatelli, R. Bowser, A. Chio, B. J. Traynor, C. Moglia, S. Cammarosano, A. Canosa, S. Gallo, M. Brunetti, I. Ossola, K. Marinou, L. Papetti, F. Pisano, G. L. Pinter, A. Conte,

M. Luigetti, M. Zollino, S. Lattante, G. Marangi, V. La Bella, R. Spataro, T. Colletti, F. Giannini, S. Battistini, C. Ricci, C. Caponnetto, G. Mancardi, P. Mandich, F. Salvi, I. Bartolomei, J. Mandrioli, P. Sola, C. Lunetta, S. Penco, M. R. Monsurro, G. Tedeschi, F. L. Conforti, A. Gambardella, A. Quattrone, P. Volanti, G. Floris, A. Cannas, V. Piras, F. Marrosu, M. G. Marrosu, M. R. Murru, M. Pugliatti, L. D. Parish, A. Sotgiu, G. Solinas, L. Ulgheri, A. Ticca, I. Simone, G. Logroscino, and A. Pirisi. Mutations in the Matrin 3 gene cause familial amyotrophic lateral sclerosis. *Nat. Neurosci.*, 17(5):664–666, May 2014. 7

P. A. Jonsson, K. Ernhill, P. M. Andersen, D. Bergemalm, T. Brannstrom, O. Gredal, P. Nilsson, and S. L. Marklund. Minute quantities of misfolded mutant superoxide dismutase-1 cause amyotrophic lateral sclerosis. *Brain*, 127(Pt 1):73–88, Jan 2004. 33

P. A. Jonsson, K. S. Graffmo, P. M. Andersen, T. Brannstrom, M. Lindberg, M. Oliveberg, and S. L. Marklund. Disulphide-reduced superoxide dismutase-1 in CNS of transgenic amyotrophic lateral sclerosis models. *Brain*, 129(Pt 2):451–464, Feb 2006a. 30

P. A. Jonsson, K. S. Graffmo, T. Brannstrom, P. Nilsson, P. M. Andersen, and S. L. Marklund. Motor neuron disease in mice expressing the wild type-like D90A mutant superoxide dismutase-1. *J. Neuropathol. Exp. Neurol.*, 65(12):1126–1136, Dec 2006b. 32

P. I. Joyce, P. Mcgoldrick, R. A. Saccon, W. Weber, P. Fratta, S. J. West, N. Zhu, S. Carter, V. Phatak, M. Stewart, M. Simon, S. Kumar, I. Heise, V. Bros-Facer, J. Dick, S. Corrochano, M. J. Stanford, T. V. Luong, P. M. Nolan, T. Meyer, S. Brandner, D. L. Bennett, P. H. Ozdinler, L. Greensmith, E. M. Fisher, and A. Acevedo-Arozena. A novel SOD1-ALS mutation separates central and peripheral effects of mutant SOD1 toxicity. *Hum. Mol. Genet.*, 24(7):1883–1897, Apr 2015. 32

C. Jung, C. M. Higgins, and Z. Xu. Mitochondrial electron transport chain complex

dysfunction in a transgenic mouse model for amyotrophic lateral sclerosis. *J. Neurochem.*, 83(3):535–545, Nov 2002. 18

E. Kabashi, J. N. Agar, D. M. Taylor, S. Minotti, and H. D. Durham. Focal dysfunction of the proteasome: a pathogenic factor in a mouse model of amyotrophic lateral sclerosis. *J. Neurochem.*, 89(6):1325–1335, Jun 2004. 30

E. Kabashi, P. N. Valdmanis, P. Dion, D. Spiegelman, B. J. McConkey, C. Vande Velde, J. P. Bouchard, L. Lacomblez, K. Pochigaeva, F. Salachas, P. F. Pradat, W. Camu, V. Meininger, N. Dupre, and G. A. Rouleau. TARDBP mutations in individuals with sporadic and familial amyotrophic lateral sclerosis. *Nat. Genet.*, 40(5):572–574, May 2008. 7

E. Kabashi, L. Lin, M. L. Tradewell, P. A. Dion, V. Bercier, P. Bourgouin, D. Rochefort, S. Bel Hadj, H. D. Durham, C. Vande Velde, G. A. Rouleau, and P. Drapeau. Gain and loss of function of ALS-related mutations of TARDBP (TDP-43) cause motor deficits in vivo. *Hum. Mol. Genet.*, 19(4):671–683, Feb 2010. 35, 63, 98, 108, 178

E. Kabashi, V. Bercier, A. Lissouba, M. Liao, E. Brustein, G. A. Rouleau, and P. Drapeau. FUS and TARDBP but not SOD1 interact in genetic models of amyotrophic lateral sclerosis. *PLoS Genet.*, 7(8):e1002214, Aug 2011a. 38, 40, 63, 98, 108

E. Kabashi, E. Brustein, N. Champagne, and P. Drapeau. Zebrafish models for the functional genomics of neurogenetic disorders. *Biochim. Biophys. Acta*, 1812(3): 335–345, Mar 2011b. 28, 178

E. Kabashi, J. N. Agar, M. J. Strong, and H. D. Durham. Impaired proteasome function in sporadic amyotrophic lateral sclerosis. *Amyotroph Lateral Scler*, 13(4):367–371, Jun 2012. 18, 21

E. Kabashi, H. El Oussini, V. Bercier, F. Gros-Louis, P. N. Valdmanis, J. McDearmid, I. A. Mejier, P. A. Dion, N. Dupre, D. Hollinger, J. Sinniger, S. Dirrig-Grosch, W. Camu, V. Meininger, J. P. Loeffler, F. Rene, P. Drapeau, G. A. Rouleau, and

L. Dupuis. Investigating the contribution of VAPB/ALS8 loss of function in amyotrophic lateral sclerosis. *Hum. Mol. Genet.*, 22(12):2350–2360, Jun 2013. 63, 98, 108

A. V. Kalueff, A. M. Stewart, and R. Gerlai. Zebrafish as an emerging model for studying complex brain disorders. *Trends Pharmacol. Sci.*, 35(2):63–75, Feb 2014. 195

K. Kawakami, A. Shima, and N. Kawakami. Identification of a functional transposase of the Tol2 element, an Ac-like element from the Japanese medaka fish, and its transposition in the zebrafish germ lineage. *Proc. Natl. Acad. Sci. U.S.A.*, 97(21): 11403–11408, Oct 2000. 104, 105, 106

T. Kawamata, H. Akiyama, T. Yamada, and P. L. McGeer. Immunologic reactions in amyotrophic lateral sclerosis brain and spinal cord tissue. *Am. J. Pathol.*, 140(3): 691–707, Mar 1992. 16

H. H. Kazazian. Mobile elements: drivers of genome evolution. *Science*, 303(5664): 1626–1632, Mar 2004. 105

B. A. Keller, K. Volkening, C. A. Droppelmann, L. C. Ang, R. Rademakers, and M. J. Strong. Co-aggregation of RNA binding proteins in ALS spinal motor neurons: evidence of a common pathogenic mechanism. *Acta Neuropathol.*, 124(5):733–747, Nov 2012. 18

M. Kellis, B. W. Birren, and E. S. Lander. Proof and evolutionary analysis of ancient genome duplication in the yeast Saccharomyces cerevisiae. *Nature*, 428(6983):617– 624, Apr 2004. 60

K. P. Kenna, P. T. van Doormaal, A. M. Dekker, N. Ticozzi, B. J. Kenna, F. P. Diekstra, W. van Rheenen, K. R. van Eijk, A. R. Jones, P. Keagle, A. Shatunov, W. Sproviero, B. N. Smith, M. A. van Es, S. D. Topp, A. Kenna, J. W. Miller, C. Fallini, C. Tiloca, R. L. McLaughlin, C. Vance, C. Troakes, C. Colombrita,

G. Mora, A. Calvo, F. Verde, S. Al-Sarraj, A. King, D. Calini, J. de Belleroche, F. Baas, A. J. van der Kooi, M. de Visser, A. L. Ten Asbroek, P. C. Sapp, D. McKenna-Yasek, M. Polak, S. Asress, J. L. Munoz-Blanco, T. M. Strom, T. Meitinger, K. E. Morrison, G. Lauria, K. L. Williams, P. N. Leigh, G. A. Nicholson, I. P. Blair, C. S. Leblond, P. A. Dion, G. A. Rouleau, H. Pall, P. J. Shaw, M. R. Turner, K. Talbot, F. Taroni, K. B. Boylan, M. Van Blitterswijk, R. Rademakers, J. Esteban-Perez, A. Garcia-Redondo, P. Van Damme, W. Robberecht, A. Chio, C. Gellera, C. Drepper, M. Sendtner, A. Ratti, J. D. Glass, J. S. Mora, N. A. Basak, O. Hardiman, A. C. Ludolph, P. M. Andersen, J. H. Weishaupt, R. H. Brown, A. Al-Chalabi, V. Silani, C. E. Shaw, L. H. van den Berg, J. H. Veldink, J. E. Landers, S. D'Alfonso, L. Mazzini, G. P. Comi, R. Del Bo, M. Ceroni, S. Gagliardi, G. Querin, C. Bertolin, V. Pensato, B. Castellotti, S. Corti, C. Cereda, L. Corrado, and G. Soraru. NEK1 variants confer susceptibility to amyotrophic lateral sclerosis. *Nat. Genet.*, 48(9):1037–1042, Sep 2016. 7, 187

S. Khan, K. Ahmad, E. M. Alshammari, M. Adnan, M. H. Baig, M. Lohani, P. Somvanshi, and S. Haque. Implication of Caspase-3 as a Common Therapeutic Target for Multineurodegenerative Disorders and Its Inhibition Using Nonpeptidyl Natural Compounds. *Biomed Res Int*, 2015:379817, 2015. 101

M. C. Kiernan, S. Vucic, B. C. Cheah, M. R. Turner, A. Eisen, O. Hardiman, J. R. Burrell, and M. C. Zoing. Amyotrophic lateral sclerosis. *Lancet*, 377(9769):942–955, Mar 2011. 173

H. J. Kim, N. C. Kim, Y. D. Wang, E. A. Scarborough, J. Moore, Z. Diaz, K. S. MacLea, B. Freibaum, S. Li, A. Molliex, A. P. Kanagaraj, R. Carter, K. B. Boylan, A. M. Wojtas, R. Rademakers, J. L. Pinkus, S. A. Greenberg, J. Q. Trojanowski, B. J. Traynor, B. N. Smith, S. Topp, A. S. Gkazi, J. Miller, C. E. Shaw, M. Kottlors, J. Kirschner, A. Pestronk, Y. R. Li, A. F. Ford, A. D. Gitler, M. Benatar, O. D. King, V. E. Kimonis, E. D. Ross, C. C. Weihl, J. Shorter, and J. P. Taylor. Mutations in prion-like domains in hnRNPA2B1 and hnRNPA1 cause multisystem proteinopathy and ALS. *Nature*, 495(7442):467–473, Mar 2013. 7

J. Kim, Y. H. Liao, C. Ionita, A. E. Bale, B. Darras, and G. Acsadi. Mitochondrial Membrane Protein-Associated Neurodegeneration Mimicking Juvenile Amyotrophic Lateral Sclerosis. *Pediatr. Neurol.*, 64:83–86, Nov 2016. 7

Y. Kino, C. Washizu, M. Kurosawa, M. Yamada, H. Miyazaki, T. Akagi, T. Hashikawa, H. Doi, T. Takumi, G. G. Hicks, N. Hattori, T. Shimogori, and N. Nukina. FUS/TLS deficiency causes behavioral and pathological abnormalities distinct from amyotrophic lateral sclerosis. *Acta Neuropathol Commun*, 3:24, Apr 2015. 39, 40

F. Knopf, K. Schnabel, C. Haase, K. Pfeifer, K. Anastassiadis, and G. Weidinger. Dually inducible TetON systems for tissue-specific conditional gene expression in zebrafish. *Proc. Natl. Acad. Sci. U.S.A.*, 107(46):19933–19938, Nov 2010. 132, 138

D. Kokel and R. T. Peterson. Using the zebrafish photomotor response for psychotropic drug screening. *Methods Cell Biol.*, 105:517–524, 2011. 98

D. Kokel, T. W. Dunn, M. B. Ahrens, R. Alshut, C. Y. Cheung, L. Saint-Amant, G. Bruni, R. Mateus, T. J. van Ham, T. Shiraki, Y. Fukada, D. Kojima, J. R. Yeh, R. Mikut, J. von Lintig, F. Engert, and R. T. Peterson. Identification of nonvisual photomotor response cells in the vertebrate hindbrain. *J. Neurosci.*, 33(9):3834–3843, Feb 2013. 98

M. Koppers, A. M. Blokhuis, H. J. Westeneng, M. L. Terpstra, C. A. Zundel, R. Vieira de Sa, R. D. Schellevis, A. J. Waite, D. J. Blake, J. H. Veldink, L. H. van den Berg, and R. J. Pasterkamp. C9orf72 ablation in mice does not cause motor neuron degeneration or motor deficits. *Ann. Neurol.*, 78(3):426–438, Sep 2015. 42

D. J. Koss, L. Robinson, B. D. Drever, K. Pluci?ska, S. Stoppelkamp, P. Veselcic, G. Riedel, and B. Platt. Mutant Tau knock-in mice display frontotemporal dementia relevant behaviour and histopathology. *Neurobiol. Dis.*, 91:105–123, 07 2016. 196

C. Krueger, K. Pfleiderer, W. Hillen, and C. Berens. Tetracycline derivatives: alternative effectors for Tet transregulators. *BioTechniques*, 37(4):546, 548, 550, Oct 2004. 133

J. Kuhle, R. L. Lindberg, A. Regeniter, M. Mehling, A. J. Steck, L. Kappos, and A. Czaplinski. Increased levels of inflammatory chemokines in amyotrophic lateral sclerosis. *Eur. J. Neurol.*, 16(6):771–774, Jun 2009. 19

R. Kurita, H. Sagara, Y. Aoki, B. A. Link, K. Arai, and S. Watanabe. Suppression of lens growth by alphaA-crystallin promoter-driven expression of diphtheria toxin results in disruption of retinal cell organization in zebrafish. *Dev. Biol.*, 255(1): 113–127, Mar 2003. 170

K. M. Kwan, E. Fujimoto, C. Grabher, B. D. Mangum, M. E. Hardy, D. S. Campbell, J. M. Parant, H. J. Yost, J. P. Kanki, and C. B. Chien. The Tol2kit: a multisite gateway-based construction kit for Tol2 transposon transgenesis constructs. *Dev. Dyn.*, 236(11):3088–3099, Nov 2007. 49, 51, 52, 53, 105, 106, 107, 134

T. J. Kwiatkowski, D. A. Bosco, A. L. Leclerc, E. Tamrazian, C. R. Vanderburg, C. Russ, A. Davis, J. Gilchrist, E. J. Kasarskis, T. Munsat, P. Valdmanis, G. A. Rouleau, B. A. Hosler, P. Cortelli, P. J. de Jong, Y. Yoshinaga, J. L. Haines, M. A. Pericak-Vance, J. Yan, N. Ticozzi, T. Siddique, D. McKenna-Yasek, P. C. Sapp, H. R. Horvitz, J. E. Landers, and R. H. Brown. Mutations in the FUS/TLS gene on chromosome 16 cause familial amyotrophic lateral sclerosis. *Science*, 323(5918): 1205–1208, Feb 2009. 7

K. Kyrylkova, S. Kyryachenko, M. Leid, and C. Kioussi. Detection of apoptosis by TUNEL assay. *Methods Mol. Biol.*, 887:41–47, 2012. 97

C. Lagier-Tourenne, M. Baughn, F. Rigo, S. Sun, P. Liu, H. R. Li, J. Jiang, A. T. Watt, S. Chun, M. Katz, J. Qiu, Y. Sun, S. C. Ling, Q. Zhu, M. Polymenidou, K. Drenner, J. W. Artates, M. McAlonis-Downes, S. Markmiller, K. R. Hutt, D. P. Pizzo, J. Cady, M. B. Harms, R. H. Baloh, S. R. Vandenberg, G. W. Yeo, X. D. Fu, C. F. Bennett, D. W. Cleveland, and J. Ravits. Targeted degradation of sense and antisense C9orf72 RNA foci as therapy for ALS and frontotemporal degeneration. *Proc. Natl. Acad. Sci. U.S.A.*, 110(47):E4530–4539, Nov 2013. 42

A. S. Laird, A. Van Hoecke, L. De Muynck, M. Timmers, L. Van den Bosch, P. Van Damme, and W. Robberecht. Progranulin is neurotrophic in vivo and protects against a mutant TDP-43 induced axonopathy. *PLoS ONE*, 5(10):e13368, Oct 2010. 35, 62, 63, 98, 178

R. C. Laker, P. Xu, K. A. Ryall, A. Sujkowski, B. M. Kenwood, K. H. Chain, M. Zhang, M. A. Royal, K. L. Hoehn, M. Driscoll, P. N. Adler, R. J. Wessells, J. J. Saucerman, and Z. Yan. A novel MitoTimer reporter gene for mitochondrial content, structure, stress, and damage in vivo. *J. Biol. Chem.*, 289(17):12005–12015, Apr 2014. 194

P. Y. Lam, E. A. Harvie, and A. Huttenlocher. Heat shock modulates neutrophil motility in zebrafish. *PLoS ONE*, 8(12):e84436, 2013. 129

K. M. Lamar and E. M. McNally. Genetic Modifiers for Neuromuscular Diseases. *J Neuromuscul Dis*, 1(1):3–13, 2014. 44

D. Langenau. *Cancer and Zebrafish: Mechanisms, Techniques, and Models.* Advances in Experimental Medicine and Biology. Springer International Publishing, 2016. ISBN 9783319306544. URL https://books.google.com.au/books?id=jrAqDAAAQBAJ.

N. A. Lanson, A. Maltare, H. King, R. Smith, J. H. Kim, J. P. Taylor, T. E. Lloyd, and U. B. Pandey. A Drosophila model of FUS-related neurodegeneration reveals genetic interaction between FUS and TDP-43. *Hum. Mol. Genet.*, 20(13):2510–2523, Jul 2011. 38, 40

S. H. Lecker, A. L. Goldberg, and W. E. Mitch. Protein degradation by the ubiquitin-proteasome pathway in normal and disease states. *J. Am. Soc. Nephrol.*, 17(7):1807–1819, Jul 2006. 20

A. Lee, S. L. Rayner, A. De Luca, S. S. L. Gwee, M. Morsch, V. Sundaramoorthy, H. Shahheydari, A. Ragagnin, B. Shi, S. Yang, K. L. Williams, E. K. Don, A. K. Walker, K. Y. Zhang, J. J. Yerbury, N. J. Cole, J. D. Atkin, I. P. Blair, M. P. Molloy, and R. S. Chung. Casein kinase II phosphorylation of cyclin F at serine 621 regulates

the Lys48-ubiquitylation E3 ligase activity of the SCF(cyclin F) complex. *Open Biol*, 7(10), Oct 2017a. 180, 184, 186, 198

A. Lee, S. L. Rayner, S. S. L. Gwee, A. De Luca, H. Shahheydari, V. Sundaramoorthy, A. Ragagnin, M. Morsch, R. Radford, J. Galper, S. Freckleton, B. Shi, A. K. Walker, E. K. Don, N. J. Cole, S. Yang, K. L. Williams, J. J. Yerbury, I. P. Blair, J. D. Atkin, M. P. Molloy, and R. S. Chung. Pathogenic mutation in the ALS/FTD gene, CCNF, causes elevated Lys48-linked ubiquitylation and defective autophagy. *Cell. Mol. Life Sci.*, Aug 2017b. 15, 92, 95, 180, 184, 190, 198

C. G. Lee, A. P. Farrell, A. Lotto, M. J. MacNutt, S. G. Hinch, and M. C. Healey. The effect of temperature on swimming performance and oxygen consumption in adult sockeye (Oncorhynchus nerka) and coho (O. kisutch) salmon stocks. *J. Exp. Biol.*, 206(Pt 18):3239–3251, Sep 2003. 167

J. Lee, S. J. Hyeon, H. Im, H. Ryu, Y. Kim, and H. Ryu. Astrocytes and Microglia as Non-cell Autonomous Players in the Pathogenesis of ALS. *Exp Neurobiol*, 25(5): 233–240, Oct 2016. 174

Y. B. Lee, H. J. Chen, J. N. Peres, J. Gomez-Deza, J. Attig, M. Stalekar, C. Troakes, A. L. Nishimura, E. L. Scotter, C. Vance, Y. Adachi, V. Sardone, J. W. Miller, B. N. Smith, J. M. Gallo, J. Ule, F. Hirth, B. Rogelj, C. Houart, and C. E. Shaw. Hexanucleotide repeats in ALS/FTD form length-dependent RNA foci, sequester RNA binding proteins, and are neurotoxic. *Cell Rep*, 5(5):1178–1186, Dec 2013. 41, 43

R. Lemmens, A. Van Hoecke, N. Hersmus, V. Geelen, I. D'Hollander, V. Thijs, L. Van Den Bosch, P. Carmeliet, and W. Robberecht. Overexpression of mutant superoxide dismutase 1 causes a motor axonopathy in the zebrafish. *Hum. Mol. Genet.*, 16(19): 2359–2365, Oct 2007. 30, 32, 62, 63, 98, 178

A. Levasseur and P. Pontarotti. The role of duplications in the evolution of genomes highlights the need for evolutionary-based approaches in comparative genomics. *Biol. Direct*, 6:11, Feb 2011. 60

E. D. Levin. Zebrafish assessment of cognitive improvement and anxiolysis: filling the gap between in vitro and rodent models for drug development. *Rev Neurosci*, 22(1): 75–84, 2011. 196, 197

M. Lewandoski. Conditional control of gene expression in the mouse. *Nat. Rev. Genet.*, 2(10):743–755, Oct 2001. 128

J. Li, K. X. Huang, and W. D. Le. Establishing a novel C. elegans model to investigate the role of autophagy in amyotrophic lateral sclerosis. *Acta Pharmacol. Sin.*, 34(5): 644–650, May 2013a. 32

J. Li, Z. Chen, L. Y. Gao, A. Colorni, M. Ucko, S. Fang, and S. J. Du. A transgenic zebrafish model for monitoring xbp1 splicing and endoplasmic reticulum stress in vivo. *Mech. Dev.*, 137:33–44, Aug 2015a. 106, 194

M. Li, V. O. Ona, C. Guegan, M. Chen, V. Jackson-Lewis, L. J. Andrews, A. J. Olszewski, P. E. Stieg, J. P. Lee, S. Przedborski, and R. M. Friedlander. Functional role of caspase-1 and caspase-3 in an ALS transgenic mouse model. *Science*, 288 (5464):335–339, Apr 2000. 101, 102

W. Li and Y. Ye. Polyubiquitin chains: functions, structures, and mechanisms. *Cell. Mol. Life Sci.*, 65(15):2397–2406, Aug 2008. 20

Y. Li, P. Ray, E. J. Rao, C. Shi, W. Guo, X. Chen, E. A. Woodruff, K. Fushimi, and J. Y. Wu. A Drosophila model for TDP-43 proteinopathy. *Proc. Natl. Acad. Sci. U.S.A.*, 107(7):3169–3174, Feb 2010. 35

Y. Li, Y. Guo, X. Wang, X. Yu, W. Duan, K. Hong, J. Wang, H. Han, and C. Li. Trehalose decreases mutant SOD1 expression and alleviates motor deficiency in early but not end-stage amyotrophic lateral sclerosis in a SOD1-G93A mouse model. *Neuroscience*, 298:12–25, Jul 2015b. 190

Z. Li, W. Zheng, Z. Wang, Z. Zeng, H. Zhan, C. Li, L. Zhou, C. Yan, J. M. Spitsbergen, and Z. Gong. A transgenic zebrafish liver tumor model with inducible Myc expression

reveals conserved Myc signatures with mammalian liver tumors. *Dis Model Mech*, 6 (2):414–423, Mar 2013b. 132

N. F. Liachko, C. R. Guthrie, and B. C. Kraemer. Phosphorylation promotes neuro-toxicity in a Caenorhabditis elegans model of TDP-43 proteinopathy. *J. Neurosci.*, 30(48):16208–16219, Dec 2010. 35

M. Lichtenberg, A. Mansilla, V. R. Zecchini, A. Fleming, and D. C. Rubinsztein. The Parkinson's disease protein LRRK2 impairs proteasome substrate clearance without affecting proteasome catalytic activity. *Cell Death Dis*, 2:e196, Aug 2011. 188

G. J. Lieschke and P. D. Currie. Animal models of human disease: zebrafish swim into view. *Nat. Rev. Genet.*, 8(5):353–367, May 2007. 28, 104, 195

C. L. Lin, L. A. Bristol, L. Jin, M. Dykes-Hoberg, T. Crawford, L. Clawson, and J. D. Rothstein. Aberrant RNA processing in a neurodegenerative disease: the cause for absent EAAT2, a glutamate transporter, in amyotrophic lateral sclerosis. *Neuron*, 20(3):589–602, Mar 1998. 18

M. J. Lin, C. W. Cheng, and C. K. Shen. Neuronal function and dysfunction of Drosophila dTDP. *PLoS ONE*, 6(6):e20371, 2011. 35

S. Lin, N. Gaiano, P. Culp, J. C. Burns, T. Friedmann, J. K. Yee, and N. Hopkins. In-tegration and germ-line transmission of a pseudotyped retroviral vector in zebrafish. *Science*, 265(5172):666–669, Jul 1994. 104, 105

S. C. Ling, M. Polymenidou, and D. W. Cleveland. Converging mechanisms in ALS and FTD: disrupted RNA and protein homeostasis. *Neuron*, 79(3):416–438, Aug 2013. 4, 5, 16, 180

M. M. Lino, C. Schneider, and P. Caroni. Accumulation of SOD1 mutants in postna-tal motoneurons does not cause motoneuron pathology or motoneuron disease. *J. Neurosci.*, 22(12):4825–4832, Jun 2002. 31

D. Liu, J. Wen, J. Liu, and L. Li. The roles of free radicals in amyotrophic lateral sclerosis: reactive oxygen species and elevated oxidation of protein, DNA, and membrane phospholipids. *FASEB J.*, 13(15):2318–2328, Dec 1999. 29

J. Liu, C. Lillo, P. A. Jonsson, C. Vande Velde, C. M. Ward, T. M. Miller, J. R. Subramaniam, J. D. Rothstein, S. Marklund, P. M. Andersen, T. Brannstrom, O. Gredal, P. C. Wong, D. S. Williams, and D. W. Cleveland. Toxicity of familial ALS-linked SOD1 mutants from selective recruitment to spinal mitochondria. *Neuron*, 43(1): 5–17, Jul 2004. 31

R. Liu, J. S. Althaus, B. R. Ellerbrock, D. A. Becker, and M. E. Gurney. Enhanced oxygen radical production in a transgenic mouse model of familial amyotrophic lateral sclerosis. *Ann. Neurol.*, 44(5):763–770, Nov 1998. 19

Y. Liu, A. Pattamatta, T. Zu, T. Reid, O. Bardhi, D. R. Borchelt, A. T. Yachnis, and L. P. Ranum. C9orf72 BAC Mouse Model with Motor Deficits and Neurodegenerative Features of ALS/FTD. *Neuron*, 90(3):521–534, May 2016. 43

T. E. Lloyd and J. P. Taylor. Flightless flies: Drosophila models of neuromuscular disease. *Ann. N. Y. Acad. Sci.*, 1184:1–20, Jan 2010. 27

R. Loew, N. Heinz, M. Hampf, H. Bujard, and M. Gossen. Improved Tet-responsive promoters with minimized background expression. *BMC Biotechnol.*, 10:81, Nov 2010. 131

A. Lopez, S. E. Lee, K. Wojta, E. M. Ramos, E. Klein, J. Chen, A. L. Boxer, M. L. Gorno-Tempini, D. H. Geschwind, L. Schlotawa, N. V. Ogryzko, E. H. Bigio, E. Rogalski, S. Weintraub, M. M. Mesulam, A. Fleming, G. Coppola, B. L. Miller, and D. C. Rubinsztein. A152T tau allele causes neurodegeneration that can be ameliorated in a zebrafish model by autophagy induction. *Brain*, 140(4):1128–1146, Apr 2017. 195

R. Lopez-Gonzalez, Y. Lu, T. F. Gendron, A. Karydas, H. Tran, D. Yang, L. Petrucelli, B. L. Miller, S. Almeida, and F. B. Gao. Poly(GR) in C9ORF72-Related ALS/FTD

Compromises Mitochondrial Function and Increases Oxidative Stress and DNA Damage in iPSC-Derived Motor Neurons. *Neuron*, 92(2):383–391, Oct 2016. 41

J. Lowe. New pathological findings in amyotrophic lateral sclerosis. *J. Neurol. Sci.*, 124 Suppl:38–51, Jul 1994. 18

L. Lu, S. Wang, L. Zheng, X. Li, E. A. Suswam, X. Zhang, C. G. Wheeler, L. B. Nabors, N. Filippova, and P. H. King. Amyotrophic lateral sclerosis-linked mutant SOD1 sequesters Hu antigen R (HuR) and TIA-1-related protein (TIAR): implications for impaired post-transcriptional regulation of vascular endothelial growth factor. *J. Biol. Chem.*, 284(49):33989–33998, Dec 2009. 31

A. A. Luty, J. B. Kwok, C. Dobson-Stone, C. T. Loy, K. G. Coupland, H. Karlstrom, T. Sobow, J. Tchorzewska, A. Maruszak, M. Barcikowska, P. K. Panegyres, C. Zekanowski, W. S. Brooks, K. L. Williams, I. P. Blair, K. A. Mather, P. S. Sachdev, G. M. Halliday, and P. R. Schofield. Sigma nonopioid intracellular receptor 1 mutations cause frontotemporal lobar degeneration-motor neuron disease. *Ann. Neurol.*, 68(5):639–649, Nov 2010. 7

Z. Ma, P. Zhu, M. Pang, L. Guo, N. Chang, J. Zheng, X. Zhu, C. Gao, H. Huang, Z. Cui, J. W. Xiong, J. Peng, and J. Chen. A novel inducible mutagenesis screen enables to isolate and clone both embryonic and adult zebrafish mutants. *Sci Rep*, 7(1):10381, Sep 2017.

I. R. Mackenzie and M. Neumann. Molecular neuropathology of frontotemporal dementia: insights into disease mechanisms from postmortem studies. *J. Neurochem.*, 138 Suppl 1:54–70, Aug 2016. 196

I. R. Mackenzie, E. H. Bigio, P. G. Ince, F. Geser, M. Neumann, N. J. Cairns, L. K. Kwong, M. S. Forman, J. Ravits, H. Stewart, A. Eisen, L. McClusky, H. A. Kretzschmar, C. M. Monoranu, J. R. Highley, J. Kirby, T. Siddique, P. J. Shaw, V. M. Lee, and J. Q. Trojanowski. Pathological TDP-43 distinguishes sporadic amyotrophic lateral sclerosis from amyotrophic lateral sclerosis with SOD1 mutations. *Ann. Neurol.*, 61(5):427–434, May 2007. 16, 30

S. Magadum, U. Banerjee, P. Murugan, D. Gangapur, and R. Ravikesavan. Gene duplication as a major force in evolution. *J. Genet.*, 92(1):155–161, Apr 2013. 60

S. Majmudar, J. Wu, and S. Paganoni. Rehabilitation in amyotrophic lateral sclerosis: why it matters. *Muscle Nerve*, 50(1):4–13, Jul 2014. 23

Y. Manabe, H. Warita, T. Murakami, M. Shiote, T. Hayashi, I. Nagano, M. Shoji, and K. Abe. Early decrease of redox factor-1 in spinal motor neurons of presymptomatic transgenic mice with a mutant SOD1 gene. *Brain Res.*, 915(1):104–107, Oct 2001. 187

S. Mantovani, S. Garbelli, A. Pasini, D. Alimonti, C. Perotti, M. Melazzini, C. Bendotti, and G. Mora. Immune system alterations in sporadic amyotrophic lateral sclerosis patients suggest an ongoing neuroinflammatory process. *J. Neuroimmunol.*, 210(1-2): 73–79, May 2009. 19

B. Marin, F. Boumediene, G. Logroscino, P. Couratier, M. C. Babron, A. L. Leutenegger, M. Copetti, P. M. Preux, and E. Beghi. Variation in worldwide incidence of amyotrophic lateral sclerosis: a meta-analysis. *Int J Epidemiol*, 46(1):57–74, Feb 2017. 4

M. Marino, S. Papa, V. Crippa, G. Nardo, M. Peviani, C. Cheroni, M. C. Trolese, E. Lauranzano, V. Bonetto, A. Poletti, S. DeBiasi, L. Ferraiuolo, P. J. Shaw, and C. Bendotti. Differences in protein quality control correlate with phenotype variability in 2 mouse models of familial amyotrophic lateral sclerosis. *Neurobiol. Aging*, 36 (1):492–504, Jan 2015. 30

M. Markaki and N. Tavernarakis. Modeling human diseases in Caenorhabditis elegans. *Biotechnol J*, 5(12):1261–1276, Dec 2010. 27

H. Maruyama, H. Morino, H. Ito, Y. Izumi, H. Kato, Y. Watanabe, Y. Kinoshita, M. Kamada, H. Nodera, H. Suzuki, O. Komure, S. Matsuura, K. Kobatake, N. Morimoto, K. Abe, N. Suzuki, M. Aoki, A. Kawata, T. Hirai, T. Kato, K. Ogasawara,

A. Hirano, T. Takumi, H. Kusaka, K. Hagiwara, R. Kaji, and H. Kawakami. Mutations of optineurin in amyotrophic lateral sclerosis. *Nature*, 465(7295):223–226, May 2010. 7, 189

E. P. McCann, K. L. Williams, J. A. Fifita, I. S. Tarr, J. O'Connor, D. B. Rowe, G. A. Nicholson, and I. P. Blair. The genotype-phenotype landscape of familial amyotrophic lateral sclerosis in Australia. *Clin. Genet.*, 92(3):259–266, Sep 2017. 6, 7, 8

B. McClintock. The origin and behavior of mutable loci in maize. *Proc. Natl. Acad. Sci. U.S.A.*, 36(6):344–355, Jun 1950. 105

P. A. McCombe and R. D. Henderson. Effects of gender in amyotrophic lateral sclerosis. *Gend Med*, 7(6):557–570, Dec 2010. 4, 127

P. A. McCombe and R. D. Henderson. The Role of immune and inflammatory mechanisms in ALS. *Curr. Mol. Med.*, 11(3):246–254, Apr 2011. 16

L. McGurk, A. Berson, and N. M. Bonini. Drosophila as an In Vivo Model for Human Neurodegenerative Disease. *Genetics*, 201(2):377–402, Oct 2015. 27

A. T. Melvin, G. S. Woss, J. H. Park, M. L. Waters, and N. L. Allbritton. Measuring activity in the ubiquitin-proteasome system: from large scale discoveries to single cells analysis. *Cell Biochem. Biophys.*, 67(1):75–89, Sep 2013. 189

E. F. Mendez and R. Sattler. Biomarker development for C9orf72 repeat expansion in ALS. *Brain Res.*, 1607:26–35, May 2015. 41

P. Menon, M. C. Kiernan, and S. Vucic. Cortical hyperexcitability precedes lower motor neuron dysfunction in ALS. *Clin Neurophysiol*, 126(4):803–809, Apr 2015. 19

D. A. Meshalkina, E. V. Kysil, J. E. Warnick, K. A. Demin, and A. V. Kalueff. Adult zebrafish in CNS disease modeling: a tank that's half-full, not half-empty, and still filling. *Lab Anim (NY)*, 46(10):378–387, Oct 2017. 195

D. Metzger and R. Feil. Engineering the mouse genome by site-specific recombination. *Curr. Opin. Biotechnol.*, 10(5):470–476, Oct 1999. 128

A. Meyer and M. Schartl. Gene and genome duplications in vertebrates: the one-to-four (-to-eight in fish) rule and the evolution of novel gene functions. *Curr. Opin. Cell Biol.*, 11(6):699–704, Dec 1999. 61

T. Meyer, A. Schwan, J. S. Dullinger, J. Brocke, K. T. Hoffmann, C. H. Nolte, A. Hopt, U. Kopp, P. Andersen, J. T. Epplen, and P. Linke. Early-onset ALS with long-term survival associated with spastin gene mutation. *Neurology*, 65(1):141–143, Jul 2005. 7

R. G. Miller, J. D. Mitchell, M. Lyon, and D. H. Moore. Riluzole for amyotrophic lateral sclerosis (ALS)/motor neuron disease (MND). *Cochrane Database Syst Rev*, (2):CD001447, 2002. 22

K. R. Mills and K. A. Nithi. Corticomotor threshold is reduced in early sporadic amyotrophic lateral sclerosis. *Muscle Nerve*, 20(9):1137–1141, Sep 1997. 173

J. Mitchell, P. Paul, H. J. Chen, A. Morris, M. Payling, M. Falchi, J. Habgood, S. Panoutsou, S. Winkler, V. Tisato, A. Hajitou, B. Smith, C. Vance, C. Shaw, N. D. Mazarakis, and J. de Belleroche. Familial amyotrophic lateral sclerosis is associated with a mutation in D-amino acid oxidase. *Proc. Natl. Acad. Sci. U.S.A.*, 107(16):7556–7561, Apr 2010. 7

J. C. Mitchell, P. McGoldrick, C. Vance, T. Hortobagyi, J. Sreedharan, B. Rogelj, E. L. Tudor, B. N. Smith, C. Klasen, C. C. Miller, J. D. Cooper, L. Greensmith, and C. E. Shaw. Overexpression of human wild-type FUS causes progressive motor neuron degeneration in an age- and dose-dependent fashion. *Acta Neuropathol.*, 125 (2):273–288, Feb 2013. 40

J. C. Mitchell, R. Constable, E. So, C. Vance, E. Scotter, L. Glover, T. Hortobagyi, E. S. Arnold, S. C. Ling, M. McAlonis, S. Da Cruz, M. Polymenidou, L. Tessarolo,

D. W. Cleveland, and C. E. Shaw. Wild type human TDP-43 potentiates ALS-linked mutant TDP-43 driven progressive motor and cortical neuron degeneration with pathological features of ALS. *Acta Neuropathol Commun*, 3:36, Jun 2015. 35

S. Mizielinska, S. Gronke, T. Niccoli, C. E. Ridler, E. L. Clayton, A. Devoy, T. Moens, F. E. Norona, I. O. C. Woollacott, J. Pietrzyk, K. Cleverley, A. J. Nicoll, S. Pickering-Brown, J. Dols, M. Cabecinha, O. Hendrich, P. Fratta, E. M. C. Fisher, L. Partridge, and A. M. Isaacs. C9orf72 repeat expansions cause neurodegeneration in Drosophila through arginine-rich proteins. *Science*, 345(6201):1192–1194, Sep 2014. 42, 43

N. Mizushima and M. Komatsu. Autophagy: renovation of cells and tissues. *Cell*, 147 (4):728–741, Nov 2011. 191

I. Momose, D. Tatsuda, S. Ohba, T. Masuda, D. Ikeda, and A. Nomoto. In vivo imaging of proteasome inhibition using a proteasome-sensitive fluorescent reporter. *Cancer Sci.*, 103(9):1730–1736, Sep 2012. 189

K. Mori, S. M. Weng, T. Arzberger, S. May, K. Rentzsch, E. Kremmer, B. Schmid, H. A. Kretzschmar, M. Cruts, C. Van Broeckhoven, C. Haass, and D. Edbauer. The C9orf72 GGGGCC repeat is translated into aggregating dipeptide-repeat proteins in FTLD/ALS. *Science*, 339(6125):1335–1338, Mar 2013. 41

M. Morsch, R. Radford, A. Lee, E. K. Don, A. P. Badrock, T. E. Hall, N. J. Cole, and R. Chung. In vivo characterization of microglial engulfment of dying neurons in the zebrafish spinal cord. *Front Cell Neurosci*, 9:321, 2015. 52

F. L. Muller, W. Song, Y. Liu, A. Chaudhuri, S. Pieke-Dahl, R. Strong, T. T. Huang, C. J. Epstein, L. J. Roberts, M. Csete, J. A. Faulkner, and H. Van Remmen. Absence of CuZn superoxide dismutase leads to elevated oxidative stress and acceleration of age-dependent skeletal muscle atrophy. *Free Radic. Biol. Med.*, 40(11):1993–2004, Jun 2006. 33

C. Munch, R. Sedlmeier, T. Meyer, V. Homberg, A. D. Sperfeld, A. Kurt, J. Prudlo, G. Peraus, C. O. Hanemann, G. Stumm, and A. C. Ludolph. Point mutations of

the p150 subunit of dynactin (DCTN1) gene in ALS. *Neurology*, 63(4):724–726, Aug 2004. 7

T. Murakami, S. P. Yang, L. Xie, T. Kawano, D. Fu, A. Mukai, C. Bohm, F. Chen, J. Robertson, H. Suzuki, G. G. Tartaglia, M. Vendruscolo, G. S. Kaminski Schierle, F. T. Chan, A. Moloney, D. Crowther, C. F. Kaminski, M. Zhen, and P. St George-Hyslop. ALS mutations in FUS cause neuronal dysfunction and death in Caenorhabditis elegans by a dominant gain-of-function mechanism. *Hum. Mol. Genet.*, 21(1): 1–9, Jan 2012. 39, 40

M. Nagai, M. Aoki, I. Miyoshi, M. Kato, P. Pasinelli, N. Kasai, R. H. Brown, and Y. Itoyama. Rats expressing human cytosolic copper-zinc superoxide dismutase transgenes with amyotrophic lateral sclerosis: associated mutations develop motor neuron disease. *J. Neurosci.*, 21(23):9246–9254, Dec 2001. 30, 33

I. Nagano, T. Murakami, Y. Manabe, and K. Abe. Early decrease of survival factors and DNA repair enzyme in spinal motor neurons of presymptomatic transgenic mice that express a mutant SOD1 gene. *Life Sci.*, 72(4-5):541–548, Dec 2002. 187

T. Nakagawa, H. Zhu, N. Morishima, E. Li, J. Xu, B. A. Yankner, and J. Yuan. Caspase-12 mediates endoplasmic-reticulum-specific apoptosis and cytotoxicity by amyloid-beta. *Nature*, 403(6765):98–103, Jan 2000. 30

M. Nassif, U. Woehlbier, and P. A. Manque. The Enigmatic Role of C9ORF72 in Autophagy. *Front Neurosci*, 11:442, 2017. 8

M. Neumann, L. K. Kwong, D. M. Sampathu, J. Q. Trojanowski, and V. M. Lee. TDP-43 proteinopathy in frontotemporal lobar degeneration and amyotrophic lateral sclerosis: protein misfolding diseases without amyloidosis. *Arch. Neurol.*, 64(10): 1388–1394, Oct 2007. 7, 16, 21, 34, 180

K. Newton, M. L. Matsumoto, I. E. Wertz, D. S. Kirkpatrick, J. R. Lill, J. Tan, D. Dugger, N. Gordon, S. S. Sidhu, F. A. Fellouse, L. Komuves, D. M. French, R. E. Ferrando, C. Lam, D. Compaan, C. Yu, I. Bosanac, S. G. Hymowitz, R. F. Kelley,

and V. M. Dixit. Ubiquitin chain editing revealed by polyubiquitin linkage-specific antibodies. *Cell*, 134(4):668–678, Aug 2008. 20, 187

L. K. Nguyen, W. Kolch, and B. N. Kholodenko. When ubiquitination meets phosphorylation: a systems biology perspective of EGFR/MAPK signalling. *Cell Commun. Signal*, 11:52, Jul 2013. 186

M. D. Nguyen, M. Boudreau, J. Kriz, S. Couillard-Despres, D. R. Kaplan, and J. P. Julien. Cell cycle regulators in the neuronal death pathway of amyotrophic lateral sclerosis caused by mutant superoxide dismutase 1. *J. Neurosci.*, 23(6):2131–2140, Mar 2003. 188

A. L. Nishimura, M. Mitne-Neto, H. C. Silva, A. Richieri-Costa, S. Middleton, D. Cascio, F. Kok, J. R. Oliveira, T. Gillingwater, J. Webb, P. Skehel, and M. Zatz. A mutation in the vesicle-trafficking protein VAPB causes late-onset spinal muscular atrophy and amyotrophic lateral sclerosis. *Am. J. Hum. Genet.*, 75(5):822–831, Nov 2004. 7

W. Norton and L. Bally-Cuif. Adult zebrafish as a model organism for behavioural genetics. *BMC Neurosci*, 11:90, Aug 2010. 195

M. Ogawa, H. Shidara, K. Oka, M. Kurosawa, N. Nukina, and Y. Furukawa. Cysteine residues in Cu,Zn-superoxide dismutase are essential to toxicity in Caenorhabditis elegans model of amyotrophic lateral sclerosis. *Biochem. Biophys. Res. Commun.*, 463(4):1196–1202, Aug 2015. 32

Y. Ohki, A. Wenninger-Weinzierl, A. Hruscha, K. Asakawa, K. Kawakami, C. Haass, D. Edbauer, and B. Schmid. Glycine-alanine dipeptide repeat protein contributes to toxicity in a zebrafish model of C9orf72 associated neurodegeneration. *Mol Neurodegener*, 12(1):6, 01 2017. 42, 43

T. Ohta. Evolution by gene duplication revisited: differentiation of regulatory elements versus proteins. *Genetica*, 118(2-3):209–216, Jul 2003. 60

A. Okado-Matsumoto and I. Fridovich. Amyotrophic lateral sclerosis: a proposed mechanism. *Proc. Natl. Acad. Sci. U.S.A.*, 99(13):9010–9014, Jun 2002. 31

K. Okamoto, Y. Mizuno, and Y. Fujita. Bunina bodies in amyotrophic lateral sclerosis. *Neuropathology*, 28(2):109–115, Apr 2008. 16

A. Opattova, M. Cente, M. Novak, and P. Filipcik. The ubiquitin proteasome system as a potential therapeutic target for treatment of neurodegenerative diseases. *Gen. Physiol. Biophys.*, 34(4):337–352, Oct 2015. 184

A. Orlacchio, C. Babalini, A. Borreca, C. Patrono, R. Massa, S. Basaran, R. P. Munhoz, E. A. Rogaeva, P. H. St George-Hyslop, G. Bernardi, and T. Kawarai. SPATACSIN mutations cause autosomal recessive juvenile amyotrophic lateral sclerosis. *Brain*, 133(Pt 2):591–598, Feb 2010. 7

D. M. Ornitz, R. W. Moreadith, and P. Leder. Binary system for regulating transgene expression in mice: targeting int-2 gene expression with yeast GAL4/UAS control elements. *Proc. Natl. Acad. Sci. U.S.A.*, 88(3):698–702, Feb 1991. 128, 129

J. G. O'Rourke, L. Bogdanik, A. K. M. G. Muhammad, T. F. Gendron, K. J. Kim, A. Austin, J. Cady, E. Y. Liu, J. Zarrow, S. Grant, R. Ho, S. Bell, S. Carmona, M. Simpkinson, D. Lall, K. Wu, L. Daughrity, D. W. Dickson, M. B. Harms, L. Petrucelli, E. B. Lee, C. M. Lutz, and R. H. Baloh. C9orf72 BAC Transgenic Mice Display Typical Pathologic Features of ALS/FTD. *Neuron*, 88(5):892–901, Dec 2015. 43

R. W. Orrell, J. J. Habgood, J. S. de Belleroche, and R. J. Lane. The relationship of spinal muscular atrophy to motor neuron disease: investigation of SMN and NAIP gene deletions in sporadic and familial ALS. *J. Neurol. Sci.*, 145(1):55–61, Jan 1997. 7

D. Orsucci, V. Calsolaro, M. Mancuso, and G. Siciliano. Neuroprotective effects of tetracyclines: molecular targets, animal models and human disease. *CNS Neurol Disord Drug Targets*, 8(3):222–231, Jun 2009. 165

S. K. Panda, B. Wefers, O. Ortiz, T. Floss, B. Schmid, C. Haass, W. Wurst, and R. Kuhn. Highly efficient targeted mutagenesis in mice using TALENs. *Genetics*, 195(3):703–713, Nov 2013. 199

U. B. Pandey, Z. Nie, Y. Batlevi, B. A. McCray, G. P. Ritson, N. B. Nedelsky, S. L. Schwartz, N. A. DiProspero, M. A. Knight, O. Schuldiner, R. Padmanabhan, M. Hild, D. L. Berry, D. Garza, C. C. Hubbert, T. P. Yao, E. H. Baehrecke, and J. P. Taylor. HDAC6 rescues neurodegeneration and provides an essential link between autophagy and the UPS. *Nature*, 447(7146):859–863, Jun 2007. 189

P. Panula, Y. C. Chen, M. Priyadarshini, H. Kudo, S. Semenova, M. Sundvik, and V. Sallinen. The comparative neuroanatomy and neurochemistry of zebrafish CNS systems of relevance to human neuropsychiatric diseases. *Neurobiol. Dis.*, 40(1): 46–57, Oct 2010. 28, 195

D. Paquet, R. Bhat, A. Sydow, E. M. Mandelkow, S. Berg, S. Hellberg, J. Falting, M. Distel, R. W. Koster, B. Schmid, and C. Haass. A zebrafish model of tauopathy allows in vivo imaging of neuronal cell death and drug evaluation. *J. Clin. Invest.*, 119(5):1382–1395, May 2009. 122, 195

N. Parkinson, P. G. Ince, M. O. Smith, R. Highley, G. Skibinski, P. M. Andersen, K. E. Morrison, H. S. Pall, O. Hardiman, J. Collinge, P. J. Shaw, and E. M. Fisher. ALS phenotypes with mutations in CHMP2B (charged multivesicular body protein 2B). *Neurology*, 67(6):1074–1077, Sep 2006. 7

C. Parng, W. L. Seng, C. Semino, and P. McGrath. Zebrafish: a preclinical model for drug screening. *Assay Drug Dev Technol*, 1(1 Pt 1):41–48, Nov 2002. 97

P. N. Patsalos and E. Perucca. Clinically important drug interactions in epilepsy: interactions between antiepileptic drugs and other drugs. *Lancet Neurol*, 2(8):473–481, Aug 2003. 166

S. T. Paulukonis, E. M. Roberts, J. P. Valle, N. N. Collins, P. B. English, and W. E.

Kaye. Survival and Cause of Death among a Cohort of Confirmed Amyotrophic Lateral Sclerosis Cases. *PLoS ONE*, 10(7):e0131965, 2015. 4

E. Pennisi. Molecular evolution. Genome duplications: the stuff of evolution? *Science*, 294(5551):2458–2460, Dec 2001. 60

D. I. Perez, C. Gil, and A. Martinez. Protein kinases CK1 and CK2 as new targets for neurodegenerative diseases. *Med Res Rev*, 31(6):924–954, Nov 2011. 187

O. M. Peters, G. T. Cabrera, H. Tran, T. F. Gendron, J. E. McKeon, J. Metterville, A. Weiss, N. Wightman, J. Salameh, J. Kim, H. Sun, K. B. Boylan, D. Dickson, Z. Kennedy, Z. Lin, Y. J. Zhang, L. Daughrity, C. Jung, F. B. Gao, P. C. Sapp, H. R. Horvitz, D. A. Bosco, S. P. Brown, P. de Jong, L. Petrucelli, C. Mueller, and R. H. Brown. Human C9ORF72 Hexanucleotide Expansion Reproduces RNA Foci and Dipeptide Repeat Proteins but Not Neurodegeneration in BAC Transgenic Mice. *Neuron*, 88(5):902–909, Dec 2015. 43

S. R. Pfohl, M. T. Halicek, and C. S. Mitchell. Characterization of the Contribution of Genetic Background and Gender to Disease Progression in the SOD1 G93A Mouse Model of Amyotrophic Lateral Sclerosis: A Meta-Analysis. *J Neuromuscul Dis*, 2 (2):137–150, 2015. 29

T. Philips and W. Robberecht. Neuroinflammation in amyotrophic lateral sclerosis: role of glial activation in motor neuron disease. *Lancet Neurol*, 10(3):253–263, Mar 2011. 174

T. Philips and J. D. Rothstein. Rodent Models of Amyotrophic Lateral Sclerosis. *Curr Protoc Pharmacol*, 69:1–21, Jun 2015. 45

V. Picher-Martel, P. N. Valdmanis, P. V. Gould, J. P. Julien, and N. Dupre. From animal models to human disease: a genetic approach for personalized medicine in ALS. *Acta Neuropathol Commun*, 4(1):70, Jul 2016. 18

J. H. Postlethwait, Y. L. Yan, M. A. Gates, S. Horne, A. Amores, A. Brownlie, A. Donovan, E. S. Egan, A. Force, Z. Gong, C. Goutel, A. Fritz, R. Kelsh, E. Knapik, E. Liao,

B. Paw, D. Ransom, A. Singer, M. Thomson, T. S. Abduljabbar, P. Yelick, D. Beier, J. S. Joly, D. Larhammar, F. Rosa, M. Westerfield, L. I. Zon, S. L. Johnson, and W. S. Talbot. Vertebrate genome evolution and the zebrafish gene map. *Nat. Genet.*, 18(4):345–349, Apr 1998. 61

J. H. Postlethwait, I. G. Woods, P. Ngo-Hazelett, Y. L. Yan, P. D. Kelly, F. Chu, H. Huang, A. Hill-Force, and W. S. Talbot. Zebrafish comparative genomics and the origins of vertebrate chromosomes. *Genome Res.*, 10(12):1890–1902, Dec 2000. 61

A. Pramatarova, J. Laganiere, J. Roussel, K. Brisebois, and G. A. Rouleau. Neuron-specific expression of mutant superoxide dismutase 1 in transgenic mice does not lead to motor impairment. *J. Neurosci.*, 21(10):3369–3374, May 2001. 31

K. Prussing, A. Voigt, and J. B. Schulz. Drosophila melanogaster as a model organism for Alzheimer's disease. *Mol Neurodegener*, 8:35, Nov 2013. 27

E. Quarta, R. Bravi, I. Scambi, R. Mariotti, and D. Minciacchi. Increased anxiety-like behavior and selective learning impairments are concomitant to loss of hippocampal interneurons in the presymptomatic SOD1(G93A) ALS mouse model. *J. Comp. Neurol.*, 523(11):1622–1638, Aug 2015. 33

S. Rainier, M. Bui, E. Mark, D. Thomas, D. Tokarz, L. Ming, C. Delaney, R. J. Richardson, J. W. Albers, N. Matsunami, J. Stevens, H. Coon, M. Leppert, and J. K. Fink. Neuropathy target esterase gene mutations cause motor neuron disease. *Am. J. Hum. Genet.*, 82(3):780–785, Mar 2008. 7

R. Rakhit, P. Cunningham, A. Furtos-Matei, S. Dahan, X. F. Qi, J. P. Crow, N. R. Cashman, L. H. Kondejewski, and A. Chakrabartty. Oxidation-induced misfolding and aggregation of superoxide dismutase and its implications for amyotrophic lateral sclerosis. *J. Biol. Chem.*, 277(49):47551–47556, Dec 2002. 31

N. Ramesh and U. B. Pandey. Autophagy Dysregulation in ALS: When Protein Aggregates Get Out of Hand. *Front Mol Neurosci*, 10:263, 2017. 189

T. Ramesh, A. N. Lyon, R. H. Pineda, C. Wang, P. M. Janssen, B. D. Canan, A. H. Burghes, and C. E. Beattie. A genetic model of amyotrophic lateral sclerosis in zebrafish displays phenotypic hallmarks of motoneuron disease. *Dis Model Mech*, 3 (9-10):652–662, 2010. 30, 32, 98, 108, 168, 171

S. Ranganathan and R. Bowser. Alterations in G(1) to S phase cell-cycle regulators during amyotrophic lateral sclerosis. *Am. J. Pathol.*, 162(3):823–835, Mar 2003. 188

S. Ranganathan, S. Scudiere, and R. Bowser. Hyperphosphorylation of the retinoblastoma gene product and altered subcellular distribution of E2F-1 during Alzheimer's disease and amyotrophic lateral sclerosis. *J. Alzheimers Dis.*, 3(4):377–385, Aug 2001. 188

T. Ravid and M. Hochstrasser. Diversity of degradation signals in the ubiquitin-proteasome system. *Nat. Rev. Mol. Cell Biol.*, 9(9):679–690, Sep 2008. 20

D. B. Re, V. Le Verche, C. Yu, M. W. Amoroso, K. A. Politi, S. Phani, B. Ikiz, L. Hoffmann, M. Koolen, T. Nagata, D. Papadimitriou, P. Nagy, H. Mitsumoto, S. Kariya, H. Wichterle, C. E. Henderson, and S. Przedborski. Necroptosis drives motor neuron death in models of both sporadic and familial ALS. *Neuron*, 81(5): 1001–1008, Mar 2014. 96

I. M. Redelsperger, T. Taldone, E. R. Riedel, M. L. Lepherd, N. S. Lipman, and F. R. Wolf. Stability of Doxycycline in Feed and Water and Minimal Effective Doses in Tetracycline-Inducible Systems. *J. Am. Assoc. Lab. Anim. Sci.*, 55(4):467–474, 2016. 133

L. T. Reiter and E. Bier. Using Drosophila melanogaster to uncover human disease gene function and potential drug target proteins. *Expert Opin. Ther. Targets*, 6(3): 387–399, Jun 2002. 26

A. E. Renton, E. Majounie, A. Waite, J. Simon-Sanchez, S. Rollinson, J. R. Gibbs, J. C. Schymick, H. Laaksovirta, J. C. van Swieten, L. Myllykangas, H. Kalimo, A. Paetau, Y. Abramzon, A. M. Remes, A. Kaganovich, S. W. Scholz, J. Duckworth, J. Ding,

D. W. Harmer, D. G. Hernandez, J. O. Johnson, K. Mok, M. Ryten, D. Trabzuni, R. J. Guerreiro, R. W. Orrell, J. Neal, A. Murray, J. Pearson, I. E. Jansen, D. Sondervan, H. Seelaar, D. Blake, K. Young, N. Halliwell, J. B. Callister, G. Toulson, A. Richardson, A. Gerhard, J. Snowden, D. Mann, D. Neary, M. A. Nalls, T. Peuralinna, L. Jansson, V. M. Isoviita, A. L. Kaivorinne, M. Holtta-Vuori, E. Ikonen, R. Sulkava, M. Benatar, J. Wuu, A. Chio, G. Restagno, G. Borghero, M. Sabatelli, D. Heckerman, E. Rogaeva, L. Zinman, J. D. Rothstein, M. Sendtner, C. Drepper, E. E. Eichler, C. Alkan, Z. Abdullaev, S. D. Pack, A. Dutra, E. Pak, J. Hardy, A. Singleton, N. M. Williams, P. Heutink, S. Pickering-Brown, H. R. Morris, P. J. Tienari, B. J. Traynor, A. Calvo, S. Cammarosano, C. Moglia, A. Canosa, S. Gallo, M. Brunetti, I. Ossola, G. Mora, K. Marinou, L. Papetti, A. Conte, M. Luigetti, V. La Bella, R. Spataro, T. Colletti, S. Battistini, F. Giannini, C. Ricci, C. Caponnetto, G. Mancardi, P. Mandich, F. Salvi, I. Bartolomei, J. Mandrioli, P. Sola, M. Corbo, C. Lunetta, S. Penco, M. R. Monsurro, G. Tedeschi, F. L. Conforti, P. Volanti, G. Floris, A. Cannas, V. Piras, M. R. Murru, M. G. Marrosu, M. Pugliatti, A. Ticca, I. Simone, and G. Logroscino. A hexanucleotide repeat expansion in C9ORF72 is the cause of chromosome 9p21-linked ALS-FTD. *Neuron*, 72(2): 257–268, Oct 2011. 7

H. J. Rideout, I. Lang-Rollin, and L. Stefanis. Involvement of macroautophagy in the dissolution of neuronal inclusions. *Int. J. Biochem. Cell Biol.*, 36(12):2551–2562, Dec 2004. 189

G. M. Ringholz, S. H. Appel, M. Bradshaw, N. A. Cooke, D. M. Mosnik, and P. E. Schulz. Prevalence and patterns of cognitive impairment in sporadic ALS. *Neurology*, 65(4):586–590, Aug 2005. 4

M. E. Ripps, G. W. Huntley, P. R. Hof, J. H. Morrison, and J. W. Gordon. Transgenic mice expressing an altered murine superoxide dismutase gene provide an animal model of amyotrophic lateral sclerosis. *Proc. Natl. Acad. Sci. U.S.A.*, 92(3):689–693, Jan 1995. 29, 32

P. Rombough. Gills are needed for ionoregulation before they are needed for O(2) uptake in developing zebrafish, Danio rerio. *J. Exp. Biol.*, 205(Pt 12):1787–1794, Jun 2002.

D. R. Rosen. Mutations in Cu/Zn superoxide dismutase gene are associated with familial amyotrophic lateral sclerosis. *Nature*, 364(6435):362, Jul 1993. 6, 7

J. N. Rosen, M. F. Sweeney, and J. D. Mably. Microinjection of zebrafish embryos to analyze gene function. *J Vis Exp*, (25), Mar 2009. 61

J. D. Rothstein, M. Van Kammen, A. I. Levey, L. J. Martin, and R. W. Kuncl. Selective loss of glial glutamate transporter GLT-1 in amyotrophic lateral sclerosis. *Ann. Neurol.*, 38(1):73–84, Jul 1995. 19

K. J. Roux, D. I. Kim, M. Raida, and B. Burke. A promiscuous biotin ligase fusion protein identifies proximal and interacting proteins in mammalian cells. *J. Cell Biol.*, 196(6):801–810, Mar 2012. 192

L. P. Rowland. Riluzole for the treatment of amyotrophic lateral sclerosis–too soon to tell? *N. Engl. J. Med.*, 330(9):636–637, Mar 1994. 22

L. P. Rowland and N. A. Shneider. Amyotrophic lateral sclerosis. *N. Engl. J. Med.*, 344(22):1688–1700, May 2001. 1, 3

M. N. Roy, V. E. Prince, and R. K. Ho. Heat shock produces periodic somitic disturbances in the zebrafish embryo. *Mech. Dev.*, 85(1-2):27–34, Jul 1999. 129

I. Sadowski, J. Ma, S. Triezenberg, and M. Ptashne. GAL4-VP16 is an unusually potent transcriptional activator. *Nature*, 335(6190):563–564, Oct 1988. 129

S. A. Sakowski, J. S. Lunn, A. S. Busta, S. S. Oh, G. Zamora-Berridi, M. Palmer, A. A. Rosenberg, S. G. Philip, J. J. Dowling, and E. L. Feldman. Neuromuscular effects of G93A-SOD1 expression in zebrafish. *Mol Neurodegener*, 7:44, Aug 2012. 32, 63, 106, 108

S. Santana, E. P. Rico, and J. S. Burgos. Can zebrafish be used as animal model to study Alzheimer's disease? *Am J Neurodegener Dis*, 1(1):32–48, 2012. 195, 197

S. Sasaki. Endoplasmic reticulum stress in motor neurons of the spinal cord in sporadic amyotrophic lateral sclerosis. *J. Neuropathol. Exp. Neurol.*, 69(4):346–355, Apr 2010a. 18

S. Sasaki. Determination of altered mitochondria ultrastructure by electron microscopy. *Methods Mol. Biol.*, 648:279–290, 2010b. 18

S. Sasaki. Autophagy in spinal cord motor neurons in sporadic amyotrophic lateral sclerosis. *J. Neuropathol. Exp. Neurol.*, 70(5):349–359, May 2011. 18, 189

S. Sathasivam and P. J. Shaw. Apoptosis in amyotrophic lateral sclerosis–what is the evidence? *Lancet Neurol*, 4(8):500–509, Aug 2005. 96

S. Saxena, E. Cabuy, and P. Caroni. A role for motoneuron subtype-selective ER stress in disease manifestations of FALS mice. *Nat. Neurosci.*, 12(5):627–636, May 2009. 18, 30

N. W. Schiffer, S. A. Broadley, T. Hirschberger, P. Tavan, H. A. Kretzschmar, A. Giese, C. Haass, F. U. Hartl, and B. Schmid. Identification of anti-prion compounds as efficient inhibitors of polyglutamine protein aggregation in a zebrafish model. *J. Biol. Chem.*, 282(12):9195–9203, Mar 2007. 169

B. Schmid, A. Hruscha, S. Hogl, J. Banzhaf-Strathmann, K. Strecker, J. van der Zee, M. Teucke, S. Eimer, J. Hegermann, M. Kittelmann, E. Kremmer, M. Cruts, B. Solchenberger, L. Hasenkamp, F. van Bebber, C. Van Broeckhoven, D. Edbauer, S. F. Lichtenthaler, and C. Haass. Loss of ALS-associated TDP-43 in zebrafish causes muscle degeneration, vascular dysfunction, and reduced motor neuron axon outgrowth. *Proc. Natl. Acad. Sci. U.S.A.*, 110(13):4986–4991, Mar 2013. 34, 35, 61

B. M. Schwenk, H. Hartmann, A. Serdaroglu, M. H. Schludi, D. Hornburg, F. Meissner, D. Orozco, A. Colombo, S. Tahirovic, M. Michaelsen, F. Schreiber, S. Haupt,

M. Peitz, O. Brustle, C. Kupper, T. Klopstock, M. Otto, A. C. Ludolph, T. Arzberger, P. H. Kuhn, and D. Edbauer. TDP-43 loss of function inhibits endosomal trafficking and alters trophic signaling in neurons. *EMBO J.*, 35(21):2350–2370, 11 2016. 18

S. Scott, J. E. Kranz, J. Cole, J. M. Lincecum, K. Thompson, N. Kelly, A. Bostrom, J. Theodoss, B. M. Al-Nakhala, F. G. Vieira, J. Ramasubbu, and J. A. Heywood. Design, power, and interpretation of studies in the standard murine model of ALS. *Amyotroph Lateral Scler*, 9(1):4–15, 2008. 45

E. L. Scotter, H. J. Chen, and C. E. Shaw. TDP-43 Proteinopathy and ALS: Insights into Disease Mechanisms and Therapeutic Targets. *Neurotherapeutics*, 12(2):352–363, Apr 2015. 16

C. F. Sephton, B. Cenik, B. K. Cenik, J. Herz, and G. Yu. TDP-43 in central nervous system development and function: clues to TDP-43-associated neurodegeneration. *Biol. Chem.*, 393(7):589–594, Jul 2012. 7, 34

C. F. Sephton, A. A. Tang, A. Kulkarni, J. West, M. Brooks, J. J. Stubblefield, Y. Liu, M. Q. Zhang, C. B. Green, K. M. Huber, E. J. Huang, J. Herz, and G. Yu. Activity-dependent FUS dysregulation disrupts synaptic homeostasis. *Proc. Natl. Acad. Sci. U.S.A.*, 111(44):E4769–4778, Nov 2014. 40

D. G. Sfakianakis, I. Leris, and M. Kentouri. Effect of developmental temperature on swimming performance of zebrafish (danio rerio) juveniles. *Environmental Biology of Fishes*, 90(4):421–427, Apr 2011. ISSN 1573-5133. doi: 10.1007/s10641-010-9751-5. URL https://doi.org/10.1007/s10641-010-9751-5. 167

X. Shan, P. M. Chiang, D. L. Price, and P. C. Wong. Altered distributions of Gemini of coiled bodies and mitochondria in motor neurons of TDP-43 transgenic mice. *Proc. Natl. Acad. Sci. U.S.A.*, 107(37):16325–16330, Sep 2010. 35, 37

Y. Shang and E. J. Huang. Mechanisms of FUS mutations in familial amyotrophic lateral sclerosis. *Brain Res.*, 1647:65–78, 09 2016. 8

A. Sharma, A. K. Lyashchenko, L. Lu, S. E. Nasrabady, M. Elmaleh, M. Mendelsohn, A. Nemes, J. C. Tapia, G. Z. Mentis, and N. A. Shneider. ALS-associated mutant FUS induces selective motor neuron degeneration through toxic gain of function. *Nat Commun*, 7:10465, Feb 2016. 39, 40

D. D. Shaye and I. Greenwald. OrthoList: a compendium of C. elegans genes with human orthologs. *PLoS ONE*, 6(5):e20085, 2011. 26, 27

T. A. Shelkovnikova, O. M. Peters, A. V. Deykin, N. Connor-Robson, H. Robinson, A. A. Ustyugov, S. O. Bachurin, T. G. Ermolkevich, I. L. Goldman, E. R. Sadchikova, E. A. Kovrazhkina, V. I. Skvortsova, S. C. Ling, S. Da Cruz, P. A. Parone, V. L. Buchman, and N. N. Ninkina. Fused in sarcoma (FUS) protein lacking nuclear localization signal (NLS) and major RNA binding motifs triggers proteinopathy and severe motor phenotype in transgenic mice. *J. Biol. Chem.*, 288(35):25266–25274, Aug 2013. 38, 40

A. Shiber and T. Ravid. Chaperoning proteins for destruction: diverse roles of Hsp70 chaperones and their co-chaperones in targeting misfolded proteins to the proteasome. *Biomolecules*, 4(3):704–724, Jul 2014. 20

C. L. Simpson and A. Al-Chalabi. Amyotrophic lateral sclerosis as a complex genetic disease. *Biochim. Biophys. Acta*, 1762(11-12):973–985, 2006. 15

C. L. Simpson, R. Lemmens, K. Miskiewicz, W. J. Broom, V. K. Hansen, P. W. van Vught, J. E. Landers, P. Sapp, L. Van Den Bosch, J. Knight, B. M. Neale, M. R. Turner, J. H. Veldink, R. A. Ophoff, V. B. Tripathi, A. Beleza, M. N. Shah, P. Proitsi, A. Van Hoecke, P. Carmeliet, H. R. Horvitz, P. N. Leigh, C. E. Shaw, L. H. van den Berg, P. C. Sham, J. F. Powell, P. Verstreken, R. H. Brown, W. Robberecht, and A. Al-Chalabi. Variants of the elongator protein 3 (ELP3) gene are associated with motor neuron degeneration. *Hum. Mol. Genet.*, 18(3):472–481, Feb 2009. 7

R. Sivadasan, D. Hornburg, C. Drepper, N. Frank, S. Jablonka, A. Hansel, X. Lojewski, J. Sterneckert, A. Hermann, P. J. Shaw, P. G. Ince, M. Mann, F. Meissner, and

M. Sendtner. C9ORF72 interaction with cofilin modulates actin dynamics in motor neurons. *Nat. Neurosci.*, 19(12):1610–1618, 12 2016. 8

B. N. Smith, N. Ticozzi, C. Fallini, A. S. Gkazi, S. Topp, K. P. Kenna, E. L. Scotter, J. Kost, P. Keagle, J. W. Miller, D. Calini, C. Vance, E. W. Danielson, C. Troakes, C. Tiloca, S. Al-Sarraj, E. A. Lewis, A. King, C. Colombrita, V. Pensato, B. Castellotti, J. de Belleroche, F. Baas, A. L. ten Asbroek, P. C. Sapp, D. McKenna-Yasek, R. L. McLaughlin, M. Polak, S. Asress, J. Esteban-Perez, J. L. Munoz-Blanco, M. Simpson, W. van Rheenen, F. P. Diekstra, G. Lauria, S. Duga, S. Corti, C. Cereda, L. Corrado, G. Soraru, K. E. Morrison, K. L. Williams, G. A. Nicholson, I. P. Blair, P. A. Dion, C. S. Leblond, G. A. Rouleau, O. Hardiman, J. H. Veldink, L. H. van den Berg, A. Al-Chalabi, H. Pall, P. J. Shaw, M. R. Turner, K. Talbot, F. Taroni, A. Garcia-Redondo, Z. Wu, J. D. Glass, C. Gellera, A. Ratti, R. H. Brown, V. Silani, C. E. Shaw, J. E. Landers, S. D'Alfonso, L. Mazzini, G. P. Comi, R. Del Bo, M. Ceroni, S. Gagliardi, G. Querin, and C. Bertolin. Exome-wide rare variant analysis identifies TUBA4A mutations associated with familial ALS. *Neuron*, 84(2):324–331, Oct 2014. 7

E. F. Smith, P. J. Shaw, and K. J. De Vos. The role of mitochondria in amyotrophic lateral sclerosis. *Neurosci. Lett.*, Jun 2017. 18

L. L. Smith, A. H. Beggs, and V. A. Gupta. Analysis of skeletal muscle defects in larval zebrafish by birefringence and touch-evoke escape response assays. *J Vis Exp*, (82):e50925, Dec 2013. 99

H. A. Snaith, A. Anders, I. Samejima, and K. E. Sawin. New and old reagents for fluorescent protein tagging of microtubules in fission yeast; experimental and critical evaluation. *Methods Cell Biol.*, 97:147–172, 2010. 134

K. Y. Soo, M. Halloran, V. Sundaramoorthy, S. Parakh, R. P. Toth, K. A. Southam, C. A. McLean, P. Lock, A. King, M. A. Farg, and J. D. Atkin. Rab1-dependent ER-Golgi transport dysfunction is a common pathogenic mechanism in SOD1, TDP-43 and FUS-associated ALS. *Acta Neuropathol.*, 130(5):679–697, Nov 2015a. 16, 101

K. Y. Soo, J. Sultana, A. E. King, R. Atkinson, S. T. Warraich, V. Sundaramoorthy, I. Blair, M. A. Farg, and J. D. Atkin. ALS-associated mutant FUS inhibits macroautophagy which is restored by overexpression of Rab1. *Cell Death Discov*, 1:15030, 2015b. 101

S. Sorrells, C. Toruno, R. A. Stewart, and C. Jette. Analysis of apoptosis in zebrafish embryos by whole-mount immunofluorescence to detect activated Caspase 3. *J Vis Exp*, (82):e51060, Dec 2013. 96

S. Sperandio, K. Poksay, I. de Belle, M. J. Lafuente, B. Liu, J. Nasir, and D. E. Bredesen. Paraptosis: mediation by MAP kinases and inhibition by AIP-1/Alix. *Cell Death Differ.*, 11(10):1066–1075, Oct 2004. 96

O. Spreux-Varoquaux, G. Bensimon, L. Lacomblez, F. Salachas, P. F. Pradat, N. Le Forestier, A. Marouan, M. Dib, and V. Meininger. Glutamate levels in cerebrospinal fluid in amyotrophic lateral sclerosis: a reappraisal using a new HPLC method with coulometric detection in a large cohort of patients. *J. Neurol. Sci.*, 193 (2):73–78, Jan 2002. 19

J. Sreedharan, I. P. Blair, V. B. Tripathi, X. Hu, C. Vance, B. Rogelj, S. Ackerley, J. C. Durnall, K. L. Williams, E. Buratti, F. Baralle, J. de Belleroche, J. D. Mitchell, P. N. Leigh, A. Al-Chalabi, C. C. Miller, G. Nicholson, and C. E. Shaw. TDP-43 mutations in familial and sporadic amyotrophic lateral sclerosis. *Science*, 319(5870):1668–1672, Mar 2008. 7

C. Stadler, E. Rexhepaj, V. R. Singan, R. F. Murphy, R. Pepperkok, M. Uhlen, J. C. Simpson, and E. Lundberg. Immunofluorescence and fluorescent-protein tagging show high correlation for protein localization in mammalian cells. *Nat. Methods*, 10 (4):315–323, Apr 2013. 166

N. R. Stallings, K. Puttaparthi, C. M. Luther, D. K. Burns, and J. L. Elliott. Progressive motor weakness in transgenic mice expressing human TDP-43. *Neurobiol. Dis.*, 40(2):404–414, Nov 2010. 35, 37

M. D. Stewart, T. Ritterhoff, R. E. Klevit, and P. S. Brzovic. E2 enzymes: more than just middle men. *Cell Res.*, 26(4):423–440, Apr 2016. 20

C. Stribl, A. Samara, D. Trumbach, R. Peis, M. Neumann, H. Fuchs, V. Gailus-Durner, M. Hrab? de Angelis, B. Rathkolb, E. Wolf, J. Beckers, M. Horsch, F. Neff, E. Kremmer, S. Koob, A. S. Reichert, W. Hans, J. Rozman, M. Klingenspor, M. Aichler, A. K. Walch, L. Becker, T. Klopstock, L. Glasl, S. M. Holter, W. Wurst, and T. Floss. Mitochondrial dysfunction and decrease in body weight of a transgenic knock-in mouse model for TDP-43. *J. Biol. Chem.*, 289(15):10769–10784, Apr 2014. 35

G. W. Stuart, J. V. McMurray, and M. Westerfield. Replication, integration and stable germ-line transmission of foreign sequences injected into early zebrafish embryos. *Development*, 103(2):403–412, Jun 1988. 104, 105

G. W. Stuart, J. R. Vielkind, J. V. McMurray, and M. Westerfield. Stable lines of transgenic zebrafish exhibit reproducible patterns of transgene expression. *Development*, 109(3):577–584, Jul 1990. 105

Y. Sugano and S. C. Neuhauss. Reverse genetics tools in zebrafish: a forward dive into endocrinology. *Gen. Comp. Endocrinol.*, 188:303–308, Jul 2013. 106

V. Swarup, D. Phaneuf, C. Bareil, J. Robertson, G. A. Rouleau, J. Kriz, and J. P. Julien. Pathological hallmarks of amyotrophic lateral sclerosis/frontotemporal lobar degeneration in transgenic mice produced with TDP-43 genomic fragments. *Brain*, 134(Pt 9):2610–2626, Sep 2011. 35, 36

Y. Takahashi, Y. Fukuda, J. Yoshimura, A. Toyoda, K. Kurppa, H. Moritoyo, V. V. Belzil, P. A. Dion, K. Higasa, K. Doi, H. Ishiura, J. Mitsui, H. Date, B. Ahsan, T. Matsukawa, Y. Ichikawa, T. Moritoyo, M. Ikoma, T. Hashimoto, F. Kimura, S. Murayama, O. Onodera, M. Nishizawa, M. Yoshida, N. Atsuta, G. Sobue, J. A. Fifita, K. L. Williams, I. P. Blair, G. A. Nicholson, P. Gonzalez-Perez, R. H. Brown, M. Nomoto, K. Elenius, G. A. Rouleau, A. Fujiyama, S. Morishita, J. Goto, S. Tsuji, R. Nakamura, H. Watanabe, Y. Izumi, R. Kaji, M. Morita, K. Ogaki, A. Taniguchi,

I. Aiba, K. Mizoguchi, K. Okamoto, K. Hasegawa, M. Aoki, A. Kawata, I. Nakano, K. Abe, M. Oda, M. Konagaya, T. Imai, M. Nakagawa, T. Fujita, H. Sasaki, and M. Nishizawa. ERBB4 mutations that disrupt the neuregulin-ErbB4 pathway cause amyotrophic lateral sclerosis type 19. *Am. J. Hum. Genet.*, 93(5):900–905, Nov 2013. 7

Y. Tashiro, M. Urushitani, H. Inoue, M. Koike, Y. Uchiyama, M. Komatsu, K. Tanaka, M. Yamazaki, M. Abe, H. Misawa, K. Sakimura, H. Ito, and R. Takahashi. Motor neuron-specific disruption of proteasomes, but not autophagy, replicates amyotrophic lateral sclerosis. *J. Biol. Chem.*, 287(51):42984–42994, Dec 2012. 21

J. P. Taylor, R. H. Brown, and D. W. Cleveland. Decoding ALS: from genes to mechanism. *Nature*, 539(7628):197–206, 11 2016. 200

S. C. Taylor and A. Posch. The design of a quantitative western blot experiment. *Biomed Res Int*, 2014:361590, 2014. 94

D. Teschendorf and C. D. Link. What have worm models told us about the mechanisms of neuronal dysfunction in human neurodegenerative diseases? *Mol Neurodegener*, 4:38, Sep 2009. 27

M. T. Tetzlaff, C. Bai, M. Finegold, J. Wilson, J. W. Harper, K. A. Mahon, and S. J. Elledge. Cyclin F disruption compromises placental development and affects normal cell cycle execution. *Mol. Cell. Biol.*, 24(6):2487–2498, Mar 2004. 198, 199

V. Thermes, C. Grabher, F. Ristoratore, F. Bourrat, A. Choulika, J. Wittbrodt, and J. S. Joly. I-SceI meganuclease mediates highly efficient transgenesis in fish. *Mech. Dev.*, 118(1-2):91–98, Oct 2002. 104, 105

M. Therrien and J. A. Parker. Worming forward: amyotrophic lateral sclerosis toxicity mechanisms and genetic interactions in Caenorhabditis elegans. *Front Genet*, 5:85, 2014. 27

M. Therrien, G. A. Rouleau, P. A. Dion, and J. A. Parker. Deletion of C9ORF72 results

in motor neuron degeneration and stress sensitivity in C. elegans. *PLoS ONE*, 8(12): e83450, 2013. 42, 43

K. D. Thielsen, J. M. Moser, T. Schmitt-John, M. S. Jensen, K. Jensen, and M. M. Holm. The Wobbler mouse model of amyotrophic lateral sclerosis (ALS) displays hippocampal hyperexcitability, and reduced number of interneurons, but no presynaptic vesicle release impairments. *PLoS ONE*, 8(12):e82767, 2013. 19

T. Tian, C. Huang, J. Tong, M. Yang, H. Zhou, and X. G. Xia. TDP-43 potentiates alpha-synuclein toxicity to dopaminergic neurons in transgenic mice. *Int. J. Biol. Sci.*, 7(2):234–243, Mar 2011. 36, 121

T. Tikka, B. L. Fiebich, G. Goldsteins, R. Keinanen, and J. Koistinaho. Minocycline, a tetracycline derivative, is neuroprotective against excitotoxicity by inhibiting activation and proliferation of microglia. *J. Neurosci.*, 21(8):2580–2588, Apr 2001. 165

S. Tobisawa, Y. Hozumi, S. Arawaka, S. Koyama, M. Wada, M. Nagai, M. Aoki, Y. Itoyama, K. Goto, and T. Kato. Mutant SOD1 linked to familial amyotrophic lateral sclerosis, but not wild-type SOD1, induces ER stress in COS7 cells and transgenic mice. *Biochem. Biophys. Res. Commun.*, 303(2):496–503, Apr 2003. 33

J. Tong, C. Huang, F. Bi, Q. Wu, B. Huang, X. Liu, F. Li, H. Zhou, and X. G. Xia. Expression of ALS-linked TDP-43 mutant in astrocytes causes non-cell-autonomous motor neuron death in rats. *EMBO J.*, 32(13):1917–1926, Jul 2013. 36

H. Tran, S. Almeida, J. Moore, T. F. Gendron, U. Chalasani, Y. Lu, X. Du, J. A. Nickerson, L. Petrucelli, Z. Weng, and F. B. Gao. Differential Toxicity of Nuclear RNA Foci versus Dipeptide Repeat Proteins in a Drosophila Model of C9ORF72 FTD/ALS. *Neuron*, 87(6):1207–1214, Sep 2015. 43

B. J. Traynor, M. Alexander, B. Corr, E. Frost, and O. Hardiman. Effect of a multidisciplinary amyotrophic lateral sclerosis (ALS) clinic on ALS survival: a population

based study, 1996-2000. *J. Neurol. Neurosurg. Psychiatr.*, 74(9):1258–1261, Sep 2003. 22

K. J. Tsai, C. H. Yang, Y. H. Fang, K. H. Cho, W. L. Chien, W. T. Wang, T. W. Wu, C. P. Lin, W. M. Fu, and C. K. Shen. Elevated expression of TDP-43 in the forebrain of mice is sufficient to cause neurological and pathological phenotypes mimicking FTLD-U. *J. Exp. Med.*, 207(8):1661–1673, Aug 2010. 35

P. H. Tu, P. Raju, K. A. Robinson, M. E. Gurney, J. Q. Trojanowski, and V. M. Lee. Transgenic mice carrying a human mutant superoxide dismutase transgene develop neuronal cytoskeletal pathology resembling human amyotrophic lateral sclerosis lesions. *Proc. Natl. Acad. Sci. U.S.A.*, 93(7):3155–3160, Apr 1996. 30

M. R. Turner, J. Barnwell, A. Al-Chalabi, and A. Eisen. Young-onset amyotrophic lateral sclerosis: historical and other observations. *Brain*, 135(Pt 9):2883–2891, Sep 2012. 4

M. R. Turner, A. Al-Chalabi, A. Chio, O. Hardiman, M. C. Kiernan, J. D. Rohrer, J. Rowe, W. Seeley, and K. Talbot. Genetic screening in sporadic ALS and FTD. *J. Neurol. Neurosurg. Psychiatr.*, Jun 2017. 5

A. Uchida, H. Sasaguri, N. Kimura, M. Tajiri, T. Ohkubo, F. Ono, F. Sakaue, K. Kanai, T. Hirai, T. Sano, K. Shibuya, M. Kobayashi, M. Yamamoto, S. Yokota, T. Kubodera, M. Tomori, K. Sakaki, M. Enomoto, Y. Hirai, J. Kumagai, Y. Yasutomi, H. Mochizuki, S. Kuwabara, T. Uchihara, H. Mizusawa, and T. Yokota. Non-human primate model of amyotrophic lateral sclerosis with cytoplasmic mislocalization of TDP-43. *Brain*, 135(Pt 3):833–846, Mar 2012. 29

J. Ugolino, Y. J. Ji, K. Conchina, J. Chu, R. S. Nirujogi, A. Pandey, N. R. Brady, A. Hamacher-Brady, and J. Wang. Loss of C9orf72 Enhances Autophagic Activity via Deregulated mTOR and TFEB Signaling. *PLoS Genet.*, 12(11):e1006443, Nov 2016. 42

K. Umeda, T. Ishizuka, H. Yawo, and W. Shoji. Position- and quantity-dependent responses in zebrafish turning behavior. *Sci Rep*, 6:27888, Jun 2016. 98

S. Urlinger, U. Baron, M. Thellmann, M. T. Hasan, H. Bujard, and W. Hillen. Exploring the sequence space for tetracycline-dependent transcriptional activators: novel mutations yield expanded range and sensitivity. *Proc. Natl. Acad. Sci. U.S.A.*, 97 (14):7963–7968, Jul 2000. 131

M. Urushitani, J. Kurisu, K. Tsukita, and R. Takahashi. Proteasomal inhibition by misfolded mutant superoxide dismutase 1 induces selective motor neuron death in familial amyotrophic lateral sclerosis. *J. Neurochem.*, 83(5):1030–1042, Dec 2002. 30

A. Vaccaro, A. Tauffenberger, D. Aggad, G. Rouleau, P. Drapeau, and J. A. Parker. Mutant TDP-43 and FUS cause age-dependent paralysis and neurodegeneration in C. elegans. *PLoS ONE*, 7(2):e31321, 2012. 35, 40

F. van Bebber, D. Paquet, A. Hruscha, B. Schmid, and C. Haass. Methylene blue fails to inhibit Tau and polyglutamine protein dependent toxicity in zebrafish. *Neurobiol. Dis.*, 39(3):265–271, Sep 2010. 169

M. van Blitterswijk, M. DeJesus-Hernandez, and R. Rademakers. How do C9ORF72 repeat expansions cause amyotrophic lateral sclerosis and frontotemporal dementia: can we learn from other noncoding repeat expansion disorders? *Curr. Opin. Neurol.*, 25(6):689–700, Dec 2012. 8

P. Van Damme, A. Van Hoecke, D. Lambrechts, P. Vanacker, E. Bogaert, J. van Swieten, P. Carmeliet, L. Van Den Bosch, and W. Robberecht. Progranulin functions as a neurotrophic factor to regulate neurite outgrowth and enhance neuronal survival. *J. Cell Biol.*, 181(1):37–41, Apr 2008. 62

P. Van Damme, W. Robberecht, and L. Van Den Bosch. Modelling amyotrophic lateral sclerosis: progress and possibilities. *Dis Model Mech*, 10(5):537–549, May 2017. 26, 28, 29

V. M. Van Deerlin, J. B. Leverenz, L. M. Bekris, T. D. Bird, W. Yuan, L. B. Elman, D. Clay, E. M. Wood, A. S. Chen-Plotkin, M. Martinez-Lage, E. Steinbart, L. Mc-Cluskey, M. Grossman, M. Neumann, I. L. Wu, W. S. Yang, R. Kalb, D. R. Galasko, T. J. Montine, J. Q. Trojanowski, V. M. Lee, G. D. Schellenberg, and C. E. Yu. TARDBP mutations in amyotrophic lateral sclerosis with TDP-43 neuropathology: a genetic and histopathological analysis. *Lancet Neurol*, 7(5):409–416, May 2008. 7

L. Van Den Bosch, P. Van Damme, E. Bogaert, and W. Robberecht. The role of excitotoxicity in the pathogenesis of amyotrophic lateral sclerosis. *Biochim. Biophys. Acta*, 1762(11-12):1068–1082, 2006. 17

J. van Eersel, Y. D. Ke, A. Gladbach, M. Bi, J. Gotz, J. J. Kril, and L. M. Ittner. Cytoplasmic accumulation and aggregation of TDP-43 upon proteasome inhibition in cultured neurons. *PLoS ONE*, 6(7):e22850, 2011. 18, 21

M. A. van Es, J. H. Veldink, C. G. Saris, H. M. Blauw, P. W. van Vught, A. Birve, R. Lemmens, H. J. Schelhaas, E. J. Groen, M. H. Huisman, A. J. van der Kooi, M. de Visser, C. Dahlberg, K. Estrada, F. Rivadeneira, A. Hofman, M. J. Zwarts, P. T. van Doormaal, D. Rujescu, E. Strengman, I. Giegling, P. Muglia, B. Tomik, A. Slowik, A. G. Uitterlinden, C. Hendrich, S. Waibel, T. Meyer, A. C. Ludolph, J. D. Glass, S. Purcell, S. Cichon, M. M. Nothen, H. E. Wichmann, S. Schreiber, S. H. Vermeulen, L. A. Kiemeney, J. H. Wokke, S. Cronin, R. L. McLaughlin, O. Hardiman, K. Fumoto, R. J. Pasterkamp, V. Meininger, J. Melki, P. N. Leigh, C. E. Shaw, J. E. Landers, A. Al-Chalabi, R. H. Brown, W. Robberecht, P. M. Andersen, R. A. Ophoff, and L. H. van den Berg. Genome-wide association study identifies 19p13.3 (UNC13A) and 9p21.2 as susceptibility loci for sporadic amyotrophic lateral sclerosis. *Nat. Genet.*, 41(10):1083–1087, Oct 2009. 7

T. J. van Ham, J. Mapes, D. Kokel, and R. T. Peterson. Live imaging of apoptotic cells in zebrafish. *FASEB J.*, 24(11):4336–4342, Nov 2010. 106, 194

A. Van Hoecke, L. Schoonaert, R. Lemmens, M. Timmers, K. A. Staats, A. S. Laird, E. Peeters, T. Philips, A. Goris, B. Dubois, P. M. Andersen, A. Al-Chalabi, V. Thijs,

A. M. Turnley, P. W. van Vught, J. H. Veldink, O. Hardiman, L. Van Den Bosch, P. Gonzalez-Perez, P. Van Damme, R. H. Brown, L. H. van den Berg, and W. Robberecht. EPHA4 is a disease modifier of amyotrophic lateral sclerosis in animal models and in humans. *Nat. Med.*, 18(9):1418–1422, Sep 2012. 7

W. van Rheenen, A. Shatunov, A. M. Dekker, R. L. McLaughlin, F. P. Diekstra, S. L. Pulit, R. A. van der Spek, U. Vosa, S. de Jong, M. R. Robinson, J. Yang, I. Fogh, P. T. van Doormaal, G. H. Tazelaar, M. Koppers, A. M. Blokhuis, W. Sproviero, A. R. Jones, K. P. Kenna, K. R. van Eijk, O. Harschnitz, R. D. Schellevis, W. J. Brands, J. Medic, A. Menelaou, A. Vajda, N. Ticozzi, K. Lin, B. Rogelj, K. Vrabec, M. Ravnik-Glava?, B. Koritnik, J. Zidar, L. Leonardis, L. D. Gro?elj, S. Millecamps, F. Salachas, V. Meininger, M. de Carvalho, S. Pinto, J. S. Mora, R. Rojas-Garcia, M. Polak, S. Chandran, S. Colville, R. Swingler, K. E. Morrison, P. J. Shaw, J. Hardy, R. W. Orrell, A. Pittman, K. Sidle, P. Fratta, A. Malaspina, S. Topp, S. Petri, S. Abdulla, C. Drepper, M. Sendtner, T. Meyer, R. A. Ophoff, K. A. Staats, M. Wiedau-Pazos, C. Lomen-Hoerth, V. M. Van Deerlin, J. Q. Trojanowski, L. Elman, L. McCluskey, A. N. Basak, C. Tunca, H. Hamzeiy, Y. Parman, T. Meitinger, P. Lichtner, M. Radivojkov-Blagojevic, C. R. Andres, C. Maurel, G. Bensimon, B. Landwehrmeyer, A. Brice, C. A. Payan, S. Saker-Delye, A. Durr, N. W. Wood, L. Tittmann, W. Lieb, A. Franke, M. Rietschel, S. Cichon, M. M. Nothen, P. Amouyel, C. Tzourio, J. F. Dartigues, A. G. Uitterlinden, F. Rivadeneira, K. Estrada, A. Hofman, C. Curtis, H. M. Blauw, A. J. van der Kooi, M. de Visser, A. Goris, M. Weber, C. E. Shaw, B. N. Smith, O. Pansarasa, C. Cereda, R. Del Bo, G. P. Comi, S. D'Alfonso, C. Bertolin, G. Soraru, L. Mazzini, V. Pensato, C. Gellera, C. Tiloca, A. Ratti, A. Calvo, C. Moglia, M. Brunetti, S. Arcuti, R. Capozzo, C. Zecca, C. Lunetta, S. Penco, N. Riva, A. Padovani, M. Filosto, B. Muller, R. J. Stuit, I. Blair, K. Zhang, E. P. McCann, J. A. Fifita, G. A. Nicholson, D. B. Rowe, R. Pamphlett, M. C. Kiernan, J. Grosskreutz, O. W. Witte, T. Ringer, T. Prell, B. Stubendorff, I. Kurth, C. A. Hubner, P. N. Leigh, F. Casale, A. Chio, E. Beghi, E. Pupillo, R. Tortelli, G. Logroscino, J. Powell, A. C. Ludolph, J. H. Weishaupt,

W. Robberecht, P. Van Damme, L. Franke, T. H. Pers, R. H. Brown, J. D. Glass, J. E. Landers, O. Hardiman, P. M. Andersen, P. Corcia, P. Vourc'h, V. Silani, N. R. Wray, P. M. Visscher, P. I. de Bakker, M. A. van Es, R. J. Pasterkamp, C. M. Lewis, G. Breen, A. Al-Chalabi, L. H. van den Berg, and J. H. Veldink. Genome-wide association analyses identify new risk variants and the genetic architecture of amyotrophic lateral sclerosis. *Nat. Genet.*, 48(9):1043–1048, Sep 2016. 7, 187

C. Vance, B. Rogelj, T. Hortobagyi, K. J. De Vos, A. L. Nishimura, J. Sreedharan, X. Hu, B. Smith, D. Ruddy, P. Wright, J. Ganesalingam, K. L. Williams, V. Tripathi, S. Al-Saraj, A. Al-Chalabi, P. N. Leigh, I. P. Blair, G. Nicholson, J. de Belleroche, J. M. Gallo, C. C. Miller, and C. E. Shaw. Mutations in FUS, an RNA processing protein, cause familial amyotrophic lateral sclerosis type 6. *Science*, 323(5918):1208–1211, Feb 2009. 7, 8

M. R. Vargas and J. A. Johnson. Astrogliosis in amyotrophic lateral sclerosis: role and therapeutic potential of astrocytes. *Neurotherapeutics*, 7(4):471–481, Oct 2010. 174

S. Vinsant, C. Mansfield, R. Jimenez-Moreno, V. Del Gaizo Moore, M. Yoshikawa, T. G. Hampton, D. Prevette, J. Caress, R. W. Oppenheim, and C. Milligan. Characterization of early pathogenesis in the SOD1(G93A) mouse model of ALS: part II, results and discussion. *Brain Behav*, 3(4):431–457, Jul 2013. 18

A. Voigt, D. Herholz, F. C. Fiesel, K. Kaur, D. Muller, P. Karsten, S. S. Weber, P. J. Kahle, T. Marquardt, and J. B. Schulz. TDP-43-mediated neuron loss in vivo requires RNA-binding activity. *PLoS ONE*, 5(8):e12247, Aug 2010. 35

S. Vucic and M. C. Kiernan. Novel threshold tracking techniques suggest that cortical hyperexcitability is an early feature of motor neuron disease. *Brain*, 129(Pt 9):2436–2446, Sep 2006. 173

S. Vucic, G. A. Nicholson, and M. C. Kiernan. Cortical hyperexcitability may precede the onset of familial amyotrophic lateral sclerosis. *Brain*, 131(Pt 6):1540–1550, Jun 2008. 173

A. J. Waite, D. Baumer, S. East, J. Neal, H. R. Morris, O. Ansorge, and D. J. Blake. Reduced C9orf72 protein levels in frontal cortex of amyotrophic lateral sclerosis and frontotemporal degeneration brain with the C9ORF72 hexanucleotide repeat expansion. *Neurobiol. Aging*, 35(7):5–1779, Jul 2014. 42

A. K. Walker and J. D. Atkin. Stress signaling from the endoplasmic reticulum: A central player in the pathogenesis of amyotrophic lateral sclerosis. *IUBMB Life*, 63 (9):754–763, Sep 2011. 37

A. K. Walker, K. J. Spiller, G. Ge, A. Zheng, Y. Xu, M. Zhou, K. Tripathy, L. K. Kwong, J. Q. Trojanowski, and V. M. Lee. Functional recovery in new mouse models of ALS/FTLD after clearance of pathological cytoplasmic TDP-43. *Acta Neuropathol.*, 130(5):643–660, Nov 2015. 34, 36, 37, 132

C. M. Walsh. Grand challenges in cell death and survival: apoptosis vs. necroptosis. *Front Cell Dev Biol*, 2:3, 2014. 96

J. Wang, G. Xu, V. Gonzales, M. Coonfield, D. Fromholt, N. G. Copeland, N. A. Jenkins, and D. R. Borchelt. Fibrillar inclusions and motor neuron degeneration in transgenic mice expressing superoxide dismutase 1 with a disrupted copper-binding site. *Neurobiol. Dis.*, 10(2):128–138, Jul 2002. 32

J. Wang, H. Slunt, V. Gonzales, D. Fromholt, M. Coonfield, N. G. Copeland, N. A. Jenkins, and D. R. Borchelt. Copper-binding-site-null SOD1 causes ALS in trans-genic mice: aggregates of non-native SOD1 delineate a common feature. *Hum. Mol. Genet.*, 12(21):2753–2764, Nov 2003. 30, 32

J. Wang, G. Xu, H. Li, V. Gonzales, D. Fromholt, C. Karch, N. G. Copeland, N. A. Jenkins, and D. R. Borchelt. Somatodendritic accumulation of misfolded SOD1-L126Z in motor neurons mediates degeneration: alphaB-crystallin modulates aggre-gation. *Hum. Mol. Genet.*, 14(16):2335–2347, Aug 2005. 33

J. Wang, G. W. Farr, D. H. Hall, F. Li, K. Furtak, L. Dreier, and A. L. Horwich. An ALS-linked mutant SOD1 produces a locomotor defect associated with aggregation

and synaptic dysfunction when expressed in neurons of Caenorhabditis elegans. *PLoS Genet.*, 5(1):e1000350, Jan 2009a. 30, 31, 32

J. W. Wang, J. R. Brent, A. Tomlinson, N. A. Shneider, and B. D. McCabe. The ALS-associated proteins FUS and TDP-43 function together to affect Drosophila locomotion and life span. *J. Clin. Invest.*, 121(10):4118–4126, Oct 2011. 38, 39, 40

L. Wang, H. X. Deng, G. Grisotti, H. Zhai, T. Siddique, and R. P. Roos. Wild-type SOD1 overexpression accelerates disease onset of a G85R SOD1 mouse. *Hum. Mol. Genet.*, 18(9):1642–1651, May 2009b. 32

E. E. Wanker, E. Scherzinger, V. Heiser, A. Sittler, H. Eickhoff, and H. Lehrach. Membrane filter assay for detection of amyloid-like polyglutamine-containing protein aggregates. *Meth. Enzymol.*, 309:375–386, 1999. 169

B. A. Warmus, D. R. Sekar, E. McCutchen, G. D. Schellenberg, R. C. Roberts, L. L. McMahon, and E. D. Roberson. Tau-mediated NMDA receptor impairment underlies dysfunction of a selectively vulnerable network in a mouse model of frontotemporal dementia. *J. Neurosci.*, 34(49):16482–16495, Dec 2014. 196

J. D. Warren, J. D. Rohrer, and M. N. Rossor. Clinical review. Frontotemporal dementia. *BMJ*, 347:f4827, Aug 2013. 3

T. Watanabe, M. Tanaka, K. Watanabe, Y. Takamatsu, and A. Tobe. [Research and development of the free radical scavenger edaravone as a neuroprotectant]. *Yakugaku Zasshi*, 124(3):99–111, Mar 2004. 22

M. R. Watson, R. D. Lagow, K. Xu, B. Zhang, and N. M. Bonini. A drosophila model for amyotrophic lateral sclerosis reveals motor neuron damage by human SOD1. *J. Biol. Chem.*, 283(36):24972–24981, Sep 2008. 30, 32

T. Weber and R. Koster. Genetic tools for multicolor imaging in zebrafish larvae. *Methods*, 62(3):279–291, Aug 2013. 96

C. P. Webster, E. F. Smith, P. J. Shaw, and K. J. De Vos. Protein Homeostasis in Amyotrophic Lateral Sclerosis: Therapeutic Opportunities? *Front Mol Neurosci*, 10:123, 2017. 2, 16, 180, 182, 184

I. Wegorzewska and R. H. Baloh. TDP-43-based animal models of neurodegeneration: new insights into ALS pathology and pathophysiology. *Neurodegener Dis*, 8(4):262–274, 2011. 37

I. Wegorzewska, S. Bell, N. J. Cairns, T. M. Miller, and R. H. Baloh. TDP-43 mutant transgenic mice develop features of ALS and frontotemporal lobar degeneration. *Proc. Natl. Acad. Sci. U.S.A.*, 106(44):18809–18814, Nov 2009. 35

D. Wehner, C. Jahn, and G. Weidinger. Use of the TetON System to Study Molecular Mechanisms of Zebrafish Regeneration. *J Vis Exp*, (100):e52756, Jun 2015. 132

C. Welinder and L. Ekblad. Coomassie staining as loading control in Western blot analysis. *J. Proteome Res.*, 10(3):1416–1419, Mar 2011. 94

X. Wen, W. Tan, T. Westergard, K. Krishnamurthy, S. S. Markandaiah, Y. Shi, S. Lin, N. A. Shneider, J. Monaghan, U. B. Pandey, P. Pasinelli, J. K. Ichida, and D. Trotti. Antisense proline-arginine RAN dipeptides linked to C9ORF72-ALS/FTD form toxic nuclear aggregates that initiate in vitro and in vivo neuronal death. *Neuron*, 84(6): 1213–1225, Dec 2014. 42

M. C. West, L. J. Campbell, J. J. Willoughby, and A. M. Jensen. Two types of transgenic lines for doxycycline-inducible, cell-specific gene expression in zebrafish ultraviolet cone photoreceptors. *Gene Expr. Patterns*, 14(2):96–104, Mar 2014. 132

M. Westerfield. *The Zebrafish book.* University of Oregon Press, Eugene, 4 edition, 2000. 55, 123

K. E. Wickliffe, A. Williamson, H. J. Meyer, A. Kelly, and M. Rape. K11-linked ubiquitin chains as novel regulators of cell division. *Trends Cell Biol.*, 21(11):656–663, Nov 2011. 20

K. L. Williams, S. Topp, S. Yang, B. Smith, J. A. Fifita, S. T. Warraich, K. Y. Zhang, N. Farrawell, C. Vance, X. Hu, A. Chesi, C. S. Leblond, A. Lee, S. L. Rayner, V. Sundaramoorthy, C. Dobson-Stone, M. P. Molloy, M. van Blitterswijk, D. W. Dickson, R. C. Petersen, N. R. Graff-Radford, B. F. Boeve, M. E. Murray, C. Pottier, E. Don, C. Winnick, E. P. McCann, A. Hogan, H. Daoud, A. Levert, P. A. Dion, J. Mitsui, H. Ishiura, Y. Takahashi, J. Goto, J. Kost, C. Gellera, A. S. Gkazi, J. Miller, J. Stockton, W. S. Brooks, K. Boundy, M. Polak, J. L. Munoz-Blanco, J. Esteban-Perez, A. Rabano, O. Hardiman, K. E. Morrison, N. Ticozzi, V. Silani, J. de Belleroche, J. D. Glass, J. B. Kwok, G. J. Guillemin, R. S. Chung, S. Tsuji, R. H. Brown, A. Garcia-Redondo, R. Rademakers, J. E. Landers, A. D. Gitler, G. A. Rouleau, N. J. Cole, J. J. Yerbury, J. D. Atkin, C. E. Shaw, G. A. Nicholson, and I. P. Blair. CCNF mutations in amyotrophic lateral sclerosis and frontotemporal dementia. *Nat Commun*, 7, 2016. 7, 15, 46, 89, 92, 95, 180, 184, 188, 192, 193, 195, 198, 209

T. L. Williamson and D. W. Cleveland. Slowing of axonal transport is a very early event in the toxicity of ALS-linked SOD1 mutants to motor neurons. *Nat. Neurosci.*, 2(1):50–56, Jan 1999. 19

H. Wils, G. Kleinberger, J. Janssens, S. Pereson, G. Joris, I. Cuijt, V. Smits, C. Ceuterick-de Groote, C. Van Broeckhoven, and S. Kumar-Singh. TDP-43 transgenic mice develop spastic paralysis and neuronal inclusions characteristic of ALS and frontotemporal lobar degeneration. *Proc. Natl. Acad. Sci. U.S.A.*, 107(8):3858–3863, Feb 2010. 35, 37

C. Wilson, H. J. Bellen, and W. J. Gehring. Position effects on eukaryotic gene expression. *Annu. Rev. Cell Biol.*, 6:679–714, 1990. 104, 120

F. A. Wininger, R. Zeng, G. S. Johnson, M. L. Katz, G. C. Johnson, W. W. Bush, J. M. Jarboe, and J. R. Coates. Degenerative myelopathy in a Bernese Mountain Dog with a novel SOD1 missense mutation. *J. Vet. Intern. Med.*, 25(5):1166–1170, 2011. 33

P. C. Wong, C. A. Pardo, D. R. Borchelt, M. K. Lee, N. G. Copeland, N. A. Jenkins, S. S. Sisodia, D. W. Cleveland, and D. L. Price. An adverse property of a familial ALS-linked SOD1 mutation causes motor neuron disease characterized by vacuolar degeneration of mitochondria. *Neuron*, 14(6):1105–1116, Jun 1995. 18, 30, 32

C. H. Wu, C. Fallini, N. Ticozzi, P. J. Keagle, P. C. Sapp, K. Piotrowska, P. Lowe, M. Koppers, D. McKenna-Yasek, D. M. Baron, J. E. Kost, P. Gonzalez-Perez, A. D. Fox, J. Adams, F. Taroni, C. Tiloca, A. L. Leclerc, S. C. Chafe, D. Mangroo, M. J. Moore, J. A. Zitzewitz, Z. S. Xu, L. H. van den Berg, J. D. Glass, G. Siciliano, E. T. Cirulli, D. B. Goldstein, F. Salachas, V. Meininger, W. Rossoll, A. Ratti, C. Gellera, D. A. Bosco, G. J. Bassell, V. Silani, V. E. Drory, R. H. Brown, and J. E. Landers. Mutations in the profilin 1 gene cause familial amyotrophic lateral sclerosis. *Nature*, 488(7412):499–503, Aug 2012a. 7

L. S. Wu, W. C. Cheng, and C. K. Shen. Targeted depletion of TDP-43 expression in the spinal cord motor neurons leads to the development of amyotrophic lateral sclerosis-like phenotypes in mice. *J. Biol. Chem.*, 287(33):27335–27344, Aug 2012b. 34, 36

Z. Xi, Y. Yunusova, M. van Blitterswijk, S. Dib, M. Ghani, D. Moreno, C. Sato, Y. Liang, A. Singleton, J. Robertson, R. Rademakers, L. Zinman, and E. Rogaeva. Identical twins with the C9orf72 repeat expansion are discordant for ALS. *Neurology*, 83(16):1476–1478, Oct 2014. 3, 44

L. Xia, L. Zheng, and J. L. Zhou. Transcriptional and morphological effects of tamoxifen on the early development of zebrafish (Danio rerio). *J Appl Toxicol*, 36(6): 853–862, Jun 2016. 129

Y. F. Xu, T. F. Gendron, Y. J. Zhang, W. L. Lin, S. D'Alton, H. Sheng, M. C. Casey, J. Tong, J. Knight, X. Yu, R. Rademakers, K. Boylan, M. Hutton, E. McGowan, D. W. Dickson, J. Lewis, and L. Petrucelli. Wild-type human TDP-43 expression causes TDP-43 phosphorylation, mitochondrial aggregation, motor deficits, and early mortality in transgenic mice. *J. Neurosci.*, 30(32):10851–10859, Aug 2010. 35, 37

Y. F. Xu, Y. J. Zhang, W. L. Lin, X. Cao, C. Stetler, D. W. Dickson, J. Lewis, and L. Petrucelli. Expression of mutant TDP-43 induces neuronal dysfunction in transgenic mice. *Mol Neurodegener*, 6:73, Oct 2011. 36

Z. Xu, M. Poidevin, X. Li, Y. Li, L. Shu, D. L. Nelson, H. Li, C. M. Hales, M. Gearing, T. S. Wingo, and P. Jin. Expanded GGGGCC repeat RNA associated with amyotrophic lateral sclerosis and frontotemporal dementia causes neurodegeneration. *Proc. Natl. Acad. Sci. U.S.A.*, 110(19):7778–7783, May 2013. 43

K. Yamanaka, S. J. Chun, S. Boillee, N. Fujimori-Tonou, H. Yamashita, D. H. Gutmann, R. Takahashi, H. Misawa, and D. W. Cleveland. Astrocytes as determinants of disease progression in inherited amyotrophic lateral sclerosis. *Nat. Neurosci.*, 11 (3):251–253, Mar 2008. 31

S. Yanase, A. Onodera, P. Tedesco, T. E. Johnson, and N. Ishii. SOD-1 deletions in Caenorhabditis elegans alter the localization of intracellular reactive oxygen species and show molecular compensation. *J. Gerontol. A Biol. Sci. Med. Sci.*, 64(5):530–539, May 2009. 32

H. Yang, G. Wang, H. Sun, R. Shu, T. Liu, C. E. Wang, Z. Liu, Y. Zhao, B. Zhao, Z. Ouyang, D. Yang, J. Huang, Y. Zhou, S. Li, X. Jiang, Z. Xiao, X. J. Li, and L. Lai. Species-dependent neuropathology in transgenic SOD1 pigs. *Cell Res.*, 24 (4):464–481, Apr 2014. 29, 33, 44

A. Yokoseki, A. Shiga, C. F. Tan, A. Tagawa, H. Kaneko, A. Koyama, H. Eguchi, A. Tsujino, T. Ikeuchi, A. Kakita, K. Okamoto, M. Nishizawa, H. Takahashi, and O. Onodera. TDP-43 mutation in familial amyotrophic lateral sclerosis. *Ann. Neurol.*, 63(4):538–542, Apr 2008. 7

N. Yoshinari, K. Ando, A. Kudo, M. Kinoshita, and A. Kawakami. Colored medaka and zebrafish: transgenics with ubiquitous and strong transgene expression driven by the medaka β-actin promoter. *Dev. Growth Differ.*, 54(9):818–828, Dec 2012. 107

J. Yrjanheikki, R. Keinanen, M. Pellikka, T. Hokfelt, and J. Koistinaho. Tetracyclines inhibit microglial activation and are neuroprotective in global brain ischemia. *Proc. Natl. Acad. Sci. U.S.A.*, 95(26):15769–15774, Dec 1998. 165

A. Yu, Y. Shibata, B. Shah, B. Calamini, D. C. Lo, and R. I. Morimoto. Protein aggregation can inhibit clathrin-mediated endocytosis by chaperone competition. *Proc. Natl. Acad. Sci. U.S.A.*, 111(15):E1481–1490, Apr 2014. 31

L. Yu, V. Tucci, S. Kishi, and I. V. Zhdanova. Cognitive aging in zebrafish. *PLoS ONE*, 1:e14, Dec 2006. 196

S. Yuan and Z. Sun. Microinjection of mRNA and morpholino antisense oligonucleotides in zebrafish embryos. *J Vis Exp*, (27), May 2009. 61

B. Zakeri and G. D. Wright. Chemical biology of tetracycline antibiotics. *Biochem. Cell Biol.*, 86(2):124–136, Apr 2008. 133

D. W. Zang and S. S. Cheema. Degeneration of corticospinal and bulbospinal systems in the superoxide dismutase 1(G93A G1H) transgenic mouse model of familial amyotrophic lateral sclerosis. *Neurosci. Lett.*, 332(2):99–102, Oct 2002. 30

K. Zhang, C. J. Donnelly, A. R. Haeusler, J. C. Grima, J. B. Machamer, P. Steinwald, E. L. Daley, S. J. Miller, K. M. Cunningham, S. Vidensky, S. Gupta, M. A. Thomas, I. Hong, S. L. Chiu, R. L. Huganir, L. W. Ostrow, M. J. Matunis, J. Wang, R. Sattler, T. E. Lloyd, and J. D. Rothstein. The C9orf72 repeat expansion disrupts nucleocytoplasmic transport. *Nature*, 525(7567):56–61, Sep 2015a. 41

Q. Zhang, J. Cheng, and Q. Xin. Effects of tetracycline on developmental toxicity and molecular responses in zebrafish (Danio rerio) embryos. *Ecotoxicology*, 24(4): 707–719, May 2015b. 134

X. Zhang, S. Chen, L. Song, Y. Tang, Y. Shen, L. Jia, and W. Le. MTOR-independent, autophagic enhancer trehalose prolongs motor neuron survival and ameliorates the autophagic flux defect in a mouse model of amyotrophic lateral sclerosis. *Autophagy*, 10(4):588–602, Apr 2014. 190

Y. J. Zhang, T. F. Gendron, J. C. Grima, H. Sasaguri, K. Jansen-West, Y. F. Xu, R. B. Katzman, J. Gass, M. E. Murray, M. Shinohara, W. L. Lin, A. Garrett, J. N. Stankowski, L. Daughrity, J. Tong, E. A. Perkerson, M. Yue, J. Chew, M. Castanedes-Casey, A. Kurti, Z. S. Wang, A. M. Liesinger, J. D. Baker, J. Jiang, C. Lagier-Tourenne, D. Edbauer, D. W. Cleveland, R. Rademakers, K. B. Boylan, G. Bu, C. D. Link, C. A. Dickey, J. D. Rothstein, D. W. Dickson, J. D. Fryer, and L. Petrucelli. C9ORF72 poly(GA) aggregates sequester and impair HR23 and nucleocytoplasmic transport proteins. *Nat. Neurosci.*, 19(5):668–677, 05 2016. 8, 42

H. Zhou, C. Huang, H. Chen, D. Wang, C. P. Landel, P. Y. Xia, R. Bowser, Y. J. Liu, and X. G. Xia. Transgenic rat model of neurodegeneration caused by mutation in the TDP gene. *PLoS Genet.*, 6(3):e1000887, Mar 2010. 36, 121, 126, 131

S. Zhu, I. G. Stavrovskaya, M. Drozda, B. Y. Kim, V. Ona, M. Li, S. Sarang, A. S. Liu, D. M. Hartley, D. C. Wu, S. Gullans, R. J. Ferrante, S. Przedborski, B. S. Kristal, and R. M. Friedlander. Minocycline inhibits cytochrome c release and delays progression of amyotrophic lateral sclerosis in mice. *Nature*, 417(6884):74–78, May 2002. 165

U. Ziemann, M. Winter, C. D. Reimers, K. Reimers, F. Tergau, and W. Paulus. Impaired motor cortex inhibition in patients with amyotrophic lateral sclerosis. Evidence from paired transcranial magnetic stimulation. *Neurology*, 49(5):1292–1298, Nov 1997. 173

H. Zinszner, J. Sok, D. Immanuel, Y. Yin, and D. Ron. TLS (FUS) binds RNA in vivo and engages in nucleo-cytoplasmic shuttling. *J. Cell. Sci.*, 110 (Pt 15):1741–1750, Aug 1997. 38

P. Zwiegers and C. Shaw. Disparity of outcomes: the limits of modeling amyotrophic lateral sclerosis in murine models and translating results clinically. *Journal of Controversies in Biomedical Research*, 1(1):4–22, 2015. 45